UNIVERSITY COLLEGE LONDON
Research Department of Structural and Molecular Biology

The role of Grb2 in FGFR2IIIc-mediated early signalling complexes

Chi-Chuan Lin

September 2010

Thesis submitted for award of the degree of Doctor of Philosophy by the University College London

Supervisor: Professor John E. Ladbury

Abstract

Receptor tyrosine kinases (RTKs) regulate cellular processes by undergoing autophosphorylation on their tyrosine residues upon ligand binding. Phosphotyrosine residues also provide binding sites for adaptor protein binding. Grb2 has been shown to play a role in RTK pathways by recruiting other signalling proteins. Previously we showed the direct binding of Grb2 SH3 domain to the last 15 residues of FGFR2 C-terminal tail. In the present study, it is demonstrated that the direct binding of full-length Grb2 to FGFR2 cytoplasmic domain is a 2:1 binding event. Importantly, the direct binding may induce an apparent FGFR2 conformational change and enhance the FGFR2 phosphorylation. It is also shown that the effect of Grb2 on FGFR2 phosphorylation is mediated by the Grb2 C-SH3 domain. In addition, both N-SH3 domain and SH2 domain of Grb2 may play a role in the enhancement of the C-SH3 domain-mediated FGFR2 phosphorylation by stabilising Grb2 polypeptide structure, thus increasing the binding affinity toward FGFR2.

This study also shows Grb2 phosphorylation by FGFR2 mediated by the direct binding of Grb2 to the C-terminal of FGFR2. Three phosphorylation sites on Grb2 are identified; *in vitro* FGFR2 phosphorylation and ERK1/2 activation studies suggest that Grb2 phosphorylation may play a role in regulating FGFR2-mediated signalling pathway. Moreover, the interactions between Grb2 and SHP2, as well as FGFR2 and SHP2 have been characterised. It is also demonstrated that the binding of Grb2 to FGFR2 can prevent SHP2 binding to FGFR2, which is important in regulating FGFR2 activation. Finally, a model for the recruitment of FGFR2-Grb2-SHP2 signalling complex is proposed, in which Grb2 and SHP2 control FGFR2 early signalling complex formation. This study provides new insights into the role of Grb2 in the FGFR2-mediated signalling pathway.

Declaration

I confirm that the work presented in this thesis is my own which was conducted between 2006 and 2010. Information derived from other sources is indicated within the work.

…….

Chi-Chuan Lin

Acknowledgements

I would like to thank Professor John Ladbury for the opportunity to pursue a PhD in his group and for his supervision, helpful advice and guidance. I also thank Dr. Mark Williams and Professor Mark Marsh for helpful input and discussions.

In particular, I would like to thank Dr. Zamal Ahmed and Dr. Roger George for their help and support. Their expertise and confidence in me allowed me to conduct my research independently. I also want to thank Dr. Fernando Melo for his help in the ITC studies and Dr. Loren Stagg for his help in the SPR studies.

I also would like to thank the great UCL 6th floor members: Paul, Annika, Sunita, Claire, Tjelvar, Ellie, Ragini, Dipali, Dave, Anderson, Helene, Marilia, Toshi, Xioalin, Kate and Masooma. Thank you guys; you are the best team I have ever had. And thanks Kin. It is more than fair to say that without her I would not have achieved this goal.

Finally, I would like to thank my lovely parents for their support and understanding.

Table of Contents

List of Figures

List of Tables

Abbreviations

CH	Collagen homology (domain)
DAG	Diacylglycerol
EGF	Epidermal growth factor
EGFR	Epidermal growth factor receptor
ERK1/2	Extracellular signal regulated kinase 1 and 2
FGF	Fibroblast growth factor
FGFR	Fibroblast growth factor receptor
FRS2	Fibroblast growth factor receptor substrate 2
Gab1	Grb2-associated binder 1
Grb2	Growth factor receptor binding protein 2
HEK 293	Human embryonic kidney cell line
IP3	Inositol(1,4,5)triphosphate
MAPK	Mitogen activated protein kinase
NGF	Nerve growth factor
PC12	Rat phaeochromocytoma cell line
PDGF	Platelet-derived growth factor
PDGFR	Platelet-derived growth factor receptor
PH	Pleckstrin homology (domain)
PI3K	Phosphatidylinositol 3 kinase
PKC	Protein kinase C
PTB	Phosphotyrosine binding (domain)
RTK	Receptor tyrosine kinase
Sf9	Spodoptera frugiperda
SHP2	Src homology 2-containing tyrosine phosphatase
SH2	Src homology 2 (domain)
SH3	Src homology 3 (domain)
Sos	Son of sevenless
VEGF	Vascular endothelial growth factor
VEGFR	Vascular endothelial growth factor receptor

Chapter 1

Introduction

1.1 Receptor Tyrosine Kinases (RTKs)

1.1.1 General introduction

Protein tyrosine kinases (PTKs) play critical roles in signal transduction cascades by catalysing the phosphorylation of the tyrosine residues of signalling proteins. Two types of protein tyrosine kinases have been identified: non-receptor tyrosine kinases and RTKs[1, 2]. Extracellular signalling molecules such as hormones, neurotransmitters, cytokines and growth factors modulate the activities of vertebrate cells (e.g., cell growth and differentiation). These extracellular signals are transmitted through a class of transmembrane proteins known as receptors. One type of transmembrane receptor is the receptor tyrosine kinase (RTK) family, which consists of PTKs that can transfer phosphate groups from ATP molecules to tyrosine residues[3]. The tyrosine kinase activity of a receptor is important for its ability to activate signal transduction pathways and achieve downstream regulation[4] .

1.1.2 Signalling by RTKs

1.1.2.1 Cellular responses by RTKs

Upon ligand binding, the tyrosine residues of RTKs undergo autophosphorylation. Phosphotyrosine residues in the cytoplasmic domains of the receptor are selective binding sites for downstream intracellular signalling proteins. The recognition and

specific binding of intracellular signalling proteins to RTKs result in the formation of a signalling complex and activation of the downstream signalling pathway, therefore inducing the cellular response to growth factors. The responses of any given receptor are usually cell-type specific. For example, activation of the FGF receptor in PC12 cells leads to neurite outgrowth and cell differentiation, but in NIH3T3 cells, FGF receptor activation results in proliferation[5]. The following sections outline three major signalling pathways downstream of activated RTKs.

1.1.2.2 The Ras/Raf/MEK/ERK pathway

Activated RTKs recruit Grb2-Sos complexes to the plasma membrane. Sos acts as a guanine nucleotide exchange factor for Ras by promoting the exchange of GDP to GTP bound to Ras, leading to Ras activation. Ras is a critical mediator of RTK signalling and is responsible for the activation of downstream signalling. Activated Ras activates the protein kinase activity of Raf, the first component of the MAP kinase cascade. Activated Raf phosphorylates and activates MEK, and activated MEK then activates the extracellular regulated kinase 1/2 (ERK1/2) by phosphorylation. Activated ERK1/2 kinase then phosphorylates its downstream targets, leading to the regulation of various cellular functions[6]. Raf, MEK and ERK1/2 are all serine/threonine protein kinases.

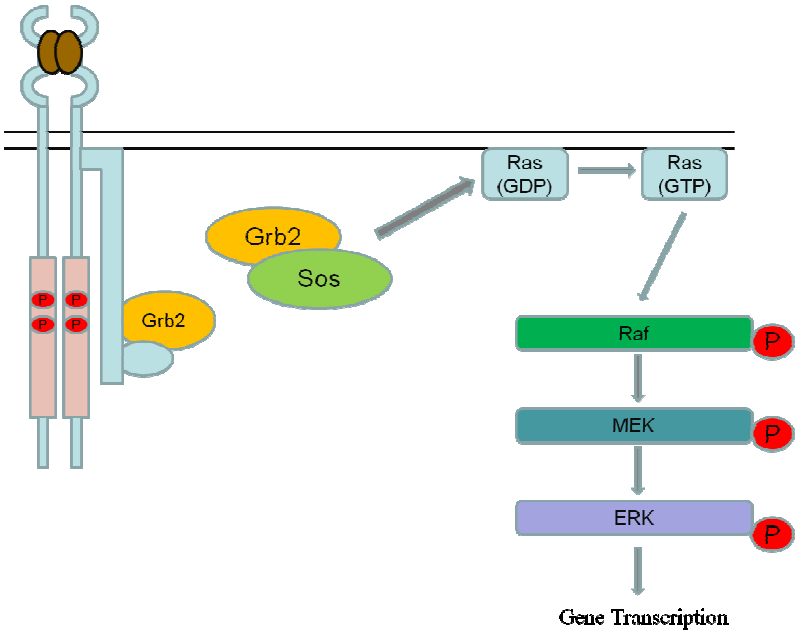

Figure 1.1: The Ras/Raf/MEK/ERK pathway. Activated RTK recruits the Grb2-Sos complex and activates Ras. The GTP-bound (activated) Ras then activates the downstream Raf/MEK/ERK pathway.

1.1.2.3 The PLCγ pathway

PLCγ is a 150-kDa phosphoprotein that associates with activated RTKs upon ligand binding[7]. Activated PLCγ cleaves phosphatidyl-inositol-4,5-bisphosphate to inositol trisphosphate (IP3) and diacylglycerol (DAG); DAG remains on the membrane and IP3 is released into the cytosol. IP3 and DAG are important second messengers; IP3 binds to the endoplasmic reticulum and releases Ca^{2+} into the cytosol, where Ca^{2+} activates various cellular processes. In the presence of Ca^{2+}, DAG activates protein kinase C, which phosphorylates cellular proteins.

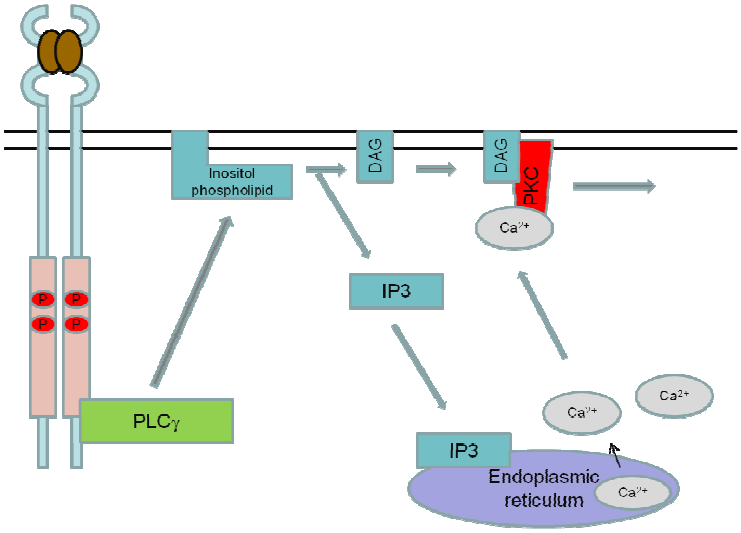

Figure 1.2: The PLCγ pathway. Activated RTK interacts with and activates PLCγ, which then catalyses the hydrolysis of inositol phospholipid to produce the second messengers IP3 and DAG. IP3 induces the release of calcium from the endoplasmic reticulum, thus allowing DAG to activate PKC.

1.1.2.4 The phosphatidylinositol 3-kinase (PI3-kinase) pathway

Phosphatidylinositol 3-kinases (PI3-kinases) are a family of enzymes involved in cellular functions such as cell growth and cell survival through inhibition of apoptosis. The PI3-kinase family can be divided into Class I, Class II and Class III according to their primary structure, regulation, and *in vitro* lipid substrate specificity. Only the Class I PI3-kinases can activate Akt in cells. PI3-kinase can be activated by RTKs, and active PI3-kinase phosphorylates the D-3 position of the inositol ring in inositol phospholipids to produce phosphatidylinositol 3-phosphate (PI(3)P), phosphatidylinositol (3,4)-bisphosphate ($PI(3,4)P_2$) and phosphatidylinositol (3,4,5)-trisphosphate ($PI(3,4,5)P_3$). $PI(3,4)P_2$ and $PI(3,4,5)P_3$ activate PDK1 by

binding to it, and activated PDK1 then phosphorylates Akt, thus activating the Akt pathway [8, 9].

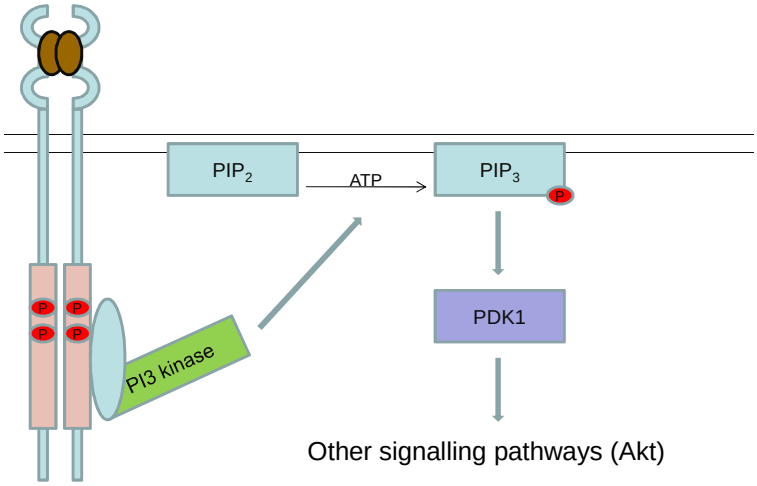

Figure 1.3: The PI3 kinase pathway. Activated RTK recruits and activates PI3 kinase. The activated PI3-kinase phosphorylates the phospholipid PIP_2 to form PIP_3, which activates the protein-serine/threonine kinase Akt pathway.

1.1.3 Structural Features of RTKs

1.1.3.1 RTK families

RTKs are found in all multicellular eukaryotic organisms, and 59 genes encoding different RTKs have been identified in the human genome. All RTKs have a similar architecture, with an extracellular domain, a single transmembrane region, and an intracellular region with protein tyrosine kinase activity and a C-terminal tail[10]. Human RTKs can be divided into 20 subfamilies according to their structural characteristics and the sequence homology in their extracellular domains, which are specific for their biological ligands (Figure 1.4).

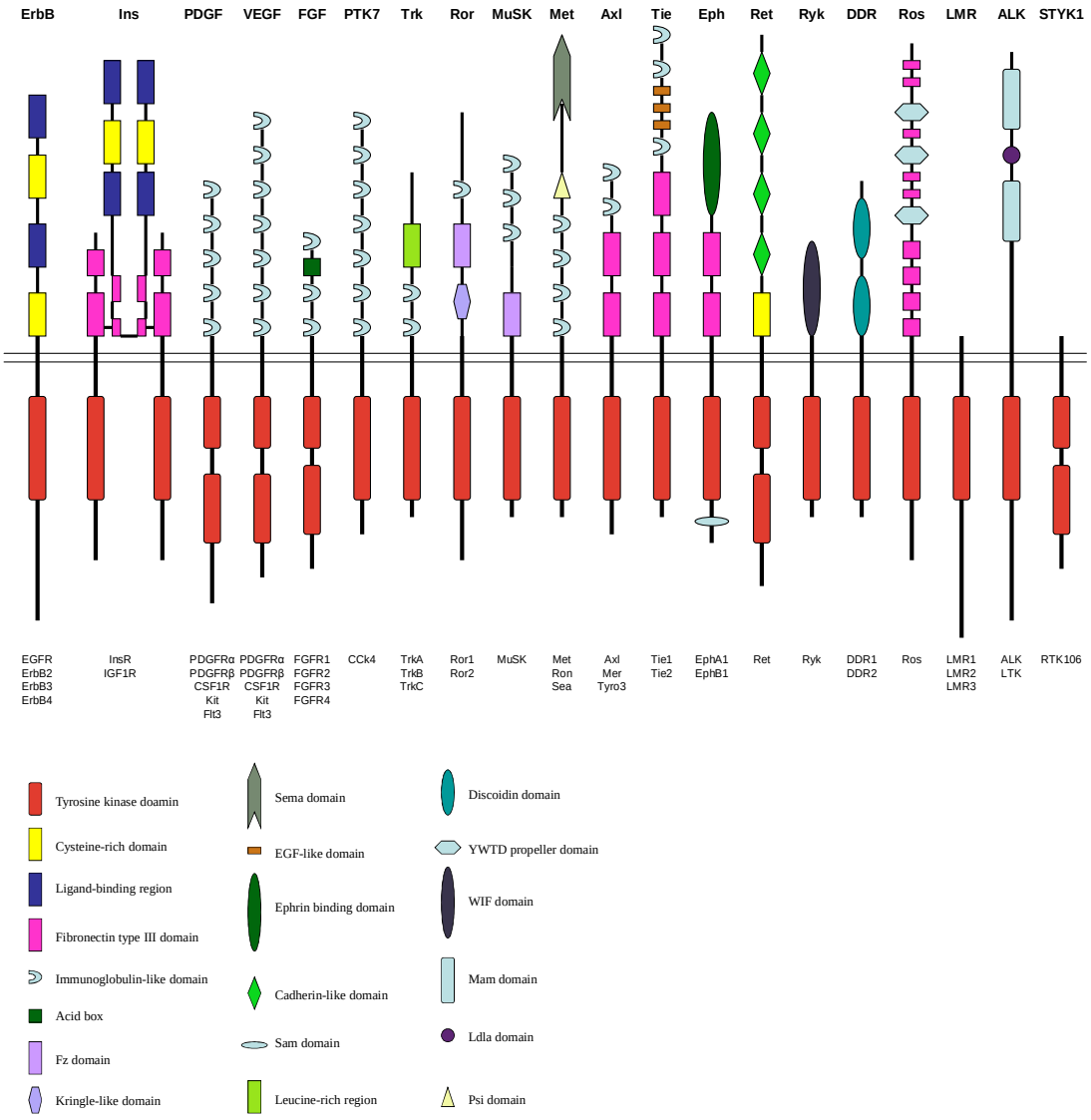

Figure 1.4: Overview of RTK families. Human RTKs can be divided into 20 subfamilies according to the differences in their extracellular domain structures. Adapted from Lemmon and Schlessinger, Cell, **141**, 1117-34 (2010)[11].

1.1.3.2 RTK domain composition and features

The N-termini of RTKs have a signal peptide sequence that is followed by an extracellular domain. The signal peptide targets the protein to the secretory pathway. The signal peptide and the extracellular domain are secreted outside the cellular membrane, where the extracellular domain plays its role as the ligand-binding domain.

This N-terminal extracellular domain is usually glycosylated and contains a distinctive pattern of cysteines, which form structural motifs. Different receptors have different extracellular motifs. For example, the fibroblast growth factor receptor (FGFR) subfamily has two or three immunoglobulin domains, whereas the epidermal growth factor receptor (EGFR) subfamily has two cysteine-rich regions. The extracellular domains of the various receptors form binding pockets specific for their biological ligands[12]. Asides from providing the binding site for signalling molecules, the extracellular domain also functions as a point of adhesion with other cell surface proteins. Further, the extracellular domain plays a critical role in receptor dimerisation following ligand binding, which is necessary for RTK signalling[13, 14].

The transmembrane domain has hydrophobic and basic residues that function as a stop-transfer signal. The transmembrane domain anchors the receptor in the correct orientation, stabilises the dimeric conformation of activated receptors, and transmits biological signals to the plasma membrane upon receptor dimerisation. Studies have indicated that mutations in the transmembrane domains of FGFR and EGFR can cause ligand-independent RTK activation[15, 16, 17].

Most RTKs share a highly conserved intracellular catalytic domain that consists of approximately 250 amino acids and has high sequence similarity among RTKs, including 13 conserved residues in all of the 59 human RTK sequences[18, 19]. The intracellular catalytic domain catalyses the phosphorylation reaction and interacts with and activates downstream signalling proteins. Moreover, structural studies focused on several protein kinases also provide evidence that the protein kinase catalytic domains have conserved architectures[20-24]. Although the catalytic domains of RTKs are highly conserved, there are differences between the intracellular sequences of various subfamilies. For example, platelet-derived growth factor receptor (PDGFR) and FGFR have an insertion region in their protein tyrosine kinase domains that splits this domain into two parts. Moreover, different RTK subfamilies use different sites to interact with docking proteins, essential components of the cellular signalling network that mediate the formation of the signalling complex. For example, a highly conserved sequence on the FGFR juxtamembrane region binds constitutively to the FRS2 PTB domain without FGFR activation. However, the NPQpY motif of nerve growth factor receptor (NGFR) binds to the FRS2 PTB domain only when NGFR is activated[25].

1.1.4 Ligand binding and RTK activation

Extracellular ligand binding is the first step in the activation of receptor signalling pathways. Ligand binding induces a conformational change in the extracellular domain, which in turn causes receptor dimerisation, resulting in the autophosphorylation or transphosphorylation of specific tyrosine residues in the cytoplasmic domain[1, 26, 27]. Different ligands use different mechanisms to induce receptor dimerisation. Dimeric growth factors such as vascular endothelial growth factor (VEGF) exist as homodimers and bind to their receptors in a 2:2 complex to induce receptor dimerisation. On the other hand, Cunningham *et al*. proposed a monomeric growth factor binding mechanism. Their study indicates that the binding of one molecule of human growth factor to one molecule of its receptor can promote the binding of the second receptor molecule to this complex and induce dimerisation of receptor extracellular domains[28]. Receptor dimerisation is further stabilised by additional interactions between the two receptors' extracellular domains[29-31].

The dimerisation of receptors is important for the activation of the intrinsic catalytic activity and autophosphorylation of receptor protein tyrosine kinases[32]. The tyrosine kinase domain of all RTKs is highly conserved; this domain contains the ATP binding sequence GlyXGlyXXGlyX(15-20)Lys[26, 33]. Mutagenesis studies performed both *in*

vitro and *in vivo* demonstrate that the lysine residue in the EGF and PDGF receptors is necessary for ATP binding and kinase activity[34-36]. Sequence alignments also reveal a glutamate residue (E651 in PDGFR) conserved in all protein tyrosine kinases. This conserved glutamate residue is involved in coordinating ATP and forming a salt bridge to the lysine residue in the above sequence[13]. Another conserved sequence that is found in the catalytic loop of receptor protein tyrosine kinases is HisArgAspLeuAlaAlaArgAsn, in which the Asp residue is believed to be the catalytic base. This conserved sequence not only exists in protein tyrosine kinases but can also be found in protein serine/threonine kinases[13]. Finally, the kinase activity of the receptor protein tyrosine kinase is increased by dimerisation, causing transphosphorylation between the two receptor monomers[37]. The transphosphorylation within the receptor dimer results in the activation of the dimeric tyrosine kinase domain and causes the phosphorylation of cytoplasmic substrate proteins. A mutagenesis study demonstrated that transphosphorylation is necessary for the activation or phosphorylation of the downstream substrate proteins[13]. This suggests that the tyrosine autophosphorylation in receptor protein tyrosine kinases has two important roles: the stimulation of the intrinsic catalytic activity of the receptor and the creation of binding sites for downstream Src homology 2 (SH2) domain- or phosphotyrosine-binding (PTB) domain-containing signalling proteins[38]. Further

studies demonstrate that the phosphorylation of tyrosine residues on a receptor induces a conformational change that allows for the binding of signalling proteins containing SH2 or PTB domains[39-41].

1.1.5 The formation of early signalling complexes (ESCs)

RTKs undergo phosphorylation at specific sites upon stimulation. This leads to the recruitment of signalling proteins such as Grb2 and Shc to the activated/phosphorylated RTKs via their SH2 or PTB domains. These recruited signalling proteins may be phosphorylated or may constitute platforms for other signalling proteins. To prevent incorrect crosstalk between different signalling pathways, the recruitment takes place among a defined group of proteins and in a precise order.

1.1.5.1 Specificity of signal transduction

One characteristic of signalling proteins involved in RTK signalling pathways is that they contain different types of domains, which means small protein modules with highly homologous primary and tertiary structures. Several different signalling domains have been reported, such as Src homology 2 (SH2), Src homology 3 (SH3),

and the phosphotyrosine-binding (PTB) domains[42]. These domains interact with other signalling proteins by recognising specific motifs on their targets.

The original dogma described an RTK signal transduction process as a linear pathway that requires a series of protein-protein interactions[43]. However, it is not obvious how the signalling can be specific when individual proteins participate in a number of pathways and how different proteins sharing common signalling domains transmit signals in a pathway-specific manner. Thus, each protein-protein interaction must have a high level of specificity to ensure that the entire signalling pathway is secure and that there is no interruption between different signalling pathways. However, it remains unclear how these proteins can be specific for one pathway.

The specificity of a domain-mediated protein-protein interaction is reflected as the binding affinity (K_D) of the interaction compared with those of any other competing interactions. Ladbury *et al*. determined that at least a 1000-fold difference in binding affinity is required to distinguish a specific interaction from non-specific interactions because a cell can have hundreds of signalling proteins composed of the same homologous domains[44, 45]. To investigate the specificity with which each domain recognises its binding partner in an RTK signalling pathway, several binding studies

have been performed using SH2, PTB and SH3 domains with their corresponding peptides. The following sections outline several studies on the specificity of binding by these domains.

1.1.5.2 Specificity in SH2 domains

SH2 domains are ~100 amino acid-long sequences with a structure composed of an anti-propeller β-sheet flanked by two α-helices[46]. SH2 domains regulate signalling pathways by recognising and binding to phosphotyrosine residues on their target proteins[39, 47-49]. Approximately 110 signalling proteins that contain a total of 120 SH2 domains are involved in controlling tyrosine kinase signalling pathways in humans[50-55].

Because cells possess many different proteins containing the SH2 domain, it is important to understand how SH2 domain-containing signalling proteins recognise their specific targets. Several groups have employed phosphopeptide library screens to study the sequence specificity of the phosphopeptide binding sites of SH2 domains (Table 1.1). For example, phosphopeptide screening results reported by Songyang *et al*. demonstrate that the SH2 domains from Src, Fyn, Lck, Abl, Crk and Sem5 have higher selectivities toward pY-X1-X2-I/P (X1 and X2 are hydrophilic residues)

compare with that of other phosphopeptides. The residues positioned from -2 to +4 surrounding this sequence are important for determining the selectivity of given phosphopeptides to certain SH2 domains[56]. For instance, the Src SH2 domain recognises the sequence pYEEI, whereas the Sem5 SH2 domain recognises the sequence pYLNV/P. However, this study also revealed that some SH2 domains can also bind to degenerate sequences with similar specificities, e.g., the Src SH2 domain can also bind to pYDNI or pYTEM.

Table 1.1: Amino acids preferentially selected by different SH2 domains at the pY+1, pY+2 or pY+3 positions. The numbers indicate the enrichment values of the residues selected. Adapted from Songyang, Cell, 1993, 72, 767[56].

Recognition specificities of SH2 domains			
SH2 domain	pY+1	pY+2	pY+3
Src	E (2.5)	E (2.6)	I (3.6)
	D (1.7)	N (2.4)	M (2.5)
	T (1.7)	Y (2.0)	L (2.3)
Fyn	E (3.2)	E (3.7)	I (4.2)
	T (2.0)	D (1.7)	V (2.5)
		Q (1.6)	M (2.0)
Lck	E (3.5)	E (2.5)	I (3.4)
	T (1.7)	D (1.5)	V (2.2)
	Q (1.6)		M (2.1)
Abl	E (2.8)	N (3.5)	P (3.0)
	T (2.4)	E (2.2)	V (2.2)
	M (2.1)	D (1.8)	L (2.2)
Crk	D (2.6)	H (2.9)	P (7.3)
	K (2.3)	F (1.9)	L (1.7)
	N (1.6)	R (1.7)	
Nck	D (5.8)	E (3.6)	P (3.0)
			D (2.8)
			V (2.7)
Sem5	L (2.3)	N (4.6)	V (1.7)
	V (2.0)		P (1.7)
	I (1.9)		
	M (1.8)		

Structural studies demonstrate that the pY residue interacts with a positively charged pocket within the SH2 domain. This binding site involves charge-charge interactions and hydrogen-bonds[42, 57]. The C-terminal residues of pY are bound in three different ways (Figure 1.5). First, the pY+1 and pY+2 residues extend across the polar surface, and the pY+3 residue inserts into the left pocket[46]. Second, the C-terminal residues of the pY extension bend to interact with a hydrophobic BG loop formed between helix αB and strand βG[58]. Third, the pY+2 residue is forced to adopt a β-turn conformation, resulting in an interaction between the hydrophobic side chain and the SH2 binding site surface[59].

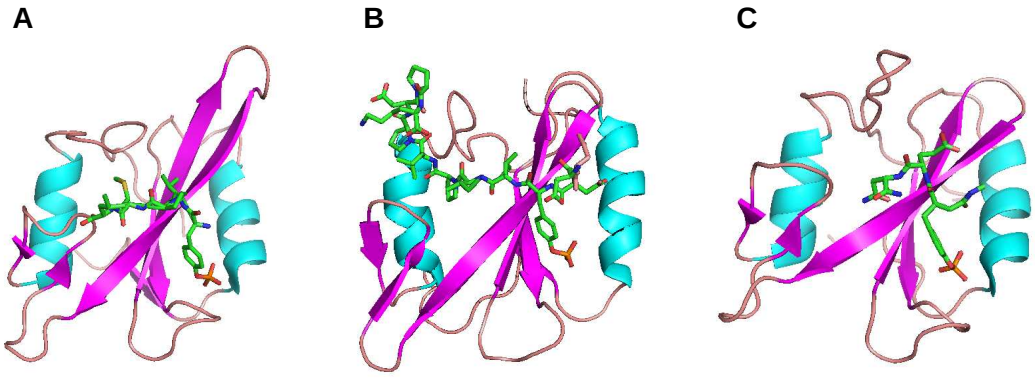

Figure 1.5: Structures of (A) the Src SH2 domain in complex with a phosphotyrosine peptide. Adapted from Waksman *et al.*, Nature, **358**, 646-53 (1992). PDB code: 1SHA. (B) The PLCγ SH2 domain in complex with a phosphotyrosine peptide. Adapted from Pascal *et al.*, Cell, **77**,461-72 (1994). PDB code: 2PLE. (C) The Grb2 SH2 domain in complex with a phosphotyrosine peptide. Adapted from DeLorbe *et al.*, J Am Chem Soc, **131**, 16758-70 (2009). PDB code: 3KFJ[59].

However, these studies did not explain the specificity with which SH2 domains bind to phosphotyrosine-containing proteins. According to reports by Ladbury *et al.*[8, 39], thermodynamic data from isothermal titration calorimetry (ITC) studies focusing on the interactions between phosphotyrosine-containing peptides and the Src SH2 domain reveal a lack of specificity in SH2 domain-phosphopeptide binding (Table 1.2). Different peptides with different residues at their pY+1, pY+2 or pY+3 positions have similar binding affinities, ranging from 0.18 to 6.25 μM, which are clearly not at the levels of affinity required for specific binding because the differences between these binding affinities are below 1000-fold[60].

Table 1.2: Binding of phosphotyrosine peptides to the Src SH2 domain. ITC was used to measure the interactions of a series of phosphotyrosine peptides with different amino acids in their pY+1, pY+2 or pY+3 positions. Adapted from Ladbury, Acta Crystallogr D Biol Crystallogr**, D63**, 26-31 (2007)[60].

Binding of tyrosyl phosphopeptides to the Src SH2 domain	
Peptide	Kd (μM)
PQpYEEIPI	0.25
Peptides with substitution in pY+1 position	
PQpYQEIPI	0.47
PQpYDEIPI	0.18
PQpYAEIPI	0.34
PQpYGEIPI	6.25
Peptides with substitution in pY+2 position	
PQpYEYIPI	0.66
PQpYEQIPI	0.53
PQpYEDIPI	0.42
PQpYEAIPI	1.04
PQpYEGIPI	1.96
Peptides with substitution in pY+3 position	
PQpYEELPI	0.43
PQpYEEVPI	0.46
PQpYEEAPI	1.75
PQpYEEGPI	0.39

In contrast, studies performed using phosphotyrosine peptides to explore the interactions between SH2 domains and phosphotyrosine may be oversimplified because screening short peptide cannot sufficiently represent native proteins[45, 61, 62]. An X-ray crystal structure of the FGFR1 cytoplasmic domain in complex with PLCγ SH2 domains is an ideal model to study interactions between SH2 domains and phosphotyrosine-containing proteins in their native states (Figure 1.6)[62].

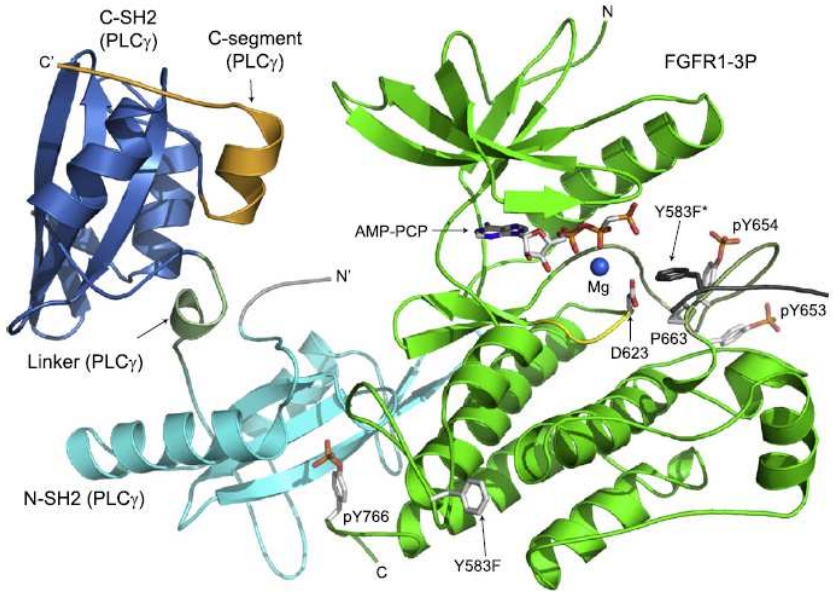

Figure 1.6: Crystal structure of the activated FGFR1-PLCγ SH2 domain complex. The structure of FGFR1 is shown in green, the N-SH2 domain of PLCγ is shown in cyan and the C-SH2 domain of PLCγ is shown in blue. The A-loop is shown in pale green, and the catalytic loop is shown in yellow. The ATP analogue, phosphotyrosines (pY653, pY654 and pY766) and the catalytic base (D623) are shown in stick representations. Taken from Bae *et al*., Cell, **138**, 514-24 (2009)[62].

The SH2-phosphorylation binding specificity is determined by the primary SH2 domain binding site, i.e., the N-SH2 domain of PLCγ binding to the pYDLD motif of FGFR1 is a typical SH2 domain-phosphotyrosine interaction that involves a pY binding pocket and a hydrophobic binding pocket. Surprisingly, the structure suggests that asides from the canonical phosphorylation-dependent binding, the binding of the N-SH2 domain of PLCγ to activated FGFR1 is also controlled by a secondary binding site that contributes the "selectivity" to the interaction (Figure 1.7). The secondary binding site is divided into hydrophobic sub-site I and hydrophilic sub-site II based on the hydrophobic and hydrophilic characteristics of the binding sites.

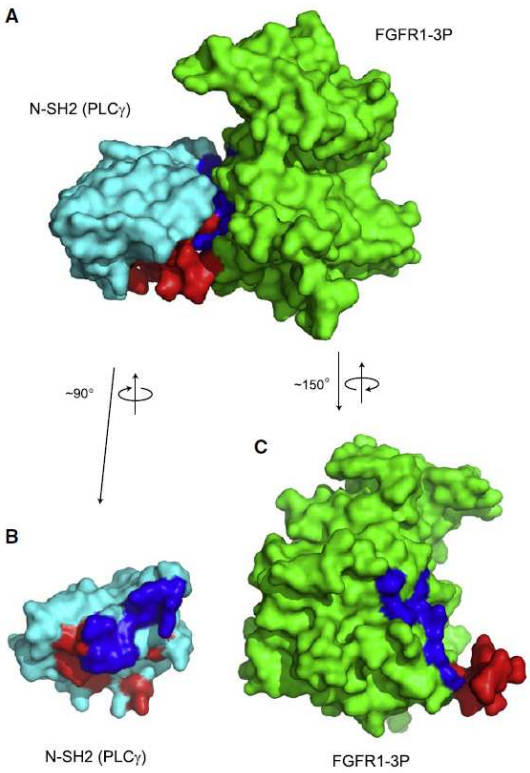

Figure 1.7: Interactions between activated FGFR1 and PLCγ. Interactions mediated by the primary binding site (phosphotyrosine-dependent) are coloured red. Interactions mediated by the secondary binding site are coloured blue. Taken from Bae *et al*., Cell, **138**, 514-24 (2009)[62].

Sequence alignments of the N-SH2 and C-SH2 domains from different species reveal that the residues responsible for the phosphotyrosine-dependent primary binding site are conserved across species. However, the residues responsible for the secondary binding site can only be found in the N-SH2 domain. *In vitro* binding studies using ITC demonstrate that the N-SH2 and C-SH2 domains have similar binding affinities to a phosphopeptide derived from FGFR1 (0.43 µM for the N-SH2 domain and 1.87 µM for the C-SH2 domain). However, when the native protein was used instead of the

phosphopeptide, the N-SH2 domain exhibited a higher binding affinity (0.03 μM) towards the native FGFR1 protein[62].

Although the difference in binding affinity is less than what Ladbury *et al*. suggested (i.e., that meaningful specificity requires at least a 1000-fold difference in affinity), this study provides new insight into studying the specificity of SH2 domain interactions.

1.1.5.3 Specificity in PTB domains

PTB domains also recognise and bind to phosphotyrosine-containing cellular signalling proteins. Common PTB domains have a structure of seven antiparallel β-strands, forming a central β-sandwich motif, as well as a C-terminal α-helix[63]. According to their structural differences, PTB domains can be divided into three families: IRS-1/Dok-like, Shc-like and Dab-like[64]. The first PTB domain was identified as a 186-residue module in Shc, a scaffold protein in signalling cascades. This domain can also bind to a conserved phosphotyrosine-containing sequence NPXpY or NXXpY (where X represents any residue) in activated receptor protein tyrosine kinases[65, 66].

Ligand recognition of PTB domains is more diverse than that of SH2 domains. In contrast to SH2 domains, the presence of a phosphotyrosine is not required for PTB domain-mediated binding, and PTB binding is more dependent on the surrounding β-strand antiparallel motif[67-69]. PTB domains lack specificity. For example, the FRS2 PTB domain can bind to both NPXpY and AVHKLAKSIPLRRQVYVS with similar binding affinities[25, 70].

1.1.5.4 Specificity in SH3 domains

SH3 domains were first identified as a conserved sequence in the N-terminus of Src[71]. SH3 domains are small 55- to 70-amino acid domains that are found in many cellular signalling proteins, such as PLCγ and PI-3 kinase[72-75]. SH3 domains have a compact β-barrel structure[76]. An early study performed by Rodaway *et al*. indicates that most SH3 domain-containing proteins are membrane-associated, suggesting that SH3 domain may be involved in subcellular localisation[77]. Further studies have demonstrated that SH3 domains play a role in the reorganisation of signalling proteins to their targets through interactions with proline-rich sequences[78]. Several structural studies reveal the molecular details of the SH3-proline-rich motif interaction. Interactions between SH3 domains and proline-rich motifs are mediated by hydrophobic interactions and are typically rather weak. The binding site within SH3

domain consists of conserved aromatic residues that form an exposed hydrophobic patch on the protein surface[76, 79-81]. SH3 domains also have preferences for arginine and leucine residues. Peptide library screens have found that the proline-rich peptides bound to SH3 domains can be divided into two classes. Class I has the consensus sequence RXLPP(L/R)P, whereas class II has the sequence XPPLPXR. Due to the conserved arginine residues located at the N-terminus of Class I peptides and the C-terminus of Class II peptides, it is proposed that peptides of these two classes bind to SH3 domains in reverse orientations[82]. Studies also indicate that SH3 domains may form a dimer when they bind to ligands. This ligand-mediated SH3 dimerisation is stabilised by the peptide ligand[83-85].

The specificity of SH3 domain binding has been addressed using peptide library screening. Although the C-terminal residues of the proline-rich motif do not provide additional specificity, the difference in binding affinities among different proline-rich peptides is clearly < 40-fold (Table 1.3)[45], suggesting that no high level of specificity is achieved. For example, the Fyn SH3 domain has similar binding affinities towards the Sos and p85 peptides (20 and 16 μM, respectively); thus, the SH3 domain cannot distinguish between these different binding partners in cells.

Table 1.3: Binding of proline-rich peptides to SH3 domains. The differences in the affinities from these binding studies are < 100-fold, suggesting that SH3 domain binding is non-specific. Adapted from Ladbury and Arold, Chem Biol, **7**, R3-8 (2000)[45].

Recognition specificities of SH3 domains		
SH3 domain	Peptides	K_D (μM)
Abl	RAPTMPPPLPP (3BP-1)	34
Abl	PPAYPPPPVP (3BP-2)	5
Fyn	PVRPQVPLRPPMT (Nef)	202
Fyn	PPRPTPVAPGSSKT(p85)	50
Fyn	HSIAGPPVPPR (Sos 1-4)	20
Fyn	RAPTMPPPLPP (3BP-1)	34
Fyn	PPAYPPPPVP (3BP-2)	34
Fyn	PPRPTPVAPGSSKT(p85)	16
Grb2	VPPPVPPRRR (Sos)	5
Grb2	GTDEVPVPPPVPPRRRPESA (hSos)	21
p85	RKLPPRPSK (peptide libraries)	9
Src	RALPPLPRY (peptide libraries)	8
Src	HSIAGPPVPPR (Sos 1-4)	26

1.1.5.5 Early signalling complexes (ESCs) provide specificity

Meaningful specificities require at least a 1000-fold difference between a specific interaction and a non-specific interaction[45]. Linear processing of a signal that employs individual protein-protein interactions would require a high level of specificity to avoid any cross reaction between signalling pathways. However, as described above, binding studies of SH2, PTB and SH3 domains reveal that the differences in binding affinity are < 100-fold (i.e., all three domains lack the specificity required to prevent cross-talk between different cell signalling pathways). Thus, linear processing of signals is not sufficient to ensure mutually exclusive pathways.

It has become clear that the stimulation of RTKs results in the assembly of a number of signalling proteins at the membrane. This formation of signalling complexes requires multiple interactions, potentially increasing the interaction affinity between two interacting proteins by providing the correct positioning of binding sites, making the interaction specific with respect to other binding partners. This increase in affinity would reduce the chance of non-specific interactions with other competing proteins. The formation of ESCs both explains the specificity of a signalling pathway and provides several features for the control of signalling pathways[43].

1.2 Fibroblast Growth Factor Receptor Signalling

1.2.1 The FGFR family

1.2.1.1 FGFR subfamilies and isoforms

Different promoters and alternative splicing in cells result in the formation of different types of FGFRs. The FGFR family consists of at least four types: FGFR1 (*flg*)[86, 87], FGFR2 (*bek*)[88], FGFR3[89], and FGFR4[90, 91]. Further, alternative splicing of FGFR mRNA results in the formation of three different isoforms of the Ig-like domain III in FGFRs, termed IIIa, IIIb, and IIIc (Figure 1.8)[92-95], which confers ligand-binding specificities on the receptors. The b isoform is mainly expressed in epithelial lineages, whereas the c isoform is expressed in mesenchymal lineages[96-99].

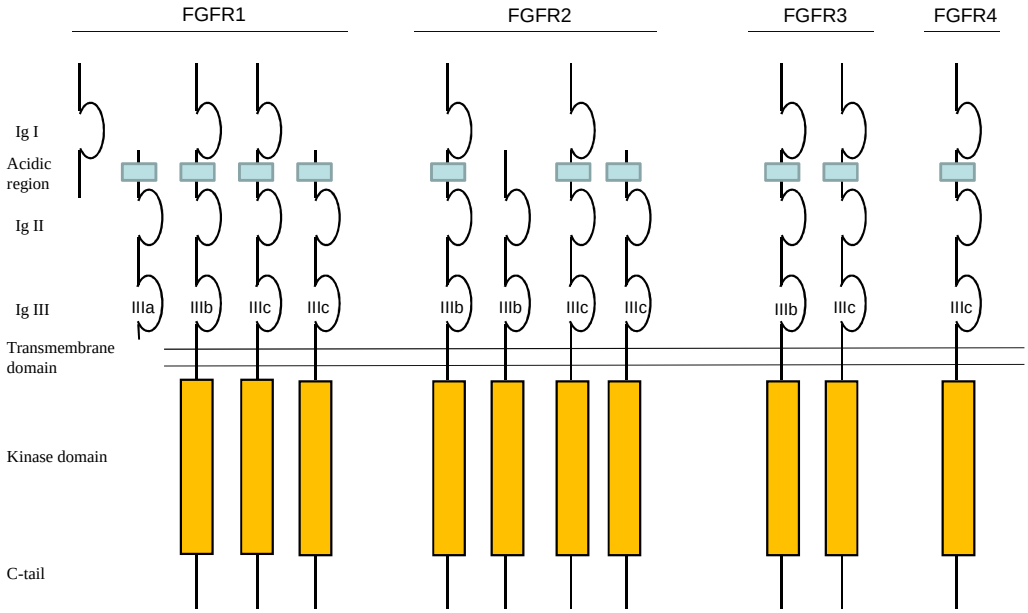

Figure 1.8: Various FGFR isoforms. Numerous splicing forms of FGFR. Some isoforms have truncated extracellular domains (in particular, Ig I is often missing). Secreted forms lack the transmembrane domain. Adapted from Johnson and Williams, Adv. Cancer Res, **60**, 1-41 (1993)[100].

1.2.1.2 Fibroblast growth factors

In humans, 22 different FGFs have been identified to date (FGF15 is only known to exist in mice). FGF3, 4, 8, 17 and 19 are expressed during embryonic development, while FGF1, 2, 5, 6, 7, 9, 10, 11, 12, 13, 14, 16, 18, 20, 21, 22 and 23 are expressed in both embryonic and adult tissues[101]. FGFs play important roles in DNA synthesis, cell migration, the regulation of cell growth, embryogenesis, and angiogenesis[100-102]. In vertebrates, these 22 FGFs are highly conserved in gene structure and amino acid sequence. Most FGFs have peptide sequences that allow them to be secreted from cells. Although FGF9, 16, and 20 do not have these peptides, they are still found outside the cell. FGF1 and FGF2 are found on the cell surface and within the extracellular matrix, and FGF11-14 remain inside cells. While some FGFs contain nuclear localisation signals and can be found in the nucleus, the role of these nuclear FGFs remains unclear[101].

FGF9 was used in this PhD study. Previous studies by our group indicate that FGFR2IIIc is highly phosphorylated even in unstimulated cells, and the level of FGFR2IIIc phosphorylation can only be increased upon FGF9 stimulation[103-105].

1.2.1.3 Heparin sulphate proteoglycans (HSPGs)

Heparin, a highly sulphated glycosaminoglycan, is found in various mammalian tissues including the liver, lung and intestines. Heparins are glycosaminoglycan family carbohydrates and have molecular weights ranging from 3 to 40 kDa. The basic structure of heparin consists of repeating sulphated disaccharide units. The main disaccharide unit in the heparin backbone is O-sulphated and N-sulphated glucosamine; iduronate and glucuronate residues are also prominent[106].

Heparin can link to proteins after chain elongation and modification, creating complexes called HSPGs. These complexes are macromolecules located on the surface of vertebrate and invertebrate cells. HSPGs have several important biological functions in embryonic morphogenesis, angiogenesis and tissue repair[106].

1.2.1.4 The Interaction between FGF and heparin

FGFs alone are unable to bind and activate FGFRs without heparin[107]. Indeed, HSPGs are necessary components of the FGF signalling pathway[108, 109]. FGFs have a strong affinity for heparin and HSPGs. FGF-heparin complexes can bind to FGFRs and initiate downstream signalling cascades affecting gene expression, thus regulating cell growth, development and migration.

HSPGs bind and activate cellular growth factors through their heparin sulphate chains[110]. Heparin forms very tight complexes with groups of mammalian cellular growth factors, including FGF[107, 111], VEGF[112] and heparin-binding EGF[113]. Studies performed by Mansukhani *et al*. indicate that cell surface HSPGs can also enhance the binding of several types of FGF to FGFR2[114]. According to this study, binding of FGF to FGFR2 induces the phosphorylation of FGFR2 and leads to a mitogenic response; the binding affinity of FGF to FGFR2 can be greatly enhanced by the addition of heparin. In addition to increasing the binding affinity of FGF to FGFR, heparins and cell surface HSPGs also play important roles in protecting FGF from heat inactivation and proteolysis[115-119]. The degree of sulphation and the length of heparin in HSPGs affects the ability of FGF2 to bind FGFR1 and heparin[120]. This study demonstrates that the binding of FGF2 to its receptor requires heparin molecules containing at least eight to 10 sugar units. Also, FGF bound to highly sulphated heparin-derived polysaccharides has a greater receptor binding ability than FGF bound to heparin with a low level of sulphation.

FGF4 provides an excellent example of the regulation of FGF and FGFR binding by heparin. FGF4 is found in tumours and is related to limb development and embryogenesis[121, 122]. FGF4 is known to bind and activate FGFR2 rather than FGFR1

at low heparin concentrations[123]. However, the low binding affinity of FGF4 to FGFR1 can be increased using a higher concentration of heparin. This study supports the model that the activation of different types of FGF receptors by FGF may be determined by different concentrations of heparin at the cell surface. However, there is no significant difference between the binding of FGF1 to FGFR1 or FGFR2 at the same heparin concentration, and the increase in heparin concentration has no effect on the binding affinity of FGF1 to FGFR1[123]. Brickman *et al*. used peptides homologous to the heparin binding region of the receptor to investigate whether HSPGs with different specificities for FGF2 also have different affinities for different FGF receptors[124]. The results demonstrate that the basic residues of the Ig-like domain 2 of FGFR 1 can form a heparin-binding site. Peptides homologous to this region of FGFR1 inhibit mitogenesis *in vivo*, but FGFR2, 3 and 4 do not elicit the same response. These findings indicate that unique heparin sulphate domains interact with specific cell-surface receptors and direct different cellular responses.

1.2.2 The cellular context of FGFRs

FGFR signalling is important in the regulation of cellular functions, such as differentiation, survival and proliferation. FGFR1 signalling is the best-studied component of the FGFR signalling pathway, and the initial signalling events are quite

similar between FGFR1 and FGFR4 due to the highly conserved sequence homology in their RTK domains[125].

While many growth factors can bind to more than one receptor, the various roles of these receptors in signalling pathways remain unclear. A study comparing FGFR1 and FGFR4 signalling in BaF3 cells and L6 cells revealed that both FGFR1 and FGFR4 have high binding affinities to FGF1, and both have similar degrees of receptor activation upon FGF1 stimulation. However, FGFR1 has a stronger downstream response: tyrosine phosphorylation of PLCγ and ERK2, and only FGFR1 activation induced the phosphorylation of an unidentified 80-kDa protein[125]. Another study using the chimeric receptor FGFR4/R1C, which contains the FGFR4 extracellular domain and the FGFR1 intracellular domain, demonstrates that this chimeric receptor exhibits the same FGF-induced proliferation response as FGFR1 upon FGF1 stimulation. Therefore, this result suggests that the intracellular domains of FGFRs determine their functional capacities[126]. Moreover, a study performed by Raffioni using chimeric receptors in PC12 cells indicates that FGFR1, FGFR3 and FGFR4 mainly use FRS2 and PLCγ but not Shc to transduce signals, and these FGFRs have similar signalling responses. This study demonstrates that the major difference

between FGFRs is the level of receptor autophosphorylation; specifically, FGFR1 and FGFR3 have higher phosphorylation levels compared to FGFR4[127].

Haugsten *et al*. transfected each of the FGFR1-4 proteins into HeLa cells to study the intracellular trafficking of FGF1 in an effort to understand the differences between FGFR1, FGFR2, FGFR3 and FGFR4. Their study revealed that FGF1 is slowly degraded in cells expressing FGFR4. FGFR1-3 are ubiquitinylated on several lysine residues, can be transported to lysosomes with their bound ligands and are degraded in the lysosomes after endocytosis. Thus, these data suggest that differences exist between various FGFRs[128].

1.2.3 General structural overview of FGFRs

1.2.3.1 Extracellular domains

FGFRs have common structural features: they have three Ig-like domains in their extracellular domain (D1~D3), a transmembrane domain and an intracellular domain containing a highly conserved PTK domain. The Ig-like domains 2 and 3 (D2 and D3) are necessary for ligand binding; an acidic box between D1 and D2 participates in the regulation of FGF binding to FGFR. Alternative exon splicing results in the expression of FGFR with or without the Ig-like domain 1. The FGFR α isoforms

possess three Ig-like domains (D1, D2, and D3), whereas the β isoforms contain two Ig-like domains (D2 and D3)[129, 130]. A study performed by Johnson *et al*. indicates that both isoforms can respond to FGF1 and FGF2. Furthermore, Wang *et al*. indicate that the lack of D1 can increase the binding affinity to both FGF and heparin[130]. A crystal structure of the FGFR3c-FGF 1 complex reported by Olsen *et al*. (2004) displays that D1 and the linker region between D1 and D2 are disordered, suggesting that D1 and the linker are not responsible for FGF ligand binding. However, real-time binding assay results also demonstrate that the FGFR3c with 3 Ig-like domains have a lower affinity for both FGF and heparin compared to the FGFR3c with two Ig-like domains. This study proposes that the FGFR with three Ig-like domains possesses an autoinhibition function[131].

Several groups have explored the interaction between FGF, heparin and FGFR from a structural perspective. In 1999, Plotnikov *et al*. determined the crystal structure of immunoglobulin-like domains 2 and 3 with their ligand, FGF2; two FGF2:FGFR1 complexes form a twofold symmetric dimer via the binding of ligand to Ig-like domains 2 and 3 (D2 and D3) (Figure 1.9). They also investigated ligand-receptor and receptor-receptor interactions that stabilise dimerisation, though they did not find evidence of a direct FGF-FGFR interaction. Instead, they propose a positively

charged heparin-binding canyon within the FGF2-FGFR1 crystal structure. Although heparin is not present in this crystal structure, this model still provides detailed information on how a growth factor binds to an extracellular domain of a receptor and how dimerisation occurs between receptors[132].

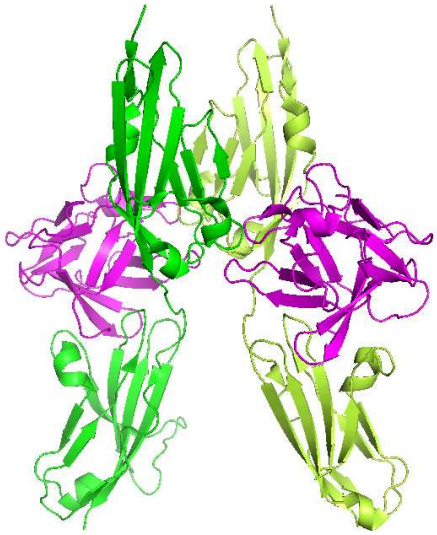

Figure 1.9: Dimeric structure of FGF2-FGFR1. Monomers of the D2-D3 domain of FGFR1 are shown in light and dark green, and FGF1 is shown in purple. This structure shows that two FGF2-FGFR1 complexes form a twofold FGF2-FGFR1 symmetric dimer. Adapted from Plotnikov *et al*., Cell, **98**, 641-50 (1999). FGF2-FGFR1 structure PDB code: 1CVS[132].

Two crystal structures, FGF1-FGFR1 and FGF2-FGFR2, have been determined to study the interaction between FGF and FGFR (Figure 1.10). The FGF1-FGFR1 D2 region and FGF2-FGFR2 D2 region interactions are very similar (mainly mediated by hydrophobic interactions), whereas the interactions of FGF ligands to D3 regions are mediated by hydrogen bonds. In the FGF2-FGFR2 structure, the interactions between

FGF2 and the D3 region are mediated by FGF2 making contact with the ordered βC′-βE loop via five hydrogen bonds. The FGF2-FGFR1 structure also displays the interaction between FGF2 and the ordered βC′-βE loop of the FGFR1 D3 region. However, in the FGF1-FGFR1 structure, the βC′-βE loop is disordered due to the lack of interaction between FGF1 and the FGFR1 D3 region. Gln-58 and Val-88 of FGF2 contribute to the interactions between FGF2 and FGFR2 D3. Substituting Gln-58 and Val-88 with Ser-47 and Pro-79 in FGF1 prevents the interaction with the βC′-βE loop, therefore making this loop disordered. This structural information was used to explain the binding specificity of FGF-FGFR[133].

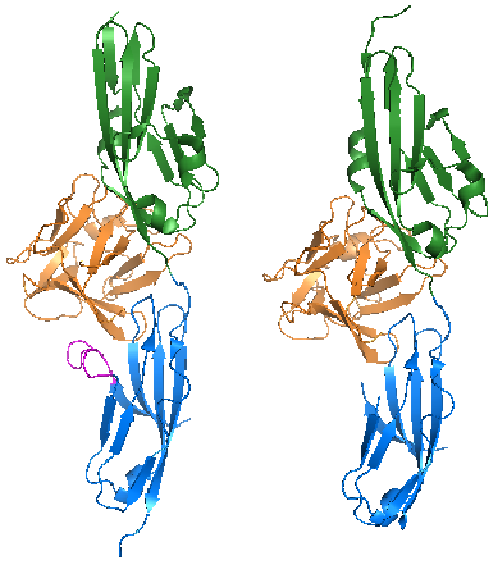

Figure 1.10: Structures of the FGF2-FGFR2 (left) and FGF1-FGFR1 (right) complexes. The D2 and D3 domains are coloured in green and blue, respectively. FGF1 and FGF2 are shown in orange. The ordered βC′-βE loop is shown in purple in the FGF2-FGFR2 complex structure. The βC′-βE loop in the FGF1-FGFR1 complex is disordered. Adapted from Plotnikov *et al.*, Cell, **101**, 413-24 (2000). FGF2-FGFR2 structure PDB code: 1EV2, FGF1-FGFR structure PDB code: 1EVT[133].

Stauber *et al*. (2000) also published a crystal structure of the complex between FGF1 and the Ig-like domains 2 and 3 of FGFR2; this crystal structure is also a dimeric 1:1 ligand:receptor complex. Moreover, they produced a model of a ligand:heparin:receptor complex that provides fundamental information on the interaction between heparin, FGFs and FGF receptors[134]. A model of the FGF2-FGFR1-heparin-like glycosaminoglycan (HLGAG) complex was proposed in which the two domains of a single FGFR1 molecule wrap around a single FGF2 protein, indicating a role for the HLGAG in the complex with FGF2 and FGFR1, suggesting HLGAG-mediated FGF dimerisation or oligomerisation[135]. The crystal structure of the dimeric FGF1-FGFR2-heparin complex was reported in 2000 (Figure 1.11). This structural model provides clear information on the FGF1-FGFR2-heparin interaction. The complex is assembled by two FGF1 molecules linked to one heparin molecule in the centre that forms a bridge between two FGFR2 molecules (2:2:1 FGF:FGFR:heparin)[136].

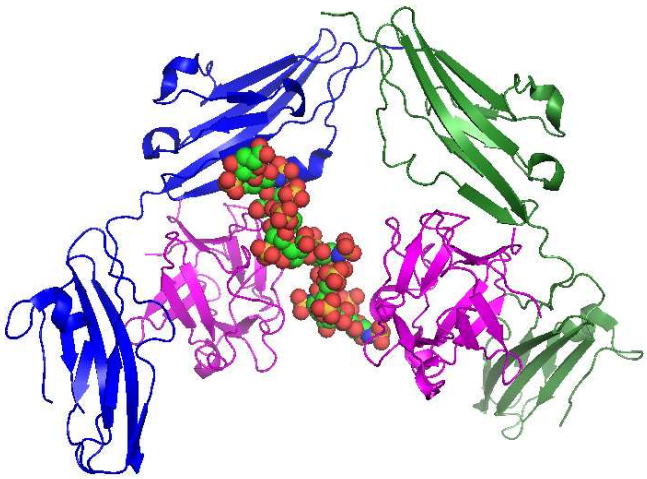

Figure 1.11: Structure of the FGF1-FGFR2-heparin complex. The D2-D3 domains of FGFR2 are shown in green and blue. FGF1 is presented in purple, and heparin is depicted in a CPK representation. This structure shows that the dimeric form of FGFR2 is induced by two FGF1 molecules and one heparin. Adapted from Pellengrini *et al*., Nature, **407**, 1029-34 (2000). FGF1-FGFR2-heparin structure PDB code: 1E0O[136].

A crystal structure of a 2:2:2 FGF:FGFR:heparin complex has also been reported. In contrast to the heparin-mediated formation of the twofold symmetric dimer formed by two FGF-FGFR complexes, this structure shows that each FGF-FGFR complex contains one decasaccharide molecule. This structure is proposed to exist when shorter heparin molecules are used for FGF-stimulated FGFR activation[137].

1.2.3.2 FGFR tyrosine kinase domain structure

The crystal structures of the FGFR1 tyrosine kinase domain in complex with an ATP analogue and in the unliganded form were solved by Mohammadi *et al*. Figure 1.12 shows the overall structure of the FGFR1 tyrosine kinase domain. The N-terminal

lobe comprises five anti-parallel β strands (β1 – β5) and one α helix (αC), while the N-terminal lobe has the ATP binding site located in the loop between strands β1 and β2. The C-terminal lobe has two β strands (β7, β8) and seven α helices (α D, αE, αEF, αF, αG, αH, and αI). The catalytic loop located between αE and β7 contains an aspartic acid residue that functions as the catalytic base in the phosphotransfer reaction of FGFR1 tyrosine kinase. The activation loop (A-loop) that serves as the substrate binding site has two tyrosine autophosphorylation residues, Tyr653 and Tyr654, and these residues are conserved in all FGFRs.

Phosphorylation of these tyrosine residues within the A-loop is critical for the activation of kinase activity and the biological control of the receptor in several different cellular receptors, such as the insulin receptor and FGFR[138, 139]. The crystal structure of the non-phosphorylated kinase domain of the insulin receptor suggests a molecular mechanism in which the receptor tyrosine kinase domain has a low activity before the autophosphorylation of the A-loop[140]. This significant activation of protein tyrosine kinase activity stimulated by A-loop phosphorylation is both important in receptor protein tyrosine kinases and plays a critical role in non-receptor protein tyrosine kinases such as Src and JAK2[141, 142].

Moreover, comparing the FGFR1 kinase domain structure with the insulin receptor kinase domain structure indicates that the main difference between the kinase domains is in the conformation of their activation loops. Hubbard *et al.* provide evidence for the different conformations of the A-loop between the FGF and insulin receptors[143]. In the FGFR1 kinase domain, residues Arg-661 and Pro-663 in the A-loop have the ability to interfere with the binding of substrate peptides but not with the binding of ATP, whereas the critical residue in the activation loop that blocks the binding of substrate peptide in insulin receptor kinase is Tyr-1162. This finding suggests that FGFR1 kinase may also have an autoinhibitory mechanism.

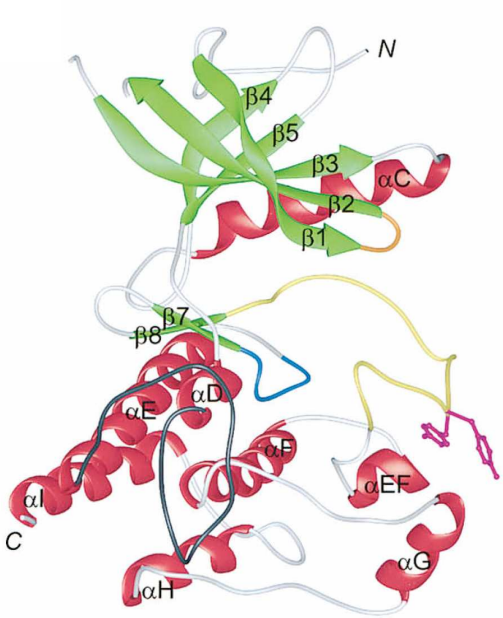

Figure 1.12: FGFR1 kinase structure. The α-helices are coloured red, and the β-strands are green. The nucleotide-binding loop is shown in orange, the catalytic loop is shown in blue and the activation A-loop is shown in yellow. The side chains of Tyr-653 and Tyr-654 are shown in purple. Taken from Mohammadi *et al.*, Cell, **86**, 577-87 (1996)[139].

Crystal structures of the non-phosphorylated FGFR2 kinase domain and A-loop phosphorylated FGFR2 kinase domain, together with an ATP analogue and a peptide substrate (FGFR2 C-terminal tail, residues 764-778), were solved (Figure 1.13). The overall architectures of nonphospho-FGFR2 kinase and phospho-FGFR2 kinase are bilobate like that of the FGFR1 kinase domain, the insulin receptor kinase domain and other protein serine/threonine kinases with known 3D structures[139, 140, 143-145]. Briefly, the N-terminal lobe of FGFR2 kinase, which has an ATP binding site, consists of one α-helix (αC) and a β-sheet comprised of five anti-parallel β-stands (β1-5). The C-terminal lobe, which is responsible for kinase activation, substrate binding and catalysis, contains seven α-helices (αD, αE, αF, αEF, αG, αH, and αI) and two β-strands (β7 and β8). Two major architectural changes can be detected when the A-loop of FGFR2 kinase is phosphorylated. First, the N-lobe moves towards the C-lobe. Second, the A-loop conformation is rearranged and makes contact with the RD pocket. Arginine and aspartate residues have been demonstrated to be important in regulating tyrosine kinase activity[144, 146]. These conformational changes are necessary for ATP and substrate binding and to increase kinase catalytic efficiency.

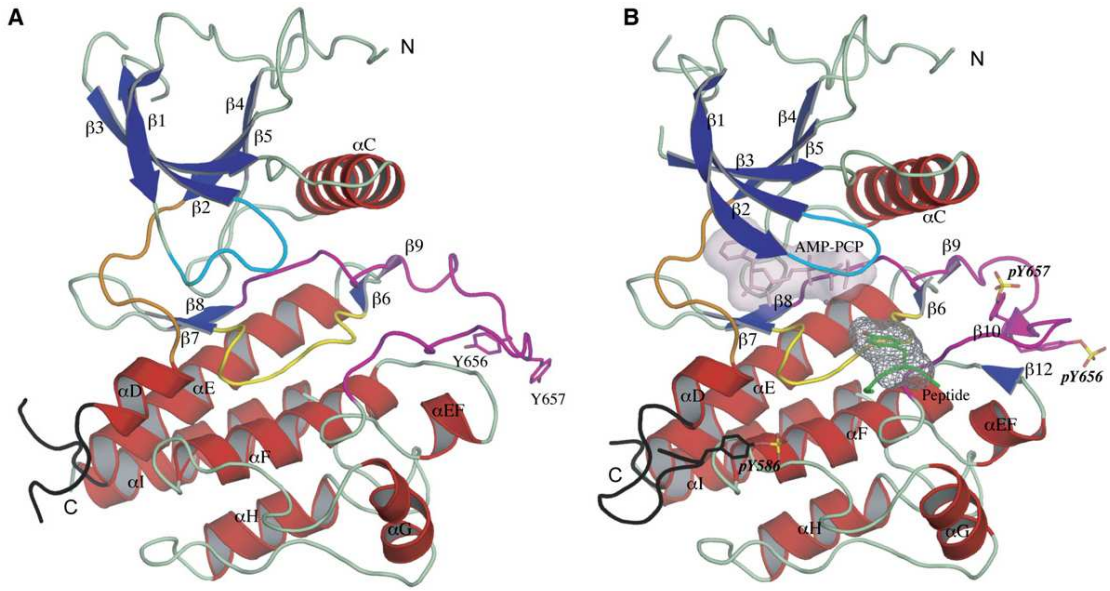

Figure 1.13: Structures of non-phosphorylated FGFR2 kinase domain and A-loop phosphorylated FGFR2 kinase domain. The α-helices are coloured red, and the β-strands are blue. The nucleotide-binding loop is shown in cyan, the catalytic loop is shown in yellow, the kinase hinge is shown in orange, and the activation A-loop is shown in magenta. In the A-loop phosphorylated structure, AMP-PCP and the substrate peptide are labelled. Taken from Chen *et al*., Mol Cell, **27**,717-30 (2007)[147].

Importantly, this group also reported seven non-phosphorylated pathogenic FGFR2 kinase domain structures (N549H: PDB code 2PWL; N549T: PDB code 2PZ5; E565G: PDB code 2PY3; E565A: PDB code 2QO8; K641R: PDB code 2PZR; K526E: PDB code 2PZP; and K659N: PDB code 2PVY). These pathogenic mutants result in constitutive kinase activation. Comparing these structures suggests the existence of an autoinhibitory mechanism regulated by a molecular brake in the kinase hinge region. These pathogenic mutants regulate the molecular brake through different mechanisms, such as directly or indirectly disengaging the molecular brake

or forcing the A-loop to adapt the active conformation, resulting in constitutive kinase activation[147].

1.2.4 Activation of FGFRs

1.2.4.1 FGF binding and FGFR activation

The activity of the FGF signalling pathway is regulated by the binding affinities of FGFs for FGFRs[91, 95]. Further, the binding specificities are determined by the alternative splicing in the ligand-binding domain of FGFRs, which results in a large combinatorial group of potential FGF-FGFR interactions.

Early *in vitro* binding assays performed by Miki *et al*. demonstrate that FGFR2IIIb isoform binds to FGF7, while FGFR2IIIc does not. Furthermore, FGFR2IIIb has a lower binding affinity for FGF2 than FGFR2IIIc[95]. Later, Chellaiah *et al*. cloned an alternatively spliced form of FGFR3 corresponding to FGFR1IIIc and FGFR2IIIc, which has a restricted ligand-binding specificity. Compared to FGFR3, FGFR2IIIc has a higher binding affinity for both FGF2 and FGF7, though the splicing pattern of FGFR3 is similar to that of FGFR2. Additionally, chimeric FGFR3 carrying the exon domain III isoform b from FGFR2IIIb exhibits high binding affinities to FGF2 and FGF7. This suggests that the Ig-like domain III, which is generated by alternative

mRNA splicing, plays an important role in regulating FGF ligand specificity[94]. In contrast, Ornitz *et al* created mitogenically responsive cell lines that express all known FGFRs. Their study demonstrated that FGF1 is the only ligand that can activate all FGF splice variants (FGFR1IIIb, FGFR1IIIc, FGFR2IIIb, FGFR2IIIc, FGFR3IIIb, FGFR3IIIc and FGFR4). Using FGF1 as an internal standard, they also measured the relative activity of FGF2, 3, 4, 5, 6, 7, 8, and 9. Xu *et al.* also determined the relative activity of FGF 8, 17 and 18 compared with FGF1 mitogenetic activity as the internal standard. Moreover, Zhang *et al*. extended Ornitz's study and determined the relative activities of FGF 10-23. These studies provide further evidence of the receptor specificity of FGFs[148-150].

1.2.4.2 Dimerisation and phosphorylation of FGFR

FGFs mediate their biological functions by binding to the Ig-like domains of FGFRs, resulting in dimerisation and phosphorylation of multiple tyrosine residues on the cytoplasmic domain of the receptors. Early studies indicate that FGF1 and FGF2 can dimerise when they bind to heparin molecules, thereby causing the dimerisation and activation of FGFR[151, 152]. This property is important in achieving the binding of growth factors to their cellular receptors and the formation of dimeric receptors[14, 153]. Unlike other dimeric growth factors, such as PDGF, FGFs are unable to induce the

activation of FGFRs without HSPGs. The binding of FGF2 to HSPGs is important for FGFR activation and the subsequent induction of biological responses. A study performed by Ornitz *et al*. indicates that FGF2 binding to its cellular receptor requires heparin, and the presence of heparin is important for the induction of mitogenesis in living cells[154]. This study also proposes that the binding of heparin to FGF can induce a conformational change in FGF, and this conformational change is involved in the dimerisation of FGFRs.

Conversely, several studies also reveal that though heparin can increase the binding affinity of FGF2 to its receptor (Ig-like domain of FGFR1), heparin is not actually required for the binding of basic FGF to its receptor[155]. An *in vitro* study performed using the FGFR2 extracellular ligand-binding domain also indicate that heparin is not required for the ligand-receptor interaction. However, the addition of heparin can cause the oligomerisation of FGF1; this oligomerisation allows FGF1 to induce the dimerisation of FGFR via the FGF1-heparin complex[152].

Oligomeric receptors also have higher kinase activities and ligand binding affinities than monomeric receptors[156]. *In vivo* and *in vitro* research carried out by Bellot *et al.* has also indicated the mechanism of ligand-induced transphosphorylation between

different FGFR molecules. NIH3T3 cells co-transfected with kinase-negative full-length FGFR2 and the truncated kinase domain of FGFR2 have the ability to phosphorylate kinase-negative full-length FGFR2 when FGF1 is added[157]. This result provides evidence that the autophosphorylation of FGFR occurs via an intermolecular mechanism. Moreover, transphosphorylation also occurs between different types of FGFRs, i.e., both homologous transphosphorylation (FGFR2 to FGFR2) and heterologous transphosphorylation (FGFR2 to FGFR1 and FGFR1 to FGFR2) occur. This study provides strong evidence that the autophosphorylation of FGFR occurs via an intermolecular transphosphorylation mechanism, and because most cell types express more than one type of FGFR, the heterologous transphosphorylation of FGFR may have a role in signal transduction[157].

1.2.4.3 The phosphorylation of the intracellular region in FGFR1 is an ordered process

The binding of FGF to its cellular receptor not only induces the activation of intrinsic protein tyrosine kinase activity and the autophosphorylation of the receptors but also induces the phosphorylation of substrate proteins[158]. PLCγ, which serves as the main target protein of several receptor tyrosine kinases, associates with the PDGFR[159], EGFR[160] and FGFR[7] signalling pathways. Several studies indicate that the

autophosphorylation of receptor tyrosine kinase can induce the phosphorylation of PLCγ, the downstream signalling molecule of ligand-induced receptor signalling pathways[158-160,7]. Tyr-766 in the C-terminus of FGFR1 has been identified as the phosphorylated residue that provides the binding site for the SH2 domain of PLCγ[161]. A study performed by Mohammadi *et al*. (1992) explored the role of Tyr-766 in FGFR signalling. The mutant FGF receptor (Y766F) is unable to interact with PLCγ and cannot induce the hydrolysis of phosphatidylinositol. Moreover, the elimination of the hydrolysis of phosphatidylinositol does not affect FGF-induced mitogenesis. However, mutant Y766F FGFR can undergo an autophosphorylation reaction, and this mutant FGFR still has the ability to phosphorylate several cellular proteins and stimulate DNA synthesis[162].

Another six autophosphorylation sites of FGFR1 have been identified: Tyr-463, Tyr-583, Tyr-585, Tyr-653, Tyr-654, and Tyr-730[139]. Both Tyr-653 and Tyr-654 are important for the activation of FGFR1 tyrosine kinase activity *in vitro* and *in vivo*. Studies of FGFR1 mutants with phenylalanine substitutions Y653F, Y654F, and Y653/654F reveal that the phosphorylation level of FGFR1 and PLCγ makes no difference to the wild type FGFR1 and Y653F mutant. However, the phosphorylation of FGFR1 and PLCγ is very weak in the Y654F mutant, and no phosphorylated PLCγ

is detected in Y653/654F. Moreover, because Tyr-653 and Tyr-654 are conserved in all four FGF receptor types, the homologous regions appear to be important for receptor activation.

Mohammadi *et al*. also show that the autophosphorylation of tyrosine residues on FGFR1 is an ordered event: tyrosine 653 is autophosphorylated prior to tyrosine 654, and tyrosine 583 is autophosphorylated prior to tyrosine 585[139]. Recently, Furdui *et al*. also indicated that tyrosine phosphorylation occurs in a sequential and ordered manner on FGFR1. The detailed phosphorylation order of the FGFR1 cytoplasmic domain has been identified as follows: 1) Y653 in the activation loop, 2) Y583 in the kinase insert domain, 3) Y463 in the juxtamembrane domain, 4) Y585 in the kinase insert domain, and 5) Y654 in the activation domain[163]. This precise sequential reaction suggests that correct signalling may result from the observed phosphorylation pattern. They also demonstrate that the rate of substrate catalysis increases greatly after the phosphorylation of Y653 (50 times) and Y654 (500 times). These data suggest that phosphorylation at different time points may activate different signalling pathways.

1.2.5 The formation of ESCs of FGFR

The docking protein FRS2 constitutively interacts with FGFR1 through the binding of the FRS2 PTB domain to the juxtamembrane region[25]. Recruitment of FRS2 to activated FGFR2 also results in the phosphorylation of FRS2, which forms a complex with Grb2-Sos upon FGF stimulation, therefore connecting to the MAPK signalling cascade[164, 165]. It has been shown that four Grb2 molecules bind to one tyrosine-phosphorylated FRS2 directly via the Grb2 SH2 domain. The Grb2 C-SH3 domain can also mediate the recruitment of Gab 1 to FRS2, followed by the recruitment of PI3-kinase and the activation of the Akt pathway[165-167].

Tyrosine-phosphorylated FRS2 also provides binding sites for the phosphatase SHP2. SHP2 also binds to phosphorylated FRS2 via the SHP2 N-SH2 domain[168, 169]. The binding of SHP2 to the FGFR-FRS2 complex leads to the tyrosine phosphorylation of SHP2 and the recruitment of Grb2 to the FGFR-FRS2-SHP2 complex through the interaction between Grb2 and phosphorylated SHP2[164, 170, 171]. Upon FGF stimulation, PLCγ interacts with activated FGFR at Tyr-766 via its SH2 domain, therefore activating the PLCγ pathway[162, 172].

Previous studies performed by our group also indicate the indirect recruitment of Shc to FGFR[104] and the direct interaction of Grb2 and FGFR2[173]. These results provide new insight into the regulation of the FGFR signalling pathway (Figure 1.14).

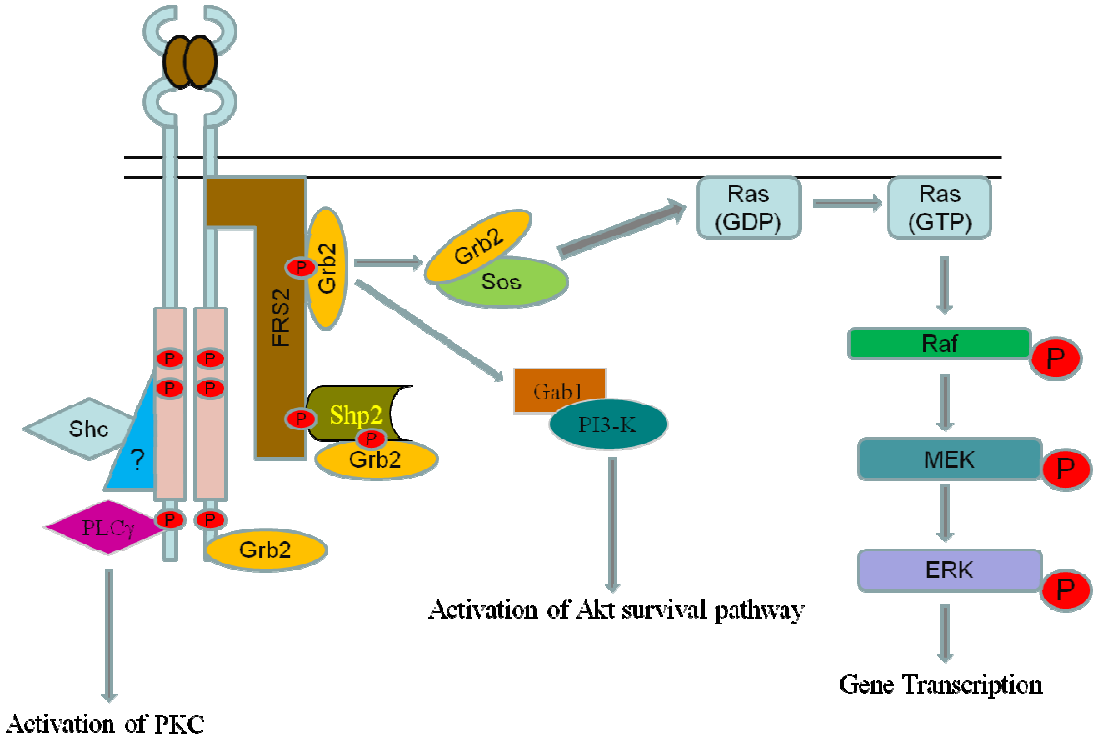

Figure 1.14: Signal transduction from FGFR via the formation of multi-protein complexes. Formation of a multi-protein complex via multivalent interactions with various signalling proteins leads to the activation of additional receptor activation-specific pathways[174].

1.3 The Signalling Adaptor Protein Grb2

1.3.1 General introduction to Grb2

The phosphorylation and activation of RTKs results in the recruitment of cellular signalling proteins that contain SH2 domains, which can recognise and bind to the phosphotyrosine residues of activated receptors[175]. Some of these proteins, such as PLCγ, SHP2 and PI3K, have enzymatic activities that can catalyse different reactions to maintain normal cell functions. However, other proteins such as Grb2 (growth factor receptor-bound protein) do not have any enzymatic activities. These proteins serve as adaptor proteins to link the activated RTKs to their downstream targets.

Grb2 was first isolated and cloned in 1992[54]; it contains an SH2 domain flanked by two SH3 domains. Mammalian Grb2 and its homologues have been isolated and identified, such as Sem-5 from *Caenorhabditis elegans*[176] and Ash from rats[177]. Of the Grb2 amino acid sequence, 63% is similar to the *C. elegans* protein Sem-5, which is an important protein in vulval development and myoblast migration[176].

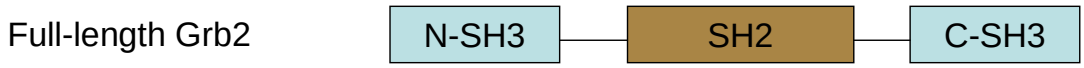

Figure 1.15: Diagram of Grb2 domains. Grb2 has an SH2 domain flanked by two SH3 domains.

A spliced isoform of Grb2 named Grb3-3 has a deletion of the SH2 domain from residues 60 to 100. Grb3-3 retains SH3 domain functions but does not bind to phosphotyrosine-containing proteins. Therefore, Grb3-3 is thought to be a suppressor of Grb2 function and has been implicated in apoptosis[178, 179].

1.3.2 The role of Grb2 in RTK signalling

1.3.2.1 Grb2 function

Grb2 plays an important role in several RTK signalling pathways by interacting with other signalling receptors, enzymes or adaptor proteins via its SH2 or SH3 domains. For example, non-phosphorylated Grb2 interacts with PDGFR by recognising phosphotyrosine residues through its SH2 domain[54, 180, 181]. The SH2 domain of Grb2 recognises and binds to the pYXNX motif with a preference for residues Q, V, and Y at the P+1 position and F, Q, and Y at the P+3 position[56] .

Microinjection studies performed by Lowenstein *et al*. indicate that injection of Grb2 or H-Ras alone into quiescent rat embryo fibroblast cells has no effect on mitogenesis, while injecting both together stimulates DNA synthesis. This suggests that Grb2 has a positive effect on the Ras-mediated cell signalling pathway, and both the SH2 and SH3 domains are important for stimulating DNA synthesis[54]. Subsequent

microinjection experiments using an anti-Ash/Grb2 antibody revealed that the antibody can abrogate the cellular effects of EGF and PDGF, resulting in the inhibition of DNA synthesis and causing a reversion in Rac-regulated actin fibre assembly to the unstimulated level. These results led to a proposed role for Ash/Grb2 in controlling RTK signalling transduction to Ras and Rac as a linker joining RTK activation to downstream signalling[16, 180, 182-184].

1.3.2.2 The Grb2-Sos interaction is SH3 domain-dependent

Sos, the guanine nucleotide exchange factor of Ras to activated receptors, constitutively associates with Grb2 in mammalian cells[185-187]. Two different Sos proteins, Sos1 and Sos2, are found in mammalian cells. Sos1 and Sos2 share 65% similarity in their amino acid sequences, but their C-terminal regions are quite different, with the conserved region restricted only to the short proline-rich motif [185, 188]. Both *in vitro* and *in vivo* studies performed by Yang *et al*. indicate that hSos1 and hSos2 have different binding affinities to Grb2, and the higher affinity of hSos2 for Grb2 may be due to the existence of an extra SH3 binding motif and the relative positions of the binding domains within the C-terminal domain of hSos2. Therefore, hSos1 and hSos2 are proposed to have different roles in receptor-mediated Ras-activation based on their interactions with Grb2. Moreover, this study also

demonstrates that both the N-SH3 and C-SH3 domains are involved in Grb2-Sos complex formation[189].

NMR structures reported by Goudreau *et al*. show that the Grb2 N-SH3 domain is highly similar to other human SH3 domain-containing proteins, such as Spectrin[76, 190]. The SH3 domains of these proteins have a compact β-barrel structure consisting of five to six antiparallel β-strands and a C-terminal α-helix. Further experiments have investigated the SH3 domain-mediated Grb2-Sos interaction at the molecular level. Studies have also revealed the NMR structure of the Grb2 N-SH3 domain with the proline-rich peptide derived from the hSos C-terminal proline-rich region. The SH3 domain sequences form an exposed hydrophobic patch on the surface of the protein, and the peptide binds to the hydrophobic patch at the conserved aromatic residues[191-194].

1.3.2.3 The Grb2-Shc interaction is SH2 domain-dependent

Another important cellular signalling protein involved in the receptor-Grb2 interaction is Shc, which has a domain architecture consisting of a PTB domain, a collagen homology 1 (CH1) domain and an SH2 domain. The ShcA family has three isoforms: p46, p52 and p66. All three isoforms are known to serve as signalling

adaptors that can form complexes with activated EGFRs and therefore control their downstream signalling pathways, which regulates the proliferation of mammalian cells[195]. p52 and p46 Shc isoforms activate the Ras and MAP kinase pathway, while p66 participates in the regulation of the cellular response to oxidative stress and lifespan[196].

The Shc protein associates with activated EGFR on the cellular membrane following EGF stimulation[197]. An early study indicates that the Shc p46 and p52 isoforms are tyrosine phosphorylated in Rat-2 v-Src cells, and a Grb2-Shc complex can be immunoprecipitated in these cells. Additionally, phosphorylated Shc recruits and forms a stable complex with Grb2-Sos through the Grb2 SH2 domain in response to growth factor stimulation[181, 198-200]. Moreover, a short YV/IN motif has been identified on Shc as the binding site for the Grb2 SH2 domain[181].

1.3.2.4 The Grb2-Sos complex in RTK signalling

The Grb2-Sos complex binds to activated growth factor receptors directly or indirectly via other proteins such as Shc adaptor protein, Syp or SHP2[54, 198, 201].

A study performed by Buday *et al*. indicates that the Grb2/Sos complex associates with activated EGFR through Grb2 upon EGF stimulation in Rat-1 fibroblast cells. The formation of the EGFR-Grb2-Sos complex also alters the subcellular localisation of Sos to the membrane. Furthermore, an earlier study demonstrates that the rate of GTP binding to Ras is increased when Rat-1 cells are stimulated with EGF. Therefore, the formation of activated EGFR-Grb2-Sos complexes in Rat-1 cells is believed to play a key role in Ras activation[202]. EGF-induced Ras and MAPK activation are also enhanced when Grb2 is overexpressed[203]. Further studies have identified the interaction between Grb2 and Sos; both *in vivo* and *in vitro* experiments performed by Chardin *et al*. reveal that downstream Ras signalling is mediated by Grb2 coupling the activated RTKs and the C-terminal region of Sos through its SH3 domain[185].

In contrast, insulin-stimulated ERK activation is mediated by the Grb2-Sos complex recruiting tyrosine phosphorylated Shc and IRS-1 via the Grb2 SH2 domain. However, there is no evidence of Grb2 phosphorylation by the activated insulin receptor[181, 204]. Several studies also suggest that the interaction of the Grb2-Sos complex with phosphorylated Shc *in vitro* can initiate GTP binding to Ras[198], suggesting a mechanism by which the Grb2-Sos complex may regulate Ras activation[198, 205]. Moreover, Shc is also tyrosine-phosphorylated upon PDGF stimulation, and

tyrosine-phosphorylated Shc mediates the interaction between the Grb2-Sos complex and the activated PDGFR. The membrane-associated PDGFR-Shc-Grb2-Sos complex is important for proliferation in response to PDGF stimulation[206].

1.3.3 Grb2 structure

The crystal structure of dimeric Grb2 was solved in 1995 (Figure 1.16). Both the SH2 and SH3 domains of Grb2 have classic structures. The SH2 domain is composed of a central antiparallel β-sheet flanked by two α-helices, while both the N-SH3 and C-SH3 domains contain five antiparallel β-sheets[207].

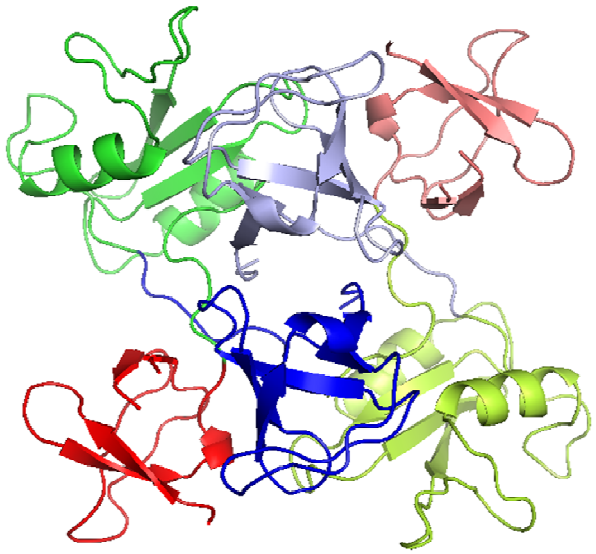

Figure 1.16: Dimeric Grb2 structure. Two Grb2 molecules are shown. The N-SH3, SH2 and C-SH3 domains of Grb2 molecule A are shown in red, green and blue, respectively. The N-SH3, SH2 and C-SH3 domains of Grb2 molecule B are shown in pink, light green and purple, respectively. Adapted from Maignan *et al*., Science, **268**, 291-3 (1995). PDB code: 1GRI[207].

The SH3 domains are not in contact with the SH2 domain (Figure 1.17). The two SH3 domains interact with each other via Van der Waals forces with five H-bonds within 1000 $Å^2$, which is weaker than typical protein-protein interactions. This unusually weak interaction suggests that the two SH3 domains of a Grb2 monomer can adopt different orientations, making Grb2 a flexible adaptor. A further NMR solution structure study of Grb2 performed by Yuzawa *et al*. also indicates that the Grb2 SH2 domain is connected to the C-SH3 domain through a flexible linker, and at least 20 different structures can be seen in solution. Moreover, the flexibility of Grb2 may be important for target recognition and binding[208].

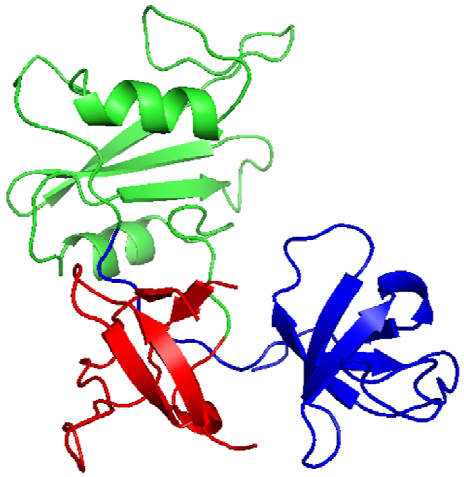

Figure 1.17: Grb2 monomer structure. The N-SH3, SH2 and C-SH3 domains of the Grb2 monomer are shown in red, green and blue, respectively. The structure shows that all three binding sites of Grb2 are fully accessible. Adapted from Maignan *et al.*, Science, **268**, 291-3 (1995). PDB code: 1GRI[207].

1.4 Protein Tyrosine Phosphatases (PTPs) and Signalling

1.4.1 PTP, Protein tyrosine phosphatase

1.4.1.1 Protein phosphatases

In contrast to kinases, protein phosphatases function to dephosphorylate proteins. The coordinated action of the tyrosine phosphorylation and dephosphorylation processes of certain proteins in cells is the key to the regulation of cell signalling[209].

Protein phosphatases can be grouped into three main classes according to their sequences, structures and catalytic functions: 1) the phosphoprotein phosphatase (PPP) family (PP1, PP2A, PP2B, PP4, PP5, PP6, PP7, (2) the PTP super-family, and 3) the aspartate-based protein phosphatases[210].

1.4.1.2 PTP families

The human genome encodes 107 PTPs that can be divided into four families according to the amino acid sequences of the catalytic domains: class I Cys-based PTPs (99 proteins), class II Cys-based PTPs (one protein), class III Cys-based PTPs (three proteins), and Asp-based PTPs (four proteins)[211].

Among class I PTPs, 38 are considered “classical PTPs” and can be classified into two different groups: classical receptor PTPs (RPTPs, 21 proteins), which are transmembrane, receptor-like PTPs; and classical non-receptor PTPs (NRPTPs, 17 proteins)[211, 212].

Receptor-like PTPs are transmembrane receptors that contain PTPase domains. All RPTPs have an extracellular domain followed by a transmembrane region and a C-terminal catalytic cytoplasmic domain. Some receptor-like PTPs contain the fibronectin type III (FN-III) repeat region, immunoglobulin-like domains, MAM domains or carbonic anhydrase (CA)-like domains in their extracellular regions. The cytoplasmic region generally contains two copies of the PTPase domain, though the second domain is usually inactive. All subclasses of RPTPs are expressed only in the nervous system, except for type I RPTPs. Although RPTPs are thought to be ligand receptors, their ligands are still largely unknown[213].

Non-receptor PTPs (intracellular PTPs) lack transmembrane regions and are targeted via their N- and/or C-terminal regulatory sequences to multiple intracellular locations. They can be divided into two groups according to their substrate specificities. The first group is phosphotyrosine-specific phosphatases, including PTP1B, STEP,

PTP-SL, and SH2 domain-containing phosphatases (SHP1 and SHP2). The second group contains phosphatases that can dephosphorylate both phosphotyrosines and phosphoserines/threonines, known as dual specificity phosphatases.

1.4.2 Signalling by SHP2

SHP2 is required for ERK/MAP kinase pathway activation in most RTK signalling pathways. However, the mechanism by which SHP2 mediates Ras/ERK activation is not completely understood.

1.4.2.1 SHP2 as an adaptor protein

Studies reveal that SHP2 can directly interact with activated EGFR and PDGFR or indirectly through binding to other tyrosine-phosphorylated adaptor proteins, such as FRS2 and Gab1, through SHP2 SH2 domains[170, 214-216]. Tyr 1009 of activated PDGFR is the binding site for SHP2, and both *in vivo* and *in vitro* binding studies carried out by Kazlauskas *et al.* demonstrate that the N-terminal SH2 domain directly binds to the activated growth factor receptor. Moreover, the research by Kazlauskas *et al.* also indicates that SHP2 is serine/threonine-phosphorylated and has trace tyrosine phosphorylation in A431 cells in the unstimulated state[217]. The presence of EGF significantly increases the tyrosine phosphorylation level of SHP2[215]. Several studies

propose that SHP2 functions as an adaptor protein. Stimulation by EGF or PDGF leads to SHP2 phosphorylation at Tyr 542 and Tyr 580, which can provide binding sites for the Grb2 SH2 domain, therefore recruiting the Grb2/Sos complex to the cell membrane and activating the Ras pathway[201, 218, 201, 219]. However, early studies reveal that tyrosine phosphorylation of SHP2 has no effect on EGF and PDGF signalling in 293 cells or on FGF-induced ERK activation in *Xenopus* embryos[220, 221]. Surprisingly, Hadari *et al*[170]. indicate that SHP2 binds to tyrosine-phosphorylated FRS2 via the SHP2 N-SH2 domain in the FGF signalling pathway; this interaction leads to tyrosine phosphorylation of SHP2 and Grb2-SHP2 complex formation. The binding of tyrosine phosphorylated-SHP2 to tyrosine phosphorylated-FRS2 is necessary in FGF-induced MAP kinase activation and cell differentiation in PC12 cells. This result suggests that tyrosine phosphorylation of SHP2 may play a role in growth factor-induced MAP kinase activation. Tyrosine phosphorylation of SHP2 is required for FGF and PDGF-induced ERK activation but not for EGF signalling in fibroblasts. Additional data also show that Tyr 542 is the major Grb2 SH2 domain binding site in tyrosine-phosphorylated SHP2, though Grb2 binding to tyrosine phosphorylated-SHP2 is not necessary in SHP2-mediated Ras/ERK activation. It is proposed that tyrosine phosphorylation of SHP2 may be important in certain kinds of growth factor-induced Ras/ERK activation. However, it is also suggested that SHP2

may be important in regulating the MAP kinase pathway through PTP activity but not in acting as an adaptor protein for the Grb2/Sos complex[222].

1.4.2.2 SHP2-IRS1 interaction, SHP2 activation and signalling by SHP2

Studies on the insulin receptor reveal that SHP2 does not bind to the tyrosine phosphorylated form of the receptor and is not tyrosine phosphorylated as part of the insulin response of 3T3-L1 adipocytes. Instead, upon insulin treatment, SHP2 associates with the phosphotyrosine-containing sequence of IRS 1 (insulin stimulation results in at least 12 potential tyrosine phosphorylation sites in IRS1) on the YIDL motif via the SH2 domain of SHP2 in both *in vitro* and *in vivo* experiments[214, 215, 223]. These results suggest a model of insulin receptor-IRS1-SHP2 signalling complex formation[214]. To understand the role of IRS-1 in SHP2 activation, Sugimoto *et al*. performed *in vitro* binding experiments and SHP2 activity studies. Their surface plasmon resonance data suggest that the SH2 domains of SHP2 have different binding affinities towards IRS-1 phosphopeptides (N-SH2 prefers pY1172, whereas C-SH2 prefers pY1222). In contrast, PTPase assay results also demonstrate that both pY1172 and pY1222 have the ability to increase SHP2 activity, and pY1222 has a significant dose-dependence when compared with pY1172. This study proposes an allosteric activation mechanism in which SHP2 binds two individual

phosphotyrosine-containing motifs to its N-SH2 and C-SH2 domains, resulting in activation of the phosphatase domain and dephosphorylation of the third phosphotyrosine-containing motif[224]. SHP2 is also proposed to be a positive factor in growth factor-stimulated cell proliferation[225]. Noguchi *et al*. further identified that catalytically inactivated SHP2 (C459S) specifically inhibits insulin-stimulated Ras/MAP kinase activity in CHO cells, while insulin-stimulated PI3-kinase activity is not affected by catalytically inactive SHP2. Moreover, tyrosine phosphorylated-Shc binds to Grb2 and forms a complex with Grb2 and Sos. Grb2 also binds to IRS-1, linking IRS-1 to Sos and therefore leading to Ras activation in response to insulin stimulation[181, 200, 204]. However, catalytically inactivated SHP2 has no effect on the formation of Grb2-IRS-1 and Grb2-Shc complexes, suggesting that SHP2 regulates an upstream signalling protein that is necessary for insulin-induced Ras activation. Although it is indicated that the binding of SHP2 to IRS-1 plays a part in regulating Ras activation by controlling an unknown upstream element of the Grb2 and Shc pathways, the precise mechanism by which this occurs remains unclear[226].

An *in vivo* study reveals that the expression of the catalytically inactive mutant of SHP2 (C459S) has no effect on insulin receptor phosphorylation, Shc phosphorylation or IRS-1 phosphorylation but it does decrease insulin-induced MAPK activation and

reduces insulin-stimulated mitogenesis by suppressing DNA synthesis. Moreover, a 120-kDa phosphoprotein that is suggested to be a potential insulin-induced MAPK activation regulator interacts with the SH2 domain of SHP2 upon insulin stimulation[227].

1.4.2.3 SHP2-Gab1 interaction, SHP2 activation and signalling by SHP2

Deb *et al*. demonstrate that SHP2 activity is required for EGFR-induced MAPK activation in COS-7 cells overexpressing SHP2. Moreover, their results reveal that SHP2 has no effect on the Grb2-Shc, Shc-EGFR or Grb2-EGFR interactions, which also supports the idea that SHP2 regulates Ras/MAPK activation by controlling an upstream element of the Grb2 and Shc pathways[228].

SHP2-Gab1 interaction is important in epidermal proliferation. Studies focused on EGFR signalling pathways indicate that Gab1 Y627F and SHP2 C459S inhibit epidermal proliferation and enhance differentiation. Gab1, a member of a docking protein family that can bind to activated receptors and be tyrosine phosphorylated, recruits signalling proteins and plays a role in activating MAPK and PI3-kinase[229-234]. Gab1 is also the major binding protein for SHP2 in EGF-stimulated cells[235]. Cunnick *et al*. characterised the Gab1-SHP2 interaction to study the mechanism by which

SHP2 activation mediates MAPK activation. Western blotting results suggest that the N-SH2 and C-SH2 domains of SHP2 bind to pY627 and pY659 of Gab1, respectively, upon EGF stimulation, and binding both pY627 and pY659 is essential for SHP2 PTPase activation. Gab1 mutants deficient in SHP2-binding have negative effects on Ras/ERK2 activation. Therefore, one possible mechanism is that activated SHP2 mediates ERK2 activation via the binding of SHP2 to Gab1[236, 237]. Another study provides a more detailed mechanism for SHP2-mediated ERK activation, revealing that Gab1 PH domain and SHP2 binding residues (Y627 and Y659) are important for the Gab1-SHP2 interaction and are necessary for c-Src, Ras, MEK1 and ERK2 activation. Therefore, Gab1 may serve as a carrier to target SHP2 to the membrane to activate a signalling step upstream of Src and Ras[238].

A possible molecular mechanism proposed by Yehenew *et al*. explains the positive role of SHP2 in growth factor-stimulated pathways. PTPase activity is necessary for EGF-induced Ras-ERK1/2 activation. SHP2 inhibits the translocation of Ras-GAP to the plasma membrane, and therefore, Ras-GAP cannot inactive Ras[239].

1.4.3 SHP2 domain composition and structure

1.4.3.1 SHP2 domain composition

Two vertebrate SH2 domain-containing PTPs, SHP1 and SHP2, have been identified as the subfamily of NRPTPs. SHPs have two N-terminal SH2 domains (N-SH2 and C-SH2), a PTP domain and a C-terminal hydrophilic tail. The 240- to 250-amino acid PTP domain has a signature PTP motif ([I/V]HCxAGxxR[S/T]G, where the nucleophilic cysteine is essential for enzyme activity), is specific for hydrolysing phosphotyrosine, and is flanked by regulatory sequences. The C-terminal tail contains two tyrosine phosphorylation sites that can be variously phosphorylated by different protein tyrosine kinases. SHP2 also has proline-rich domains, and it is suggested that these act as binding sites for other SH3 domain-containing proteins.

1.4.3.2 SHP2 structure and regulation

The SHP2 crystal structure has been solved at 2.0-Å resolution (residues 1-527, C-terminally truncated). Both the N-SH2 and C-SH2 domains have the conserved SH2 fold, a large four-stranded-β-sheet flanked by two α-helices. The PTP domain has nine α-helices and 14 β-strands, and the signature PTP motif was found in βM and αG connected by loop MG. The signature motif and the other residues required for catalysis form a catalytic cleft at the phosphotyrosine binding pocket (Fig 1.18).

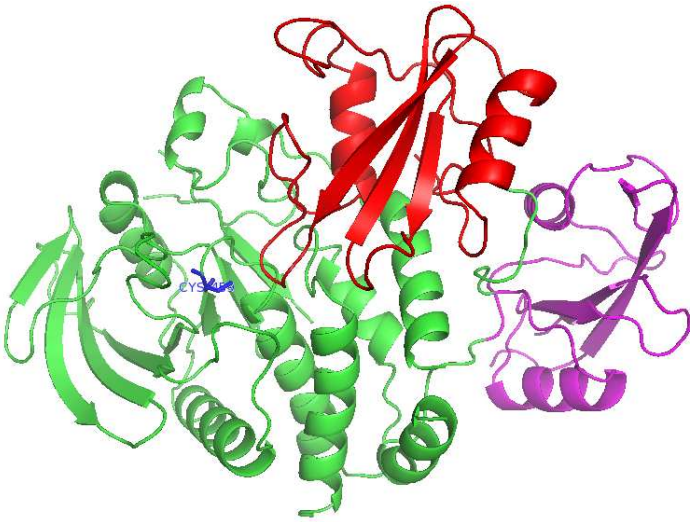

Figure 1.18: Structure of SHP2 (residues 1-527). The N-SH2 domain is shown in red, and the C-SH2 domain is shown in purple. The catalytic PTP is shown in green. Cys-459 is coloured blue. Adapted from Hof *et al*., Cell, **92**, 441-50 (1998). PDB code: 2SHP[240].

It remains unclear why phosphotyrosine-containing proteins preferentially bind to the N-SH2 or C-SH2 domain of SHP2 (also SHP1). A study performed by Beebe *et al*. using a phosphotyrosine peptide library screen indicates that the N-SH2 domain of SHP1 selects for peptides with a leucine at the P-2 position; it recognises and binds to phosphopeptides with consensus sequences of LXpY(M/F)X(F/M) and LXpYAXL (X represents any amino acid). However, the C-SH2 domain almost exclusively selects phosphopeptides with (V/I/L)XpYAX(L/V) sequences, which are present in immuno-receptor tyrosine-based inhibitory motifs (ITIMs)[241, 242].

The SHP2 crystal structure also suggests an autoinhibition mechanism. In the absence of its phosphotyrosine target, the N-SH2 domain inserted into the catalytic cleft of the

PTP domain results in mutual allosteric inhibition and blocking of the catalytic site, converting the SHP2 into the inactive form.

However, the phosphatase activity can be markedly increased using a phosphotyrosine peptide to compete with the N-SH2 domain for binding to the PTP domain. Moreover, using a peptide containing two phosphotyrosines that occupy both N-SH2 and C-SH2 domains can increase the phosphatase activity significantly more than the signal phosphotyrosine peptide does to the N-SH2 domain[243].

The C-terminal tail also plays an important role in the regulation of SHP1/SHP2 function. An *in vitro* assay performed by Pei *et al*. demonstrates that the last 35 amino acids of SHP1 are important for phosphatase activity; the C-terminally truncated version has enhanced phosphatase activity[244]. Lu *et al*. suggest an intramolecular mechanism of regulation of SHP2; phospho-Tyr 542 and phospho-Tyr 580 can interact with the N-SH2 domain and C-SH2 domain, respectively, thereby inhibiting PTP activity[245]. Poole *et al*. also conclude that there are three possible mechanisms by which the C-terminal tail participated in SHP2 activity regulation: 1) Tyrosine phosphorylation of the C-terminal tail, as phosphorylated Tyr 542 and Tyr 580 at the SHP2 C-terminal tail have been suggested to function as the binding sites for the Grb2

SH2 domain, therefore connecting SHP2 to the MAP kinase pathway. However, the role of tyrosine phosphorylation of SHP2 in regulating signalling remains unclear. Tyrosine mutants of SHP2 have no effect on FGF signalling in *Xenopus*[221]. 2) Serine and threonine phosphorylation of SHP2 by PKC and MAP kinase has been reported in response to EGF stimulation both *in vitro* and in PC12 cells[246, 247]. Serine phosphorylation sites are located at Ser 576 and Ser 591, within the SHP2 C-terminal tail. The effect of serine and threonine phosphorylation on the activity of SHP2 activity is not clear. Zhao's result shows that serine phosphorylation has no effect on SHP2 activity[246], whereas Peraldi's data indicate that threonine phosphorylation may decrease SHP2 activity[247]. 3) The proline-rich motif may recruit SH3 domains. Only SHP2 (but not SHP1) has a proline-rich region. However, there is no direct evidence that this proline-rich motif interacts with any SH3 domains. Additionally, a study of FGF signalling in *Xenopus* reveals that the C-terminal tail of SHP2 has no effect on phosphatase activity[221, 248].

1.5 Objectives

1.5.1 The importance of precise protein recruitment in signalling pathways

Cell signalling is initiated by external signals that are transduced into cells via membrane-bound receptors. To preserve the integrity of a signal transduction pathway without any corruption from other pathways, a critical step is the protein-protein interactions that mediate the formation of specific signalling complexes for each signalling pathway at the plasma membrane. The signalling complex is an assembly of multi-molecular protein complexes formed by sequential binding through domain-specific interactions. Schuller has shown the receptor type-specific recruitment of signalling complex formation in TrkA, EGFR and FGFR. Her study indicates that the differential recruitment of FRS2, Sos, Grb2 and Shc in these three different signalling pathways is an important mechanism of determining signalling specificity[249].

One of the questions regarding the FGFR2 signalling pathway that remains unclear is the molecular mechanism of the protein-protein interactions in the FGFR2 signalling complex. This study focuses on the roles of Grb2 in FGFR2 activation and in FGFR2-mediated formation of the early signalling complex.

1.5.2 Investigation of the regulation of Grb2 in FGFR2 signalling activation

Grb2 mediates EGFR signalling by directly interacting with activated EGFR through the Grb2 SH2 domain. However, a study by our group revealed that the interaction between Grb2 and FGFR2 is SH3 domain-dependent, and the Grb2-FGFR2 interaction is important in regulating SHP2 function[173]. Past studies of the biological function of Grb2 focused on the downstream responses of RTK signalling pathways. Grb2 is best known for its ability to link activated RTKs, such as EGFR or PDGFR, to the activation of Ras and its downstream signalling cascades such as the ERK1/2 pathway[16, 180, 182-184, 202, 203, 206]. The first part of this study focuses on investigating the role of Grb2 in FGFR2 activation/phosphorylation in early signalling events.

1.5.3 Investigation of the regulation of Grb2 recruitment to FGFR2

Biophysical studies have investigated the direct binding of the Grb2 SH3 domain to FGFR2 using FGFR2 sequence-derived peptides[173], but the molecular mechanism of the Grb2-FGFR2 interaction has not yet been elucidated. Therefore, the second part of the current study focuses on the molecular mechanism of FGFR2-mediated formation of the early signalling complex and the regulation of this process by Grb2. Because little is currently known about Grb2 phosphorylation and its role in the FGFR2

signalling pathway, this study also examines the ability of FGFR2 to induce tyrosine phosphorylation of Grb2 and the role of Grb2 tyrosine mutants in FGFR2 activation and downstream signalling.

Chapter 2

Materials and Methods

2.1 Materials

2.1.1Chemicals

All chemicals used in this study were purchased from Sigma, Merck, Melford or Fisher unless otherwise stated.

2.1.2 Enzymes and growth factor

Enzymes and growth factor	Supplier
Vent DNA polymerase	NEB
T4 DNA polymerase	NEB
Calf intestinal phosphatase (CIP)	NEB
Restriction endonucleases	NEB or Promega
T4 DNA ligase	NEB
RNase	Invitrogen
Thrombin protease	Sigma
Recombinant human FGF9	R&D systems

2.1.3 Kits and other materials

Kits and other materials	Supplier
Talon superflow resin	Clontech
Glutathiones agarose	Clontech or Sigma
DEAE sepharose	GE
Superdex 75	GE
Superdex 200	GE
Protein A agarose	Sigma
Protein G agarose	Sigma
Protease inhibitor cocktail set III	EMD
Lipofectamine 2000 transfection reagent	Invitrogen
Genejuice transfection reagent	EMD
Immobilon-P PVDF membrane	Millipore

QIAprep spin miniprep kit	Qiagen
QIAquick gel extraction kit	Qiagen
Enhanced chemiluminescence substrate	Thermo Scientific
X-ray film	Kodak

2.1.4 Bacterial cell culture reagents

2.1.4.1 Bacterial growth media

Luria-Bertani (LB) broth was used as the growth medium for *E. coli* culture.

Luria-Bertani (LB) broth

1.0% (w/v) tryptone
0.5% (w/v) yeast extract
0.5% (w/v) sodium chloride
The medium was autoclaved and appropriate antibiotics were used for selection.

Antibiotic working concentrations

Ampicillin: 50 µg/ml (prerpared in H_2O, following by 0.22 µm filtration)

Carbenicillin : 250 µg/ml (prerpared in H_2O, following by 0.22 µm filtration)

Kanamycin: 50 µg/ml (prerpared in H_2O, following by 0.22 µm filtration)

Chlormphenicol: 50 µg/ml (prerpared in 100% ethanol)

LB-Agar plates

1.0% (w/v) agar powder was added to LB broth following by autoclaving. Plates containing appropriate antibiotic were prepared after the LB-agar was cooled to 50 ^{o}C.

2.1.4.2 E. coli glycerol stocks

Glycerol stocks were prepared by mixing 400 µl 50% autoclaved glycerol and 600 µl *E. coli* overnight culture. Stocks were stored at -80 ^{o}C.

2.1.5 Insect cell culture reagents

Insect-Xpress Protein–Free Medium and Dulbecco's PBS were purchased from Lonza. Fetal bovine serum was supplied by Biosera. Gentamycin sulphate and Pen/Strep Fungizone Mixture were purchased from Cambrex. Trypan blue solution was purchased from Novagen.

2.1.6 Mammalian cell culture reagents

HEK 293 complete growth medium

Dulbecco's modified Eagle's Medium (DMEM) and Dulbecco's PBS were purchased from Lonza. Fetal bovine serum was supplied by Biosera. Gentamycin sulphate and Pen/Strep Fungizone Mixture were purchased from Cambrex.

Starvation medium

DMEM medium without fetal bovine serum for HEK 293 cells.

2.1.7 Cell lines and Bacterial strains

Cell lines and bacterial strains	Use
HEK 293	For transfection and protein production
HEK 293 stable expressing WT-FGFR2	For transfection and protein production
Sf9	For infection, virus production and protein production
DH5α	For plasmid DNA production and protein expression
BL21 (DE3)	For protein expression
Rosetta 2	For protein expression

2.1.8 Antibodies

Antibody	Epitope	Host species	Supplier
Bek antibody (C-8)	C-terminus	Mouse	Santa Cruz
Bek antibody (C-17)	C-terminus	Rabbit	Santa Cruz
Grb2 antibody (F-3)	1-68	Mouse	Santa Cruz
Grb2 antibody (C-7)	54-164	Mouse	Santa Cruz
Grb2 antibody (C-23)	C-terminus	Rabbit	Santa Cruz
p-Tyr antibody	N/A	Mouse	Santa Cruz
p44/42 MAPK (ERK1/2) antibody	C-terminus of rat p44 MAP kinase	Mouse	Cell Signaling
p44/42 MAPK (ERK1/2) antibody	C-terminus of rat p44 MAP kinase	Rabbit	Cell Signaling
Phospho- p44/42 MAPK (ERK1/2) antibody	Synthetic phosphopeptide corresponding to residues surrounding Thr202/Tyr204 of human p44 MAP kinase	Mouse	Cell Signaling
Phospho- p44/42 MAPK (ERK1/2) antibody	Synthetic phosphopeptide corresponding to residues surrounding Thr202/Tyr204 of human p44 MAP kinase	Rabbit	Cell Signaling
GST antibody	immunising animals with a GST fusion protein	Rabbit	Cell Signaling
Anti-mouse secondary antibody, HRP conjugated	N/A	Horse	Cell Signaling
Anti-rabbit secondary antibody, HRP conjugated	N/A	Goat	Cell Signaling

2.1.9 Plasmids

Plasmid	Characteristics	Source
pcDNA6 Myc/His B	Mammalian expression vector with a Myc tag and a His tag	Invitrogen
pcDNA-MBP	Mammalian expression vector with a MBP tag	This study
pcDNA-Myc-MBP	Mammalian expression vector with a Myc tag and a MBP tag	This study
pcDNA-Myc-Strep	Mammalian expression vector with a Myc tag and a Strep tag	This study
pcDNA-Myc-MBP-WT-FGFR2	Mammalian expression vector that expresses C-terminal Myc-MBP-tagged wild-type full-length FGFR2	This study
pcDNA-Myc-Strep-WT-FGFR2	Mammalian expression vector that expresses C-terminal Myc-Strep-tagged wild-type full-length FGFR2	This study
pcDNA-Myc-MBP-WT-CYTO	Mammalian expression vector that expresses C-terminal Myc-MBP-tagged FGFR2 cytoplasmic domain	This study
pcDNA-Myc-Strep-WT-CYTO	Mammalian expression vector that expresses C-terminal Myc-Strep-tagged FGFR2 cytoplasmic domain	This study
pBAC4x1	Insect cell expression vector	Novagen
pBAC4x1- WT-FGFR2-MBP	Insect cell expression vector that expresses C-terminal MBP-tagged wild-type full-length FGFR2	This study
pBAC4x1- WT-CYTO-MBP	Insect cell expression vector that expresses C-terminal MBP-tagged FGFR2 cytoplasmic	This study

	domain	
pBAC4x1- WT-EX-MBP	Insect cell expression vector that expresses C-terminal MBP-tagged FGFR2 extracellular domain	This study
pBAC4x1- WT-FGFR2-His	Insect cell expression vector that expresses C-terminal His-tagged wild-type full-length FGFR2	This study
pBAC4x1- WT-CYTO-His	Insect cell expression vector that expresses C-terminal His-tagged FGFR2 cytoplasmic domain	This study
pBAC4x1- WT-EX-His	Insect cell expression vector that expresses C-terminal His-tagged FGFR2 extracellular domain	This study
pET28a	His-tagged bacterial expression vector	Novagen
pET28a-Grb2	His-tagged bacterial expression vector that express wild type full length Grb2	(173)
pET33b	His-tagged bacterial expression vector	Novagen
pET33b-CYTO	Bacterial expression vector that expresses N-terminal His-tagged FGFR2 cytoplasmic domain	This study
pET33b-kinase	Bacterial expression vector that expresses N-terminal His-tagged FGFR2 kinase domain	This study
pET33b-C58	Bacterial expression vector that expresses N-terminal His-tagged FGFR2 C-terminal 58 amino acids	This study
pGEX2T	Bacterial expression vector that used for expression of GST-fused protein	GE
pGEX2T-Grb2	Bacterial expression vector that expresses GST-fused wild-type full-length Grb2	(173)
pGEX2T-N-SH3	Bacterial expression vector that	(173)

	expresses GST-fused Grb2 N-SH3 domain	
pGEX2T-C-SH3	Bacterial expression vector that expresses GST-fused Grb2 C-SH3 domain	(173)
pGEX2T-NSH3-SH2	Bacterial expression vector that expresses GST-fused Grb2 Nsh3-SH2 domain	(173)
pGEX2T-SH2-CSH3	Bacterial expression vector that expresses GST-fused Grb2 SH2-CSH3 domain	(173)
pGEX2T-Grb2 R/A	Bacterial expression vector that expresses GST-fused full-length Grb2 R86A mutant	(173)
pGEX4T2-NSH3-CSH3	Bacterial expression vector that expresses GST-fused Grb2 NSH3-CSH3 domain	(173)
pGEX4T2	Bacterial expression vector that used for expression of GST-fused protein	GE
pGEX4T2-2SH2	Bacterial expression vector that expresses GST-fused SHP2 NSH2-CSH2 domain	This study
pGEX4T2-N-SH2	Bacterial expression vector that expresses GST-fused SHP2 N-SH2 domain	This study
pGEX4T2-C-SH2	Bacterial expression vector that expresses GST-fused SHP2 C-SH2 domain	This study
pGEX4T2-2SH2-R32A	Bacterial expression vector that expresses GST-fused SHP2 NSH2 R32A-CSH2 domain mutant	This study
pGEX4T2-2SH2-R138A	Bacterial expression vector that expresses GST-fused SHP2 NSH2-CSH2 R138A domain mutant	This study
pGEX4T2-2SH2-R32/138A	Bacterial expression vector that	This study

	expresses GST-fused SHP2 NSH2 R32A-CSH2 R138A domain mutant	
pGEX4T2-C58	Bacterial expression vector that expresses GST-fused FGFR2 C-terminal 58 amino acids	This study
pET33b-SHP2	Bacterial expression vector that expresses N-terminal His-tagged wild-type full-length SHP2	This study

2.1.10 Stock solutions

Coomassie blue stain solution
0.2% (w/v) Coomassie brilliant blue R
40% (w/v) methanol
10% (w/v) acetic acid

Coomassie blue destain solution
40% (w/v) methanol
10% (w/v) acetic acid

Lysis buffer
20 mM Tris-HCl pH 7.5
138 mM NaCl
1 mM EGTA
20 mM β-glycerophosphate
10% (w/v) glycerol
1 mM sodium orthovanadate
20 mM sodium fluoride
1% (v/v) protease inhibitor cocktail set III

Midiprep Solution I
50 mM glucose
25 mM Tris-HCl pH 8.0
10 mM EDTA
Autoclaved and stored at 4^{o}C, add 4 μg/ml lysozyme before using.

Midiprep Solution II
0.2 M NaOH
1% (w/v) SDS
Freshly prepared

Midiprep Solution III
8 M ammonium acetate
Autoclaved and stored at room temperature.

Native-PAGE running buffer (10x)
1.9 M glycine
250 mM Tris-base

PBS (10x)
80 g NaCl
2 g KCl
14.4 g Na_2HPO_4
2.4 g KH_2PO_4
Adjust pH to 7.4 with HCl. Bring volume to 1 litre, autoclave or sterilize by filtration.

PBS (1x)
137 mM NaCl
2.7 mM KCl
100 mM Na_2HPO_4
2 mM KH_2PO_4
pH 7.4

Ponceau S stain buffer
0.1% (w/v) Ponceau S
5% (v/v) acetic acid

Rapid screening buffer
5 mM EDTA
10% (w/v) sucrose
0.25% (w/v) sodium lauryl sulphate (SDS)
100 mM NaOH
60 mM KCl
0.05% (w/v) bromophenol blue

SDS-PAGE/Native-PAGE stacking gel buffer
1.0 M Tris-HCl pH 6.8

SDS-PAGE/Native-PAGE resolving gel buffer
1.5 M Tris-HCl pH 8.8

SDS-PAGE running buffer (10x)
1.9 M glycine
250 mM Tris-base
10% (w/v) sodium lauryl sulphate (SDS)

Silver stain fix solution
40% (v/v) ethanol
10% (v/v) acetic acid

Silver stain sensitise solution
0.005% (w/v) NN
0.004% (w/v) sodium thiosulfate
40% (v/v) ethanol
10% (v/v) acetic acid

Silver stain destain solution
40% (v/v) ethanol
10% (v/v) acetic acid

Silver stain silver nitrate solution
0.25% (w/v) silver nitrate
0.03% (w/v) formaldehyde

Silver stain develop solution
3% (w/v) potassium carbonate
0.03% (w/v) formaldehyde
0.0004% (w/v) sodium thiosulfate

Silver stain stop solution
1.5% (w/v) EDTA

Stripping buffer
62.5 mM Tris-HCl pH 6.7
2% (w/v) SDS
0.7% (V/V) β-mercaptoethanol

TBE buffer (10x)
890 mM Tris-base
890 mM boric acid
20 mM EDTA

TBS (10x)
500 mM Tris-HCl
1.5 M sodium chloride
pH 7.4

TBS-T (1x)
100 ml 10x stock solution
1 mM EDTA
0.01% (v/v) Tween-20

Transfer buffer (10x)
1.9 M glycine
250 mM Tris-Base

Transfer buffer (1x)
100 ml 10x stock solution
200 ml methanol
700 ml ddH_2O

HBS (2x)
42 mM HEPES pH 7.05
274 mM NaCl
10 mM KCl
1.5 mM Na_2HPO_4
2% (w/v) glucose

6x DNA loading dye
0.25% (w/v) bromophenol blue
0.25% (w/v) xylene xyanol
30% (v/v) glycerol

6x Native loading buffer
300 mM Tris-HCl, pH 6.8
60% (v/v) glycerol
0.6% (w/v) bromophenol blue

6x Laemmli loading buffer
300 mM Tris-HCl pH 6.8
12% (w/v) SDS
60% (v/v) glycerol
0.6% (w/v) bromophenol blue
30 mM DTT (added before use)

2.2 General Molecular Biological Protocols

2.2.1 DNA manipulation

2.2.1.1 DNA extraction

Recombinant plasmids obtained from transformed *E. coli* DH5α cells were purified using the QIAprep Spin Miniprep Kit (Qiagen). Briefly, single colony from transformed *E. coli* DH5α culture was grown overnight in 5 ml LB media containing antibiotic at 37^{o}C and 180 rpm. Purification was performed using a QIAprep Spin Miniprep Kit (Qiagen) according to the manufacture's protocol. The bacterial cells were lysed using P1 alkaline buffer containing RNase, and the lysate was neutralised

and adjusted to high-salt binding condition using P2 and P3 buffer. Plasmid DNA was bound to silica spin column while remaining RNA, cellular proteins and salts were removed by spinning down and washing using ethanol containing PB buffer. The purified plasmid DNA was eluted from the QIAprep spin column using EB buffer (Tris containing buffer, pH 7.0 – 8.5).

2.2.1.2 Agarose gel electrophoresis and DNA extraction from agarose gels

Agarose gel electrophoresis was used to separate and confirm the size of PCR products and to separate restriction-enzyme digested DNA fragments. Agarose was dissolved in TAE buffer (40 mM 2-amino-2-hydroxymethyl-1,3-propanediol (Tris)-Acetate and 1 mM ethylene-diamine-tetraacetic acid (EDTA)). Gels were set in the apparatus provided. DNA samples were prepared by adding 1x DNA loading buffer (0.1% bromophenol blue, 20 mM Tris and 20% glycerol). The 100 bp or 1 kb ladders (New England Biolabs, NEB) were used as molecular weight standards. Electrophoresis was carried out in TAE buffer at a constant voltage of 60 V. Trace amount of ethidium bromide was added to the running buffer in order to visualise the DNA. The resolved DNA bands were visualised on UV-transilluminators.

DNA fragments were extracted from the gel using the QIAquick Gel Extraction Kit (Qiagen) according to the manufacturer's protocol. Provided, agarose was dissolved using buffer QE. DNA was absorbed to the silica-membrane of the spin column. Salts were washed away by the ethanol-containing PE buffer. The DNA was subsequently eluted with buffer EB (10 mM Tris pH 8.5).

2.2.1.3 Determination of DNA concentration

Double strand DNA has an absorbance at a wavelength of 260 nm. An OD_{260}=1 is equivalent to a DNA concentration of 50 µg/ml. The DNA concentration was measured using 1 µl of sample in a Nanodrop Spectrophotometer.

2.2.1.4 Restriction enzyme digestion

Restriction enzymes were purchased from NEB. Reactions were performed in 50 µl volumes using

2 µg of DNA
2 µl of each restriction enzyme
5 µl of recommended buffer
0.5 µl of 100x bovine serum albumin.

Enzyme digestion reactions were incubated at 37^{o}C for 2 hours or overnight according to manufacturer's protocol. Digested products were then electrophoresed on an

agarose gel and subsequently extracted and purified using QIAquick Gel Extraction Kit (Qiagen).

2.2.1.5 DNA ligation and transformation

DNA ligations were set up in 10 µl volumes using

3:1 molar ratio of insert to vector (~20 ng vector DNA)
400 U of T4 DNA ligase (NEB)
1x T4 DNA ligation buffer (NEB), containing 1 mM ATP

Calculation of insert amount:

Insert Mass (ng) = 3×[Insert Length (bp)/Vector Length (bp)]× Vector Mass (ng)

The ligation mixture was mixed well and left overnight at room temperature.

DNA was introduced into bacterial strain by chemical transformation. Method for competent cell preparation was described in section 2.2.3. For transformation, competent bacteria DH5α were thawed on ice for 12 minutes. 10 µl of ligation mixture was added and left on ice for 30 minutes. The cells were then heat shocked at 42^{o}C for 2 minutes and transferred to ice for another 5 minutes. 1 ml of LB broth was added to the cells which were then incubated at 37^{o}C and 180 rpm for 45 minutes. Cells were then spun down at 4^{o}C and 800 rpm for 1 minute. Culture medium was

discarded; 100 µl of LB was used to resuspend these cells and plated onto agar supplemented with the appropriate antibiotic and incubated overnight at 37^{o}C.

2.2.1.6 Rapid screening of plasmid DNA

Plasmid DNA rapid screening was performed to check if the colonies contain inserts. The method involved in lysing bacteria and extract genomic DNA, plasmid DNA and RNA. The entire extraction product is subjected to agarose gel electrophoresis.

Cells were picked and resuspended in 20 µl of rapid screen buffer and incubated on ice for five minutes followed by incubating at 37^{o}C for 5 minutes. The reactions were pelleted by centrifugation at 13,000 rpm for 10 minutes and the samples were run on agarose gels. The sizes of the plasmids were compared with the original plasmid without insert.

2.2.1.7 DNA sequencing

All DNA constructs created by molecular cloning were sequenced with appropriate primers to make sure the gene sequence is correct and the open reading frame was

intact. Purified plasmid DNA and primers were sent to the sequencing facility of Wolfson Institute of Biomedical Research for sequencing.

2.2.2 DNA amplification

2.2.2.1 Polymerase chain reaction

Oligonucleotide primers were synthesised (Sigma) in order to amplify various genes by polymerase chain reaction (PCR). PCR amplification was performed in 50 µl reaction volumes; the reaction mixture is listed follow:

- 1x ThermoPol Reaction Buffer (20 mM Tris-HCl, 10 mM $(NH_4)_2SO_4$, 10 mM KCl, 2 mM $MgSO_4$ and 0.1 % Triton X-100, pH 8.8 at 25°C)
- 0.2 mM of each deoxynucleoside triphosphates
- 0.4 µM of upstream primer
- 0.4 µM of downstream primer
- 25 ng of DNA template
- 2 units (U) of Vent polymerase
- 5% DMSO

Thermo cycles (35 cycles of melting step-annealing step-extension step):

Initial melting step:	95^{o}C, 5 minutes
Melting step:	95^{o}C, 1 minute
Annealing step:	appropriate temperature, 1 minute
Extension step:	72^{o}C, 1 minute/ kbp
Final extension step:	72^{o}C, 10 minutes

Different annealing temperatures were used according to the Tm values of primers. The PCR amplified products were analysed on an agarose gel and purified using QIAquick Gel Extraction Kit (Qiagen).

2.2.2.2 Mutagenesis

Oligonucleotide primers were synthesised (Sigma) in order to perform site-directed mutagenesis by polymerase chain reaction (PCR) as in section 2.2.2.1.

Thermo cycles (18 cycles of melting step-annealing step-extension step):

Initial melting step:	95^{o}C, 5 minutes
Melting step:	95^{o}C, 1 minute
Annealing step:	55 ^{o}C, 1 minute
Extension step:	68^{o}C, 1 minute/ kbp
Final extension step:	68^{o}C, 10 minutes

The PCR products were further incubated with 1 µl of DpnI (20,000U/ml) at 37^{o}C for one hour in order to digest the parental plasmid DNA since DpnI only recognises its restriction site when methylated. Following by clean-up the digestion product, 20 µl of the reaction were transformed into DH5α competent cells (transformation: 2.2.1.5).

2.2.3 Preparation of competent cells

The bacterial strains used in this study are *E. coli* DH5α for cloning of microbacterial DNA and expression of proteins, and *E. coli* BL21 (DE3) for the expression of proteins.

Competent DH5α cells or BL21(DE3) were made by rubidium chloride methods; 1 ml overnight culture was seeded into 100 ml LB, and incubated at 180 rpm, 37ºC until OD_{600} reaches 0.35. Cells were pelleted at 3500g at 4ºC for 15 min. After discarding the supernatant, 0.4x original culture volume of TFB I solution was used to resuspend the cell pellet. After 30 min of incubation on ice, pelleted cells again at 3500g at 4ºC for 15 min, and 0.04x volume of TFB II solution was added to resuspend the cell pellet. Competent cells for transformation were aliquoted and stored at -80ºC.

- TFB I Solution

Potassium acetate: 30 mM

Rubidium chloride: 100 mM

Calcium chloride: 10 mM

Manganese chloride: 50 mM

Glycerol: 15%

pH value was adjusted to 5.8 with dilute acetic acid

- TFB II Solution

MOPS: 10 mM

Rubidium chloride: 10 mM

Calcium chloride: 75 mM

Glycerol: 15%

pH value was adjusted to 6.5 with 1 M NaOH

2.3 Cell Biological Methods

2.3.1 HEK 293 cells

Human Embryonic Kidney 293 (HEK 293) cells were used were from regular laboratory stock. Cells were maintained and grown in Dulbecco's Modified Eagle's Medium (DMEM) containing 4.5 g/L glucose, 4 mM L-glutamine, 10% fetal calf serum (FCS), 0.05 mg/ml gentamycin sulphate (Cambrex), and 1x Pen/Strep Fungizone Mixture (Cambrex) at 37°C in a 5% CO_2 humidified incubator. The cells were split and the culture medium was changed every three to five days when the cell density reached 80%. Cell stocks were frozen in DMEM medium containing 20% FCS and 10% DMSO and stored in liquid nitrogen. All cell culture work was carried out in a tissue culture hood (HeraSafe, Heraeus)

2.3.2 Sf9 cells

Sf9 cells were purchased from Novagen. Cells were maintained and grown in Insect-Xpress Protein–Free Medium (Lonza) containing 10% fetal bovine serum (FBS), 0.05 mg/ml gentamycin sulphate (Cambrex), and 1x Pen/Strep Fungizone Mixture (Cambrex). The Sf9 cell culture was maintained and grown in a temperature-controlled orbital shaker at 170 rpm and 27ºC. Cells were passaged every 3-4 days to ensure the cell density was below 4×10^6 cells/ml and cell viability was higher than 95%. Cell number and viability were checked using Trypan Blue Exclusion Method. Briefly, cells and trypan blue solution (Novagen) were mixed 1:1 and then applied immediately to a hemocytometer. Cells were counted using a light microscopic; trypan blue solution stains dead cells only, therefore both cell number and cell viability were calculated.

A 35×10 mm culture dish (Sarstedt) was used for co-transfection. 0.5×10^6 cells/dish of Sf9 cells was seeded in 1 ml BacVector Insect Cell Medium 1 hour before co-transfection. Dishes were incubated at 27ºC for 1 hour to allow cells to attach to the plates.

2.3.3 Mammalian cell transfection

2.3.3.1 Preparation of DNA for transfection

Large amounts of highly concentrated DNA were required for efficient transfection. A single bacterial colony transformed with appropriate plasmid was grown at 37^{o}C and 180 rpm with appropriate antibiotic. The cells were pelleted by centrifugation at 4,000 rpm for 20 minutes at 4^{o}C. Cells were resuspended in 5 ml of solution I containing 4 μg/ml of lysozyme and incubated on ice for 5 minutes. 10 ml of freshly prepared solution II was added and mixed by inverting gently four to six times. The insoluble cell components were precipitated by adding 5 ml of solution III, followed by spinning down at 18,000rpm for 10 minutes at 20^{o}C. 0.7x volume of isopropanol was added to precipitated plasmid DNA; precipitated plasmid DNA was pelleted by centrifugation at 18,000rpm for 60 minutes at 20^{o}C. Plasmid DNA pellet was washed using 70% ice-cold ethanol. Pelleted DNA was dissolved using appropriate volume of EB. In order to remove RNA, the DNA solution was treated with 10 μg/ml RNase A and incubated at 37^{o}C for 20 minutes. The RNase and trace amount of cellular proteins were removed by adding equal volume of phenol/chloroform. The two layers were separated by centrifugation at 13,000rpm at 20^{o}C for 3 minutes. The top layer containing DNA was transferred to a new tube. 2.5x volume of 100% ice-cold ethanol was added to precipitate plasmid DNA. The DNA was pelleted by centrifugation at

18,000 rpm at 4^{o}C for 30 minutes, followed by washing with 70% ice-cold ethanol. The plasmid DNA was dried at room temperature and resuspended in 500 µl EB.

Solution I: 50 mM glucose, 10 mM EDTA and 25 mM Tris-HCl pH 8.0
Solution II: 0.2 M NaOH, 1% (w/v) SDS
Solution III: 8 M ammonium acetate

2.3.3.2 Transfection

Transfection was done using calcium phosphate transfection method in 10 ml medium in a 10 cm-dish. One day prior to transfection, the cells were plated to less than 50% confluence, in order to reach 70-75% confluence the next day. Before transfection, prepare two sets of 1.5 ml tubes. 0.5 ml 2x HBS (280 mM NaCl, 10 mM KCl, 1.5 mM Na_2HPO_4, 12 mM dextrose and 50 mM HEPES pH 7.5) was pipetted in one tube. 10 µg of DNA in 438 µl volume was mixed with 62 µl 2M $CaCl_2$ by drawing up and down in a 1 ml pipet and add dropwise to the 2X HBS and incubate at room temperature for 20 minutes. The DNA-$CaPO_4$ coprecipitate was added dropwise to the surface of the media containing the cells, and swirled to mix. After overnight incubation at 37°C in a 5% CO_2 incubator, the $CaPO_4$ containing medium was removed and the cell monolayer was washed twice with PBS. Normal culture medium was added and the

cells were incubated at 37°C in a 5% CO_2 incubator. Transient gene expression assays in transfected cells were performed 48 hours post transfection.

2.3.3.3 Generation of stable transfected cell lines

To obtain stable transfected cell line, MfeI (NEB) was used to linerised vectors to increase the chances that the vectors do not integrate in a way that disrupt the target genes. 293T cell kill curve was determined in order to obtain the minimum concentration of blasticidin required to kill untransfected cells. Briefly, 2×10^5 cells were seeded in 6 cm-dishes and incubated overnight. Medium containing different concentrations of blasticidin (1 μg/ml, 3 μg/ml, 5 μg/ml, 10 μg/ml, 15 μg/ml, 20 μg/ml, 25 μg/ml, 30 μg/ml, 35 μg/ml, 40 μg/ml and 45 μg/ml) was used to substitute culture medium. The selective medium was replenished every 3 days until the appropriate concentration of blasticidin that prevented cell growth could be determined. Cells were grown in 96-well plates for a few days until single colonies could be observed. The individual colonies were picked, expanded in 25T flasks, and protein expression levels were compared by western blotting.

2.3.3.4 Preparation of frozen cell stocks

Cells were centrifuged for 10 minutes and resuspend in freezing medium (10% DMSO, 20% FCS and 70% DMEM medium) at a concentration of 2 X 10^6 cells/0.5 mL freezing medium. Cells with freezing medium were aliquoted and placed in a styrofoam box and covered. Cell stocks were kept at -70°C for 24 hours. After 24 hours, cells were transferred into a liquid nitrogen container.

2.3.4 Insect cell transfection

2.3.4.1 Preparation of DNA and transfection

DNA preparing procedure was described in section 2.3.3.1. Transfection of transfer plasmids with lineraized virus DNA (BacMagic DNA) for the production of recombinant baculovirus was done using the liposome-mediated transfection method. For each transfection, the following co-transfection mixture was mixed in a sterile tube and incubated at room temperature for 30 min to allow the formation of transfection complexes.

- 0.5 ml BacVector Insect Cell Medium
- 2.5 µl Insect GeneJuice
- 50 ng BacMagic DNA
- 250 ng transfer vector DNA carrying target gene

Prior to the end of incubation, culture medium was removed carefully and the transfection mixture was added immediately. After an overnight incubation at 27ºC, 0.5 ml medium was added to each dish and kept for another 4 days. After incubation, the culture medium that contains recombinant baculovirus was harvested and filtered; the initial recombinant baculovirus generated was covered to avoid from light and stored at 4ºC.

2.3.4.2 Virus titer

Virus titer was determined using the FastPlax^{TM} Titer Kit (Novagen) according to the user manual. This method is based on the determination of the AcNPV gp64 glycoprotein on the cell surface after 24 hours post-infection. 1×10^{6} cells/well was seeded on 6-well plate with 2 ml of cell culture medium. Virus series dilutions (10^{-2}, 10^{-4}, 10^{-5}, 10^{-6} and 10^{-7}) were prepared for titer determination. After the cells attached to the plate, the culture medium was aspirated and virus dilutions (10^{-5}, 10^{-6} and 10^{-7}) were added drop by drop to avoid disturbing the cell monolayer. The plate was incubated at room temperature for 60 minutes with gentle rocking every 10 minutes. At the end of incubation, 2 ml of medium was added to each well followed by incubating for 24 hours in a humid incubator. Medium containing infectious virus was aspirated after 24 hours post-infection. Cells were washed with PBS and fixed with

3.7% formaldehyde solution at room temperature for 15 minutes. Blocking was done using 1% gelatin in TBST with gentle rocking. After blocking and washing with PBS, 1 ml/well of FastPlax antibody (1:10,000 in TBST) was added and incubated for 60 minutes, followed by washing with TBST three times. 1 ml/well of Goat Anti-Mouse β-gal Conjugate (1:100 in TBST) was added and incubated for 60 minutes, followed by washing with TBST three times. During the last wash, developing solution was prepared by mixing 60 µl X-Gal and 60 µl NBT to 15 ml PBS plus 5 mM $MgCl_2$. Infected cells were stained after developing solution was added and incubated at 37ºC within 60 minutes.

Virus titer could be calculated by the formula:

Pfu/ml = 5 × (number of infected cells and foci) × (dilution factor)

2.3.4.3 Virus amplification and storage

A 200 ml culture of Sf9 cells at density of 2×10^6 cells/ml was prepared in a 500 ml shaking flask. Cells were infected at a multiplicity of infection (MOI) of 0.1 and incubated with shaking at 170 rpm, 27ºC for 4-5 days. When the cells appeared to be well infected with recombinant virus, cells were harvested by centrifugation at 4000 ×

g for 20 min at 4ºC. Culture medium containing the amplified recombinant baculoviurs was filtered using 0.22 μm filter (Millipore), and stored in dark at 4ºC. The titer of the amplified recombinant baculoviurs was determined according the above description.

2.4 Protein Expression

2.4.1 Construction of the mammalian cell expression vectors

2.4.1.1 MBP-tagged mammalian cell expression vector

Gene that encodes maltose binding protein was amplified from pMAL2t1 vector (NEB) using PCR reaction. The pcDNA6 Myc/His B plasmid and the amplified MBP DNA fragment were digested using XbaI and PmeI (NEB), followed by DNA ligation and transformation. Methods for restriction enzyme digestion, DNA ligation, and plasmid DNA transformation to generate the expression vector are described in sections 2.2.1.4 and 2.2.1.5. The plasmid DNA that expresses the MBP tag was named pcDNA-MBP.

A Myc tag was also introduced into the pcDNA-MBP vector in order to introduce an antibody recognition site. The Myc tag fragment containing TEV protease cleavage

site and thrombin protease cleavage site was amplified from pcDNA6 Myc/His B plasmid. The pcDNA-MBP plasmid and the amplified Myc tag fragment were digested using HindIII and XbaI (NEB), followed by DNA ligation and plasmid DNA transformation. The plasmid DNA for mammalian cell expression that expresses both Myc tag and MBP tag containing TEV protease cleavage site and thrombin protease cleavage site was named pcDNA-Myc-MBP.

2.4.1.2 Strep-tagged mammalian cell expression vector

Another affinity tag for protein purification was chosen in order to produce protein of high purity. Strep II tag, an eight amino acid tag, based on the specific interaction between streptavidin and biotin, was generated using two complementary primers that encode Strep II tag, followed by XbaI and PmeI restriction enzyme digestion. pcDNA6-Myc-MBP expression vectors that carries either full-length FGFR2 or cytoplasmic domain of FGFR2 were also digested using XbaI and PmeI. This resulted in removal of the MBP tag which was replaced by the Strep II tag. Methods for restriction enzyme digestion, DNA ligation, and plasmid DNA transformation to generate the expression vector are described in sections 2.2.1.4 and 2.2.1.5.

2.4.2 Constructions of the insect cell expression vectors

BacMagic^{TM} DNA System (Novagen) was used in this study to generate recombinant baculovirus, eliminating the time-consuming steps of plaque purification. Plasmid DNA used for insect cell expression was generated using maltose binding protein (MBP) tagged pcDNA6.1 carrying different parts of the FGFR2 genes used in the mammalian cell expression system. 2 μg of mammalian expression plasmids were digested at 37ºC overnight using HindIII and PmeI in a total volume of 50 μl. The pBAC4x1 transfer vector (Novagen) was digested at 37ºC for overnight using AvrII. All restriction enzyme digested DNA fragments were purified using QIAquick Gel Extraction Kit (Qiagen) according to the user manual. AvrII digested pBAC4x1 transfer vector was purified to remove trace amount of protein and salts, and treated by T4 DNA polymerase (NEB) and 100 μM dNTPs at 12ºC for 15 min to blunt the digested DNA fragment. After stopping the T4 polymerase filling up reaction by adding 10 mM EDTA and heating to 72ºC for 2 minutes, the DNA was purified and digested using HindIII at 37ºC for overnight. Ligation and transformation were carried out as above.

2.4.3 Small scale protein expression tests

In order to find out the ideal condition for protein expression in Sf9 cell, tests were performed using 2×10^6 cells/ml in 50 ml medium. Different amounts of baculovirus (MOI 2, 5 and 10) were used to infect individual culture. 1 ml culture from each culture was taken every 24, 48, 72 and 96 hours after infection. Infected cells were pelleted at 1,500 rpm, 4ºC for 10 min, and lysed using 100 µl ice-cold lysis buffer (200 mM NaCl, 20 mM HEPES pH7.5, 1% Triton X-100 and 10% glycerol). Samples were run on a SDS-PAGE to test for protein expression; recombinant proteins were confirmed by western blotting.

2.4.4 Large scale protein expression

Large scale protein expression was performed using 2×10^6 cells/ml in 1 litre medium. Cells were infected at a MOI of 5, and incubated with shaking at 170 rpm and 27ºC for 2 days. Infected cells were pelleted at 1,500 rpm, 4ºC for 20 min, and lysed using suitable amount of ice-cold lysis buffer (200 mM NaCl, 20 mM HEPES pH7.5 and 10% glycerol) containing protease inhibitors (AEBSF, aprotinin, bestatin, E-64, leupeptin, pepatatin A and PMSF). After lysing, the lysate was either frozen at -80ºC or used directly for protein purification.

2.4.5 Constructions of the bacterial expression vectors

pET28a, pET33b, pGEX2T and pGEX4T2 were used to construct the expression vectors according to different requirement. Oligonucleotide primers were designed and synthesised in order to amplify various gene fragments by polymerase chain reaction (PCR). Methods for PCR amplification are described in section 2.2.2.1. Methods for restriction enzyme digestion, DNA ligation and plasmid DNA transformation to generate the expression vector are described in sections 2.2.1.4 and 2.2.1.5.

2.4.6 Bacterial culture and protein production

Luria Bertani (LB) Broth was used to grow bacterial culture. Protein expression was carried out in appropriate amount of LB medium. Individual colonies were grown overnight in 5 ml of LB broth supplemented with appropriate antibiotic at 37^{o}C and 200 rpm. The cultures were then transferred to fresh medium supplemented with appropriated antibiotic. The cells were grown at 37ºC and 180 rpm until the optical density (OD) of the larger culture reached OD_{600nm} = 0.6-0.8. The expression of protein was induced for 4 hours at 37ºC, or overnight at 20ºC with the addition of isopropyl-β-D-thiogalactopyranoside (IPTG) to a final concentration of 0.1 mM. After

the expression period the cells were pelleted at 4,000 rpm for 20 minutes and frozen at -20ºC until further use.

2.5 Protein Purification

2.5.1 Protein purification by affinity chromatography

2.5.1.1 Maltose binding protein (MBP) fused protein purification

Amylose resin (NEB) was stored in 20% filtered ethanol. Before using, amylose resin was washed with 10 column volumes of filtered water, and equilibrated with 10 times column volume of MBP wash buffer (200 mM NaCl and 20 mM HEPES pH7.5). Transfected mammalian cells or infected insect cells that expressed the MBP fused receptor proteins were lysed using suitable amount of ice-cold lysis buffer (200 mM NaCl, 20 mM HEPES pH7.5 and 10% glycerol). Cell lysate was spun at 18,000 rpm at 4ºC for 60 min. The supernatant was applied to the amylose resin. In order to remove nonspecific binding proteins, amylose resin was washed with 20 column volumes of MBP wash buffer (200 mM NaCl and 20 mM HEPES pH7.5). MBP fused receptor proteins were eluted with MBP elution buffer (20 mM maltose, 200 mM NaCl and 20 mM HEPES pH7.5). The protein identity and purity were confirmed by western blotting and silver staining. Amylose resin was regenerated using 5 column

volumes of 0.1% SDS, followed by washing with 5 column volumes of MBP wash buffer (200 mM NaCl and 20 mM HEPES pH7.5), 5 column volumes of filtered H_2O, and stored in 20% filtered ethanol at 4ºC.

2.5.1.2 Strep•Tag II -tagged protein purification

Strep•Tactin Superflow Agarose (Novagen) was stored in 20% filtered ethanol. Before using, Strep•Tactin Superflow Agarose was washed with 10 column volumes of filtered water, and equilibrated with 10 column volumes of Strep•Tactin wash buffer (150 mM NaCl, 1 mM EDTA and 100 mM Tris-HCl pH 8.0). Transfected mammalian cells that expressed the Strep•Tactin fused receptor proteins were lysed using suitable amount of ice-cold lysis buffer (200 mM NaCl, 20 mM HEPES pH7.5 and 10% glycerol). Cell lysate was spun at 18,000 rpm at 4ºC for 60 min. The supernatant was applied to Strep•Tactin resin. In order to remove nonspecific binding proteins, Strep•Tactin resin was washed with 20 column volumes of Strep•Tactin wash buffer (150 mM NaCl, 1 mM EDTA and 100 mM Tris-HCl pH 8.0). Strep•Tactin fused receptor proteins were eluted with Strep•Tactin elution buffer (2.5 mM desthiobiotin, 150 mM NaCl, 1 mM EDTA and 100 mM Tris-HCl pH 8.0). The protein identity and purity were confirmed using western blot. Strep•Tactin Superflow Agarose was regenerated using 5 column volumes of regeneration buffer (1 mM

HABA (2-[4'-hydroxy-benzeneazo]benzoic acid), 150 mM NaCl, 1 mM EDTA and 100 mM Tris-HCl pH 8.0), followed by washing with 5 column volumes of Strep•Tactin wash buffer (150 mM NaCl, 1 mM EDTA and 100 mM Tris-HCl pH 8.0), 5 column volumes of filtered H_2O, and stored in 20% filtered ethanol at 4ºC.

2.5.1.3 Proteins purification by hydroxyapatite

The MBP-fused receptor proteins were further purified using type II CHT ceramic hydroxyapatite (Biorad). Protein samples were changed into HAP wash buffer A (150 mM KCl and 10 mM potassium phosphate pH 6.8) by dialysis. Hydroxyapatite was equilibrated using HAP wash buffer A (150 mM KCl and 10 mM potassium phosphate pH 6.8). After loading and washing the column with 20 column volumes of HAP buffer A, proteins were eluted with a gradient of increasing concentration of potassium phosphate buffer at a flow rate of 0.5 ml/minute with 7 ml fractions collected (10 mM-600 mM; ÄKTA FPLC system was used to set up the gradient elution by mixing HAP wash buffer A and HAP elution buffer B (150 mM KCl and 1000 mM potassium phosphate pH 6.8). The eluted proteins were detected using UV absorbance at 280 nm and verified by SDS-PAGE analysis. Hydroxyapatite was regenerated using 5 column volumes of HAP regeneration buffer (400 mM tri-sodium phosphate pH 11), following by washing with 5 column volumes of HAP storage

buffer (10 mM potassium phosphate pH 6.8 and 0.1% sodium azide), and stored at 4ºC. This step of purification can also remove the strong binding of maltose on maltose binding protein.

2.5.1.4 Protein purification by immobilized metal ion affinity chromatography

6x histidine-tagged fusion protein (TEV-His, Grb2-His and FGF9-His) used in this study were purified as following:

All protein purification procedures were carried out at 4^{o}C. The cells were defrosted on ice and resuspended in Talon wash buffer A (250 mM NaCl, 1 mM β-mercaptoehanol and 50 mM potassium phosphate pH 8.0) and then lysed by sonication (20 x 10 sec bursts with 10 sec intervals). The lysate was centrifuged at 13,000 g for 1 hour. The supernatant was injected into the equilibrated column at a flow rate of 0.5 ml/minute. The talon column was washed with 10 column volumes of 25 mM imidazole wash buffer (25 mM imidazole, 250 mM NaCl, 1 mM β-mercaptoehanol and 50 mM potassium phosphate pH 8.0), followed by eluting with 10 column volumes of Talon elution buffer B (200 mM imidazole, 250 mM NaCl, 1 mM β-mercaptoehanol and 50 mM potassium phosphate pH 8.0) with 7 ml fractions

collected. After purification, the talon resin should be the resin should be washed with 10 column volumes of 2-(N-morpholine)-ethanesulfonic acid (MES) buffer (50 mM MES pH 5.0), followed by washing with 5 column volumes of filtered H_2O, and stored in 20% filtered ethanol at 4ºC. The eluted proteins were detected using UV absorbance at 280 nm and verified by SDS-PAGE analysis.

2.5.1.5 GST-tagged protein purification

Glutathione S-transferase-tagged (GST) fusion protein (FGF9-GST) used in this study was purified as following:

All protein purification procedures were carried out at 4^oC. The cells were defrosted on ice and resuspended in GST wash buffer A (PBS) and then lysed by sonication (20 x 10 sec bursts with 10 sec intervals). The lysate was centrifuged at 13,000 g for 1 hour. The supernatant was injected into the equilibrated column at a flow rate of 0.5 ml/minute. The GST column was washed with 10 column volumes of PBS, followed by eluting with 10 column volumes of GST elution buffer B (10 mM reduced glutathione and 50 mM Tris-HCl pH 8) with 7 ml fractions collected. The eluted proteins were detected using UV absorbance at 280 nm and verified by SDS-PAGE

analysis. The GST resin can be regenerated by washing with the following buffers sequentially: 10 column volumes of wash buffer A (1x PBS and 300 mM NaCl), 10 column volumes of wash buffer B (0.5 M NaCl and 0.1 M NaOAc pH 4.5), and 10 column volumes of wash buffer C (1x PBS and 0.5 % Triton X-100), followed by washing with 5 column volumes of filtered H_2O, and stored in 20% filtered ethanol at 4ºC.

2.5.2 TEV protease cleavage and removal

The purified MBP-fused receptor proteins were treated with TEV protease in order to cut the MBP tag. Briefly, 1 μg of TEV was used to cut 5 μg of MBP-fused receptor proteins at 4ºC for overnight. The TEV protease was removed by passing through Talon superflow agarose (Clontech). The binding flow-through, containing receptor proteins and MBP tag, was further passed through amylose resin (NEB) in order to remove the released MBP tag. The binding flow-through, containing receptor proteins, was collected and concentrated using Millipore amicon centrifugal concentrator (Millipore).

2.5.3 Thrombin protease cleavage and removal

The purified GST-fused receptor proteins were treated with thrombin protease in order to cut the GST tag. Briefly, 1 unit of thrombin was used to cut 1 mg of MBP-fused receptor proteins at 4ºC for overnight. The thrombin protease was removed by passing through Benzamidine Sepharose. The binding flow-through, containing GST tag and target proteins, was collected and passed through glutathione agarose beads to remove the GST tag and the flow-through containing target protein was concentrated using Millipore amicon centrifugal concentrator (Millipore).

2.5.4 Protein purification by ion-exchange chromatography

The receptor proteins were further purified using DEAE (GE Helthcare Life Sciences). Protein samples were changed into DEAE wash buffer A (20 mM NaCl and 20 mM HEPES pH 7.5) by dialysis. DEAE column was equilibrated using DEAE wash buffer A. After loading and washing the column with 20 column volumes of DEAE wash buffer A, proteins were eluted with a gradient of increasing concentration of potassium phosphate buffer at a flow rate of 0.5 ml/minute with 3 ml fractions collected (20 mM-600 mM NaCl; ÄKTA FPLC system was used to set up the gradient elution by mixing DEAE wash buffer A and DEAE elution buffer B (1000

mM NaCl and 20 mM HEPES pH 7.5). The eluted proteins were detected using UV absorbance at 280 nm and verified by SDS-PAGE and western blot analysis. DEAE column was regenerated using 5 column volumes of DEAE elution buffer B, followed by washing with 5 column volumes of filtered H_2O, and stored in 20% filtered ethanol at 4^oC.

2.5.5 Protein purification by size exclusion chromatography

Proteins were further purified using either a Superdex 75, or Superdex 200 pre-packaged size-exclusion chromatography column and ÄKTA FPLC system (Amersham Biosciences) at 4^oC. The column was equilibrated with 5 time column volume of gel filtration buffer (200 mM NaCl and 20 mM HEPES pH7.5). Protein samples were concentrated to less than 5 ml and injected into the equilibrated column at a flow rate of 0.5 ml/minute with 0.5-1 ml fractions collected. The eluted proteins were detected using UV absorbance at 280 nm and verified by SDS-PAGE analysis.

2.6 Protein Gel Electrophoresis

2.6.1 Sodium Dodecyl Sulphate–Polyacrylamide Gel (SDS-PAGE)

SDS-PAGE was used to separate protein samples. The gels were composed of a 5% stacking layer and different percentage of resolving layer determined by the target protein sizes. Electrophoresis was carried out using the Biorad Mini-PROTEAN II System (Biorad). Protein samples were mixed with 1x SDS loading dye (Laemmli loading dye) (100 mM Tris-HCl pH 6.8, 0.1 % bromophenol blue, 2% SDS, 5% β-mercaptoethanol and 10% glycerol) and denatured at 95^{o}C for 4 minutes. Pre-stained or Unstained Precision Plus Protein standards (Biorad) were used as molecular weight markers. Polyacrylamide gels were electrophoresed using 1X Running Buffer (0.025 M Tris, 0.192 M glycine and 0.1% SDS) at a constant voltage of 90 V through the stacking layer and 130 V through the resolving layer. Gels were stained in a staining solution (0.025% Coomassie Brilliant blue R 250, 40% methanol and 7% acetic acid). Protein bands were visualised by destaining gels in a destaining solution (40 % (v/v) methanol, 10 % (v/v) acetic acid and 50 % (v/v) H_2O).

Gel Recipes and Solutions:

	Stacking		Resolving	
Gel Percentage (%)	5	Gel Percentage (%)	7.5	10
30% Polyacrylamide (mL)	1.7	30% Polyacrylamide (mL)	2.5	3.33
1M Tris (pH6.8) (mL)	1.25	1.5M Tris (pH8.8) (mL)	2.5	2.5
10% Ammonium persulfate (mL)	0.1	10% Ammonium persulfate (mL)	0.1	0.1
10% SDS (mL)	0.1	10% SDS (mL)	0.1	0.1
TEMED (mL)	0.01	TEMED (mL)	0.008	0.004
H_2O (mL)	6.8	H_2O (mL)	4.8	3.96

2.6.2 Native gel

Native polyacrylamide gels were used to measure the size of protein complexes or separate proteins with different phosphorylation levels. The gels were run using 1x Native Running Buffer (0.025 M Tris and 0.192 M glycine) at a constant voltage (120V), and followed by coomassie blue staining, silver staining or western blotting analysis.

Gel Recipes and Solutions:

	Stacking		Separating	
Gel Percentage (%)	5	Gel Percentage (%)	7.5	10
30% Polyacrylamide (mL)	1.7	30% Polyacrylamide (mL)	2.5	3.33
1M Tris (pH6.8) (mL)	1.25	1.5M Tris (pH8.8) (mL)	2.5	2.5
10% Ammonium persulfate (mL)	0.1	10% Ammonium persulfate (mL)	0.1	0.1
TEMED (mL)	0.01	TEMED (mL)	0.008	0.004
H_2O (mL)	6.9	H_2O (mL)	4.9	4.06

2.6.3 Coommassie blue staining

After electrophoresis, gels were placed in stain solution for 60 minutes with gentle agitation. To remove non-specifically bound dye from the gels, destain solution was used to soak the gels with gentle sgitation until proteins bands could be visualised clearly.

2.6.4 Silver staining

After electrophoresis, gels were fixed in 100 mL fixing solution for 2 hours. Gels were sensitized with sensitize solution by shaking for 5 min. Upon completion of the staining, gels were destained twice, 3 minutes each using fixing solution, following by washing with water twice, 2 min each. Gels were incubated in silver solution for 20 min to form silver-dye complexes on protein. Gels were washed with water twice, 20 seconds each. Gels were soaked in the developing solution for suitable time to develop the color. EDTA stop solution was used to terminate the development.

2.6.5 Western Blot

2.6.5.1 Transfer

Proteins were separated with a 7.5% or 10% polyacrylamide gel and Prestained Precision Plus Protein standards (Biorad) or Nativemark unstained protein standard (Invitrogen) were used for molecular weight comparison. Polyvinylidene Difluoride (PVDF) membrane (Millipore) was soaked in methanol for 10 minutes before using. Following equilibration, proteins were transferred to a PVDF membrane in Mini Protean II (Bio-Rad) by electroblotting in transfer buffer (48 mM Tris, 39 mM glycine, 0.037% SDS and 20% methanol) with a constant voltage of 250 milliamps (mA) for 2 hours.

2.6.5.2 Ponceau S staining

0.1% (w/v) Ponceau S in 5% acetic acid was used to either confirm successful transfer of protein onto the PVDF membrane or to stain the protein bands for ease of manipulation. Ponceau staining is a rapid reversible detection of protein bands on membranes, the dye can be removed by washing with ddH_2O or TBS-T buffer.

2.6.5.3 Immunoblotting

Membranes were then incubated for 30 minutes in blocking buffer (5% BSA in TBS-T (140 mM NaCl, 3 mM KCl, 0.05% Tween-20 and 25 mM Tris pH 8.0) or 5% milk in TBS-T) to block the remaining protein binding sites on the membrane.

The primary antibodies were added at a dilution of 1:1000 to blocking buffer. Upon incubation for 2 hours with primary antibody, membranes were washed 3 times with TBS-T buffer. The membrane was then incubated in TBS-T buffer with 1:1000 Horseradish Peroxidase-Conjugated Immunoglobulin G antibody for 1 hour, and the membrane was subsequently washed three times in TBS-T. The membrane was incubated with Pierce ECL Western Blotting Substrate for 2 minutes. Detection was carried out using X-ray film in a dark room.

2.7 Protein Concentration Determination

2.7.1 Bradford protein assay

Protein concentrations were determined using the BioRad protein assay kit (BioRad) following the manufacturer's protocol. This method is based on the colour change of Coomassie Brilliant Blue G-250 dye, when bound to the protein residues arginine,

tryptophan, tyrosine, histidine and phenylalanine, and has an absorption maximum at 595 nm. The protein concentrations can be determined by comparing with the absorbance of the BSA standard.

2.7.2 Protein determination using absorbance at 280 nm

Proteins in solution absorb ultraviolet light with maximum absorbance at 280 nm due to the aromatic rings. Secondary, tertiary, and quaternary structure, also pH, ionic strength, etc. can affect the absorbance at 280 nm.

The protein extinction coefficient at 280nm was calculated using the equation:

E_{280nm} (cm^{-1} M^{-1}) = (number of Trp)*(5500)+(number of Tyr)*(1490)+(number of Cys)*(125)

Protein concentration can be calculated using following equation:

Concentration (molarity) = Absorbance at 280 nm /extinction coefficient

2.8 Immunoprecipitation

Whole cell lysate were used for immunoprecipitation wih selected primary antibodies to identify the presence and phosphorylation states of proteins. Generally, 1 mg of whole cell lysate was prepared in 1 ml volume for immunoprecipitation. 1 µg of the

chosen antibody was added and incubated at 4 ^{o}C for overnight with gentle rotation. After incubation, 50 µl of 50% protein A or protein G agarose beads were added and incubated for an additional four hours. The beads were spun down at 13,000 rmp for 3 minutes, supernatant was removed and the beads were washed 1 ml lysis buffer. This washing procedure was repeated for five times in order to remove non-specific binding. After the last wash, 50 µl of 2x Laemmli sample buffer were added, the sample were boiled and subjected to SDS-PAGE and western blot assay.

2.9 GST pulldown

Purified protein or total *E. coli* lysate were prepared in 1 ml volume for GST pulldown. 50 µl of 50% glutathione beads were added and incubated for overnight. The beads were spun down at 13,000 rmp for 3 minutes, supernatant was removed and the beads were washed with 1 ml lysis buffer. This washing procedure was repeated for five times in order to remove non-specific binding. After the last wash, 50 µl of 2x Laemmli sample buffer were added, the sample were boiled and subjected to SDS-PAGE and western blot assay.

2.10 *In vitro* Phosphorylation of Purified Receptor Proteins

Purified receptor proteins were phosphorylated by adding ATP and $MgCl_2$ (5 mM, and 10 mM, respectively) and incubated on ice for varied times. The phosphorylation reactions were quenched by adding EDTA (prepared in 10 mM HEPES pH 7.5) to a final concentration of 25 mM. Proteins were analysed by either SDS-PAGE, native PAGE or western blot to study the protein phosphorylation.

2.11 Isothermal Titration Calorimetry (ITC)

ITC experiments were carried out using a VP Microcal instrument (Northampton, MA) and data were analysed using ORIGIN software. All measurements were repeated at least three times. The experiments were initiated by injecting protein sample from the syringe into the calorimetry cell containing 1.8 ml of another protein sample, used a fixed temperature in a range 15 to 25^{o}C. The change in heat of each injection was recorded automatically using ORIGIN software.

2.12 Surface Plasmon Resonance (SPR) Analysis

Protein-protein interactions were analysed using a BIAcore T100 instrument (GE Healthcare). Dephosphorylated and phosphorylated FGFR2 cytoplasmic domain,

phosphorylated FGFR2 kinase domain and phosphorylated FGFR2 C-terminal tail were immobilized on CM 5 chips according to the standard amine coupling protocol. Briefly, carboxymethyl groups on the chip surface were activated with a 1:1 mixture of N-ethyl-N-(dimethyaminopropyl) carbodiimide (EDC) and N-hydroxysuccinimide (NHS). Proteins were diluted in 20 mM HEPES, pH 6.5 and injected over the activated chip surface. The unbound chip surface was blocked using ethanolamine. Proteins were immobilized to approximately 700 or 300 response units. Different concentrations of analytes were injected over the immobilized chips at a flow rate of 30 µl/min for 60 aeconds, 120 seconds or 150 seconds to obtain kinetic data. Following 180 seconds of dissociation, the sensor surface was regenerated by injection of 30 µl of 0.1% SDS and 60 µl of 500 mM NaCl. Reference responses were substrated from flow cells for each analyte injection using BiaEvaluation software. The resulting sensorgrams were anaylsed to determine the kinetic parameters.

Chapter 3

The effect of Grb2 binding on FGFR2 phosphorylation

3.1 Introduction

FGFs mediate their biological functions by binding to the Ig-like domains of FGFRs, resulting in the dimerisation and phosphorylation of multiple tyrosine residues on the cytoplasmic domain of the receptors. The phosphorylated tyrosine residues have two important roles: activating the tyrosine kinase activity and providing binding sites for other signalling proteins. Mohammadi *et al*. identified six important tyrosine phosphorylation sites on the cytoplasmic domain of FGFR1[139]. Moreover, Furdui *et al*. indicated that tyrosine phosphorylation occurs in a sequential manner in FGFR1[163]. This precise sequential reaction suggests that correct downstream signalling may be a consequence of the proposed phosphorylation pattern.

Previously, we showed the direct interaction between the Grb2 C-SH3 domain and FGFR2[173]. In this chapter, the role of Grb2 in FGFR2 phosphorylation is explored. *In vitro* studies using dot blot indicate that Grb2 binding may induce a conformational change of FGFR2, resulting in the exposure of pre-phosphorylated tyrosine residue(s). *In vitro* FGFR2 phosphorylation immunoblotting studies also suggest that the Grb2-mediated FGFR2 conformational change leads to increased FGFR2 phosphorylation. The positive regulatory effect of Grb2 on FGFR2 phosphorylation is Grb2 concentration–dependent. Isothermal titration calorimetry determinations

revealed a two-site binding model of Grb2 binding to inactivated FGFR2. Therefore, Grb2 may be involved in enhancing FGFR2 phosphorylation. Moreover, we show that Grb2 regulation of FGFR2 phosphorylation is mediated by direct binding through the C-SH3 domain. Grb2 has several flexible structures in solution, which may be important for recognising and binding to its targets[208]. Here, we show that either the N-SH3 domain or SH2 domain alone has no effect on the regulation of FGFR2 phosphorylation, but they may be important in coordinating the role of the C-SH3 domain in FGFR2 activation.

These results provide new insight into the function of Grb2. We determined that Grb2 not only may act as an adaptor protein that recruits downstream signalling proteins but may also play an important role in regulating FGFR2 signalling activity.

3.2 Results

3.2.1 Expression and purification of the functional FGFR2 cytoplasmic domain in mammalian cells, insect cells and *E. coli*

Both eukaryotic and prokaryotic protein expression systems were used in this study. The C-terminal MBP-tagged FGFR2 cytoplasmic domain (residues 309–821) was expressed and purified from stably transfected HEK 293 cells to produce proteins with post-translational modifications. Silver staining was used to confirm the purity of the samples by PAGE after eluting from amylase beads with 10 mM maltose. Figure 3.1 (A) shows the quality of the purified recombinant protein. The expected molecular weight of recombinant MBP-fused FGFR2 cytoplasmic domain is 91 kDa, and multiple bands can be seen on the silver stain gel. These additional bands were likely due to post-translational modifications, such as phosphorylation or glycosylation, of the receptor proteins in HEK 293 cells. To confirm the phosphorylation states of the recombinant cytoplasmic domain and to test if the protein was functional after purification, 10 ng of the recombinant cytoplasmic domain was incubated at 4°C with 5 mM ATP and 10 mM $MgCl_2$. Then, 50 mM EDTA was added to stop the phosphorylation reactions at various time points. SDS-PAGE and anti-phosphotyrosine blotting were used to determine the phosphorylation level of each reaction. The recombinant cytoplasmic domain had a basal level of

phosphorylation, indicating that it was tyrosine-phosphorylated in HEK 293 cells (Figure 3.1 B, 0 sec). The phosphorylation levels increased as the incubation time increased, indicating that the FGFR2 cytoplasmic domain can autophosphorylate (Figure 3.1 B, 0-300 sec). Therefore, we concluded that the purified recombinant cytoplasmic domain retains its tyrosine kinase activity. Because the purified domain was tyrosine-phosphorylated in HEK 293 cells, the protein was treated with CIP to remove phosphate groups to ensure a uniformly unphosphorylated sample as the starting material for further experiments (Figure 3.1 C). However, CIP treatment did not remove all of the phosphate groups, and a trace amount of a tyrosine phosphorylation signal could still be seen on western blots after extended exposure. These results suggest that some of the phosphotyrosines are buried within the cytoplasmic domain and are shielded from phosphatases, which may be important in maintaining signalling complexes and signal transduction *in vivo*[43].

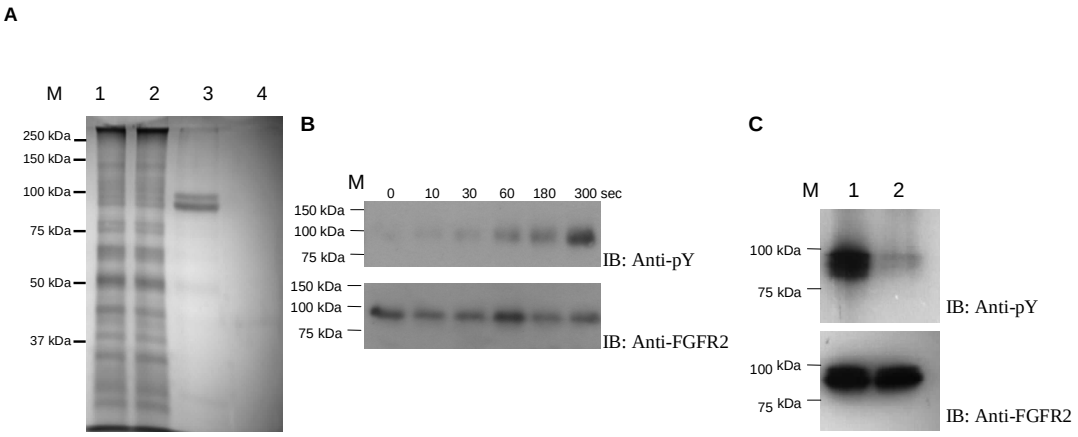

Figure 3.1: Purification and characterisation of the FGFR2 cytoplasmic domain from HEK 293 cells. The plasmid containing the FGFR2 cytoplasmic domain was transfected into HEK 293 cells by the calcium phosphate precipitation method. Cells were harvested and lysed 48 hours post-transfection. The supernatant was incubated with amylose resin for 2 hours. The beads were washed with buffer five times, and the bound MBP-fused FGFR2 cytoplasmic domain was eluted with 10 mM maltose. The purified FGFR2 cytoplasmic domain was then subject to SDS-PAGE to analyse its purity (A), activity (B) and phosphatase-treatment response (C). (A) Silver stain was used to confirm the purity of the purified receptor protein. M, protein marker; lane 1, total cell lysate; lane 2, amylase bead binding flow-through; lane 3, purified cytoplasmic domain; lane 4, elution buffer as the negative control for silver staining. (B) Tyrosine phosphorylation of recombinant FGFR2 cytoplasmic domain *in vitro*. Individual protein samples were incubated with 5 mM ATP and 10 mM $MgCl_2$, and the phosphorylation reactions were quenched by addition of 50 mM EDTA at various time points (0, 10, 30, 60, 180 and 300 sec). Samples were denatured, separated by SDS-PAGE, and immunoblotted for phosphotyrosine. (C) Dephosphorylation of the purified cytoplasmic domain. Anti-phosphotyrosine blot showing the phosphorylation states of the purified cytoplasmic domain and the CIP-treated cytoplasmic domain (upper blot); an anti-FGFR2 antibody was used to confirm equal loading in each lane (lower blot). M, protein marker; lane 1, purified cytoplasmic domain; lane 2, phosphatase-treated cytoplasmic domain. The results are representative of three independent experiments.

The C-terminal tail (last 58 residues of FGFR2) of FGFR2 has five tyrosine residues. Previous studies in our group indicate that the C-terminal tail can be tyrosine-phosphorylated and that C-terminal tyrosine-to-phenylalanine mutants cause

different FGFR2 phosphorylation patterns, suggesting a potential role for the C-terminal tail in the FGFR2-mediated signalling pathway. Therefore, constructs of the cytoplasmic domain including the C-terminal tail of FGFR2 were used to study the phosphorylation sequence of the FGFR2 cytoplasmic domain.

Native gels (5%) were used to separate FGFR2 cytoplasmic domains with different phosphorylation states. Proteins with more phosphate groups have a higher charge/mass ratio and can migrate faster in a native gel than those with lower charge/mass ratios. Purified protein (10 μg) was incubated with ATP and $MgCl_2$ in 100 μl buffer to phosphorylate receptor proteins. The reactions were quenched at different time points. Native gels were run at 35 V for 48 hours. Despite the long running time, the protein samples did not enter the separating gel. However, cytoplasmic domains with different phosphorylation levels were separated in the sample wells (Figure 3.2 A, indicated by red arrows). The gels were then run for an additional 24 hours at 150 V, and silver stain was used to detect proteins in the native gel. Two bands can be seen in lane 1 (Figure 3.2 B), indicating that proteins with two different states, both unphosphorylated and phosphorylated, were present in the sample. This result is consistent with the earlier experimental result that a trace amount of phosphorylation remained, possibly due to phosphotyrosines being buried

within the protein molecule. Surprisingly, the band pattern after 1 hour suggested that a dephosphorylation process occurred after 1-hour incubation. According to Bae *et al*., the tyrosine kinase domain of FGFR may also have phosphatase activity. When a large amount of ADP is built up in solution, the kinase domain can function as a phosphatase and dephosphorylate itself[250]. A similar experiment was carried out using a dephosphorylated FGFR2 kinase domain (residues 412–760, without the C-terminal tail). The dephosphorylated FGFR2 kinase protein samples were incubated with ATP and $MgCl_2$ and then quenched with EDTA after 5 or 10 minutes. The FGFR2 kinase domains with different phosphorylation levels were separated in a 6% native gel (Figure 3.2 C), suggesting that the C-terminus of the FGFR2 cytoplasmic domain may affect protein migration in native gels.

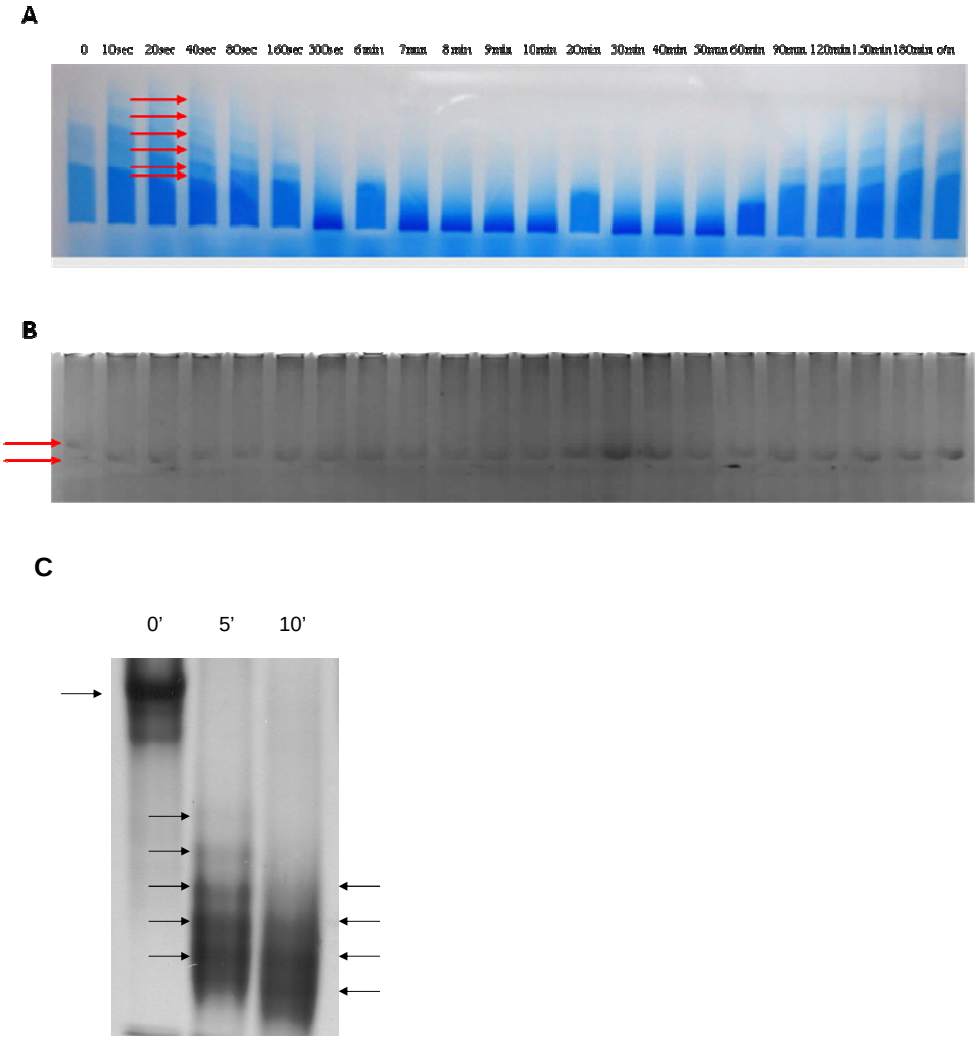

Figure 3.2: Phosphorylation order of the FGFR2 cytoplasmic domain. Native gels were used to separate the FGFR2 cytoplasmic and kinase domains with different phosphorylation states. Proteins with different phosphorylation levels can be separated according to their charge/mass ratio. Purified FGFR2 cytoplasmic domain was treated with CIP, then incubated with ATP/$MgCl_2$ and quenched with EDTA at different time points (from 10 seconds to overnight). Purified FGFR2 kinase domain was treated with CIP, then incubated with ATP/$MgCl_2$ and quenched with EDTA at 5 and 10 minutes. All protein samples were kept in their native states and subjected to native gel electrophoresis analysis. (A) Receptor protein with different phosphorylation levels was separated in the liquid phase in the sample wells. Dephosphorylation can be seen after a one-hour incubation. (B) After 120 hours of running time, receptor proteins remained at the interface of the stacking gel and separating gel. Two bands are observed in lane 1 (time 0), suggesting at least two different phosphorylation states of the protein (phosphorylated and unphosphorylated). (C) Different phosphorylation states of the FGFR2 kinase domain separated in the native gel. The results are representative of three independent experiments.

An insect cell expression system was also used to produce recombinant FGFR2 proteins. Methods for soluble protein extraction from infected insect cells are described in Chapter 2. The soluble fraction from the cells (100 μg) was used in SDS-PAGE and immunoblot experiments to confirm the presence of the receptor protein (Figure 3.3 A). The expected molecular weights of the wild-type full-length FGFR2 (C-terminal MBP/Myc-fused), cytoplasmic domain (C-terminal MBP/Myc-fused), and extracellular domain (C-terminal MBP/Myc-fused) are 124 kDa, 91 kDa and 68 kDa, respectively. A western blot of recombinant wild-type full-length FGFR2 showed multiple bands in the molecular weight range between 250 kDa and 95 kDa, which was likely due to post-translational modifications on the receptor proteins (either glycosylation or phosphorylation). The recombinant cytoplasmic domain has an expected molecular weight of 91 kDa, but it appeared to have a molecular weight around 100 kDa on the western blot, likely because of post-translational modifications on the receptor proteins (phosphorylation). The recombinant extracellular domain has an expected molecular weight at 68 kDa, but it appeared to have multiple bands in the molecular weight range between 130 kDa and 55 kDa on the western blot, which was also likely due to post-translational modifications on the receptor proteins (glycosylation). A general anti-phosphotyrosine antibody was used to study the post-translational modification

(phosphorylation) of these purified proteins. The recombinant wild-type full-length FGFR2 was highly tyrosine-phosphorylated (Figure 3.3 A, lower panel). This result suggests that the receptor is activated after production in the cells, which is likely due to the presence of growth factors in the culture medium that activate the wild-type full-length receptor and in turn induce the phosphorylation reaction of tyrosine residues in the cytoplasmic domain. The recombinant cytoplasmic domain showed a very low level of phosphorylation, which may have been due to the kinase domain using cellular free ATP to enable the autophosphorylation reaction. As expected, the extracellular domain showed no tyrosine phosphorylation. The cytoplasmic domain purification from insect cells was based on amylose and hydroxyapatite chromatographies. The MBP/Myc-tagged cytoplasmic domain was eluted from amylose resin using 10 mM maltose, followed by hydroxyapatite column chromatography (Figure 3.3 B).

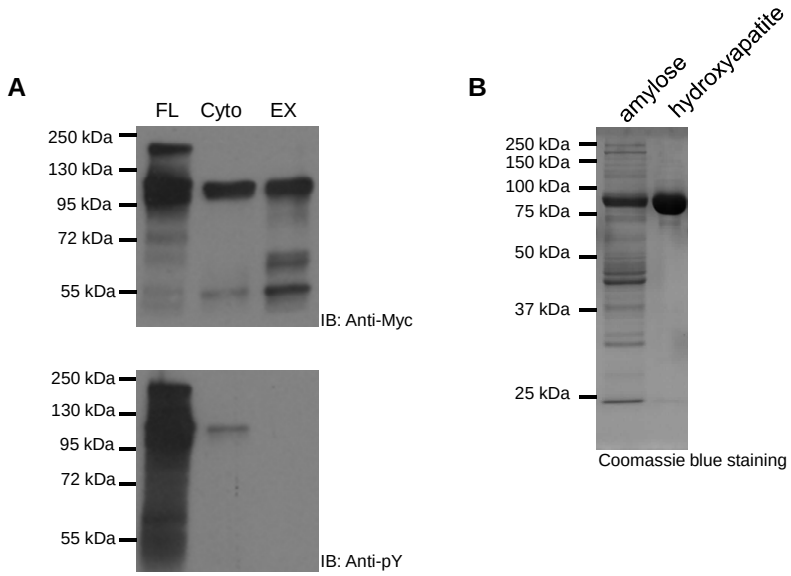

Figure 3.3: Recombinant FGFR2 protein expression and purification in insect Sf9 cells. Wild-type full-length FGFR2 plasmid, FGFR2 cytoplasmic domain plasmid and FGFR2 extracellular domain plasmid were transfected into Sf9 cells to generate recombinant viruses. After 4 days of incubation, culture media containing recombinant viruses were collected, and the virus titre was calculated. To produce recombinant proteins, Sf9 cells were infected with recombinant viruses at MOI=5. The infected cells were grown for 2 days, the cells were harvested and lysed, and the total cell lysate was used for protein expression tests. The supernatant was subjected to protein purification. (A) Expression of recombinant FGFR2 proteins in Sf9 cells. Protein expression and phosphorylation states were confirmed using an anti-Myc antibody and an anti-phosphotyrosine antibody. (B) Purification of recombinant FGFR2 cytoplasmic domain in Sf9 cells. High-purity protein was obtained after amylose and hydroxyapatite chromatographies.

Although the expression and purification of the functional recombinant FGFR2 cytoplasmic domain from eukaryotic protein expression systems (HEK 293 and Sf9 cells) was successful, only 3 μg and 700 μg of recombinant proteins could be extracted from 1 L of HEK 293 cell culture and Sf9 cell cultures, respectively. We decided that these systems do not yield enough protein for biophysical studies.

To maximise protein production, a prokaryotic protein expression system was chosen to carry out large-scale recombinant protein expression and purification. Expression and purification were performed as described in Chapter 2. The recombinant FGFR2 cytoplasmic domain was fused with a C-terminal His-tag. The purity and phosphorylation states of the purified protein were verified by SDS-PAGE and western blots (Figure 3.4). The expected molecular weight of the recombinant His-tagged FGFR2 cytoplasmic domain is 48.8 kDa, but the purified protein appeared to have a molecular weight slightly above 50 kDa, suggesting that the recombinant protein used free ATP and phosphorylated itself in *E. coli*. Western blots also showed that the purified protein had a low level of tyrosine phosphorylation during expression or purification from *E. coli* (Figure 3.4 B). Recombinant cytoplasmic domain (10 ng) was incubated at 4°C with 5 mM ATP and 10 mM $MgCl_2$ in a final volume of 50 µl. Then, 50 mM EDTA was added to stop the phosphorylation reactions at different time points. Samples were denatured and analysed to confirm the tyrosine kinase function. As shown in Figure 3.4 B, the phosphorylation levels of purified proteins increased as the incubation time increased. Thus, the prokaryotically expressed protein retains its tyrosine kinase function.

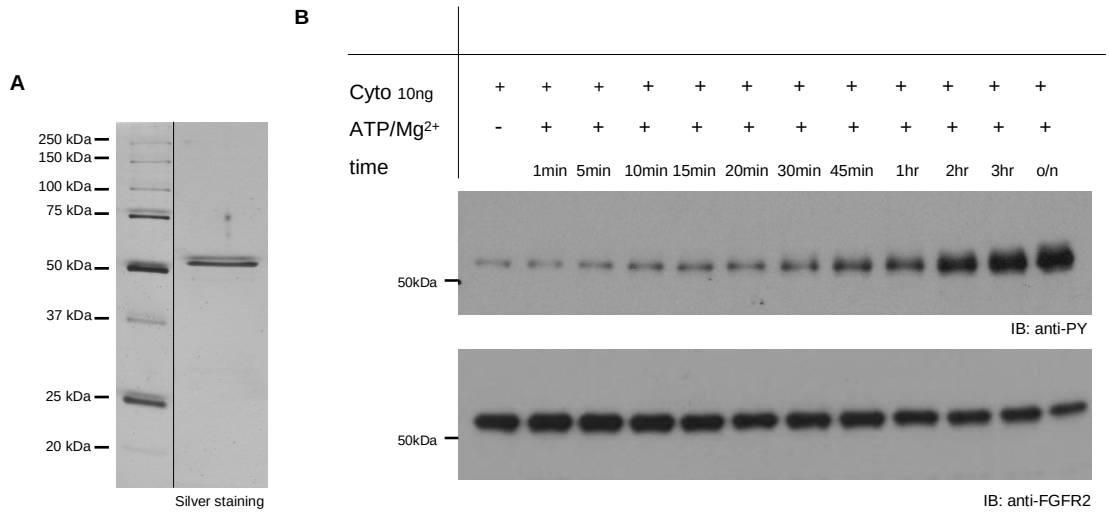

Figure 3.4: Production and characterisation of recombinant FGFR2 cytoplasmic domain in *E. coli*. The FGFR2 cytoplasmic domain plasmid was transformed into Rosetta strain *E. coli* cells to produce recombinant protein by inducing with 0.1 mM IPTG at 20℃ for 16 hours. Cells were harvested and lysed, followed by protein purification. The purified recombinant protein was subjected to SDS-PAGE and silver staining to check its purity. The activity of the protein was determined by incubating the protein with ATP/$MgCl_2$ for various times, and the phosphorylation states were confirmed using anti-phosphotyrosine immunoblot. (A) Coomassie blue staining revealed above 95% purity of the purified protein. (B) Time-dependent tyrosine phosphorylation of purified FGFR2 cytoplasmic domain *in vitro*. Phosphorylation level was determined using an anti-phosphorylation antibody (upper blot); gel loading consistency was checked using an anti-FGFR2 antibody (lower blot). The results are representative of three independent experiments.

3.2.2 *In vitro* phosphorylation of the FGFR2 cytoplasmic domain is enhanced by Grb2

Previous studies in our group have demonstrated that the Grb2 adaptor protein binds to the FGFR2 C-terminal tail directly via its C-SH3 domain; moreover, the binding of Grb2 to FGFR2 prevents site-specific dephosphorylation of FGFR2 by SHP2[173]. However, the role of Grb2 in FGFR2 activation still lacks mechanistic details. The

effect of Grb2 on the FGFR2 cytoplasmic domain phosphorylation was therefore examined using proteins from both insect cells and *E. coli*.

Receptor proteins purified from eukaryotic and prokaryotic cells had low levels of tyrosine phosphorylation (Figure 3.1, 3.2 and 3.4). However, when Grb2 was not present, only a very weak phosphotyrosine signals could be detected when the purified FGFR2 cytoplasmic domain was in its native state on the dot blot (Figure 3.5 A, lane 2). The phosphotyrosine signal could be detected when the purified receptor protein was denatured and probed with an anti-phosphorylation antibody in the absence of Grb2 (Figure 3.5 B, first panel, lane 2). When Grb2 was added to the dot blot, a stronger phosphotyrosine signal could be detected using an anti-phosphotyrosine antibody (Figure 3.5 A, lane 3). Because purified Grb2 is not tyrosine-phosphorylated in the absence of tyrosine kinase and free ATP/$MgCl_2$ (Figure 3.5 B, lane 1), the dot blot suggests that the native FGFR2 cytoplasmic domain may have a conformation that buries endogenous phosphotyrosine(s) within itself. The phosphotyrosine can only access the antibody when either the protein is denatured or Grb2 is bound to it, altering its conformation and resulting in exposure of the phosphotyrosine residue(s). However, the receptor protein mixed with Grb2 showed no increase in FGFR2 tyrosine phosphorylation, i.e., Grb2 does not enable

cis/trans phosphorylation of the receptor proteins (Figure 3.5 B, first panel, lane 2 and 3). These results suggest a potential role for Grb2 in changing the FGFR2 conformation, but this hypothesis still needs to be investigated thoroughly.

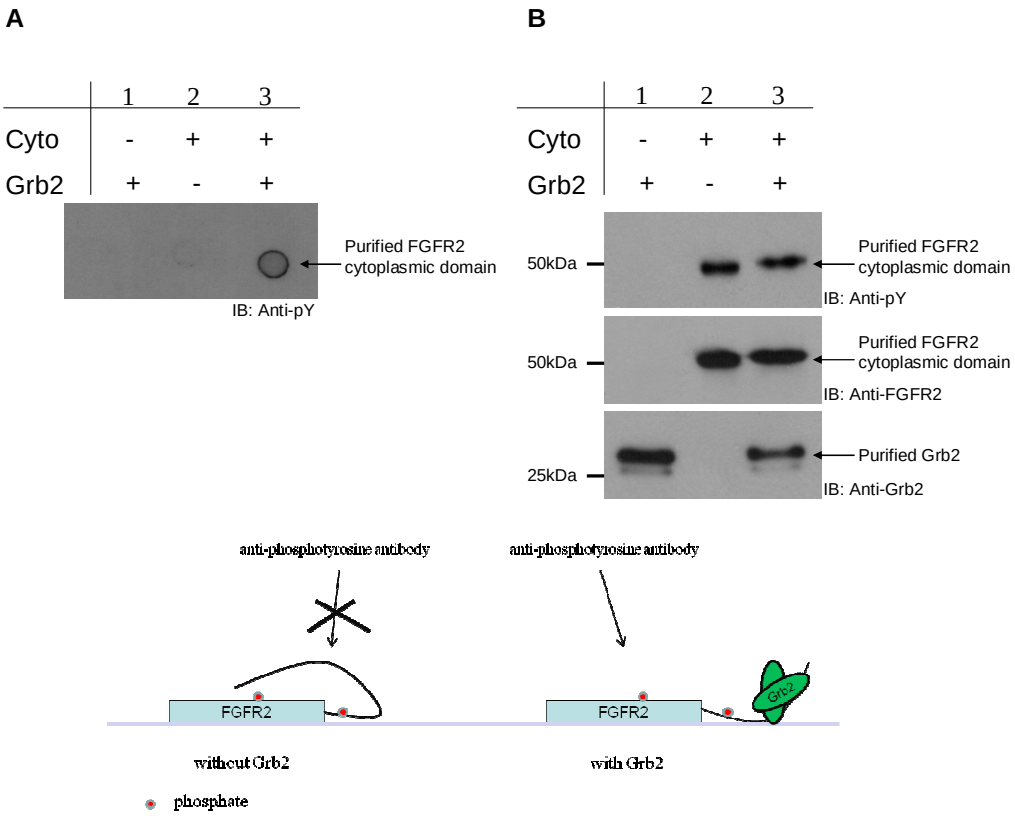

Figure 3.5: Grb2 exposes buried phosphotyrosine(s) of the FGFR2 cytoplasmic domain. Purified FGFR2 cytoplasmic domain was added onto a nitrocellulose membrane, and Grb2 protein was added to the same dot immediately. The effect of Grb2 in exposing phosphotyrosine residue(s) was examined using an anti-phosphotyrosine antibody. (A) A very weak tyrosine phosphorylation signal could be detected on the FGFR2 cytoplasmic domain without adding Grb2. However, a stronger phosphotyrosine signal could be detected when Grb2 was mixed with FGFR2 cytoplasmic domain protein. (B) Denaturing gels and anti-phosphotyrosine blots were used to examine the phosphorylation state of the purified receptor with/without the presence of Grb2. This experiment suggests that the phosphotyrosine signals seen on the dot blot may have been due to exposure of the buried phosphotyrosine(s) of the FGFR2 cytoplasmic domain by Grb2. The results are representative of two independent experiments.

The dot blot results suggest that Grb2 may induce a conformational change of the FGFR2 cytoplasmic domain. Therefore, we investigated the role of Grb2 in receptor phosphorylation. To find suitable conditions (concentrations and times) for testing the role of Grb2 in FGFR2 phosphorylation, various concentrations of the purified FGFR2 cytoplasmic domain were incubated with ATP/$MgCl_2$ in a final volume of 100 μl at 4°C for 15 minutes, 1 hour or overnight. The phosphorylation levels of the cytoplasmic domain were examined using an anti-phosphotyrosine antibody (Figure 3.6 A, upper panel). The protein concentration of the FGFR2 cytoplasmic domain was confirmed using an anti-FGFR2 antibody (Figure 3.6 A, lower panel). We determined that 10 ng of the FGFR2 cytoplasmic domain was the best condition for investigating the role of Grb2 in FGFR2 activation and for understanding the mechanism of FGFR2 activation enhanced by Grb2. Under this condition, the FGFR2 cytoplasmic domain is only phosphorylated at a low level. Therefore, if Grb2 enhances FGFR2 phosphorylation, this condition would allow for comparisons between increased intensities of phosphorylation signals.

First, to determine the role of Grb2 in FGFR2 cytoplasmic domain activation, 10 ng of FGFR2 cytoplasmic domain was mixed with various amounts of Grb2 and ATP/$MgCl_2$ in a final volume of 100 μl at 4°C for 15 minutes.

Activation/phosphorylation levels of the FGFR2 cytoplasmic domain were detected using an anti-phosphotyrosine antibody. The phosphotyrosine signal was significantly increased by Grb2 in a concentration-dependent manner (Figure 3.6 C, upper blot). These data suggest that Grb2 binds to FGFR2, thereby altering the receptor conformation and enabling FGFR2 cytoplasmic domain auto-phosphorylation.

However, the same experiment was repeated using purified FGFR2 kinase domain, which does not have the C-terminal tail (Figure 3.6 B). The result shows that Grb2 has no effect in enhancing FGFR2 kinase domain phosphorylation (Figure 3.6 D, upper blot). Because we have previously shown that Grb2 binds to the FGFR2 C-terminal tail, we propose that the direct binding of Grb2 to the FGFR2 C-terminal tail changes the FGFR2 conformation to favour its kinase activity. Thus, Grb2 binding enhances FGFR2 auto-phosphorylation.

A

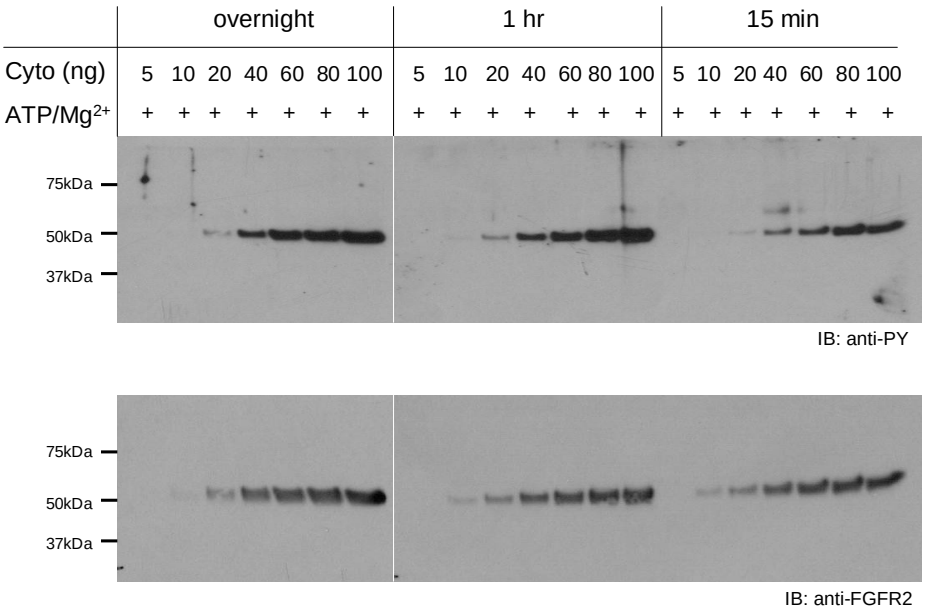
overnight
1 hr
15 min
Cyto (ng)
5 10 20 40 60 80 100 5 10 20 40 60 80 100 5 10 20 40 60 80 100
ATP/Mg2+
+ +
75kDa
50kDa
37kDa
IB: anti-PY
75kDa
50kDa
37kDa
IB: anti-FGFR2

B

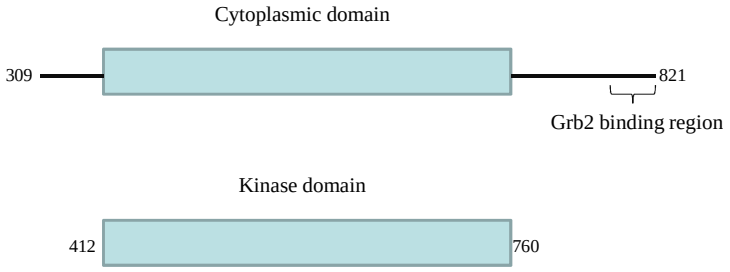
Cytoplasmic domain
309
821
Grb2 binding region
Kinase domain
412
760

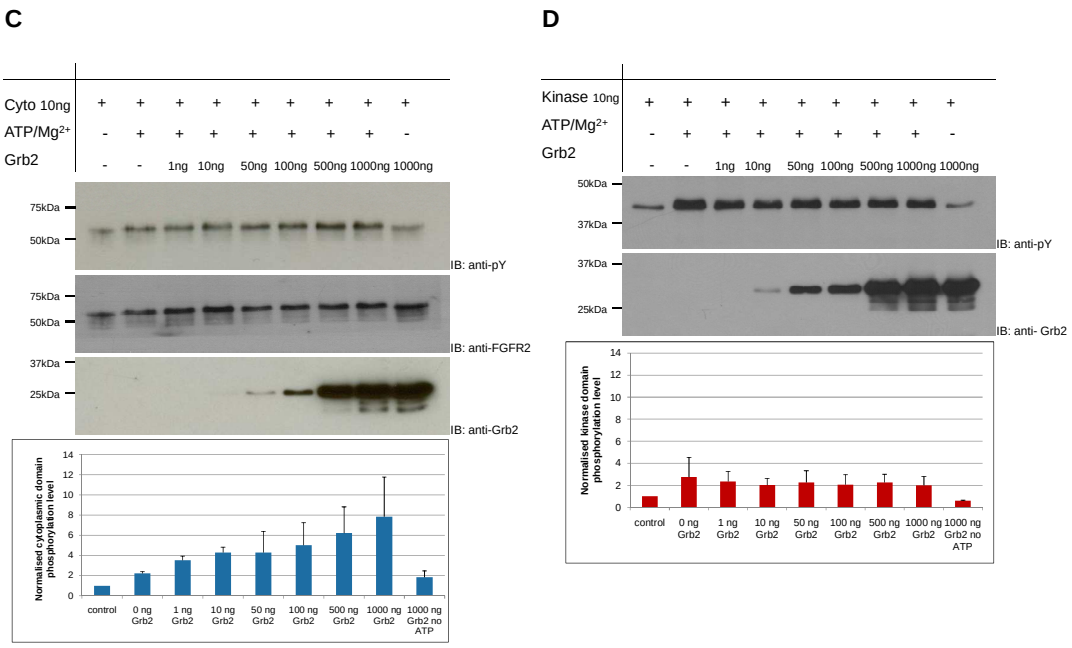

Figure 3.6: Grb2 enhances the tyrosine kinase activity of the FGFR2 cytoplasmic domain, but not the FGFR2 kinase domain. To optimise the experimental conditions, different concentrations of purified FGFR2 cytoplasmic domains were incubated with ATP/$MgCl_2$ for 15 min, 1 hour, or overnight. The phosphorylation levels of the auto-phosphorylated FGFR2 cytoplasmic domains were examined using a general anti-phosphotyrosine antibody. To compare the effects of Grb2 on the phosphorylation of the FGFR2 cytoplasmic and kinase domains, 10 ng of purified FGFR2 cytoplasmic domain or FGFR2 kinase domain was mixed with different amounts of Grb2 with/without ATP/$MgCl_2$ and incubated for 15 minutes. The amount of phosphorylation was detected by immunoblotting with an anti-phosphotyrosine antibody. (A) Different amounts of FGFR2 cytoplasmic domain, and different incubation times were used to determine the ideal conditions for further studies. Ultimately, 10 ng of FGFR2 cytoplasmic domain with ATP/$MgCl_2$ in a final volume of 100 µl for 15 minutes was chosen. (B) Illustration of the FGFR2 cytoplasmic (residues 309–821) and kinase (residues 412–760) domains. (C) Addition of Grb2 in the presence of ATP/$MgCl_2$ increases the level of FGFR2 cytoplasmic domain phosphorylation in a concentration-dependent manner. (D) Addition of Grb2 has no effect on enhancing FGFR2 kinase domain phosphorylation in the presence of ATP/$MgCl_2$. The tyrosine phosphorylation levels were detected using a general anti-phosphotyrosine antibody. To assess equal loading of the FGFR2 cytoplasmic domain, blots were stripped and re-probed with anti-FGFR2 antibody; however, there is no suitable antibody for FGFR2 kinase domain detection (Figure 3.6 B.; as opposed to the cytoplasmic domain, the kinase domain lacks the C-terminal tail and therefore cannot be detected by FGFR2 antibodies). The increased amount of Grb2 was confirmed using an anti-Grb2 antibody. The results are representative of at least two independent experiments.

3.2.3 The enhanced kinase activity of the FGFR2 cytoplasmic domain is mediated by the Grb2 C-SH3 domain

We conducted several experiments to characterise the mechanism by which direct binding of Grb2 enhances FGFR2 activation. First, several Grb2 constructs were created (Figure 3.7 A) and the recombinant proteins were purified. The role of these different Grb2 domains was examined as described above. Briefly, 10 ng of recombinant FGFR2 cytoplasmic domain was incubated with or without ATP/$MgCl_2$ and with or without Grb2 domains at various concentrations ranging from 1 ng to 1000 ng. All reactions had a final volume of 100 µl and were incubated on ice for 15 minutes. SDS-PAGE and western blotting were used to determine the FGFR2 cytoplasmic domain phosphorylation levels from all reactions (Figure 3.7 B–H).

The Grb2 R86A mutant (Arg-86 is conserved in the canonical SH2 FLI/VRES motif) caused an increase in the phosphorylation of FGFR2 cytoplasmic domain, with its maximal effect at its maximum at 10 ng protein, whereas the wild-type Grb2 augmented FGFR2 kinase activity in a concentration-dependent manner up to 1000 ng in a 100 µl solution volume (Figure 3.7 B). The Grb2 N-SH3 domain alone and the SH2 domain alone had no effects on the phosphorylation of FGFR2 cytoplasmic domain (Figure 3.7 C and D, respectively). The Grb2 C-SH3 domain alone enhanced

the phosphorylation of FGFR2 cytoplasmic domain and had its maximum effect at 10 ng (Figure 3.7 E). Therefore, we concluded that the Grb2-enhanced the phosphorylation of FGFR2 cytoplasmic domain is mediated by the Grb2 C-SH3 domain. A truncated polypeptide was also expressed, which included the Grb2 SH2 domain with either the N-SH3 domain or the C-SH3 domain, to test if the SH2 and SH3 domains cooperatively regulate the FGFR2 kinase activity. The NSH3-SH2 domain (500 ng of protein) slightly enhanced the phosphorylation of FGFR2 cytoplasmic domain, even though the N-SH3 domain alone and the SH2 domain alone had no effect. When the SH2-CSH3 domain was used, enhanced phosphorylation of FGFR2 cytoplasmic domain was observed, similar to the wild-type Grb2 or the C-SH3 domain alone.

We hypothesised that the Grb2 interaction with the cytoplasmic domain of FGFR2 occurs via the C-SH3 domain but is enhanced by the presence of the SH2 domain or another domain in the case of the NSH3-CSH3 polypeptide.

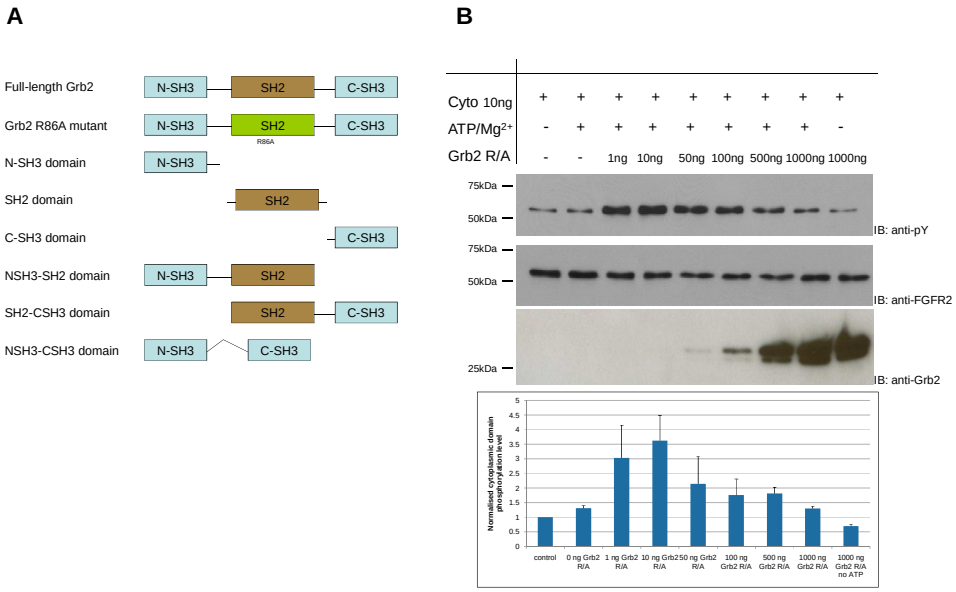
A
Full-length Grb2
N-SH3
SH2
C-SH3
Grb2 R86A mutant
R86A
N-SH3 domain
SH2 domain
C-SH3 domain
NSH3-SH2 domain
SH2-CSH3 domain
NSH3-CSH3 domain
B
Cyto 10ng
ATP/Mg2+
Grb2 R/A
control
0 ng Grb2 R/A
1 ng Grb2 R/A
10 ng Grb2 R/A
50 ng Grb2 R/A
100 ng Grb2 R/A
500 ng Grb2 R/A
1000 ng Grb2 R/A
1000 ng Grb2 R/A no ATP
75kDa
50kDa
25kDa
IB: anti-pY
IB: anti-FGFR2
IB: anti-Grb2
Normalised cytoplasmic domain phosphorylation level

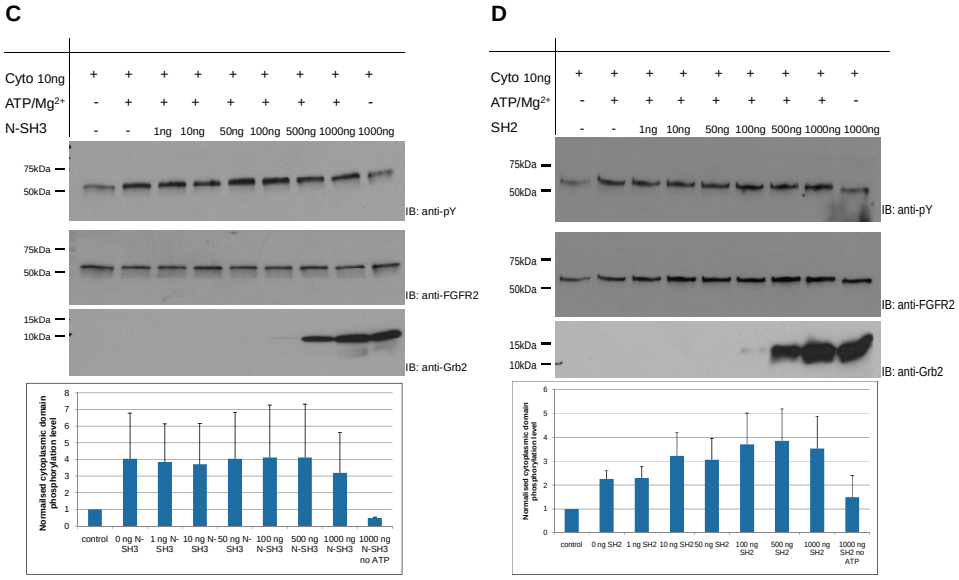
C
Cyto 10ng
ATP/Mg2+
N-SH3
control
0 ng N-SH3
1 ng N-SH3
10 ng N-SH3
50 ng N-SH3
100 ng N-SH3
500 ng N-SH3
1000 ng N-SH3
1000 ng N-SH3 no ATP
75kDa
50kDa
15kDa
10kDa
IB: anti-pY
IB: anti-FGFR2
IB: anti-Grb2
Normalised cytoplasmic domain phosphorylation level
D
Cyto 10ng
ATP/Mg2+
SH2
control
0 ng SH2
1 ng SH2
10 ng SH2
50 ng SH2
100 ng SH2
500 ng SH2
1000 ng SH2
1000 ng SH2 no ATP
75kDa
50kDa
15kDa
10kDa
IB: anti-pY
IB: anti-FGFR2
IB: anti-Grb2
Normalised cytoplasmic domain phosphorylation level

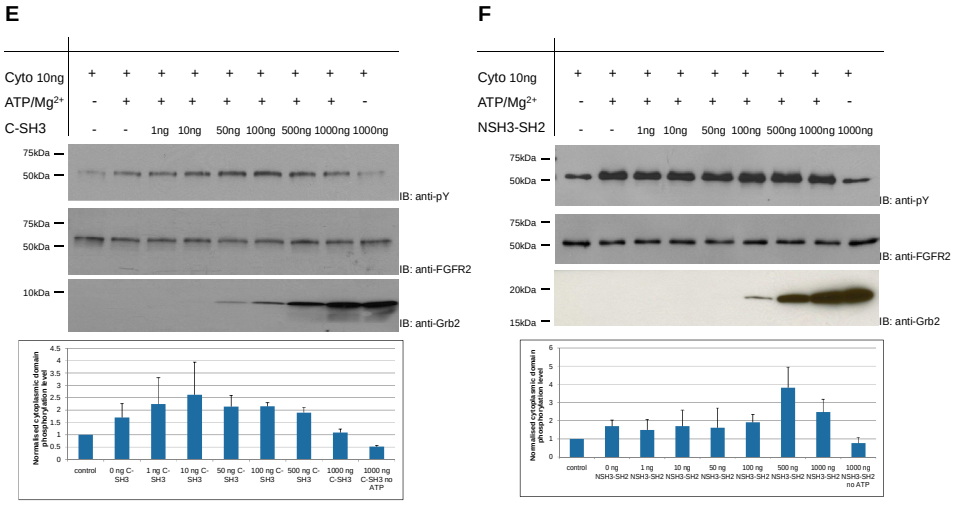
E
Cyto 10ng
ATP/Mg2+
C-SH3
control
0 ng C-SH3
1 ng C-SH3
10 ng C-SH3
50 ng C-SH3
100 ng C-SH3
500 ng C-SH3
1000 ng C-SH3
1000 ng C-SH3 no ATP
75kDa
50kDa
10kDa
IB: anti-pY
IB: anti-FGFR2
IB: anti-Grb2
Normalised cytoplasmic domain phosphorylation level
F
Cyto 10ng
ATP/Mg2+
NSH3-SH2
control
0 ng NSH3-SH2
1 ng NSH3-SH2
10 ng NSH3-SH2
50 ng NSH3-SH2
100 ng NSH3-SH2
500 ng NSH3-SH2
1000 ng NSH3-SH2
1000 ng NSH3-SH2 no ATP
75kDa
50kDa
20kDa
15kDa
IB: anti-pY
IB: anti-FGFR2
IB: anti-Grb2
Normalised cytoplasmic domain phosphorylation level

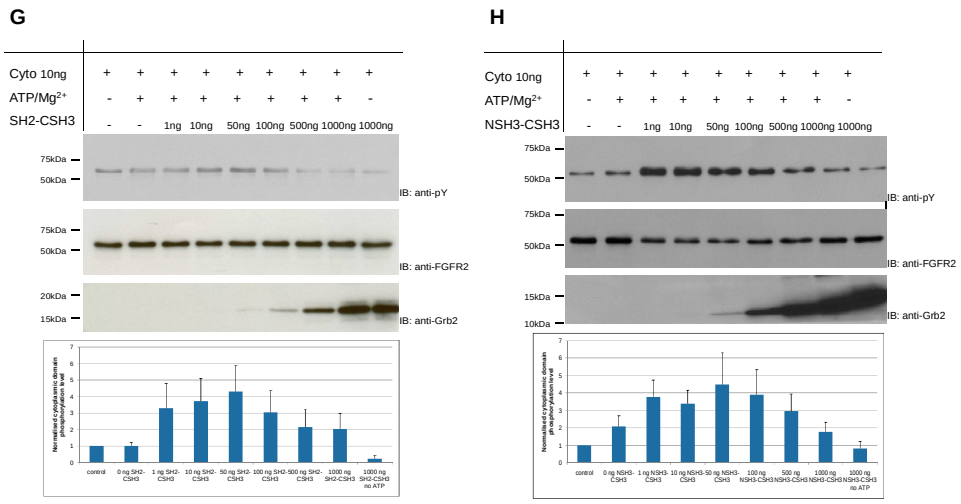

Figure 3.7: Effects of Grb2 and its various domains on the phosphorylation of FGFR2 cytoplasmic domain. Purified FGFR2 cytoplasmic domain (10 ng) was mixed with different amounts of individual domains of Grb2 with/without ATP/$MgCl_2$ and incubated for 15 minutes. The amount of phosphorylation was detected by immunoblotting with an anti-phosphotyrosine antibody. (A) Illustration of the different Grb2 domains used in this study. (B) Enhanced phosphorylation of FGFR2 cytoplasmic domain by the Grb2 R86A mutant. (C) The N-SH3 domain alone has no effect on enhancing phosphorylation of FGFR2 cytoplasmic domain. (D) The SH2 domain alone has no effect on enhancing phosphorylation of FGFR2 cytoplasmic domain. (E) Enhanced phosphorylation of FGFR2 cytoplasmic domain by the Grb2 C-SH3 domain alone. (F) Enhanced phosphorylation of FGFR2 cytoplasmic domain by the Grb2 NSH3-SH2 domain. (G) Enhanced phosphorylation of FGFR2 cytoplasmic domain by the Grb2 SH2-CSH3 domain. (H) Enhanced phosphorylation of FGFR2 cytoplasmic domain by Grb2 NSH3-C-SH3 domain. The phosphorylation of the FGFR2 cytoplasmic domain was monitored by anti-phosphotyrosine antibody. As a control, an anti-FGFR2 antibody was used to confirm that an equal amount of the FGFR2 cytoplasmic domain was used in all experiments. Increasing amounts of Grb2 and various domains were confirmed using anti-Grb2 antibodies against the N-SH3 domain (anti-Grb2 (F-9)), SH2 domain (anti-Grb2 (C-7)), and C-SH3 domain (anti-Grb2 (C-23)). The amounts of FGFR2 phosphorylation were quantified using densitometry and are represented graphically. The results are representative of at least two independent experiments.

These data suggest that the SH2 domain alone has no effect on FGFR2 cytoplasmic domain activity, but it enables the N-SH3 and C-SH3 domains to more efficiently

enhance the FGFR2 cytoplasmic domain activity by keeping the conformation of the N-SH3 and C-SH3 domains stable. The same theory can be applied to the N-SH3 and C-SH3 domains. Grb2 with the SH2 domain deletion (NSH3-CSH3) was also used to examine this protein's ability to enhance FGFR2 cytoplasmic domain activity. Notably, this construct enhanced FGFR2 cytoplasmic domain activity at a concentration of 10 ng (Figure 3.7 F), which is similar to the effect observed for wild-type Grb2 and the Grb2 R86A mutant. Together with the *in vitro* Grb2-enhanced FGFR2 cytoplasmic domain activity, these data suggest that all of the Grb2 domains are important in enhancing the FGFR2 cytoplasmic domain activity by stabilising the Grb2 conformation.

3.2.4 FGFR2 binding to Grb2

A previous study investigated the interaction between Grb2 and the FGFR2 C-terminal tail. Isothermal titration calorimetry (ITC) studies have shown direct binding of Grb2 to an unphosphorylated FGFR2 peptide corresponding to the last 15 amino acid residues with an affinity dissociation constant (K_D) of 4 μM and to a phosphorylated FGFR2 peptide corresponding to the same region with a binding affinity of 2 μM. The Grb2 C-SH3 domain binds to the same unphosphorylated and phosphorylated FGFR2 peptides with affinities between 10 to 100 μM[173]. Full-length

FGFR2 cytoplasmic domains (dephosphorylated and re-phosphorylated) and full-length Grb2 were used to investigate the FGFR2–Grb2 binding mechanism *in vitro* by biophysical methods. Both the FGFR2 cytoplasmic domain and Grb2 were expressed and purified from *E. coli*. All of the proteins exhibited purities above 98% as determined by SDS-PAGE with Coomassie blue staining. We used ITC to determine the affinity and stoichiometry of the full-length dephosphorylated FGFR2 cytoplasmic domain binding to full-length Grb2 (Figure 3.8). Grb2 was present in the calorimeter cell, and dephosphorylated FGFR2 cytoplasmic domain was loaded in the syringe. The data fit to a model corresponding to a two-site binding event, with two Grb2 molecules binding to one dephosphorylated FGFR2 cytoplasmic domain with a first dissociation constant of 0.1 µM and a second dissociation constant of 27 µM. The initial binding event had a stoichiometry of 0:5, corresponding to one molecule of FGFR2 binding to two Grb2 molecules. The second binding event had a stoichiometry of 1:1, corresponding to equal numbers of molecules interacting.

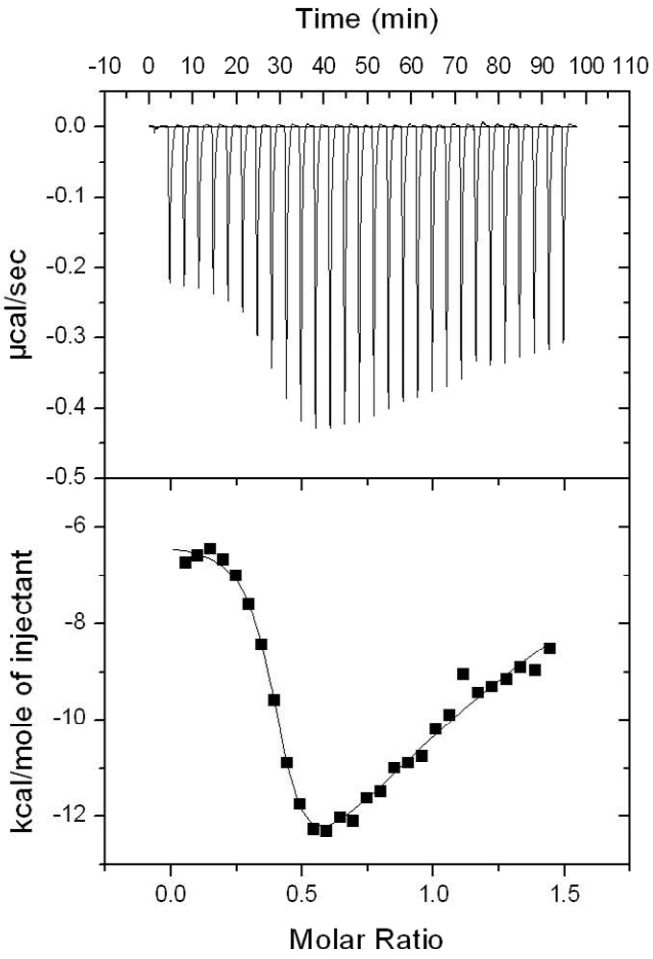

Figure 3.8: ITC measurement of the interaction between the dephosphorylated FGFR2 cytoplasmic domain with Grb2. Purified FGFR2 cytoplasmic domain was dephosphorylated using CIP. Twenty-eight 10-µl injections of dephosphorylated FGFR2 cytoplasmic domain were titrated into Grb2 at 15℃. The top panel shows the data for the baseline-corrected power versus time at 15℃, while the bottom panel shows the integrated heats and the molar ratio of the dephosphorylated FGFR2 cytoplasmic domain to Grb2. The data were corrected for the heats of dilution of the dephosphorylated FGFR2 cytoplasmic domain and fit to a two-site binding model. The results are representative of four independent experiments.

Four possible 2:1 Grb2-FGFR2 binding models can be proposed based on the ITC results (Figure 3.9). In model A, two monomeric Grb2 molecules bind to one FGFR2 molecule on two different proline-rich regions via the Grb2 C-SH3 domain. This model is plausible because the FGFR2 C-terminal tail is proline-rich and has four

PXXP motifs for SH3 domain binding (see Figure 3.9; the proline-rich regions are shown in pink, and the PXXP motifs are underlined). Moreover, our data presented above and the pull-down results indicate that the Grb2 C-SH3 domain is the major region of Grb2 involved in the Grb2–FGFR2 interaction[173]. The first Grb2 molecule binds to the proline-rich region located in the last 15 residues with a higher binding affinity, whereas the second Grb2 molecule binds to another unidentified proline-rich region with a lower binding affinity. In model B, one Grb2 molecule binds to one FGFR2 molecule at the first proline-rich region via its C-SH3 domain, and another Grb2 molecule binds to the same FGFR2 molecule at the second proline-rich region via its N-SH3 domain. This model is based on the *in vitro* GST pull-down experiment, which indicated the N-SH3 domain of Grb2 can also precipitate FGFR2 in the HEK 293 cell line expressing wild-type FGFR2, even though the same result could not be obtained using the NIH-3T3 cell line expressing endogenous FGFR2. Moreover, FLIM data have provided clear evidence that both the N-SH3 and C-SH3 domains of Grb2 bind to FGFR2 in both stimulated and unstimulated cells[173]. Altogether these results suggest a low-affinity binding of the Grb2 N-SH3 domain to FGFR2. McDonald *et al*. proposed that Grb2 may form a dimer[251]. Therefore, in models C and D, we propose that Grb2 forms a dimer and the dimeric Grb2 binds to one FGFR2 molecule via its SH3 domains.

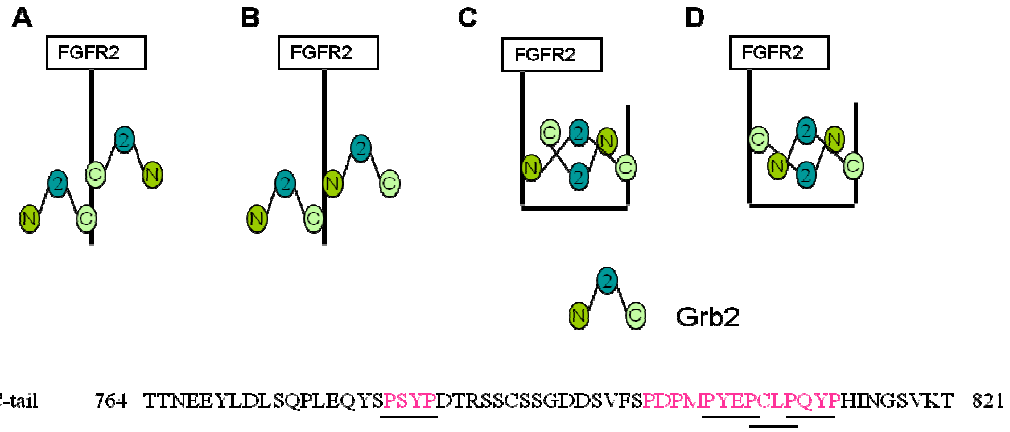

Figure 3.9: The four potential models of 2:1 Grb2-FGFR2 binding. The C-terminal tail of FGFR2 has four proline-rich regions, which could serve as binding sites for the Grb2 N-SH3 and C-SH3 domains. (A) Two Grb2 molecules bind to one FGFR2 molecule on two different proline-rich regions via their C-SH3 domains. (B) One Grb2 molecule binds to one FGFR2 molecule at the first proline-rich region via its C-SH3 domain, and another Grb2 molecule binds to the same FGFR2 molecule at the second proline-rich region via its N-SH3 domain. (C) and (D) Two Grb2 molecules form a dimer and bind to the C-terminal loop of FGFR2 via the N-SH3 domain or C-SH3 domain.

Additional studies are still needed to understand the detailed mechanism of Grb2 binding to FGFR2. First, no biophysical data support the direct binding of the N-SH3 domain to FGFR2. If such binding occurs, it would be important to determine the binding site on FGFR2 and the binding affinity of the N-SH3 domain to the full-length FGFR2 cytoplasmic domain. The C-SH3 domain interacts with FGFR2 directly *in vivo*, and an ITC binding study using purified C-SH3 domain and FGFR2 peptides also showed a binding affinity above 10 μM[173]. Second, it is unclear if the affinity of the full-length FGFR2 cytoplasmic domain will be similar to that of FGFR2 peptides. Third, the SH2 domain does not interact with FGFR2 in basal or

ligand-stimulated cells. Therefore, one of the SH2 domains might function to stabilise either the N-SH3 or C-SH3 domain structure. To examine this possibility, we tested the interactions of the NSH3-SH2 and SH2-CSH3 domains with the FGFR2 cytoplasmic domain using surface plasmon resonance (SPR) technology.

Moreover, to examine whether the SH2 domain can enhance the binding affinity to the FGFR2 cytoplasmic domain by stabilising the N-SH3 and C-SH3 domain conformations, we prepared the NSH3-SH2 and SH2-CSH3 domains for SPR studies. The NSH3-CSH3 domain was also prepared, to compare the binding status with the N-SH3 or C-SH3 domain alone. Purified dephosphorylated FGFR2 cytoplasmic domain was covalently immobilised on a CM5 chip, and different concentrations of Grb2 N-SH3, C-SH3, NSH3-SH2, SH2-CSH3 and NSH3-CSH3 domains were used as the analytes.

A range of concentrations of the Grb2 N-SH3 domain (1 µM to 400 µM) were flowed across the immobilised FGFR2 cytoplasmic domain, and direct binding was detected only at 400 µM. This may have been due to non-specific interactions, and such high concentration is probably not physiologically relevant (Figure 3.10 A).

Various concentrations of the Grb2 C-SH3 domain (1 µM to 1000 µM) showed weak binding (binding affinity above 500 µM) to immobilised FGFR2 cytoplasmic domain (Figure 3.10 B). Notably, various concentrations of the Grb2 NSH3-SH2 domain (1 µM to 753 µM) or SH2-CSH3 domain (1 µM to 471 µM) bound to the immobilised FGFR2 cytoplasmic domain exhibited binding affinities of 349 µM (Figure 3.10 C) or 135 µM (Figure 3.10 D), respectively. The SH2-deleted NSH3-CSH3 polypeptide also interacted directly with the immobilised FGFR2 cytoplasmic domain with a binding affinity of 296 µM (Figure 3.10 E). The SPR results suggest that NSH3-SH2, SH2-CSH3 and NSH3-CSH3 have stronger binding affinities for FGFR2 than the N-SH3 or C-SH3 domain alone.

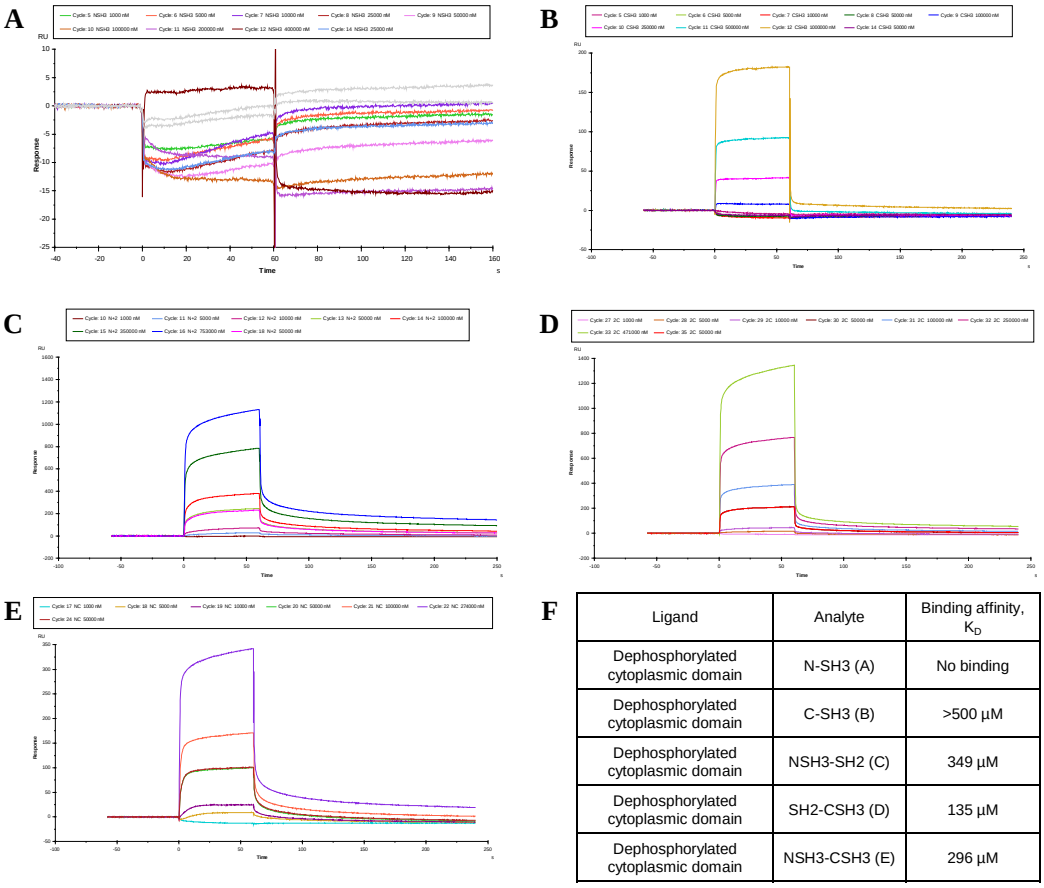

Ligand	Analyte	Binding affinity, K_D
Dephosphorylated cytoplasmic domain	N-SH3 (A)	No binding
Dephosphorylated cytoplasmic domain	C-SH3 (B)	>500 µM
Dephosphorylated cytoplasmic domain	NSH3-SH2 (C)	349 µM
Dephosphorylated cytoplasmic domain	SH2-CSH3 (D)	135 µM
Dephosphorylated cytoplasmic domain	NSH3-CSH3 (E)	296 µM

Figure 3.10: Surface plasmon resonance analysis of dephosphorylated FGFR2–Grb2 interactions. Purified FGFR2 cytoplasmic domain was dephosphorylated by CIP and immobilised on a CM5 chip. Different Grb2 domains were purified, and various concentrations of the Grb2 proteins were flowed over the chip. (A) Sensorgrams of the Grb2 N-SH3 domain binding to dephosphorylated FGFR2 cytoplasmic domain. (B) Sensorgrams of the Grb2 C-SH3 domain binding to dephosphorylated FGFR2 cytoplasmic domain. (C) Sensorgrams of the Grb2 NSH3-SH2 domain binding to dephosphorylated FGFR2 cytoplasmic domain. (D) Sensorgrams of the Grb2 SH2-CSH3 domain binding to dephosphorylated FGFR2 cytoplasmic domain. (E) Sensorgrams of the Grb2 NSH3-CSH3 domain binding to dephosphorylated FGFR2 cytoplasmic domain. (F) Summary of the binding affinities of dephosphorylated cytoplasmic domain for various Grb2 domains. The N-SH3 domain does not bind to the FGFR2 cytoplasmic domain. The C-SH3 domain binds to the FGFR2 cytoplasmic domain with a K_D>500 µM, the NSH3-SH2 domain binds to the FGFR2 cytoplasmic domain with a K_D=349 µM, the SH2-CSH3 domain binds to the FGFR2 cytoplasmic domain with a K_D=135 µM, and the NSH3-CSH3 domain binds to the FGFR2 cytoplasmic domain with a K_D=296 µM. These data suggest that direct binding of the Grb2 N-SH3 domain or C-SH3 domain to dephosphorylated FGFR2 cytoplasmic domain can be enhanced by another Grb2 domain. The biosensor chip response is shown on the *y*-axis (RU) as a function of time (*x*-axis) at 20℃. The results are representative of at least two independent experiments.

The two-site binding of Grb2 to dephosphorylated FGFR2 cytoplasmic domain and the role of Grb2 in FGFR2 activation have been investigated and are discussed above. *In vitro* FGFR2 phosphorylation studies, ITC measurements and SPR binding studies suggest a model in which the binding of Grb2 to the dephosphorylated (inactive) FGFR2 cytoplasmic domain enhances FGFR2 activity by altering the receptor conformation.

In addition, an earlier study indicates that Grb2 binds to a phosphorylated FGFR2 C-terminal peptide with a 2 μM binding affinity. Moreover, GST pull-down, immunoprecipitation, fluorescent confocal microscopy and FLIM experiments also indicate that Grb2 associates with FGF-stimulated FGFR2 both *in vitro* and *in vivo*[173]. Thus, studies in this section focused on exploring the interaction between phosphorylated (activated) FGFR2 and Grb2, using the full-length FGFR2 cytoplasmic domain rather than the phosphopeptide. To mimic the early signalling process *in vivo*, the purified FGFR2 cytoplasmic domain was autophosphorylated in the presence of ATP/$MgCl_2$ for 15 to 30 minutes. The phosphorylation reaction was quenched by the addition of EDTA, followed by size-exclusion chromatography to achieve complete buffer exchange and remove any contamination.

The interaction between the phosphorylated FGFR2 cytoplasmic domain and Grb2 was analysed by SPR. To identify whether Grb2 can bind to phosphorylated FGFR2 cytoplasmic domain via its C-SH3 domain, three different Grb2 constructs were purified: Grb2 C-SH3 domain, Grb2 R86A mutant (a conserved arginine-to-alanine mutation in the SH2 domain) and Grb2 NSH3-CSH3 domains with the deletion of the SH2 domain. The phosphorylated FGFR2 cytoplasmic domain was covalently immobilised to a CM5 sensor chip via its primary amine at about 300 RU. The Grb2 C-SH3 domain, Grb2 R86A mutant or Grb2 NSH3-CSH2 domains were passed over the chip in solution. We used sample injections of 45 µl at a flow rate of 30 µl/min. The application of a range of concentrations of Grb2 C-SH3 domain (1 µM to 1 mM), Grb2 R86A mutant protein (1 µM to 400 µM) or Grb2 NSH3-CSH3 domains (1 µM to 200 µM) to the immobilised phosphorylated FGFR2 cytoplasmic domain yielded an increase in signal resulting from specific binding of ligands, followed by a decrease in signal upon dissociation of the ligands (Figure 3.11 A, B and C). Grb2 C-SH3 bound to the phosphorylated FGFR2 cytoplasmic domain with an affinity of 104 µM (Figure 3.11 A), whereas the Grb2 R86A mutant and Grb2 NSH3-CSH3 domains bound to the phosphorylated FGFR2 cytoplasmic domain with similar binding affinities: 2.65 µM for Grb2 R86A (Figure 3.11 B) and 15.4 µM for the Grb2 NSH3-CSH3 domains (Figure 3.11 C). This SPR binding study not only shows the

direct binding of Grb2 to the phosphorylated FGFR2 cytoplasmic domain via the Grb2 SH3 domains but also supports the hypothesis that the N-SH3 domain, and probably also the SH2 domain, is important in enhancing the C-SH3 domain binding affinity toward the phosphorylated FGFR2 cytoplasmic domain by stabilising the SH3 domain structure.

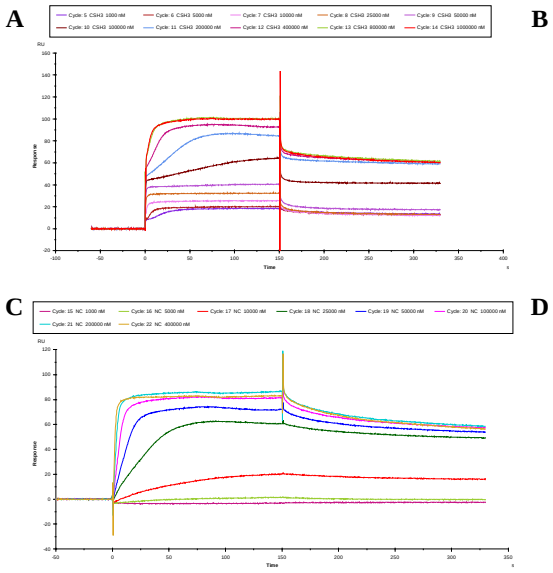

Ligand	Analyte	Binding affinity, K_D
Phosphorylated cytoplasmic domain	C-SH3 (A)	104 µM
Phosphorylated cytoplasmic domain	Grb2 R86A (B)	2.65 µM
Phosphorylated cytoplasmic domain	NSH3-CSH3 (C)	15.4 µM

Figure 3.11: Surface plasmon resonance analysis of phosphorylated FGFR2–Grb2 interactions. Purified FGFR2 cytoplasmic domain was phosphorylated by adding ATP/$MgCl_2$, followed by gel-filtration chromatography to remove any extra ATP. Phosphorylated FGFR2 cytoplasmic domain was immobilised on a CM5 chip. Different Grb2 domains were purified, and various concentrations of the Grb2 proteins were flowed over the chip. (A) Sensorgrams of the Grb2 C-SH3 domain binding to the phosphorylated FGFR2 cytoplasmic domain. (B) Sensorgrams of the Grb2 R86A mutant binding to the phosphorylated FGFR2 cytoplasmic domain. (C) Sensorgrams of the Grb2 NSH3-CSH3 domains binding to the phosphorylated FGFR2 cytoplasmic domain. (D) Summary of the binding affinities of phosphorylated cytoplasmic domain for various Grb2 proteins. The C-SH3 domain binds to the FGFR2 cytoplasmic domain with a K_D=104 µM, the Grb2 R/A mutant binds to the FGFR2 cytoplasmic domain with a K_D=2.65 µM, and the NSH3-CSH3 domain binds to the FGFR2 cytoplasmic domain with a K_D=15.4 µM. These data show the direct binding of Grb2 to the phosphorylated FGFR2 cytoplasmic domain without the Grb2 SH2 domain. The biosensor chip response is shown on the *y*-axis (RU) as a function of time (*x*-axis) at 20℃. The results are representative of two independent experiments.

3.3 Discussion – The Grb2-mediated FGFR2 phosphorylation and regulation model

The direct binding of Grb2 to FGFR2 and its function in the SHP2 regulation of FGFR2 activation have been previously described[173]. In this chapter, we investigated the role of Grb2 in FGFR2 activation and the mechanistic details of the Grb2-FGFR2 interaction.

The dot blot results suggest that Grb2 may alter the FGFR2 conformation, leading to the exposure of buried phosphotyrosine(s) (Figure 3.5). The *in vitro* FGFR2 cytoplasmic domain phosphorylation can be enhanced by Grb2 (Figure 3.6), and this activity is mediated by direct binding of Grb2 to the C-terminal tail of FGFR2 because Grb2 could not enhance FGFR2 kinase domain activation in the absence of the C-terminal tail (Figure 3.6). The investigation of how the individual domains of Grb2 affect FGFR2 phosphorylation further suggests that the FGFR2 phosphorylation enhanced by Grb2 is mainly mediated by the Grb2 C-SH3 domain (Figure 3.7), whereas the Grb2 N-SH3 and SH2 domains alone have no effect on FGFR2 phosphorylation. However, their presence helps to enhance the C-SH3 domain–mediated FGFR2 activation/phosphorylation (Figure 3.7). NMR structural studies indicate that Grb2 is dynamic in solution[208]; CD and SAXS studies also show

the flexibility of Grb2 in solution (Loren Stagg, unpublished data). Therefore, the effect of the C-SH3 domain is enhanced in the presence of N-SH3 or SH2, which might be achieved by stabilising the C-SH3 structure and thereby increasing its binding affinity for FGFR2.

We used SPR to test this hypothesis. A previous study carried out by Ahmed *et al.*[173]showed that the Grb2 C-SH3 domain alone exhibits low binding affinities for FGFR2 peptides (above 10 μM). Our SPR data also indicate that the C-SH3 domain alone has a low affinity for the dephosphorylated FGFR2 cytoplasmic domain. The observed binding between the N-SH3 domain alone and the dephosphorylated FGFR2 cytoplasmic domain may not be physiologically relevant. The inclusion of either the N-SH3 or SH2 domain with the C-SH3 domain increases the binding affinity of the C-SH3 domain (also the N-SH3 domain) toward the dephosphorylated FGFR2 cytoplasmic domain (Figure 3.10). The ITC data indicate a 2:1 stoichiometry for the Grb2:dephosphorylated FGFR2 binding model (Figure 3.8). Moreover, SPR data also demonstrate that phosphorylated FGFR2 cytoplasmic domain binds to Grb2 and that this interaction is mediated by the C-SH3 domain (Figure 3.11).

Based on these findings, we propose a mechanism of Grb2-enhanced FGFR2 activation. The binding of Grb2 to inactive/unphosphorylated FGFR2 may cause a conformational change in FGFR2, which increases the FGFR2 tyrosine kinase activity. The ITC data suggest that Grb2 also might induce FGFR2 dimerisation by bringing two FGFR2 molecules together, thereby increasing FGFR2 activity (Figure 3.12). Several Grb2 knock-out cell lines have been generated in our group to further investigate the role of Grb2 in FGFR2 signalling pathway regulation. In conclusion, this chapter presents our investigation of the role of Grb2 in the regulation of FGFR2 phosphorylation.

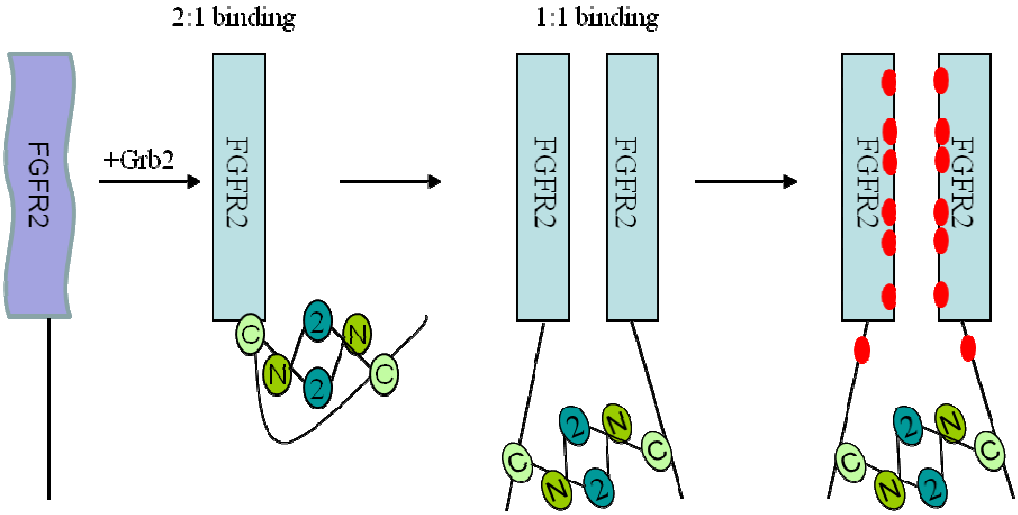

Figure 3.12: Two-site binding model of Grb2-medaited FGFR2 phosphorylation. When Grb2 is present, direct binding of Grb2 to FGFR2 is a two-site binding event; binding not only enhances the dimerisation process but also causes a conformational change in FGFR2, which leads to enhanced phosphorylation of FGFR2.

Chapter 4

Grb2 phosphorylation and its role in recruitment of the FGFR2 signalling complex

4.1 Introduction

Adaptor proteins, such as Shc, can be tyrosine-phosphorylated by tyrosine kinases. These residues provide additional binding sites for the recruitment of other signalling proteins, enabling the formation of protein complexes[252]. Grb2 plays an important role in the RTK-mediated signalling pathway[253]. To date, tyrosine phosphorylation of Grb2 and its function in cell signalling have not been investigated thoroughly. An early study indicated that Grb2 is not tyrosine-phosphorylated *in vivo* when fibroblasts are stimulated with EGF or PDGF; however, Grb2 tyrosine phosphorylation can be detected when HEK 293 cells transiently overexpress both PDGFR and Grb2[54].

Jones *et al*. reported the first clear evidence for Grb2 tyrosine phosphorylation: $pp60^{c\text{-}src}$ (Src) kinase targets Grb2 as its substrate and phosphorylates Grb2 on tyrosine 160 *in vitro*. *In vivo* experiments also show that Grb2 is tyrosine-phosphorylated by $pp60^{c\text{-}src}$ in response to PDGF stimulation[254]. A later study not only showed Grb2 can be tyrosine-phosphorylated at tyrosine 209 by a tyrosine kinase, Bcr/Abl (an oncogenic tyrosine kinase that induces chronic myeloid leukaemia (CML)-like disease in mice)[255], but also provided information about the role of phospho-Grb2 in tyrosine kinase signalling pathways. This report showed that

overexpressing Grb2 in Bcr/Abl-expressing cells causes Grb2 tyrosine phosphorylation. Moreover, Grb2 phosphorylation requires direct binding of Grb2 to Bcr/Abl. Tyrosine phosphorylation of Grb2 reduces Grb2 SH3 domain–dependent binding to Sos, but not Grb2 SH2 domain–dependent binding to Bcr/Abl. One study suggests a negative regulatory role of tyrosine-phosphorylated Grb2 in tyrosine kinase signalling[256].

Grb2 has been shown to interact with SHP2 on tyrosines 546 and 584 in 293 LA cells. A highly phosphorylated 29-kDa protein present in Grb2 immunoprecipitates in response to prolactin receptor (PRLR)–mediated JAK2 activation and is a substrate of SHP2[257]. Haines *et al*. further confirmed the identity of this phosphorylated 29-kDa protein as Grb2. Their study showed that overexpression of catalytically inactive SHP2 and activation of PRLR/JAK results in Grb2 phosphorylation[258]. Additionally, tyrosine-phosphorylated Grb2 inhibits EGF-induced MAPK activity and cell proliferation.

In this study, the first evidence of Grb2 phosphorylation by FGFR2 is reported. In addition, the docking site for Grb2 on FGFR2 appears distinct from the kinase domain. The phosphorylation sites on Grb2 are also identified. Furthermore, an *in vitro* study

using Grb2 Y/F mutants suggests that Grb2 phosphorylation may augment ERK1/2 activation upon stimulation of the FGFR2 signalling pathway. Finally, expression of FGFR2 in HEK 293 cells is shown to cause Grb2 phosphorylation; in addition, stimulation by FGF ligands leads to the dephosphorylation of Grb2, which is probably due to the FGF stimulation-dependent SHP2 activation.

The two-site binding model of Grb2 binding to inactive FGFR2 and the role of Grb2 in the regulation of FGFR2 activation has been discussed in Chapter 3. In this chapter, the interactions between FGFR2 and phosphorylated Grb2 are explored. We show that phospho-Grb2 is released from activated FGFR2, suggesting a mechanism of Grb2-regulated FGFR2 signalling. We also characterised the role of SHP2 in FGFR2 signalling complex recruitment. A previous study reported the site-specific dephosphorylation of FGFR2 by SHP2[173], demonstrating that binding of Grb2 to inactive FGFR2 inhibits SHP2 binding to FGFR2. Herein, we report the direct binding of SHP2 to activated FGFR2 on the receptor's C-terminal tail. SHP2 is also shown to directly interact with and dephosphorylate phospho-Grb2 *in vitro*.

O'Rourke and Ladbury have indicated that the formation of a signalling complex is necessary to create specificity in protein–protein interactions that transmit specific

cellular signals[43]. Results from Chapter 3 and Chapter 4 provide a detailed model of the recruitment of the FGFR2 signalling complex, and a mechanism for FGFR2 regulation is proposed.

4.2 Results

4.2.1 Grb2 tyrosine phosphorylation by FGFR2

Although Grb2 is tyrosine-phosphorylated by Bcr/Abl, EGFR[256] and pp60$^{c\text{-}src\ 254}$, it is unknown if tyrosine phosphorylation of Grb2 occurs in the FGFR signalling pathway.

To determine the ability of FGFR2 to phosphorylate Grb2, purified Grb2 and the FGFR2 cytoplasmic domain were mixed in a 2:1 molar ratio and incubated with 5 mM ATP and 10 mM $MgCl_2$ overnight. Samples were denatured and analysed by SDS-PAGE, followed by immunoblotting with an anti-phosphotyrosine antibody to investigate the phosphorylation state of Grb2. A major species of Grb2 migrated at the expected molecular weight of 28 kDa (Figure 4.1 A, lane 2). The presence of the FGFR2 cytoplasmic domain alone without ATP/$MgCl_2$ did not change the migration pattern or rate of Grb2 (Figure 4.1 A, lane 3). No phosphotyrosine signal was detected on *E. coli*–expressed Grb2 or on Grb2 incubated with the FGFR2 cytoplasmic domain alone without ATP/$MgCl_2$ (Figure 4.1 A, lane 2 and 3; Figure 4.1 B, lane 1). These results confirm that these Grb2 samples were unphosphorylated. In the presence of ATP/$MgCl_2$ and FGFR2, a Grb2 species with lower mobility appeared on a Coomassie blue–stained gel (Figure 4.1 A, lane 4) and cross-reacted with an

anti-phosphotyrosine antibody (Figure 4.1 B, lane 3), suggesting that the FGFR2 cytoplasmic domain phosphorylates Grb2 on more than one tyrosine residue.

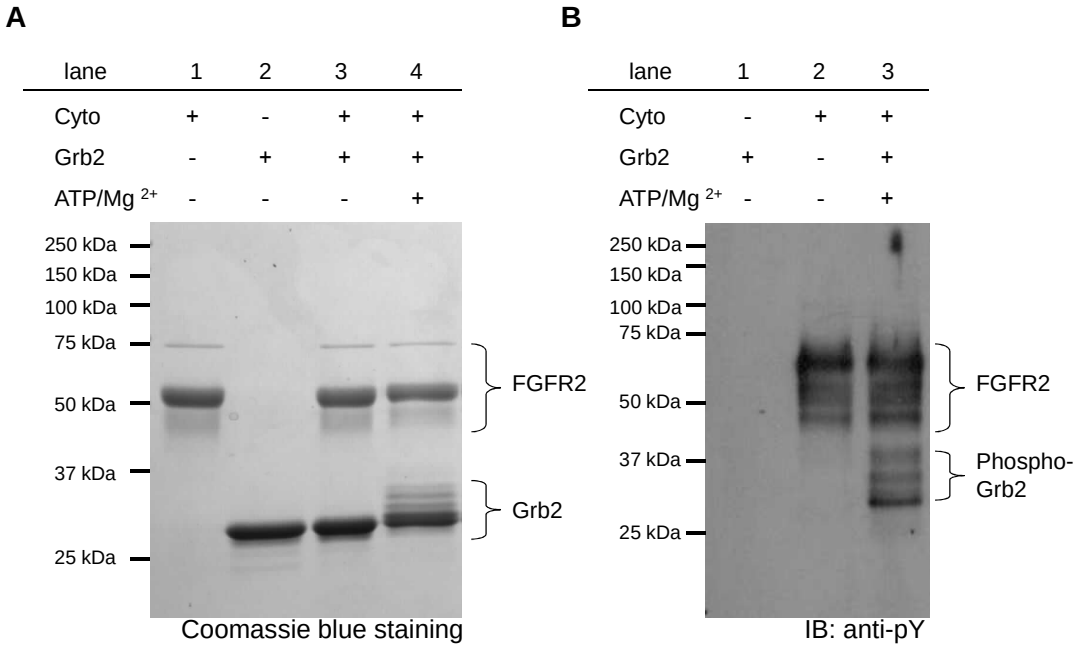

Figure 4.1: Grb2 tyrosine phosphorylation by the FGFR2 cytoplasmic domain *in vitro*. Purified FGFR2 cytoplasmic domain was used to phosphorylate Grb2 *in vitro*. Proteins were mixed in a 2:1 molar ratio and incubated with/without ATP/$MgCl_2$ overnight. Samples were denatured and analysed using SDS-PAGE followed by Coomassie blue staining or immunoblotting. Grb2 appears to form multiple bands on Coomassie blue–stained SDS-PAGE gels when mixed with the FGFR2 cytoplasmic domain in the presence of ATP/$MgCl_2$. Western blot probed with an anti-phosphotyrosine antibody confirms that these bands are tyrosine-phosphorylated. The results are representative of at least three independent experiments.

4.2.2 Direct binding of Grb2 to FGFR2 facilitates Grb2 phosphorylation

We have previously shown direct binding of Grb2 to FGFR2 via the Grb2 C-SH3 domain. The deletion of the last 10 residues in FGFR2 abolishes Grb2 binding to

FGFR2[173]. To test if direct binding of Grb2 and FGFR2 is required for Grb2 tyrosine phosphorylation, the FGFR2 cytoplasmic domain (residues 309–821) and the FGFR2 kinase domain (residues 412–760) without the C-terminal tail (Figure 4.2) were used to compare the effect on Grb2 phosphorylation *in vitro*. To avoid non-specific tyrosine phosphorylation due to protein overloading and non-physiologically relevant Grb2 phosphorylation due to long incubation times, different amounts (0.01–4 nM) of purified FGFR2 cytoplasmic and kinase domains were incubated with a constant amount of Grb2 in the presence of ATP/$MgCl_2$. All phosphorylation reactions were stopped at 15 minutes to mimic early FGFR2 signalling pathway activation *in vivo*.

The phosphorylation level of Grb2 was significantly increased in the presence of the cytoplasmic domain (2 nM and 4 nM) and ATP/$MgCl_2$ (Figure 4.2, lane 6 and 7). The minimal amount of cytoplasmic domain required to phosphorylate 500 ng of Grb2 in a 100 μl solution volume (170 nM) in the presence of ATP/$MgCl_2$ was 2 nM. Notably, the same concentration of the FGFR2 kinase domain lacking the C-terminal tail (either 2 nM or 4 nM) failed to phosphorylate Grb2 *in vitro*. The data preasented in Chapter 3 show that the interaction between FGFR2 and Grb2 occurs through the FGFR2 C-terminal tail and the Grb2 C-SH3 domain. Therefore, this result implies that binding through the C-terminal tail of FGFR2 is important for Grb2

phosphorylation. Together with previous binding results, these results suggest that Grb2 phosphorylation occurs by direct binding to FGFR2.

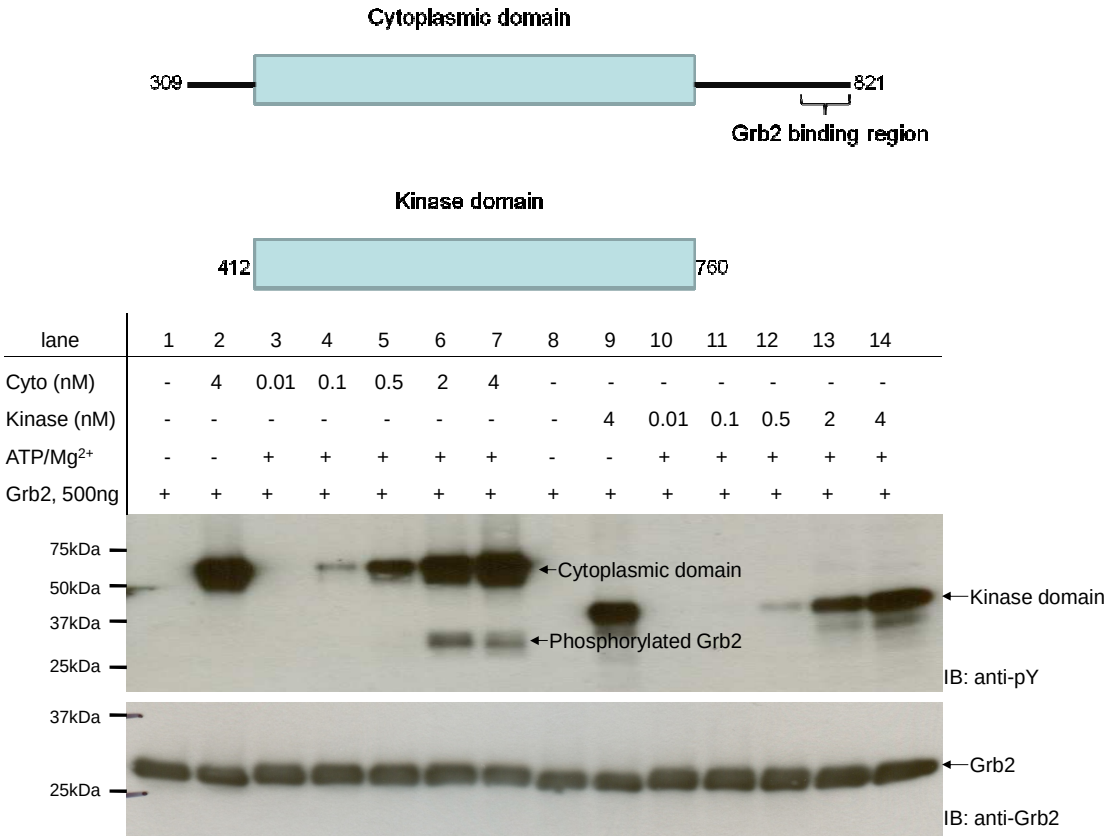

Figure 4.2: Grb2 phosphorylation requires direct binding to FGFR2. Both purified FGFR2 cytoplasmic (residues 309–821) and kinase (residues 412–760) domains were tested for their effects on Grb2 phosphorylation. Different amounts (0.01–4 nM) of FGFR2 cytoplasmic and kinase domains were mixed with 500 ng of Grb2 protein with/without ATP/$MgCl_2$ in 100 µl solution. Reactions were incubated on ice for 15 min, and samples were denatured and analysed using immunoblotting. The results show that the FGFR2 cytoplasmic domain can phosphorylate Grb2 (lane 6 and 7), whereas the FGFR2 kinase domain cannot phosphorylate Grb2 under the same conditions (lane 13 and 14), suggesting that a direct interaction via the SH3 domain of Grb2 and the FGFR2 C-terminal tail is required for Grb2 phosphorylation. The results were analysed by immunoblotting with an anti-phosphotyrosine antibody (first panel) and an anti-Grb2 antibody as the Grb2 loading control (second panel). The results are representative of two independent experiments.

Human Grb2 has seven tyrosines: residues 7, 37 and 52 in the N-terminal SH3 domain; 118 and 134 in the SH2 domain; 160 in the linker between SH2 and the C-terminal SH3 domain; and 209 in the C-terminal SH3 domain (Figure 4.3A). To characterise the nature of Grb2 phosphorylation, individual domains of Grb2 were purified and incubated with 4 nM of cytoplasmic domain with ATP/$MgCl_2$. All phosphorylation reactions were quenched at 15 minutes.

Figure 4.3A illustrates the constructs used in this part of the study. Western blotting using an anti-phosphotyrosine antibody showed that both Grb2 N-SH3 and C-SH3 domains (2000 ng/2.5 nM of each protein) were tyrosine-phosphorylated by 4 nM FGFR2 cytoplasmic domain in the presence of ATP/$MgCl_2$, whereas no tyrosine phosphorylation could be detected on the SH2 domain alone under the same conditions (Figure 4.3 B, lanes 6, 7 and 8). Notably, the phosphotyrosine signal from the C-SH3 construct was much higher than that of the N-SH3 construct (Figure 4.3 B, lower panel; the membrane was Ponceau-stained after transfer to show equal loading of the various proteins). Both of the tyrosine residues (Tyr 160 and 209) on the C-SH3 construct could have been phosphorylated, whereas only one tyrosine residue on (one of Tyr 7, 37 or 52) the N-SH3 domain was phosphorylated. Alternatively, the C-SH3 domain might have a higher binding affinity to the FGFR2 cytoplasmic domain than

the N-SH3 domain does. The C-SH3 domain binds to the FGFR2 cytoplasmic domain with a higher affinity, thus making it the preferred substrate.

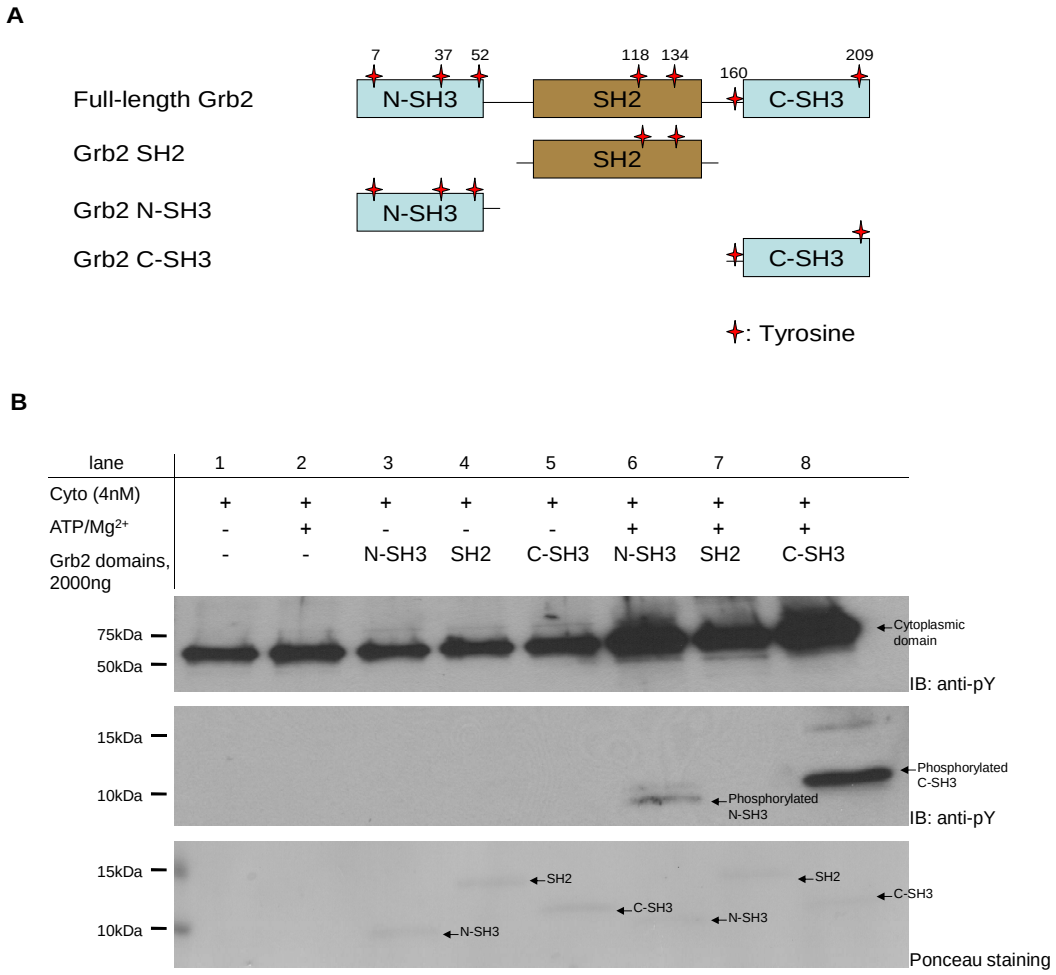

Figure 4.3: Phosphorylation of the individual domains of Grb2. Purified FGFR2 cytoplasmic domain and the Grb2 N-SH3, SH2 and C-SH3 domains were used to identify the phosphorylation status of Grb2. The FGFR2 cytoplasmic domain (4 nM) was mixed with 200 ng of the individual domains of Grb2 with/without ATP/$MgCl_2$ in 100 µl solution Reactions were incubated on ice for 15 min, and samples were denatured and analysed using immunoblotting. (A) Constructs used in this experiment. Tyrosines are indicated as stars, with the residue numbers listed. (B) Both the N-SH3 and C-SH3 domains can be phosphorylated by FGFR2 in 15 minutes in the presence of ATP/$MgCl_2$ (middle panel, lanes 6 and 8), whereas the SH2 domain is not tyrosine-phosphorylated (middle panel, lane 7). The results were analysed by immunoblotting with an anti-phosphotyrosine antibody (first and second panels). The loading control was carried out with Ponceau staining because no antibody can detect all of the constructs. The results are representative of two independent experiments.

4.2.3 Identification of the Grb2 phosphorylation sites

To identify the sites of Grb2 phosphorylation by FGFR2, two incubation times determined by preliminary studies were selected for the generation of phospho-Grb2 for mass-spectrometric analysis (Proteomics Facilities, University of Texas, MD Anderson Cancer Center). Purified Grb2 was incubated with purified FGFR2 cytoplasmic domain in the presence of ATP/$MgCl_2$, for either 15 minutes or overnight, to compare the effects of different reaction times on Grb2 phosphorylation.

Four phosphopeptides were identified from the 15-minute incubation sample, indicating that tyrosine residues 7, 52 and 160 were phosphorylated (Table 4.1). Tyrosines 7 and 52 are located in the N-SH3 domain, and tyrosine 160 is found at the linker between the SH2 and C-SH3 domains. These results further corroborate the *in vitro* domain phosphorylation experiment (Figure 4.3). On the other hand, six phosphopeptides were identified in the overnight-incubation sample, revealing that tyrosine residues 7, 37, 52, 134, and 160 were phosphorylated (Table 4.1).

An early study by our group that focused on the time-dependent FGFR2 and ERK1/2 activation indicated that FGFR2 phosphorylation/activation reaches a maximum between 5 and 30 minutes of FGF9 stimulation in HEK 293 cells expressing

wild-type FGFR2, whereas ERK1/2 phosphorylation reaches a maximum within 10 minutes of FGF2 stimulation in PC12 cells[249]. Therefore, it is reasonable to assume that the phospho-Grb2 samples from the 15-minute incubation more closely reflect the cellular reaction. Two tyrosine phosphorylation sites (phosphotyrosines 37 and 134) are suspected not to be physiologically relevant because they required prolonged exposure to the kinase.

Importantly, Bcr/Abl and $pp60^{c\text{-}src}$ phosphorylate Grb2 on tyrosines 209 and 160, respectively, whereas FGFR2 phosphorylates Grb2 on tyrosines 7, 52 and 160[254, 255]. Therefore, the phosphorylation sites of Grb2 are tyrosine kinase–specific, and these sites may play important roles in the FGFR2 signalling pathway.

Table 4.1: Mass spectrometry results for Grb2 phosphorylation sites. Grb2 protein samples were phosphorylated by the FGFR2 cytoplasmic domain in the presence of ATP/$MgCl_2$ on ice for 15 minutes or overnight. Phosphorylated Grb2 samples were denatured and separated by SDS-PAGE. Protein bands were cut and digested by trypsin, and mass-spectrometric analysis was performed by the proteomics facilities services (Proteomics Facilities, University of Texas, MD Anderson Cancer Center). We identified three phosphorylated tyrosines when Grb2 was incubated with FGFR2 in the presence of ATP/$MgCl_2$ for 15 minutes. However, five phosphotyrosines were identified when the incubation time was increased to overnight.

Sample incubation time: 15 minutes

Phosphorylated peptide identified	Phosphorylation sites identified
KY*DFKATADDELSFKR	Tyr 7
KNY*IEMKPHPWFFGKI	Tyr 52
KDGFIPKNY*IEMKPHPWFFGKI	Tyr 52
RDIEQVPQQPTY*VQALFDFDPQEDGELGFRR	Tyr 160

* Phosphorylation

Sample incubation time: overnight

Phosphorylated peptide identified	Phosphorylation sites identified
KY*DFKATADDELSFKR	Tyr 7
KY*DFKATADDELSFKRG	Tyr 7
KVLNEECDQNWY*KAELNGKD	Tyr 37
KNY*IEMKPHPWFFGKI	Tyr 52
KFNSLNELVDY*HRS	Tyr 134
RDIEQVPQQPTY*VQALFDFDPQEDGELGFRR	Tyr 160

* Phosphorylation

4.2.4 Phosphorylation of Grb2 may occur in a certain order

The order of phosphorylation of the FGFR1 kinase domain has been identified[163] and may be important in the regulation of a FGFR1 downstream signalling pathway[163, 250, 259]. As shown in Figures 4.1 and 4.2, different incubation times of Grb2 phosphorylation reactions with the FGFR2 cytoplasmic domain result in phospho-Grb2 species that migrate differently on denaturing gels: overnight incubations produce multiple bands, and 15 minute incubations yield only two bands. To investigate the relationship between the Grb2 phosphorylation level and incubation time, purified Grb2 was incubated with purified FGFR2 cytoplasmic domain in the presence of ATP/$MgCl_2$; EDTA was added to quench the phosphorylation reactions at different time points between 5 minutes and overnight. These samples were either denatured or kept in their native state.

To characterise the phosphorylation states of Grb2 at different time points, the denatured samples were separated by SDS-PAGE and analysed by immunoblotting with a general anti-phosphotyrosine antibody. The anti-phosphorylation blot shows that the Grb2 phosphotyrosine signal could be detected with only a 5-minute incubation period; however, two species were present at 10 minutes, suggesting that two tyrosines were phosphorylated. The number of phospho-Grb2 species with

different mobilities increased as the incubation time increased (Figure 4.4, upper panel). Six species with different mobilities were present in the overnight incubation sample. These results support the mass spectrometry observation that Grb2 possesses more tyrosine phosphorylation sites than the two that have been previously reported by other groups. Immunoblotting with an anti-Grb2 antibody confirmed that all of the phosphorylated species present were indeed Grb2 (Figure 4.4, lower panel). Because these data and the mass spectrometry results indicate that FGFR2 can phosphorylate Grb2 on at least five distinct tyrosine sites in a time-dependent manner, we investigated the possibility of these sites being phosphorylated sequentially.

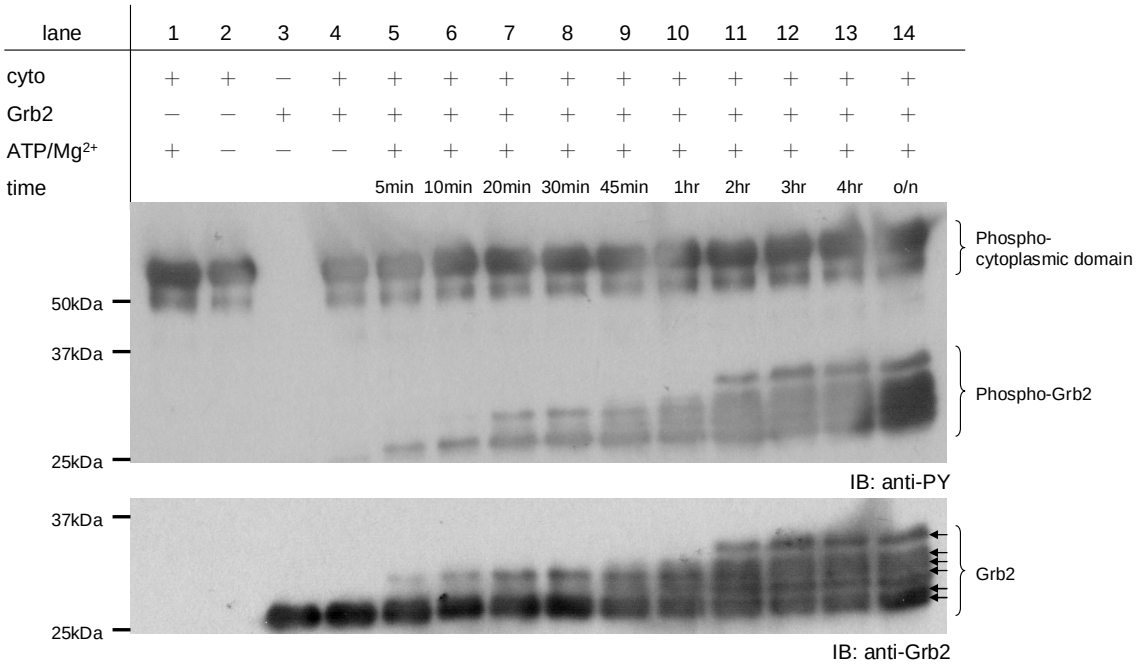

Figure 4.4: Time-dependent Grb2 phosphorylation by the FGFR2 cytoplasmic domain. Purified Grb2 was incubated with purified FGFR2 cytoplasmic domain in the presence of ATP/$MgCl_2$; EDTA was added to quench the phosphorylation reactions at different time points between 5 minutes and overnight. These samples were denatured and analysed using SDS-PAGE followed by immunoblotting. The number of Grb2 bands with different phosphorylation states increased with increasing incubation time. Activated FGFR2 cytoplasmic domain and phosphorylated Grb2 are indicated. Their phosphorylation states were detected using a general anti-phosphotyrosine antibody (upper panel). The anti-Grb2 antibody was used as the loading control and to identify Grb2 (lower panel, indicated by arrows). These results indicate that the number of phosphorylated tyrosine residues is phosphorylation time-dependent.

To investigate if FGFR2 phosphorylates Grb2 tyrosines in a certain order, we separated proteins based on their charge/mass ratios in native gels to separate phospho-Grb2 proteins with different phosphorylation levels. Native Tris-glycine (6%) gels and the above-described native phospho-Grb2 proteins were used. The reaction time course for Grb2 phosphorylation by FGFR2 was determined as shown in Figure 4.5. Notably, the phospho-Grb2 separation patterns in the native gel were similar to

the FGFR2 kinase domain phosphorylation order pattern separated in a native gel[163]. Because phosphate groups increase the net negative charge on the protein, the five resolved bands might represent Grb2 proteins with different phosphorylation states, with the most phosphorylated migrating the furthest.

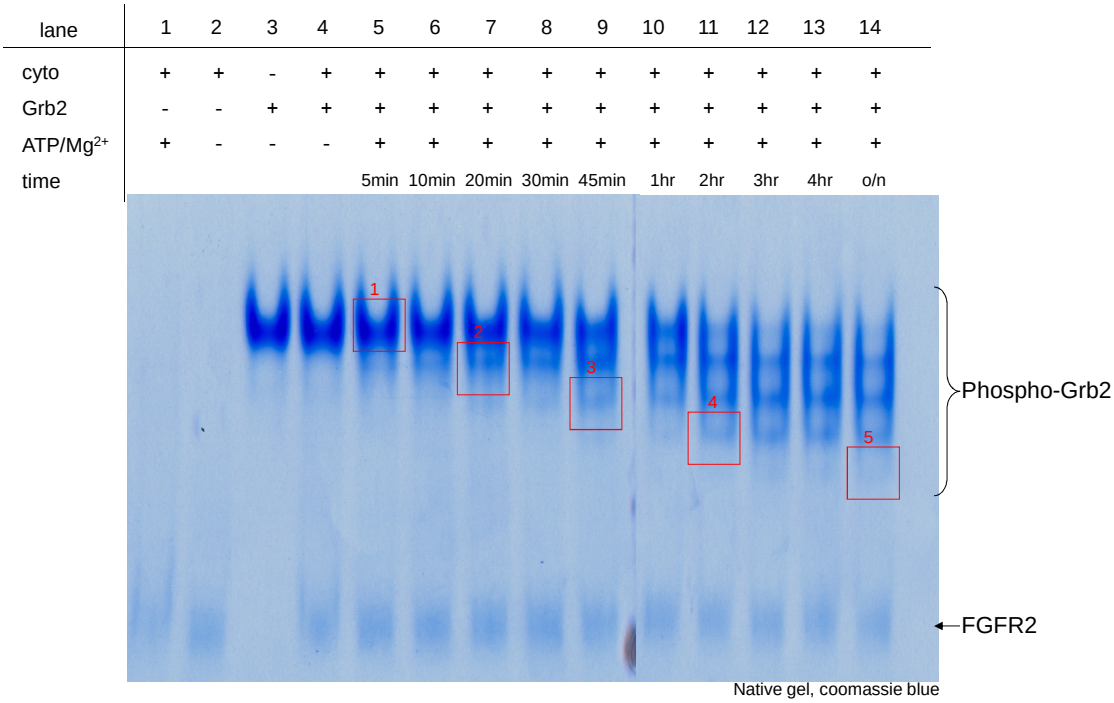

Figure 4.5: Analysis of Grb2 phosphorylation in a native gel. Purified Grb2 was mixed with purified FGFR2 cytoplasmic domain in the presence of ATP/$MgCl_2$. The phosphorylation reactions were quenched by EDTA at different time points. Samples were run for 45 minutes at 120 V. Coomassie blue staining was used to detect proteins. Bands chosen for mass spectrometry are indicated by red squares.

To identify the phosphorylation states of phospho-Grb2 in the native gel, five bands were chosen, and mass-spectrometric analysis was conducted to identify the phosphorylation states and specific residues (Figure 4.5, the chosen samples are

indicated by red squares). The mass-spectrometric data are shown in Table 4.2. Five phosphopeptides were identified in total from all five protein bands used for mass spectrometry. Three tyrosine residues, 7, 52 and 160, were confirmed to be phosphorylated, supporting previously reported mass-spectrometric data.

Table 4.2: Mass spectrometry results. Five phosphopeptides were identified in total from all five protein bands. However, only three phosphorylated tyrosines were identified.

Native phospho-Grb2 mass spectrometry

Phosphorylated peptide identified	band 1	band 2	band 3	band 4	band 5
	Number of phosphopeptides identified				
KY* DFKATADDELSFKR (Tyr 7)	0	0	2	4	9
KY* DFKATADDELSFKRG (Tyr 7)	1	0	0	0	1
KDGFIPKNY* IEMKPHPWFFGKI (Tyr 52)	1	0	2	0	0
KNY* IEMKPHPWFFGKI (Tyr 52)	2	3	5	2	1
RDIEQVPQQPTY* VQALFDFDPQEDGELGFRR (Tyr 160)	3	13	20	13	17

* Phosphorylation

Native phospho-Grb2 mass spectrometry

Phosphorylated peptide identified	band 1	band 2	band 3	band 4	band 5
	Percentage of phosphopeptide identified				
KY* DFKATADDELSFKR (Tyr 7)					
KY* DFKATADDELSFKRG (Tyr 7)	1.2	0	12.5	80	100
KDGFIPKNY* IEMKPHPWFFGKI (Tyr 52)					
KNY* IEMKPHPWFFGKI (Tyr 52)	2.6	17.6	43.8	100	100
RDIEQVPQQPTY* VQALFDFDPQEDGELGFRR (Tyr 160)	13.6	28.3	42.6	39.4	42.5

* Phosphorylation

To supplement the mass-spectrometric analysis, another FGFR2/Grb2 phosphorylation experiment was carried out. Native proteins were separated in a native gel. Certain protein bands were recovered from the native gel and denatured. SDS-PAGE and western blots were performed to characterise the components of the individual bands.

Figure 4.6 A shows the migration patterns of FGFR2, Grb2 and phospho-Grb2 in the native gel. Proteins chosen for further analysis are indicated by arrows and numbers (Figure 4.6 A, number 1 to 9). The numbers correspond to the lanes of the denaturing gel (Figure 4.6 B, lane 1 to 9). As expected, multiple bands appeared when Grb2 was incubated with the FGFR2 cytoplasmic domain in the presence of ATP/$MgCl_2$ (Figure 4.6 A, arrows 6, 7, 8 and 9). Bands 6 to 9, which were separated by SDS-PAGE according to size and immunoblotted with the anti-Grb2 antibody, were confirmed to contain Grb2 (Figure 4.6 B, upper panel, lanes 6, 7, 8 and 9). There are three possible explanations for the presence of multiple Grb2 bands. First, each band may represent a Grb2 species with a certain number of phosphorylated tyrosine residues. This possibility is partially supported by immunoblotting with a general anti-phosphotyrosine antibody, showing that these bands contained tyrosine-phosphorylated Grb2 (Figure 4.6 B, lower panel, lanes 6, 7, 8 and 9,

indicated by a red box). However, because mass spectrometry did not clearly show a sequential order for the phosphorylation of the different tyrosine residues, other factors could account for the appearance of these multiple bands. Second, Grb2 might form multimers. Because the Grb2 SH2 domain can bind to phosphotyrosine residues, a Grb2–phospho-Grb2 or phospho-Grb2–phospho-Grb2 complex could form, produce different migration patterns, and still produce the same phosphotyrosine peptides overall in the mass spectrometry experiment. Finally, as shown in previous studies in Chapter 3, Grb2 binds to FGFR2 through the C-terminal tail. In addition, Grb2 can be tyrosine-phosphorylated by FGFR2 and ATP/$MgCl_2$. Although these bands contain Grb2 proteins (Figure 4.6 B, upper panel, lanes 6, 7, 8 and 9), the FGFR2 cytoplasmic domain could also be detected in these bands when the immunoblot was stripped and re-probed with anti-FGFR2 antibody (Figure 4.6 B, second panel, lanes 6, 7, 8 and 9). Therefore, the multiple bands seen in the native gel contain (phospho-)Grb2 and the FGFR2 cytoplasmic domain. Even though the phosphotyrosine signal could be detected on the extracted Grb2 and FGFR2 proteins (Figure 4.6 B, lower panels, lanes 6, 7, 8 and 9; the phospho-Grb2 proteins are indicated by a red box), it is not clear that phospho-Grb2 still binds to FGFR2. In summary, these multiple bands might be phospho-Grb2–bound and/or (phospho-)FGFR2–bound Grb2/phospho-Grb2.

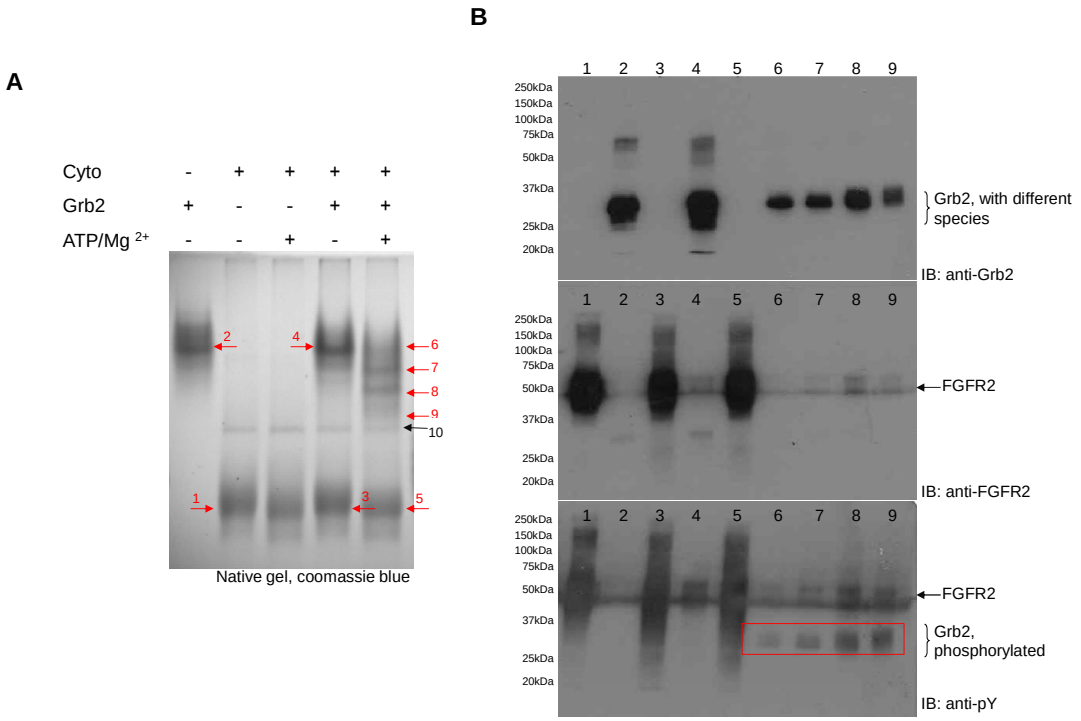

Figure 4.6: Identification of the multiple bands shown in the native gel. Purified Grb2 was mixed with the FGFR2 cytoplasmic domain with/without ATP/$MgCl_2$ for 3 hours. Samples were analysed in native gels. Coomassie blue staining was used to detect proteins. Selected bands were excised, and proteins were extracted for immunoblotting analysis. (A) All of the migration patterns of FGFR2, Grb2 and phospho-Grb2 are shown in the native gel. In the presence of the FGFR2 cytoplasmic domain and ATP/MgCl2, Grb2 forms multiple bands with different migration rates. Proteins were extracted (numbers 1 to 9; number 10 is protein contamination from the FGFR2 cytoplasmic domain and is shown with a black arrow) and denatured for immunoblotting analysis. (B) Immunoblotting results indicate that bands 6, 7, 8 and 9 contain both Grb2 and the FGFR2 cytoplasmic domain (first and second panels, probed with anti-Grb2 antibody and anti-FGFR2 antibody, respectively.). Phosphotyrosine signal could be detected in bands 6, 7, 8 and 9 (third panel, lanes 6, 7, 8 and 9). However, the interaction of phospho-Grb2 and FGFR2 remains unclear. The results are representative of two independent experiments.

4.2.5 Tyrosine-phosphorylated Grb2 does not bind to the FGFR2 cytoplasmic domain

Direct binding of Grb2 to FGFR2 is necessary for Grb2 to be tyrosine-phosphorylated by FGFR2 (Figure 4.2); however, it remains unknown if FGFR2 and phospho-Grb2 can form a stable complex. Therefore, we investigated the interaction between the FGFR2 cytoplasmic domain and phosphorylated Grb2 by ITC. Grb2 was tyrosine-phosphorylated by the cytoplasmic domain of FGFR2 cross-linked on agarose beads in the presence of ATP/$MgCl_2$ for 15 minutes. No binding was detected by ITC when phosphorylated FGFR2 cytoplasmic domain was titrated with phospho-Grb2 (Figure 4.7 A), suggesting a mechanism in which phospho-Grb2 is released from activated FGFR2 after Grb2 is tyrosine-phosphorylated by FGFR2. However, Grb2 could also be tyrosine-phosphorylated by other cellular tyrosine kinases, even though only Bcr/Abl, EGFR and $pp60^{src}$, which are not known to be involved in the FGFR2 pathway, have been identified to date.

To understand if phosphorylated Grb2 can bind to inactivated (unphosphorylated/dephosphorylated) FGFR2 when phospho-Grb2 is released from the previously bound and activated FGFR2 or when Grb2 is tyrosine-phosphorylated by other cellular tyrosine kinases, ITC experiments were performed using

phospho-Grb2 and the dephosphorylated FGFR2 cytoplasmic domain. The results show that phospho-Grb2 did not bind to inactivated (unphosphorylated/dephosphorylated) FGFR2 (Figure 4.7 B). Therefore, we conclude that phospho-Grb2 cannot bind to either unphosphorylated or phosphorylated FGFR2.

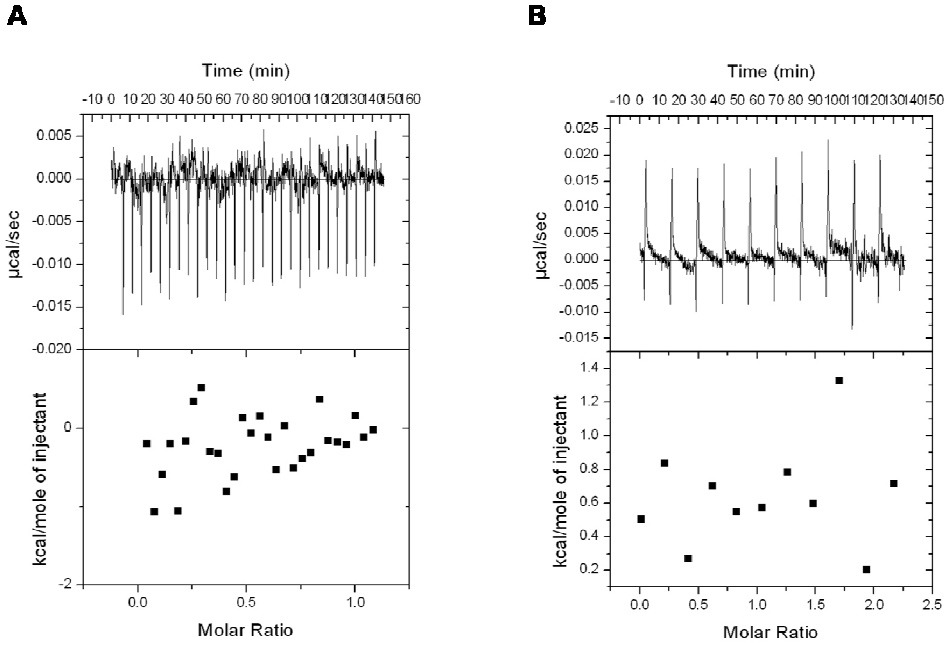

Figure 4.7: Phospho-Grb2 binding study using ITC, showing that phosphorylated Grb2 does not bind to FGFR2. Grb2 was tyrosine-phosphorylated by the FGFR2 cytoplasmic domain in the presence of ATP/MgCl2 for 15 minutes. Phosphorylated FGFR2 cytoplasmic domain was prepared by adding ATP/$MgCl_2$ and incubating on ice for 15 minutes, followed by buffer exchange. Dephosphorylated FGFR2 cytoplasmic domain was prepared by incubating with CIP overnight followed by buffer exchange. The FGFR2 cytoplasmic domain was loaded in the ITC syringe, and Grb2 was loaded in the ITC cell. All studies were done at 15℃. (A) Tyrosine-phosphorylated FGFR2 cytoplasmic domain was titrated into tyrosine-phosphorylated Grb2. No binding event could be detected. (B) Dephosphorylated FGFR2 cytoplasmic domain was titrated into tyrosine-phosphorylated Grb2. No binding event could be detected. These ITC data suggest that the phosphorylated Grb2 is released from FGFR2 once Grb2 is tyrosine-phosphorylated by FGFR2. The results are representative of four independent experiments.

4.2.6 Grb2 is tyrosine-phosphorylated in FGFR2-expressing cells and is dephosphorylated upon FGF stimulation

An earlier study carried out by Ahmed *et al*. indicated that Grb2 binds to FGFR2 but does not bind to FGFR1[173]. Figure 4.2 also shows that Grb2 is a substrate for FGFR2 *in vitro*. To evaluate whether Grb2 is a substrate for FGFR2 *in vivo* and to examine whether Grb2 phosphorylation is specific for the FGFR2 pathway rather than the FGFR1 pathway, wild-type full-length Grb2 was transfected into both non-transfected HEK 293 cells and HEK 293 cells stably expressing wild-type FGFR2. The HEK 293 cell line is ideal for this investigation as it lacks endogenous FGFR2 but possesses endogenous FGFR1.

To ascertain whether Grb2 was phosphorylated by endogenous FGFR1, Grb2 was immunoprecipitated from either serum-starved or FGF2-stimulated HEK 293 cells transiently transfected with Grb2. Only a single population was detected when probed with the anti-Grb2 antibody. No phosphotyrosine signal could be detected, indicating that Grb2 is not tyrosine-phosphorylated in the basal or stimulated state (Figure 4.8). FGF9 was used as a control to confirm the absence of FGFR2. These data suggest that Grb2 cannot be phosphorylated by FGFR1 *in vivo* and support the previous finding by Ahmed *et al*. that Grb2 does not bind to FGFR1.

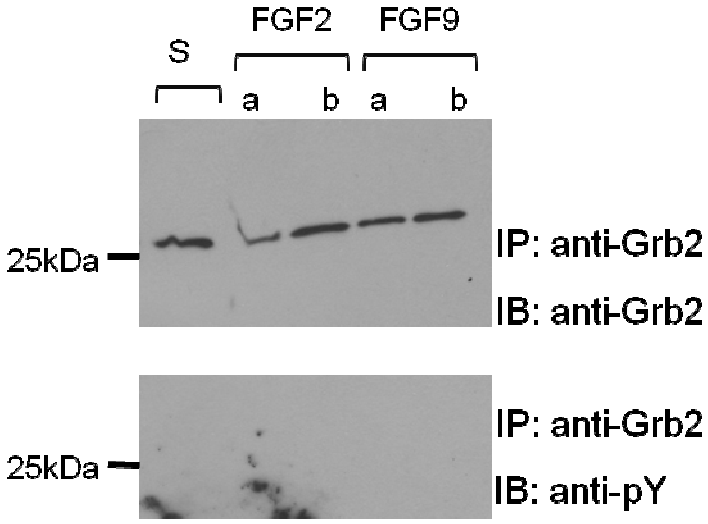

Figure 4.8: Grb2 is not tyrosine-phosphorylated in non-transfected HEK 293 cells. Grb2 plasmid was transfected into HEK 293 cells by calcium phosphate precipitation. Forty-eight hours after transfection, FGF2 was used to stimulate endogenous FGFR1 to test for its ability to phosphorylate Grb2. FGF9 was used as the control. S, serum-starved HEK 293 cells. a, 20 µl loading. b, 40 µl loading. Upon stimulation, cells were lysed in the presence of protease inhibitors and phosphatase inhibitors. Grb2 protein was immunoprecipitated, and the amount of Grb2 was detected by an anti-Grb2 antibody. The phosphorylation state was detected by an anti-phosphotyrosine antibody. No phosphorylation signal of Grb2 could be detected, suggesting that Grb2 is not phosphorylated in HEK 293 cells. The results are representative of two independent experiments.

We used HEK 293 cells stably expressing wild-type FGFR2 to investigate Grb2 phosphorylation by FGFR2 *in vivo* and the role of activated/inactivated FGFR2 in Grb2 phosphorylation. Cells were transiently transfected with wild-type Grb2 as previously described. Cells were serum-starved for 16 hours, and 10 ng/ml of FGF9 was used to stimulate FGFR2. An anti-phospho-FGFR2 (pFGFR2) antibody was used to confirm the activation of FGFR2 in response to FGF9 stimulation. An anti-phospho-ERK antibody (pERK) was used to detect the activation of FGFR2

downstream signalling upon FGF9 stimulation (Figure 4.9 A). The immunoblot was stripped and re-probed with anti-FGFR2 and anti-ERK antibodies to confirm equal loading. The transfected Grb2 was immunoprecipitated, and it appeared as multiple bands in both stimulated and unstimulated FGFR2-expressing cells. To confirm the phosphorylation states of Grb2 in these bands, a general anti-phosphotyrosine antibody (pY-99) was used. Grb2 phosphotyrosine signals could be detected in both the stimulated and unstimulated samples (Figure 4.9 B). The immunoblot was stripped and re-probed with an anti-Grb2 antibody to confirm the presence of equal amounts of Grb2.

The Grb2 phosphorylation detected from the unstimulated HEK 293 cells stably expressing wild-type FGFR2 may have been due to the low level of FGFR2 activation in the serum-starved cells (Figure 4.9 A). Surprisingly, when the HEK 293 cells stably expressing wild-type FGFR2 were stimulated with FGF9 (to activate FGFR2), the phosphorylation level of Grb2 decreased (Figure 4.9 B, FGF9 +). Therefore, we hypothesise that Grb2 is tyrosine-phosphorylated by the weakly activated FGFR2 *in vivo* and that the fully activated FGFR2 leads to activation of a tyrosine phosphatase, which then dephosphorylates the phosphorylated Grb2.

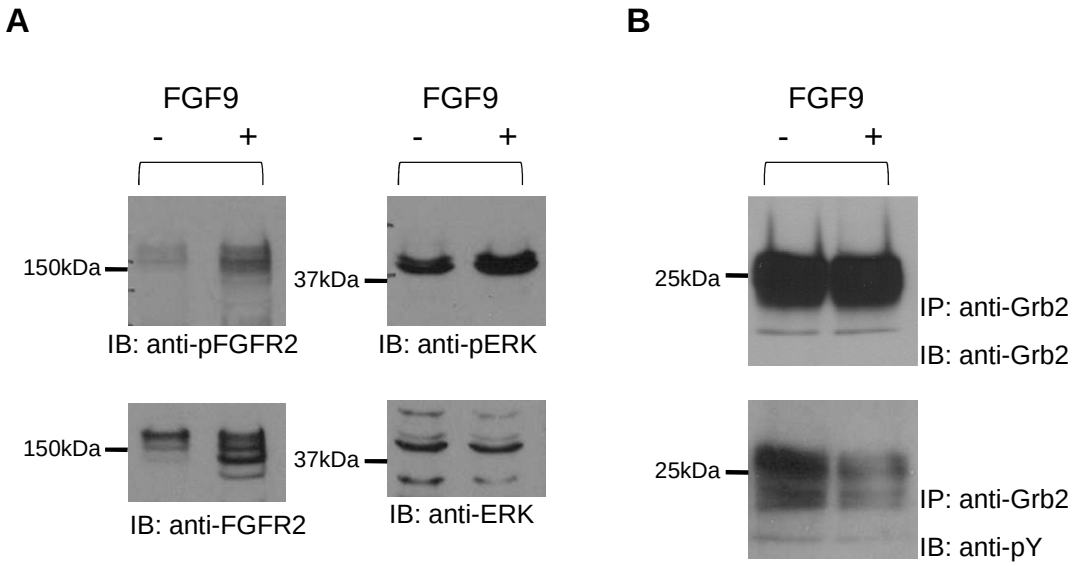

Figure 4.9: Grb2 is tyrosine-phosphorylated in the FGFR2-expressing HEK 293 cells. Grb2 plasmid was transfected into FGFR2-expressing HEK 293 cells by calcium phosphate precipitation. Forty-eight hours after transfection, cells were starved overnight and FGF9 was used to stimulate FGFR2 for 15 minutes. Cells were lysed in the presence of protease inhibitors and phosphatase inhibitors. Grb2 protein was immunoprecipitated, and the amount of Grb2 was detected by an anti-Grb2 antibody. The phosphorylation state was detected by an anti-phosphotyrosine antibody. (A) Immunoblots probed with an anti-phospho-FGFR2 antibody and an anti-phospho-ERK1/2 antibody show the activation levels of FGFR2 and ERK in the total cell lysates (Figure 4.9 A). Antibodies were used against total FGFR2 and ERK to confirm equal loading. (B) The immunoprecipitated Grb2 from both serum-starved and FGF9-stimulated cells show multiple bands. An anti-Grb2 antibody was used to confirm that these bands represent Grb2. Phosphorylation states of Grb2 species were examined using an anti-phosphotyrosine antibody. These data indicate that Grb2 is phosphorylated in FGFR2-expressing cells but might be dephosphorylated upon FGF ligand stimulation. The results are representative of two independent experiments.

4.2.7 Expression of Grb2 Y/F mutants may enhance FGFR2 activation and down-regulate FGF-mediated ERK activation upon FGF ligand stimulation

The biochemical consequences of Grb2 phosphorylation were studied by examining the effects of the expression of Grb2 Y/F mutants on FGF-stimulated FGFR2 activation and ERK1/2 activation. The data in Section 3.2.2 show that FGFR2 activation can be enhanced by direct binding of Grb2 to FGFR2, and the data in section 4.2.5 show that phospho-Grb2 does not bind to FGFR2. These data suggest that Grb2 phosphorylation plays a negative regulatory role in the activation of FGFR2; phosphorylation of Grb2 at tyrosines 7, 52 and/or 160 should reduce FGFR2 phosphorylation at the basal state in cells. To test this hypothesis, we made Grb2 constructs with mutations of tyrosine to phenylalanine at positions 7 and 52. HEK 293 cells stably expressing FGFR2 were transfected with wild-type Grb2, Grb2 Y7F or Grb2 Y52F. Then, 10 ng/ml of FGF9 was used to stimulate the cells for 15 minutes. As seen in Figure 4.9, wild-type Grb2 and mutants appear as multiple bands in HEK 293 cells stably expressing FGFR2 (Figure 4.10 A, fifth panel), suggesting that both wild-type Grb2 and mutants were phosphorylated when FGFR2 was expressed. Co-expression of FGFR2 and Grb2 Y/F mutants (Y7F and Y52F) resulted in a significant increase in the FGFR2 phosphorylation level in unstimulated cells (Figure

4.10 A, first panel and Figure 4.10 B), which may have been due to the Grb2 mutants having a higher binding affinity for FGFR2 compared with wild-type Grb2.

To explore the biochemical effects of phosphorylation on tyrosines 7 and 52 of Grb2 further, we examined the FGF-induced ERK1/2 activation. Stimulation of HEK 293 cells stably expressing FGFR2 resulted in the activation of ERK1/2 (Figure 4.10 A, third and fourth panels). FGF-induced ERK1/2 activation was slightly reduced in cells expressing the Grb2 Y7F and Y52F mutants (Figure 4.10 A, third panel and Figure 4.10 C). Because only a single experiment was done to study the effect of Grb2 phosphorylation in FGFR2 signalling, it is hard to make a definitive conclusion. These data suggest that phosphorylation of Grb2 at Tyr 7 and 52 may be able to up-regulate ERK1/2 activation after FGF stimulation.

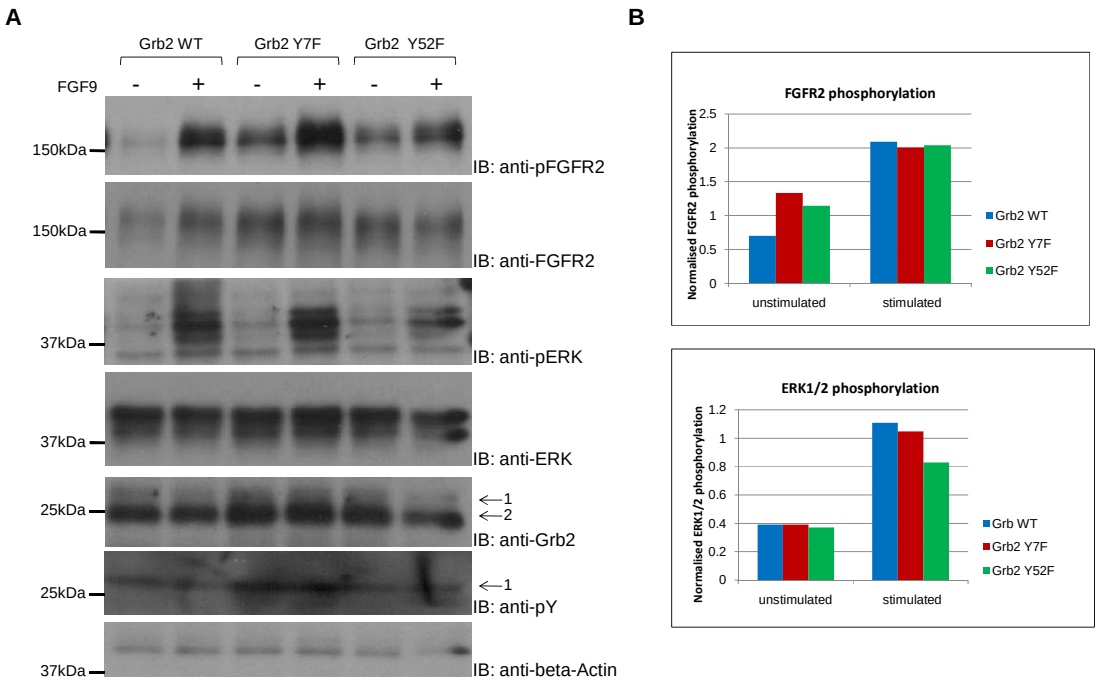

Figure 4.10: Mutation of Grb2 Tyr 7 and 52 and FGFR2 signalling pathway regulation. Grb2 mutant plasmids were transfected into FGFR2-expressing HEK 293 cells by calcium phosphate precipitation. Forty-eight hours after transfection, cells were starved overnight, and then FGF9 was used to stimulate FGFR2 for 15 minutes. Cells were lysed in the presence of protease inhibitors and phosphatase inhibitors. Total cell lysate was used to study the effect of expressing Grb2 mutants on FGFR2 signalling by probing with different antibodies. (A) FGFR2 and ERK1/2 activation. HEK 293 cells co-expressing FGFR2 and either wild-type Grb2 or Grb2 Y/F mutants were starved (lanes 1, 3 and 5) or stimulated with FGF9 for 15 min (lanes 2, 4 and 6). The lysates were analysed by immunoblotting with an anti-phospho-FGFR2 antibody (first panel), an anti-FGFR2 antibody (second panel), an anti-phospho-ERK1/2 antibody (third panel), an anti-ERK1/2 antibody (forth panel) and an anti-Grb2 antibody (fifth panel). (B) The amounts of phosphorylated FGFR2 and phosphorylated ERK1/2 were quantified using densitometry and are represented graphically. Data were normalised by dividing the intensity of the phosphorylation signal by the intensity of the corresponding total signal. Co-expression of FGFR2 and Grb2 Y/F mutants (Y7F and Y52F) results in increased FGFR2 phosphorylation in unstimulated cells and slightly reduced FGF-induced ERK1/2 activation in cells expressing the Grb2 Y7F and Y52F mutants.

4.2.8 SHP2 can bind and dephosphorylate phospho-Grb2

Previous studies[173] have proposed a potential role of SHP2 in the FGFR2 signalling pathway. Results from the previous section (section 4.2.6, Figure 4.9) raise the possibility of Grb2 dephosphorylation by a tyrosine phosphatase, so we investigated if SHP2 acts as the phosphatase. Pull-down, *in vitro* dephosphorylation and ITC experiments were conducted to examine the (phospho-)Grb2–SHP2 interaction and the role of SHP2 in Grb2 dephosphorylation.

First, various constructs of the SHP2 domains were created: the two SH2 domains (2SH2), N-SH2 domain (N-SH2), C-SH2 domain (C-SH2), 2SH2 with the conserved arginine-to-alanine mutation in the N-SH2 domain (2SH2-R32A in the FLI/VRES motif), 2SH2 with the conserved arginine-to-alanine mutation in the C-SH2 domain (2SH2-R138A) and 2SH2 with the conserved arginine-to-alanine mutation of both N-SH2 and C-SH2 domains (2SH2-R32/138A double mutant). These constructs were expressed as GST fusion proteins (Figure 4.11) for pull-down experiments.

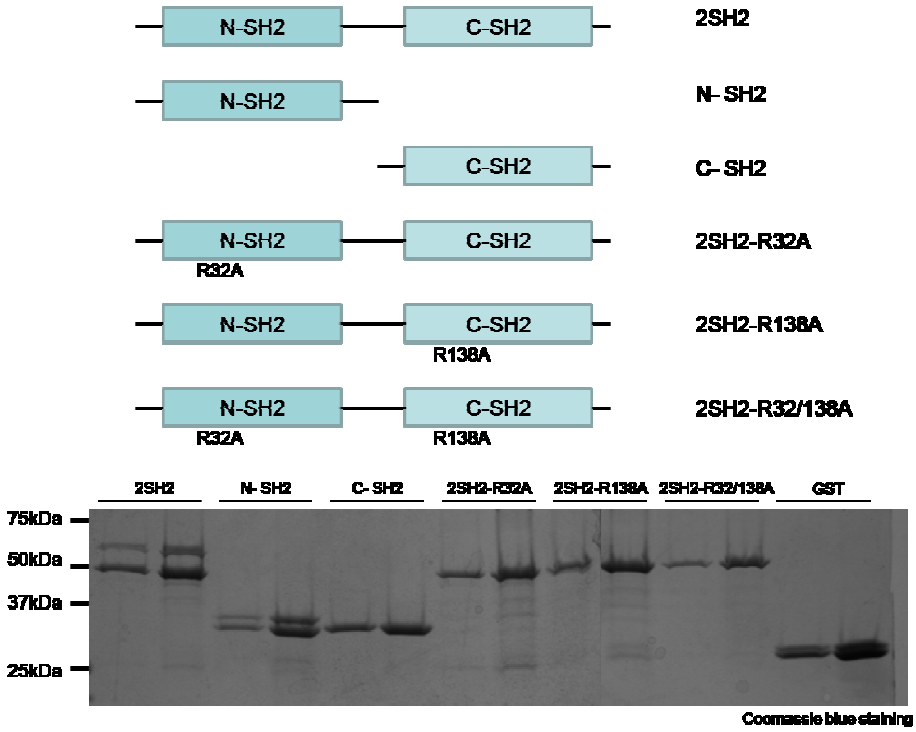

Figure 4.11: Preparation of GST-fused SHP2 proteins. The two SH2 domains of SHP2 (2SH2), N-SH2 domain (N-SH2), C-SH2 domain (C-SH2), 2SH2 with the conserved arginine-to-alanine mutation in the N-SH2 domain (2SH2-R32A), 2SH2 with the conserved arginine-to-alanine mutation in the C-SH2 domain (2SH2-R138A) and 2SH2 with the conserved arginine-to-alanine mutations in both N-SH2 and C-SH2 domains (2SH2-R32/138A) were cloned into a pGEX expression vector with N-terminally fused GST. The GST protein is not illustrated in this diagram. GST fusion proteins were expressed in *E. coli*. Cells were lysed, and the GST fusion proteins were immobilised on GST sepharose beads. Denaturing gels followed by Coomassie blue staining were used to verify protein expression and purity.

A GST pull-down experiment was carried out to investigate the effect of Grb2 phosphorylation on the Grb2–SHP2 interaction and to identify the domain required for these interactions. Grb2 was expressed in bacteria and purified; phospho-Grb2 was prepared as described in section 4.2.5. The various SHP2 constructs immobilised on agarose beads were incubated with an equal amount of either Grb2 or phosphorylated Grb2 overnight. The samples were then washed, denatured and analysed by

immunoblotting. Equal loading was verified by probing with the anti-GST antibody. The anti-Grb2 blot (Figure 4.12, first panel) shows that all constructs of the SHP2 domains were able to bind to unphosphorylated Grb2, confirming that the binding is SHP2-specific. The amount of Grb2 pulled down by the C-SH2 domain alone was significantly less than that of the N-SH2 domain alone or the 2SH2 constructs, indicating that the interaction is mediated primarily by the N-SH2 domain. Because the R/A-mutant SHP2 proteins were able to pull down Grb2, the interaction was not phosphotyrosine-dependent. All of the SHP2 constructs were also able to pull down phosphorylated Grb2. However, when probed with the anti-phosphotyrosine antibody, only the N-SH2 domain was able to pull down a significant amount of phosphorylated Grb2 (Figure 4.12, second and third panels). Taken together, these results suggest unphosphorylated Grb2 is able to bind to SHP2 *in vitro*, albeit very weakly, through the N-SH2 domain of SHP2 in a non-canonical mode. However, phosphorylated Grb2 binds to the N-SH2 domain of SHP2 via the FLI/VRES motif, and this binding is phosphotyrosine dependent.

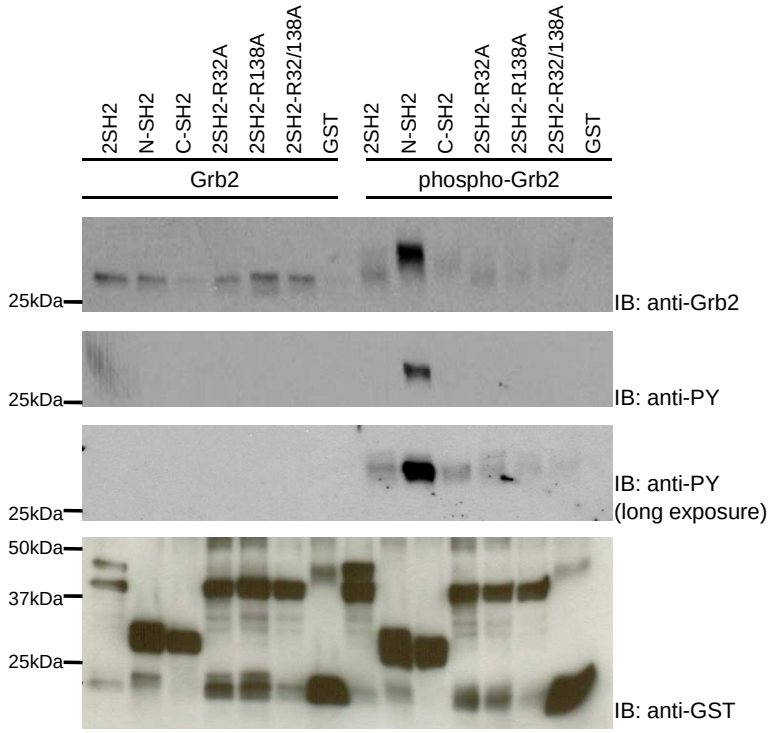

Figure 4.12: Using GST pull-down to evaluate the interactions of individual SHP2 SH2 domains with Grb2 and phospho-Grb2. GST-2SH2, GST-NSH2, GST-CSH2, GST-2SH2-R32A, GST-2SH2-R138A and GST-2SH2-R32/138A on glutathione sepharose were incubated with purified Grb2 and phospho-Grb2 overnight. The beads were washed with buffer five times, and the precipitated proteins were subjected to SDS-PAGE and western blot with an anti-Grb2 antibody (upper panel), an anti-phosphotyrosine antibody (middle panel) and an anti-GST antibody (lower panel) after stripping and re-probing. All SHP2 domains can pull down Grb2, whereas only the N-SH2 domain can pull down the phospho-Grb2 significantly. Anti-GST antibody was used to confirm the amounts of GST-SHP2 domain fusion proteins used in each precipitation experiment. The results are representative of two independent experiments.

ITC experiments were used to characterise the interactions between unphosphorylated/phosphorylated Grb2 and SHP2. The 2SH2 domain of SHP2 was titrated into full-length Grb2. No significant change in heats could be detected in the unphosphorylated Grb2–SHP2 ITC titration (Figure 4.13 A). However, when the 2SH2 domain of SHP2 was titrated into phosphorylated Grb2, a clear binding event

was detected (Figure 4.13 B), even though the isotherm does not allow for a good fit with any binding model. Previous mass spectrometry results showed that three tyrosines on Grb2 can be phosphorylated by FGFR2 in 15 minutes. Therefore, SHP2 might be able to bind to more than one phosphotyrosine residue on phospho-Grb2, which could also be an explanation for the isotherm not being a simple sigmoidal curve with a 1:1 stoichiometry.

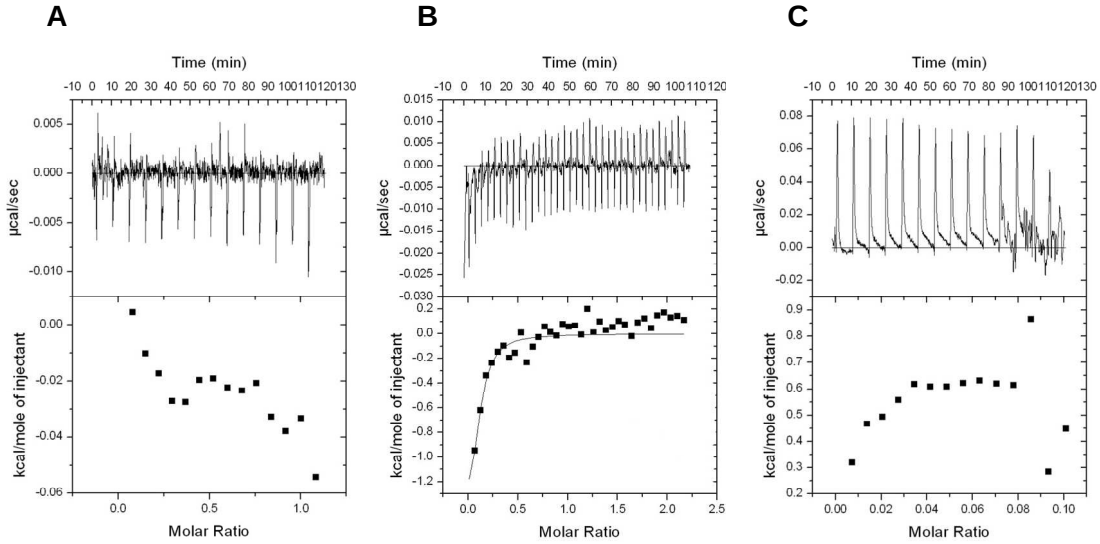

Figure 4.13: ITC measurements of SHP2 2SH2 domain binding to Grb2 and phospho-Grb2. (A) Fourteen 20-µl injections of 466 µM SHP2 2SH2 domain were titrated into 60 µM Grb2 at 15℃. (B) Thirty-five 7- µl injections of 150 µM SHP2 2SH2 domain were titrated into 15 µM phospho-Grb2 at 15℃. (C) Fourteen 20-µl injections of 466 µM SHP2 2SH2 domaindomains were titrated into buffer at 15℃. Th e top panel shows the baseline -corrected data collected at 15℃, while the bottom panel show s the integrated heats released and the molar ratio of the SHP2 2SH2 domain proteindomains to Grb2, the Grb2 N-SH3 domain, the Grb2 C-SH3 domain and phospho-Grb2. The results are representative of two independent experiments.

It is clear that SHP2 interacts with phospho-Grb2, whereas the interaction between SHP2 and unphosphorylated Grb2 is unclear. These experiments are limited because of the concentrations of proteins used. To obtain isotherms that could fit a mathematical model reasonably well, the concentration of the proteins must be at least 5 times above the K_D of the interaction for a 1:1 binding model. The interaction between unphosphorylated Grb2 and SHP2 did not result in an isotherm that clearly showed binding, which could mean that the protein concentration in the cell was well below the K_D. However, the titration between phosphorylated Grb2 and SHP2 showed that the binding sites were saturated when the molar ratio of the two components reached about 1 in the cell. Although accurate determinations for the K_D of the two events cannot be made, the K_D of full-length unphosphorylated Grb2 binding to SHP2 is well above 60 µM, whereas the K_D of full-length phosphorylated Grb2 binding to SHP2 is below 15 µM. These values corroborate the pull-down result that unphosphorylated Grb2 is a weaker binding partner for SHP2 than phosphorylated Grb2.

Another difficulty in these ITC experiments is that the change in heats of binding was too small to be detected accurately. Obtaining better biophysical parameters for these interactions will require further optimisation in conditions such as pH, buffers and

temperatures. Different constructs of the two proteins might also be helpful in better understanding the interactions.

The significance of the interaction between SHP2 and phosphorylated Grb2 was explored by a phosphorylation/dephosphorylation experiment. Purified wild-type full-length SHP2 was incubated with phosphorylated Grb2. Phosphorylated Grb2 was prepared as described before. Analysis was performed by immunoblotting with a phosphotyrosine-specific antibody, followed by stripping and re-probing with an anti-Grb2 antibody as the control for total Grb2 protein loading. Figure 4.14 shows the dephosphorylation of phospho-Grb2 by SHP2.

Taken together, the pull-down, ITC and dephosphorylation *in vitro* experiments suggest that activated FGFR2 activates SHP2 and phosphorylates Grb2 in a cellular environment; then, the activated SHP2 binds to and de-phosphorylates phosphorylated Grb2. Thus, the FGFR2 and SHP2 act as a kinase and phosphatase, respectively, for Grb2 and regulate its phosphorylation level *in vivo*.

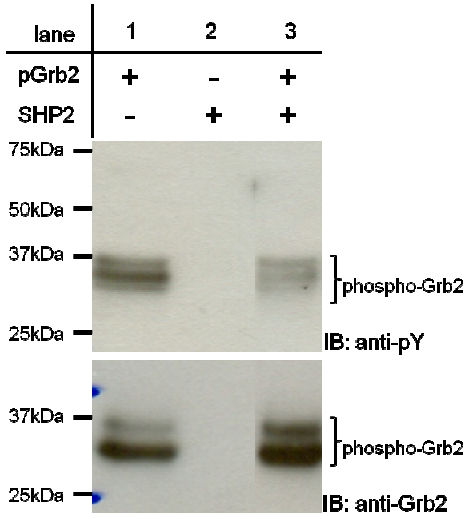

Figure 4.14: Dephosphorylation of phospho-Grb2 by SHP2. Purified wild-type full-length SHP2 was incubated with phospho-Grb2 for 30 minutes. Protein samples were denatured and analysed by SDS-PAGE and immunoblotting. The phosphorylation level of untreated phospho-Grb2 is shown in lane 1. The phosphorylation level was detected by a general anti-phosphotyrosine antibody (upper panel, lane 1). Lane 3 shows that the amount of Grb2 phosphorylation decreases when SHP2 is present (upper panel, lanes 3). An anti-Grb2 antibody was used to show the amount of phospho-Grb2 proteins used in each lane (lower panel). The results are representative of two independent experiments.

4.2.9 Interactions among FGFR2, Grb2 and SHP2

To understand the mechanism of SHP2, Grb2 and FGFR2 signalling complex formation, the Grb2 and FGFR2 cytoplasmic domains were purified, and the GST-fused SHP2 2SH2 domains were immobilised on glutathione sepharose beads. Pull-down experiments were performed using different protein combinations in the absence or presence of ATP/$MgCl_2$, as indicated in Figure 4.15. Lanes 1 and 2 show that both unphosphorylated Grb2 and dephosphorylated FGFR2 cytoplasmic domain can be precipitated by the SHP2 2SH2 domains. Although most of the SH2

domain–mediated binding was phosphotyrosine-specific, it is clear that the binding of unphosphorylated Grb2 and unphosphorylated FGFR2 cytoplasmic domain to the 2SH2 domains was phosphotyrosine-independent. However, the nature of the interactions between unphosphorylated Grb2 and the 2SH2 domains of SHP2, as well as between unphosphorylated FGFR2 cytoplasmic domain and the 2SH2 domains of SHP2, remains to be determined. Notably, when both unphosphorylated Grb2 and the FGFR2 cytoplasmic domain were present in the reaction, the amount of FGFR2 precipitated by the 2SH2 domains decreased (lane 3, first panel), whereas the presence of the unphosphorylated FGFR2 cytoplasmic domain had no effect on the amount of Grb2 precipitated by the SHP2 2SH2 domains (lane 3, third panel). The same effect was not observed when ATP was added to phosphorylated FGFR2 cytoplasmic domain and Grb2 (lanes 4 and 5). Importantly, the pull-down results from lanes 4 and 5 also confirm the previous result that phosphorylated Grb2 does not bind to phosphorylated FGFR2 (Figure 4.7), as it cannot inhibit the SHP2 2SH2 domains. This pull-down experiment reveals a possible mechanism of FGFR2–Grb2–SHP2 interaction.

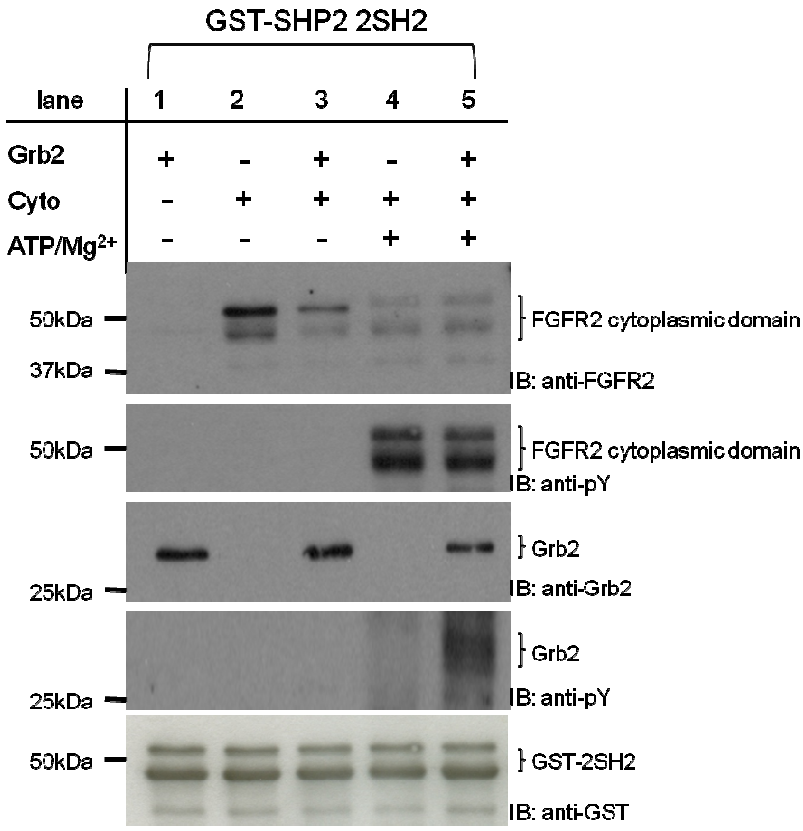

Figure 4.15: Binding of SHP2 to inactivated FGFR2 is inhibited by Grb2. GST-SHP2 2SH2 domains on glutathione sepharose were incubated with purified proteins overnight. The beads were washed with buffer five times, and the precipitated proteins were subjected to SDS-PAGE and western blot. GST-fused SHP2 2SH2 domains were used to precipitate Grb2 (lane 1), dephosphorylated FGFR2 cytoplasmic domain (lane 2), and phosphorylated FGFR2 cytoplasmic domain (lane 4). Grb2 was mixed with the dephosphorylated FGFR2 cytoplasmic domain; less dephosphorylated FGFR2 cytoplasmic domain was precipitated by the SHP2 2SH2 domains (lane 3, compared with lane 2), whereas the precipitation of phosphorylated FGFR2 cytoplasmic domain by the SHP2 2SH2 domains was not affected by either Grb2 or phospho-Grb2 (lane 5, compared with lane 4). An anti-FGFR2 antibody and anti-Grb2 antibody were used to measure the amount of FGFR2 and Grb2 precipitated by the SHP2 2SH2 domains (first and third panels), an anti-phosphotyrosine antibody was used to confirm the phosphorylation states of the FGFR2 cytoplasmic domain and Grb2 (second and forth panels), and an anti-Grb2 antibody was used as the control to show that the same amount of GST-fused SHP2 2SH2 domains was used in each lane (fifth panel). The results are representative of at least three independent experiments.

The binding of Grb2 and phospho-Grb2 to the 2SH2 domains of SHP2 by ITC is described above. To confirm the interactions between FGFR2 and SHP2, both GST pull-down and ITC experiments were performed.

GST pull-down data indicate that both phosphorylated and dephosphorylated FGFR2 cytoplasmic domain can be precipitated by the GST-tagged SHP2 2SH2 domains. Figure 4.16 shows that the SHP2 2SH2 domain binding to the dephosphorylated FGFR2 cytoplasmic domain is phosphotyrosine-independent (Figure 4.16, right panels), confirming previous results (Figure 4.15). As in the binding of Grb2 to the SHP2 2SH2 domains (Figure 4.12 and Figure 4.13), this interaction is phosphotyrosine-independent, and the binding mechanism is unclear. However, our GST pull-down results indicate that the binding of the SHP2 2SH2 domains to either phosphorylated or dephosphorylated FGFR2 is mediated through the C-SH2 domain of SHP2.

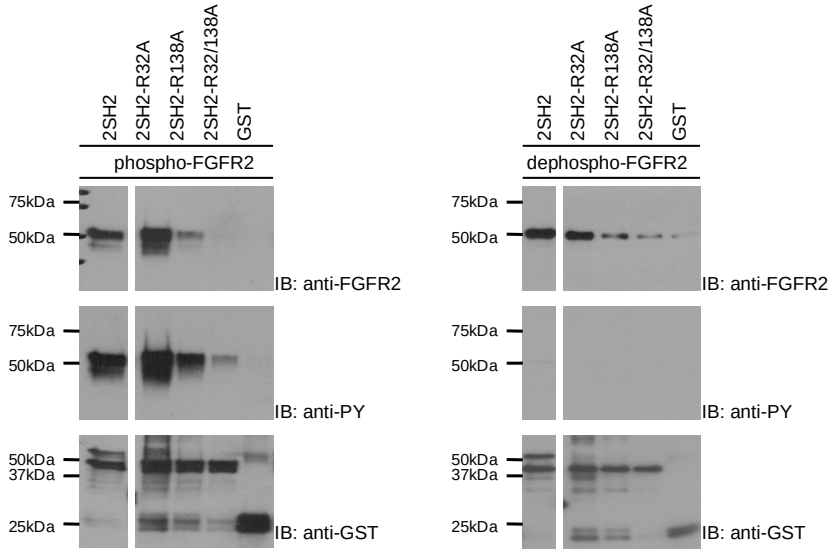

Figure 4.16: GST pull-down to evaluate the interaction of SHP2 2SH2 domains with phosphorylated FGFR2 cytoplasmic domain and dephosphorylated FGFR2 cytoplasmic domain. GST-SHP2 2SH2 domains on glutathione sepharose were incubated with purified phosphorylated FGFR2 cytoplasmic domain and dephosphorylated FGFR2 cytoplasmic domain overnight. The beads were washed with buffer five times, and the precipitated proteins were subjected to SDS-PAGE and western blot with appropriate antibodies. Both phosphorylated FGFR2 cytoplasmic domain and dephosphorylated FGFR2 cytoplasmic domain were precipitated with the SHP2 2SH2 domains and the 2SH2 domains with the conserved arginine mutated in the N-terminal SH2 domain. By contrast, the C-terminal mutant and the double mutant precipitated less phosphorylated and dephosphorylated proteins (first panel, probed with anti-FGFR2 antibody). An anti-phosphotyrosine antibody was used to confirm the phosphorylation states of the precipitated FGFR2 proteins, and an anti-GST antibody was used to confirm the amounts of GST-SHP2 domains fusion proteins used in each precipitation experiment. The results are representative of at least three independent experiments.

The GST pull-down results indicate that the binding site of SHP2 is located in the FGFR2 C-terminus. Therefore, ITC studies were performed to verify the interactions of the 2SH2 domains of SHP2 with an unphosphorylated FGFR2 C-terminal 58-residue peptide (Figure 4.17 A and B; A: actual titration; B: heats of dilution) and

a phosphorylated FGFR2 C-terminal 58-residue peptide (Figure 4.17 C and D; C: actual titration; D: heats of dilution). The tyrosine-phosphorylated C58 peptide bound to the 2SH2 domains with an affinity of 8.3 µM (Figure 4.17 C), whereas the interaction between unphosphorylated C58 peptide and the 2SH2 domains was undetectable by ITC (Figure 4.17 A).

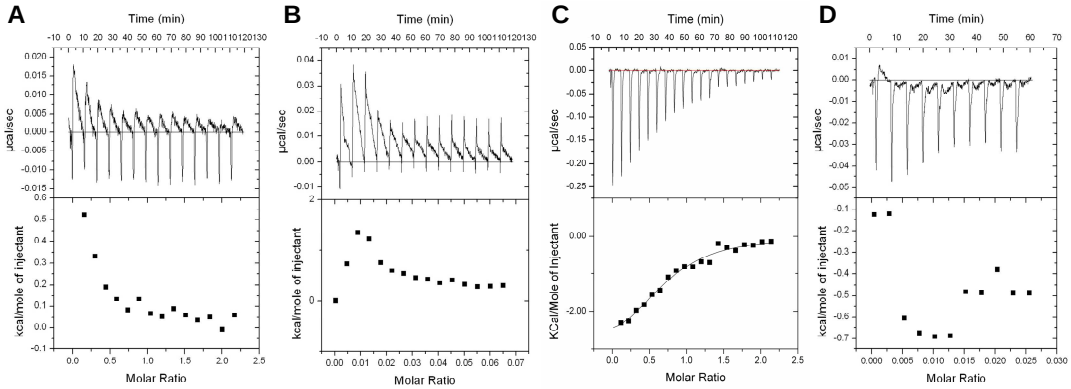

Figure 4.17: ITC measurements of SHP2 2SH2 domains binding to unphosphorylated FGFR2 C-terminal peptide (C58) (A) and phosphorylated FGFR2 C-terminal peptide (C58) (C). To examine unphosphorylated FGFR2 binding to SHP2, the 2SH2 domain peptide was loaded in the ITC syringe, whereas the unphosphorylated FGFR2 C-terminal C58 peptide was loaded in the cell. To examine phosphorylated FGFR2 binding to SHP2, the phosphorylated FGFR2 C-terminal peptide (C58) was loaded in the ITC syringe, whereas the 2SH2 domain peptide was loaded in the cell. The FGFR2 C58 peptide was expressed and purified from *E. coli*. The phosphorylated FGFR2 C58 peptide was prepared by mixing the FGFR2 cytoplasmic domain and C58 peptide in the presence of ATP/$MgCl_2$ for 30 minutes. Gel filtration was used to remove the cytoplasmic domain and free ATP. ITC experiments were carried out at 15℃. The top panel shows the baseline-corrected data collected at 15℃, while the bottom panel shows the integrated heats released and the molar ratio of FGFR2 to Grb2. (A) The 2SH2 domains were titrated into the unphosphorylated FGFR2 C-terminal peptide (C58). (B) The 2SH2 domains were titrated into buffer to measure the heats of dilution. It cannot be definitively concluded that the 2SH2 domains bind to dephosphorylated FGFR2. (C) Direct binding was measured when phosphorylated FGFR2 C-terminal peptide (C58) was titrated into the 2SH2 domains. (D) The same concentration of phosphorylated FGFR2 C-terminal peptide (C58) was titrated into buffer to measure the heats of dilution. The results are representative of two independent experiments.

4.3 Discussion

Grb2 plays an important role in RTK signalling pathways by coupling activated growth factor receptors to Sos. The Grb2–Sos complex activates the MAP kinase signal for RTKs when exposed to mitogens.

The induction of RTK intracellular signalling by growth factor stimulation must be precisely controlled to prevent improper cellular responses. For example, GTPase-activating proteins stimulate the GTPase activity of GTP-bound Ras, resulting in GDP-bound Ras and thereby permitting the control of cellular responses with unlimited transduction.

The C-terminal proline-rich domain of Sos has several MAP kinase consensus phosphorylation sites[262, 263]. ERK phosphorylates Sos both in vitro and in vivo[264]. Activation of insulin receptor results in the serine/threonine phosphorylation of Sos, followed by the dissociation of Sos–Grb2 complexes or the release of the Sos–Grb2 binary complex from the RTKs[265-267]. Therefore, serine/threonine phosphorylation of Sos has been suggested to play a negative feedback role in the Ras pathway.

In contrast to Sos phosphorylation and its role in regulating RTK signalling, Grb2 phosphorylation and its cellular function still remain largely unknown. Grb2 can be tyrosine-phosphorylated by activated RTKs in certain cell lines, and the phosphorylation of Grb2 may be another potential regulation mechanism in RTK signalling control.

However, studies by our group show that direct binding of Grb2 to FGFR2 may have two functions in controlling the FGFR2 signalling pathway. First, direct binding is involved in regulating SHP2 function towards site-specific FGFR2 dephosphorylation. Second, direct binding is important in up-regulating FGFR2 activity.

Therefore, we attempted to investigate the potency of FGFR2 in Grb2 phosphorylation and to examine the role of Grb2 phosphorylation in FGFR2-specific downstream signalling. Biophysical approaches were also used to study the effect of Grb2 phosphorylation on its binding to FGFR2. Moreover, HEK 293T cells that stably expressed FGFR2 were used to transfect Grb2 Y/F mutants in order to understand the role of Grb2 phosphorylation in the FGFR2-mediated signalling pathway. Finally, we investigated the interaction between phosphorylated Grb2 and SHP2 and the relationship among SHP2, Grb2 and FGFR2.

Using bacterially expressed recombinant proteins, we show for the first time that FGFR2 phosphorylates Grb2 *in vitro*. We found that tyrosine phosphorylation of Grb2 requires direct binding to FGFR2 via an SH3 domain–mediated interaction. Grb2 is not tyrosine-phosphorylated under the same conditions when the FGFR2 kinase domain (without the C-terminal tail, where Grb2 binds) was used instead of the whole FGFR2 cytoplasmic domain. Grb2 tyrosines 7, 52 and 160 were identified as the FGFR2 phosphorylation sites using mass spectrometry. These phosphorylation sites are different from those used by Bcr/Abl and prolactin receptor/EGF receptor, which mainly phosphorylate Grb2 on tyrosine 209. The difference in Grb2 phosphorylation sites suggests that Grb2 phosphorylation by different tyrosine kinases may have different roles in Grb2-mediated signalling pathways.

Notably, when native gel electrophoresis and SDS-PAGE were used to analyse the phosphorylated Grb2 samples, the phosphorylated Grb2 migration patterns showed a dependence on time, suggesting that the FGFR2-mediated tyrosine phosphorylation of Grb2 may happen in a certain order. However, mass spectrometry did not show any significant phosphorylation order of Grb2 when the separated bands from the native gel were subjected to analysis. We propose that (phosphorylated) Grb2 may interact with (phosphorylated) Grb2 and/or FGFR2 because the SH2 domain of Grb2 can bind

phosphotyrosine residues, thus making this mass spectrometry result controversial. The best way to determine if Grb2 phosphorylation does happen in a sequential reaction is by resolving these denatured bands by SDS-PAGE.

Grb2 binds to both phosphorylated and dephosphorylated FGFR2 directly (Chapter 3). The interactions between tyrosine-phosphorylated Grb2 and phosphorylated or dephosphorylated FGFR2 were investigated using ITC. The ITC studies did not detect any binding events with tyrosine-phosphorylated Grb2. It is possible that Grb2 phosphorylation acts as a regulator of the FGFR2 signalling pathway. First, because Grb2 can bind and stimulate FGFR2 phosphorylation, the release of Grb2 after it is phosphorylated by FGFR2 may prevent constitutive phosphorylation of FGFR2. Second, GST pull-down experiments show that the direct binding of Grb2 to FGFR2 prevents the interaction of SHP2 to FGFR2. A previous study by our group also indicated that the Grb2–FGFR2 interaction inhibits SHP2 site-specific dephosphorylation of FGFR2. Therefore, the release of phosphorylated Grb2 from FGFR2 allows SHP2 to regulate FGFR2 activation. Third, tyrosine phosphorylation of Grb2 may create sites for intermolecular binding and regulated Grb2 function and/or FGFR2 activation. However, the detailed role of Grb2 phosphorylation remains unclear.

Grb2 phosphorylation was examined *in vivo*. HEK 293 cells express endogenous FGFR1, and FGF2 is an FGFR1-specific ligand. Grb2 immunoprecipitated from HEK 293 cells did not show any tyrosine phosphorylation signal in serum-starved cells, FGF2-stimulated, or FGF9-stimulated cells. These results show that FGFR1 is not able to phosphorylate Grb2. However, Grb2 immunoprecipitated from HEK 293 cells stably expressing FGFR2 showed a Grb2 phosphorylation signal upon phosphotyrosine immunoblotting. But, when the cells were stimulated with FGF9, the phosphotyrosine signal decreased, suggesting a potential protein that could be activated by FGF9 stimulation and therefore dephosphorylate Grb2. HEK 293 cells stably expressing FGFR2 were transfected with wild-type Grb2, Grb2 Y7F or Grb2 Y52F mutant to understand the roles of Grb2 phosphorylation in FGFR2 and ERK phosphorylation. This experiment suggests that Grb2 Y7F and Y52F mutants could enhance FGFR2 phosphorylation and down-regulate FGF-induced ERK activation. This may due to altered binding affinity of Grb2 Y/F mutants towards FGFR2. However, the role of Grb2 Y/F mutants in FGFR2-mediated signalling pathway remains unknown and needs to be investigated thoroughly in the future.

Furthermore, both Grb2 and phospho-Grb2 can directly interact with the two SH2 domains of SHP2. In the unphosphorylated state of Grb2, the interaction between

Grb2 and SHP2 is mainly mediated by Grb2 SH3 domain(s) binding to the RXXK motif of the N-terminal SHP2 SH2 domain. This Grb2 SH3 domain–mediated interaction explains why all of the SH2 R/A mutants could still pull down Grb2. However, the N-terminal domain of SHP2 alone seems to play a major role in phospho-Grb2-SHP2 binding when Grb2 is phosphorylated. The ITC studies also confirm the direct interactions of Grb2 and phospho-Grb2 with SHP2, although the ideal titration curves were not obtained. Importantly, SHP2 dephosphorylated phospho-Grb2 in vitro, as shown by anti-phosphotyrosine immunoblot. Therefore, we propose that the dephosphorylation of Grb2 by SHP2 may play a role in recycling Grb2 in vivo.

In conclusion, this chapter describes the mechanism of Grb2 phosphorylation and its role in FGFR2-mediated signalling. This finding is significant because Grb2 phosphorylation may be important in regulating the FGFR2 signalling pathway. Some of the data are only based on preliminary studies, and the role of Grb2 phosphorylation in cellular signalling remains unclear. More detailed studies will be carried out to investigate the role of Grb2 phosphorylation in the FGFR2-mediated signalling pathway.

Chapter 5

Summary

The aim of this study is to investigate the role of Grb2 in FGFR2 signalling using both *in vivo* and *in vitro* approaches.

Grb2 regulates FGFR2 activation. Grb2, an adaptor protein, lacks enzymatic activity and is thought to be involved in signalling by mediating specific protein-protein interactions that lead to the formation of signalling complexes and prevent the corruption between two different signalling pathways. This study provides evidence that Grb2 not only takes part in the assembly of the early signalling complex upon FGFR2 stimulation but is also able to enhance FGFR2 phosphorylation by inducing a conformational change in FGFR2 and preventing phosphatase binding, suggesting a novel role for Grb2 in regulating FGFR2 activity.

Few reports have shown that Grb2 can be phosphorylated by tyrosine kinases, and the effect of Grb2 phosphorylation on signalling remains unclear. Grb2 is phosphorylated on tyrosine 209 upon EGF stimulation[256], and tyrosine 160 has been reported to be phosphorylated by pp60$^{c\text{-}src}$ [255]. The present study shows that Grb2 can be tyrosine phosphorylated by FGFR2 both *in vivo* and *in vitro,* dependent on the direct binding of Grb2 to the C-terminal tail of FGFR2. Three tyrosine phosphorylation sites on Grb2 have been identified: tyrosines 7, 52 and 160. These additional phosphorylation

sites suggest a different role for Grb2 phosphorylation in the FGFR2 signalling pathway compared to the EGFR signalling pathway. Exogenous expression of the Grb2 Y7F and Y52F mutants may be able to enhance the phosphorylation of FGFR2 in serum-deprived HEK293T cells. Phosphorylation of Grb2 Y7F and Y52F may reduce FGF-stimulated ERK1/2 activation, which opposes the effect of the Grb2 Y209F mutant in increasing EGF-stimulated ERK1/2 activation. These data indicate that variations in Grb2 phosphorylation may modulate different signalling pathways. However, the *in vivo* investigation of Grb2 phosphorylation and its effects on FGFR2-mediated signalling remain unclear.

Biophysical studies were used to characterise the protein-protein interactions involved in the early signalling complex formation of FGFR2 signalling. The two-site binding model of Grb2 binding to FGFR2 is presented, which offers more details than the binding studies using peptides. Additionally, Grb2 binding to phosphorylated FGFR2 *in vitro* is investigated using surface plasmon resonance (SPR), which also shows direct binding of Grb2 to phosphorylated FGFR2 via the SH3 domain of Grb2. Moreover, phospho-Grb2 has been shown to be unable to bind to FGFR2, which suggests a molecular switch mechanism for the Grb2-FGFR2 interaction.

Furthermore, we examined the role of SHP2 in FGFR2-Grb2 binding and FGFR2 activation. This study shows the direct interaction of SHP2 with activated FGFR2 and phospho-Grb2 *in vitro*. Direct binding of the SHP2 C-SH2 domain to the C-terminal tail of activated FGFR2 is thought to be important in the repression of FGFR2 activation, while direct binding of SHP2 to phospho-Grb2 is necessary for Grb2 dephosphorylation.

Taken together, this study provides new insights into the role of Grb2 in FGFR2 signalling. We present a model for FGFR2 regulation through the dynamic formation of protein-protein interactions.

5.1 The FGFR2 early signal complex recruitment model

O'Rourke and Ladbury have discussed the importance of signalling complex formation in the RTK signalling pathway[43]. Together with the studies carried out in Chapters 3 and 4, the following FGFR2 signalling complex formation and FGFR2 signalling pathway activation model is proposed (Figure 5.1). Grb2 binds to inactive FGFR2 via its C-SH3 domain, resulting in a conformational change and an increase in FGFR2 activity (Figure 5.1 A). In this state, the direct binding of Grb2 to FGFR2 inhibits the recruitment of SHP2 to FGFR2, which is important in preventing SHP2-mediated FGFR2 dephosphorylation (Figure 5.1 B). Early studies indicated that the dimerisation of the FGF receptor is due to the cooperation of the extracellular domain in binding to FGF ligands and heparan sulphate proteoglycans. However, our studies propose that Grb2 may also be able to cause the dimerisation of FGFR2. Once FGFR2 molecules begin to be activated and phosphorylated, the conformation of FGFR2 changes. The C-terminal tail of FGFR2 with Grb2 would loop back and bind to the kinase domain (unpublished data), bringing Grb2 to the kinase domain for subsequent phosphorylation (Figure 5.1 C). Phosphorylated Grb2 cannot bind to activated FGFR2 (Figure 5.1 D) and is therefore released. The SH2 domain-containing phosphatase SHP2 is then recruited to the activated FGFR2, mediated by binding of the SHP2 C-SH2 domain to the phosphotyrosine residues on

the FGFR2 C-terminal tail, causing site-specific dephosphorylation of FGFR2 (Figure 5.1 E). SHP2 can also bind to the released tyrosine-phosphorylated Grb2 via its N-SH2 domain and subsequently dephosphorylate Grb2. The SHP2-dephosphorylated Grb2 and FGFR2 are then ready for a new cycle of FGFR2 activation (Figure 5.1 F).

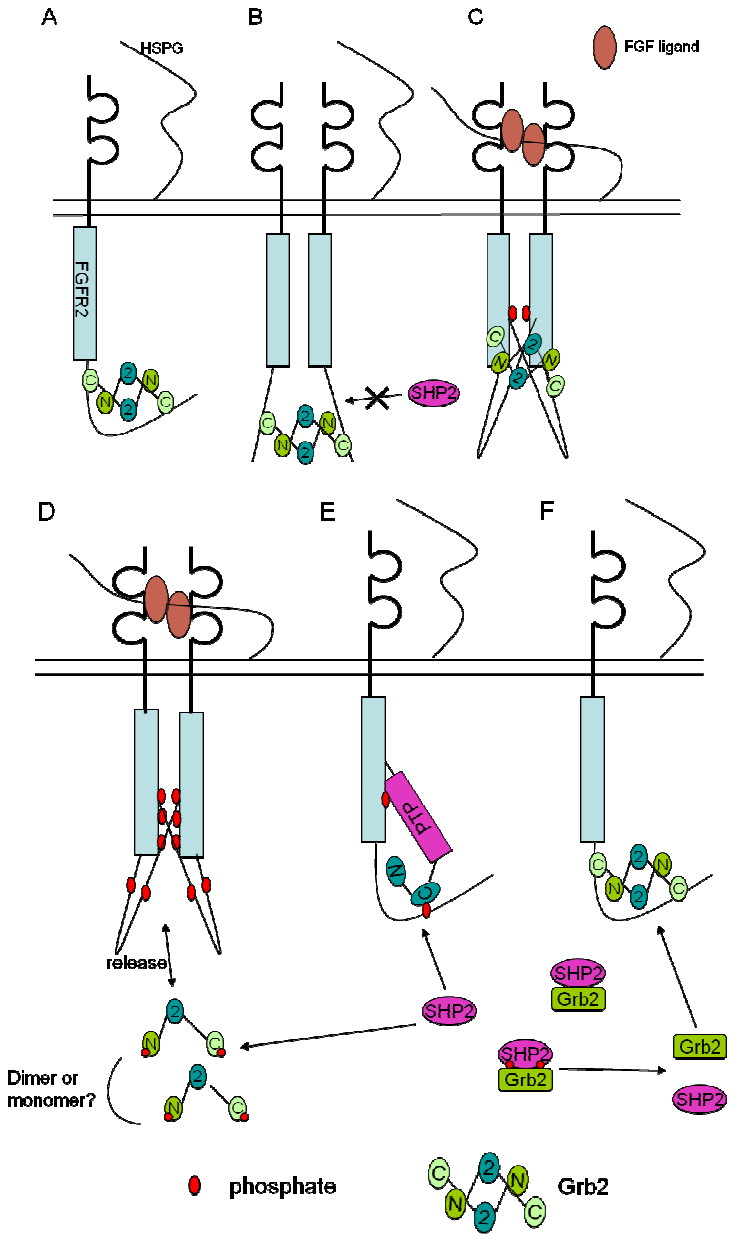

Figure 5.1: Diagrammatic representation of FGFR2 activation and the signalling complex recruitment. Grb2 binds to inactivated FGFR2 via SH3 domains, resulting in conformational change and preferential activation of FGFR2, this direct binding of Grb2 to FGFR2 also inhibits the recruitment of SHP2 to FGFR2. Grb2 is phoshporylated by the activated FGFR2, and the phosphorylated Grb2 no longer bind to the activated FGFR2. The SH2 domain-containing phosphatase SHP2 is recruited to the activated FGFR2 via binding of SHP2 C-SH2 domain to the phosphotyrosine residues on the FGFR2 C-terminal tail, and causes the site-specific dephosphorylation of FGFR. SHP2 can also binds to the released tyrosine phosphorylated Grb2 via SHP2 N-SH2 domain and dephosphorylates the phospho-Grb2. The SHP2-dephosphorylated Grb2 and FGFR2 therefore can restart the FGFR2 signalling pathway.

5.2 Future work

5.2.1 Does Grb2 binding induce conformational changes in FGFR2?

Both previous work by Ahmed *et al.*[173] and this study show direct interaction between Grb2 and FGFR2. Dot-blot experiments suggest that binding of Grb2 to FGFR2 may expose the buried phosho-tyrosines of FGFR2. Additionally, this study provides evidence that Grb2 can enhance FGFR2 phosphorylation *in vitro*. Based on these findings, we propose that the direct binding of Grb2 to FGFR2 may cause a conformational change of FGFR2 that is preferential for phosphorylation.

Direct evidence addressing a Grb2-induced FGFR2 conformational change will be dependent on structural studies. However, because there is no structural information currently available, different approaches may be used to investigate the conformational change. First, the small-angle X-ray scattering (SAXS) method will be employed to study the overall conformation of the FGFR2 cytoplasmic domain in the absence or presence of Grb2. Because the stability of Grb2-FGFR2 complexes has previously caused technical challenges, bis(sulfosuccinimidyl) suberate (BS3) will be used to cross-link Grb2 and FGFR2.

An alternative approach to determine the Grb2 binding-induced FGFR2 conformational changes will be fluorescence-based. Fluorescence resonance energy transfer (FRET) has been demonstrated to be a powerful tool for studying protein structure[268]. Using fluorescent tags, such as N-terminal-tagged CFP and C-terminal-tagged YFP, conformational changes, including the distance and the orientation of biological macromolecules, have been successfully monitored. Recently, the remarkable development of single-molecule spectroscopy has provided an advantage in studying protein conformational changes within a single molecule range[269]. However, the use of fluorescent proteins as the FRET donor or acceptor may interfere with the native protein structure and function because of their large size[270]. Therefore, Kajihara *et al.* developed the position-specific incorporation of fluorescent amino acids that function as fluorescent donors and acceptors and have limited effects on protein structure and function[271]. Most recently, Santoso *et al.* used single-molecule FRET technology to study the conformational transitions in DNA polymerase I[272].

5.2.2 The detailed model of FGFR2- Grb2 binding

Based on the two-site binding model presented in this study, it is necessary to identify the secondary binding site for Grb2 on FGFR2. Four PXXP motifs can be found on

the C-terminal tail of FGFR2; therefore, recombinant cytoplasmic domain constructs with different PXXP motif mutants (Pro to Ala mutations) will be generated for the identification of the secondary binding site.

The detailed mechanism of FGFR2 binding to Grb2 still remains unclear. To date, we can only conclude that the Grb2 C-SH3 domain is the major contributor involved in binding to the PXXP motif of FGFR2, which is reflected in our two-site binding model. However, it is not clear whether the N-SH3 domain or the C-SH3 domain mediates the secondary binding event of the two-site binding model. In this study, both isothermal titration calorimetry (ITC) and SPR approaches did not detect any interaction between the N-SH3 domain and FGFR2. However, one of our earlier studies shows direct interaction between the N-terminal SH3 domain of Grb2 and FGFR2: the GST-tagged N-SH3 domain of Grb2 is able to pull down wild-type FGFR2 from HEK 293 cells both before and after stimulation. In contrast with HEK 293 cells, the same result could not be duplicated using NIH-3T3 cells. Moreover, fluorescence lifetime imaging microscopy (FLIM) also shows direct interaction between the N-terminal SH3 domain of Grb2 and FGFR2 in unstimulated HEK 293 cells. *In vivo* binding of the Grb2 N-SH3 domain to FGFR2 may be cell type–specific.

Once the secondary binding site has been identified, amino acid sequence–relevant peptides will be synthesised, and both N-SH3 and C-SH3 domain proteins or N-SH3/C-SH3 with Grb2 will be components in a competition-binding assay using both ITC and SPR technology or the alternative fluorescent-based assay. Hopefully, this study will allow us to provide a more detailed model of the interaction between FGFR2 and Grb2.

5.2.3 The role of Grb2 phosphorylation in FGFR2-mediated signalling

This study shows that Grb2 can be tyrosine phosphorylated by FGFR2 both *in vitro* and *in vivo* and identifies the phosphorylation sites on Grb2. Although this study has shown that Grb2 phosphorylation is the key mechanism controlling FGFR2 binding, the function of Grb2 phosphorylation in FGFR2 signalling remains unclear.

In Chapter 3, we show that direct binding of Grb2 to FGFR2 is necessary for Grb2-mediated FGFR2 phosphorylation. However, *in vitro* binding studies provide clear evidence that Grb2 is released from FGFR2 once it is phosphorylated by FGFR2. Therefore, we propose a potential role for Grb2 phosphorylation in regulating FGFR2 signalling.

Our *in vivo* study proposes that Grb2 phosphorylation may be involved in regulating FGFR2 and ERK1/2 phosphorylation. However, this hypothesis is based on a single experiment prior to checking reproducibility. To rigorously investigate the role of Grb2 phosphorylation in FGFR2-mediated signalling, several additional experiments are necessary.

First, the experiment shown in Figure 4.10 needs to be repeated, and proper controls need to be employed to make a solid conclusion regarding the effects of Grb2 Y/F mutants on FGFR2 and ERK1/2 activation. The phosphorylation status of Grb2 Y/F mutants in response to FGF9 stimulation will also be examined.

Second, we have shown that Grb2 is tyrosine phosphorylated in FGFR2-expressing HEK 293 cells. Interestingly, the phosphorylation level of Grb2 goes down in response to FGF9 stimulation. SHP2 may be activated by FGFR2 in response to FGF9, in which case activated SHP2 would dephosphorylate Grb2. *In vitro* experiments have demonstrated that SHP2 can bind to phospho-Grb2 directly and that SHP2 can dephopshorylate phospho-Grb2. However, the exact role of SHP2 in Grb2 phosphorylation is still unclear. The SHP2 inhibitor NSC87877 will be included in this experiment to elucidate the role of SHP2 in Grb2 dephosphorylation. Both

serum-starved and FGF9-stimulated FGFR2-expressing cells will be treated with the SHP2 inhibitor NSC87877. Together with other NSC87877-free controls, immunoprecipitation will be carried out using an anti-Grb2 antibody, and different antibodies will be used to investigate the immunoprecipitated complex. SHP2-knockdown cell lines would be a useful material in this part of study. Both FGFR2-expressing cell lines and FGFR2-expressing/SHP2-knockdown cell lines will be used to compare the effects of SHP2 expression on Grb2 phosphorylation. Immunoprecipitation will be carried out using an anti-Grb2 antibody, and an anti-phosphotyrosine antibody will be used to illustrate the phosphorylation status of precipitated Grb2.

Finally, Li *et al.*[256] have shown that phosphorylation of Grb2 tyrosine 209 reduces its binding to Sos. Because Grb2 is phosphorylated by FGFR2 at tyrosines 7, 52 and 160, we will also examine the effects of these three tyrosine phosphorylation sites on Grb2-Sos complex formation. FGFR2-expressing cell lines transfected with different Grb2 mutants will be used to study Grb2-Sos complex formation. Immunoprecipitation will be carried out using an anti-Grb2 antibody and an anti-Sos antibody to understand the effects of variant Grb2 Y/F mutants on Grb2-Sos complex

formation. Lastly, we will examine possible contributions of Grb2 Y/F mutant expression to FGFR2-mediated signalling that lead to active Ras.

References

1. Ullrich, A. & Schlessinger, J. Signal transduction by receptors with tyrosine kinase activity. *Cell* **61**, 203-12 (1990).
2. Superti-Furga, G. Regulation of the Src protein tyrosine kinase. *FEBS Lett* **369**, 62-6 (1995).
3. Hunter, M.G. & Avalos, B.R. Phosphatidylinositol 3'-kinase and SH2-containing inositol phosphatase (SHIP) are recruited by distinct positive and negative growth-regulatory domains in the granulocyte colony-stimulating factor receptor. *J Immunol* **160**, 4979-87 (1998).
4. Russell, D.S., Gherzi, R., Johnson, E.L., Chou, C.K. & Rosen, O.M. The protein-tyrosine kinase activity of the insulin receptor is necessary for insulin-mediated receptor down-regulation. *J Biol Chem* **262**, 11833-40 (1987).
5. Marshall, C.J. Specificity of receptor tyrosine kinase signaling: transient versus sustained extracellular signal-regulated kinase activation. *Cell* **80**, 179-85 (1995).
6. Alberts, B., Johnson, A., Lewis, J., Raff, M., Roberts, K. & Walter, P. Molecular Biology of the Cell (New York and London: Garland Science 2002).
7. Burgess, W.H., Dionne, C. A., Kaplow, J., Mudd, R., Friesel, R., Zilberstein, A., Schlessinger, J. & Jaye, M. Characterization and cDNA cloning of phospholipase C-gamma, a major substrate for heparin-binding growth factor 1 (acidic fibroblast growth factor)-activated tyrosine kinase. *Mol Cell Biol* **10**, 4770-7 (1990).
8. Cantley, L.C. The phosphoinositide 3-kinase pathway. *Science* **296**, 1655-7 (2002).
9. Vanhaesebroeck, B. & Alessi, D.R. The PI3K-PDK1 connection: more than just a road to PKB. *Biochem J* **346 Pt 3**, 561-76 (2000).
10. Manning, G., Whyte, D.B., Martinez, R., Hunter, T. & Sudarsanam, S. The protein kinase complement of the human genome. *Science* **298**, 1912-34 (2002).
11. Lemmon, M.A. & Schlessinger, J. Cell signaling by receptor tyrosine kinases. *Cell* **141**, 1117-34 (2010).
12. Fantl, W.J., Johnson, D.E. & Williams, L.T. Signalling by receptor tyrosine kinases. *Annu Rev Biochem* **62**, 453-81 (1993).
13. van der Geer P, H.T. & Lindberg R.A. Receptor protein-tyrosine kinases and their signal transduction pathways. *Annu Rev Cell Biol* **10**, 251-337 (1994).

14. Heldin, C.H. Dimerization of cell surface receptors in signal transduction. *Cell* **80**, 213-23 (1995).
15. Webster, M.K. & Donoghue, D.J. Constitutive activation of fibroblast growth factor receptor 3 by the transmembrane domain point mutation found in achondroplasia. *EMBO J* **15**, 520-7 (1996).
16. Bargmann, C.I. & Weinberg, R.A. Oncogenic activation of the neu-encoded receptor protein by point mutation and deletion. *EMBO J* **7**, 2043-52 (1988).
17. Sternberg, M.J. & Gullick, W.J. Neu receptor dimerization. *Nature* **339**, 587 (1989).
18. Hanks, S.K. Eukaryotic protein kinases. *Current Opinion in Structural Biology* **1**, 315-9 (1991).
19. Hanks, S.K., Quinn, A.M. & Hunter, T. The protein kinase family: conserved features and deduced phylogeny of the catalytic domains. *Science* **241**, 42-52 (1988).
20. Bossemeyer, D., Engh, R.A., Kinzel, V., Ponstingl, H. & Huber, R. Phosphotransferase and substrate binding mechanism of the cAMP-dependent protein kinase catalytic subunit from porcine heart as deduced from the 2.0 A structure of the complex with Mn2+ adenylyl imidodiphosphate and inhibitor peptide PKI(5-24). *EMBO J* **12**, 849-59 (1993).
21. De Bondt, H.L., Rosenblatt, J., Jancarik, J., Jones, H.D., Morgan, D.O. & Kim, S.H. Crystal structure of cyclin-dependent kinase 2. *Nature* **363**, 595-602 (1993).
22. Knighton, D.R., Zheng, J.H., Ten Eyck, L.F., Ashford, V.A., Xuong, N.H., Taylor, S.S. & Sowadski, J.M. Crystal structure of the catalytic subunit of cyclic adenosine monophosphate-dependent protein kinase. *Science* **253**, 407-14 (1991).
23. Zhang, F., Strand, A., Robbins, D., Cobb, M.H. & Goldsmith, E.J. Atomic structure of the MAP kinase ERK2 at 2.3 A resolution. *Nature* **367**, 704-11 (1994).
24. Knighton, D.R., Zheng, J.H., Ten Eyck, L.F., Xuong, N.H., Taylor, S.S. & Sowadski, J.M. Structure of a peptide inhibitor bound to the catalytic subunit of cyclic adenosine monophosphate-dependent protein kinase. *Science* **253**, 414-20 (1991).
25. Ong, S.H., Guy, G.R., Hadari, Y.R., Laks, S., Gotoh, N., Schlessinger, J. & Lax, I. FRS2 proteins recruit intracellular signaling pathways by binding to diverse targets on fibroblast growth factor and nerve growth factor receptors. *Mol Cell Biol* **20**, 979-89 (2000).

26. Schlessinger, J. Signal transduction by allosteric receptor oligomerization. *Trends Biochem Sci* **13**, 443-7 (1988).
27. Jiang, G. & Hunter, T. Receptor signaling: when dimerization is not enough. *Curr Biol* **9**, R568-71 (1999).
28. Cunningham, B.C., Ultsch, M., De Vos, A.M., Mulkerrin, M.G., Clauser, K. R. & Wells, J.A. Dimerization of the extracellular domain of the human growth hormone receptor by a single hormone molecule. *Science* **254**, 821-5 (1991).
29. Greenfield, C., Hiles, I., Waterfield, M.D., Federwisch, M., Wollmer, A., Blundell, T.L. & McDonald, N. Epidermal growth factor binding induces a conformational change in the external domain of its receptor. *EMBO J* **8**, 4115-23 (1989).
30. Lax, I., Fischer, R., Ng, C., Segre, J., Ullrich, A., Givol, D. & Schlessinger, J. Noncontiguous regions in the extracellular domain of EGF receptor define ligand-binding specificity. *Cell Regul* **2**, 337-45 (1991).
31. Hurwitz, D.R., Emanuel, S. L., Nathan, M. H., Sarver, N., Ullrich, A., Felder, S., Lax, I. & Schlessinger, J. EGF induces increased ligand binding affinity and dimerization of soluble epidermal growth factor (EGF) receptor extracellular domain. *J Biol Chem* **266**, 22035-43 (1991).
32. Weiss, A. & Schlessinger, J. Switching signals on or off by receptor dimerization. *Cell* **94**, 277-80 (1998).
33. Yarden, Y. & Ullrich, A. Molecular analysis of signal transduction by growth factors. *Biochemistry* **27**, 3113-9 (1988).
34. Honegger, A.M., Kris, R.M., Ullrich, A. & Schlessinger, J. Evidence that autophosphorylation of solubilized receptors for epidermal growth factor is mediated by intermolecular cross-phosphorylation. *Proc Natl Acad Sci U S A* **86**, 925-9 (1989).
35. Chen, W.S., Lazar, C.S., Lund, K.A., Welsh, J.B., Chang, C.P., Walton, G.M., Der, C.J., Wiley, H.S., Gill, G.N. & Rosenfeld, M.G. Functional independence of the epidermal growth factor receptor from a domain required for ligand-induced internalization and calcium regulation. *Cell* **59**, 33-43 (1989).
36. Coughlin, S.R., Escobedo, J.A. & Williams, L.T. Role of phosphatidylinositol kinase in PDGF receptor signal transduction. *Science* **243**, 1191-4 (1989).
37. Schlessinger, J. & Ullrich, A. Growth factor signaling by receptor tyrosine kinases. *Neuron* **9**, 383-91 (1992).
38. Pawson, T. Protein modules and signalling networks. *Nature* **373**, 573-80 (1995).

39. Moran, M.F., Koch, C.A., Anderson, D., Ellis, C., gland, L., rtin, G.S. & Pawson, T. Src homology region 2 domains direct protein-protein interactions in signal transduction. *Proc Natl Acad Sci U S A* **87**, 8622-6 (1990).
40. Felder, S., Zhou, M., Hu, P., Urena, J., Ullrich, A., Chaudhuri, M., White, M., Shoelson, S.E. & Schlessinger, J. SH2 domains exhibit high-affinity binding to tyrosine-phosphorylated peptides yet also exhibit rapid dissociation and exchange. *Mol Cell Biol* **13**, 1449-55 (1993).
41. Panayotou, G. & Waterfield, M.D. The assembly of signalling complexes by receptor tyrosine kinases. *Bioessays* **15**, 171-7 (1993).
42. Kuriyan, J. & Cowburn, D. Modular peptide recognition domains in eukaryotic signaling. *Annu Rev Biophys Biomol Struct* **26**, 259-88 (1997).
43. O'Rourke, L. & Ladbury, J.E. Specificity is complex and time consuming: mutual exclusivity in tyrosine kinase-mediated signaling. *Acc Chem Res* **36**, 410-6 (2003).
44. Ladbury, J.E., Wright, J.G., Sturtevant, J.M. & Sigler, P.B. A thermodynamic study of the trp repressor-operator interaction. *J Mol Biol* **238**, 669-81 (1994).
45. Ladbury, J.E. & Arold, S. Searching for specificity in SH domains. *Chem Biol* **7**, R3-8 (2000).
46. Waksman, G., Kominos, D., Robertson, S.C., Pant, N., Baltimore, D., Birge, R.B., Cowburn, D., Hanafusa, H., Mayer, B.J., Overduin, M., Resh, M.D., Rios, C.B., Silverman, L. & Kuriyan, J. Crystal structure of the phosphotyrosine recognition domain SH2 of v-src complexed with tyrosine-phosphorylated peptides. *Nature* **358**, 646-53 (1992).
47. Anderson, D., Koch, C. A., Grey, L., Ellis, C., Moran, M. F. & Pawson, T. Binding of SH2 domains of phospholipase C gamma 1, GAP, and Src to activated growth factor receptors. *Science* **250**, 979-82 (1990).
48. Margolis, B., Li, N., Koch, A., Mohammadi, M., Hurwitz, D.R., Zilberstein, A., Ullrich, A., Pawson, T. & Schlessinger, J. The tyrosine phosphorylated carboxyterminus of the EGF receptor is a binding site for GAP and PLC-gamma. *EMBO J* **9**, 4375-80 (1990).
49. Mayer, B.J. & Hanafusa, H. Association of the v-crk oncogene product with phosphotyrosine-containing proteins and protein kinase activity. *Proc Natl Acad Sci U S A* **87**, 2638-42 (1990).
50. Liu, B.A., Jablonowski, K., Raina, M., Arce, M., Pawson, T. & Nash, P.D. The human and mouse complement of SH2 domain proteins-establishing the boundaries of phosphotyrosine signaling. *Mol Cell* **22**, 851-68 (2006).
51. Sadowski, I., Stone, J.C. & Pawson, T. A noncatalytic domain conserved among cytoplasmic protein-tyrosine kinases modifies the kinase function and

transforming activity of Fujinami sarcoma virus P130gag-fps. *Mol Cell Biol* **6**, 4396-408 (1986).

52. Pawson, T. Non-catalytic domains of cytoplasmic protein-tyrosine kinases: regulatory elements in signal transduction. *Oncogene* **3**, 491-5 (1988).
53. Skolnik, E.Y., Margolis, B., Mohammadi, M., Lowenstein, E., Fischer, R., Drepps, A., Ullrich, A. & Schlessinger, J. Cloning of PI3 kinase-associated p85 utilizing a novel method for expression/cloning of target proteins for receptor tyrosine kinases. *Cell* **65**, 83-90 (1991).
54. Lowenstein, E.J., Daly, R. J., Batzer, A. G., Li, W., Margolis, B., Lammers, R., Ullrich, A., Skolnik, E. Y., Bar-Sagi, D. & Schlessinger, J. The SH2 and SH3 domain-containing protein GRB2 links receptor tyrosine kinases to ras signaling. *Cell* **70**, 431-42 (1992).
55. Margolis, B. Proteins with SH2 domains: transducers in the tyrosine kinase signaling pathway. *Cell Growth Differ* **3**, 73-80 (1992).
56. Songyang, Z., Shoelson, S.E., Chaudhuri, M., Gish, G., Pawson, T., Haser, W.G., King, F., Roberts, T., Ratnofsky, S. & Lechleider, R.J. SH2 domains recognize specific phosphopeptide sequences. *Cell* **72**, 767-78 (1993).
57. Kuriyan, J. & Cowburn, D. Structures of SH2 and SH3 domains. *Curr Op Struct Biol* **3**, 828-37 (1993).
58. Pascal, S.M., Singer, A.U., Gish, G., Yamazaki, T., Shoelson, S.E., Pawson, T., Kay, L.E. & Forman-Kay, J.D. Nuclear magnetic resonance structure of an SH2 domain of phospholipase C-gamma 1 complexed with a high affinity binding peptide. *Cell* **77**, 461-72 (1994).
59. DeLorbe, J.E., Clements, J.H., Teresk, M.G., Benfield, A.P., Plake, H.R., Millspaugh, L.E. & Martin, S.F. Thermodynamic and structural effects of conformational constraints in protein-ligand interactions. Entropic paradoxy associated with ligand preorganization. *J Am Chem Soc* **131**, 16758-70 (2009).
60. Ladbury, J.E. Measurement of the formation of complexes in tyrosine kinase-mediated signal transduction. *Acta Crystallogr D Biol Crystallogr* **63**, 26-31 (2007).
61. Piccione, E., Case, R.D., Domchek, S.M., Hu, P., Chaudhuri, M., Backer, J.M., Schlessinger, J. & Shoelson, S.E. Phosphatidylinositol 3-kinase p85 SH2 domain specificity defined by direct phosphopeptide/SH2 domain binding. *Biochemistry* **32**, 3197-202 (1993).
62. Bae, J.H., Lew, E.D., Yuzawa, S., Tome, F., Lax, I. & Schlessinger, J. The selectivity of receptor tyrosine kinase signaling is controlled by a secondary SH2 domain binding site. *Cell* **138**, 514-24 (2009).

63. Zhou, M.M., Ravichandran, K.S., Olejniczak, E.F., Petros, A.M., Meadows, R.P., Sattler, M., Harlan, J.E., Wade, W.S., Burakoff, S.J. & Fesik, S.W. Structure and ligand recognition of the phosphotyrosine binding domain of Shc. *Nature* **378**, 584-92 (1995).
64. Uhlik, M.T., Temple, B., Bencharit, S., Kimple, A.J., Siderovski, D.P. & Johnson, G.L. Structural and evolutionary division of phosphotyrosine binding (PTB) domains. *J Mol Biol* **345**, 1-20 (2005).
65. Obermeier, A., Bradshaw, R.A., Seedorf, K., Choidas, A., Schlessinger, J. & Ullrich, A. Neuronal differentiation signals are controlled by nerve growth factor receptor/Trk binding sites for SHC and PLC gamma. *EMBO J* **13**, 1585-90 (1994).
66. Campbell, K.S., Ogris, E., Burke, B., Su, W., Auger, K.R., Druker, B.J., Schaffhausen, B.S., Roberts, T.M. & Pallas, D.C. Polyoma middle tumor antigen interacts with SHC protein via the NPTY (Asn-Pro-Thr-Tyr) motif in middle tumor antigen. *Proc Natl Acad Sci U S A* **91**, 6344-8 (1994).
67. Yan, K.S., Kuti, M., Yan, S., Mujtaba, S., Farooq, A., Goldfarb, M.P. & Zhou, M.M. FRS2 PTB domain conformation regulates interactions with divergent neurotrophic receptors. *J Biol Chem* **277**, 17088-94 (2002).
68. Zhang, Z., Lee, C.H., Mandiyan, V., Borg, J.P., Margolis, B., Schlessinger, J. & Kuriyan, J. Sequence-specific recognition of the internalization motif of the Alzheimer's amyloid precursor protein by the X11 PTB domain. *EMBO J* **16**, 6141-50 (1997).
69. Dhalluin, C., Yan, K.S., Plotnikova, O., Lee, K.W., Zeng, L., Kuti, M., Mujtaba, S., Goldfarb, M.P. & Zhou, M.M. Structural basis of SNT PTB domain interactions with distinct neurotrophic receptors. *Mol Cell* **6**, 921-9 (2000).
70. Xu, H., Lee, K.W. & Goldfarb, M. Novel recognition motif on fibroblast growth factor receptor mediates direct association and activation of SNT adapter proteins. *J Biol Chem* **273**, 17987-90 (1998).
71. Mayer, B.J., Hamaguchi, M. & Hanafusa, H. A novel viral oncogene with structural similarity to phospholipase C. *Nature* **332**, 272-5 (1988).
72. Stahl, M.L., Ferenz, C.R., Kelleher, K.L., Kriz, R.W. & Knopf, J.L. Sequence similarity of phospholipase C with the non-catalytic region of src. *Nature* **332**, 269-72 (1988).
73. Otsu, M., Hiles, I., Gout, I., Fry, M.J., Ruiz-Larrea, F., Panayotou, G., Thompson, A., Dhand, R., Hsuan, J. & Totty, N. Characterization of two 85 kd proteins that associate with receptor tyrosine kinases, middle-T/pp60c-src complexes, and PI3-kinase. *Cell* **65**, 91-104 (1991).

74. Koch, C.A., Anderson, D., Moran, M.F., Ellis, C. & Pawson, T. SH2 and SH3 domains: elements that control interactions of cytoplasmic signaling proteins. *Science* **252**, 668-74 (1991).
75. Pawson, T. & Gish, G.D. SH2 and SH3 domains: from structure to function. *Cell* **71**, 359-62 (1992).
76. Musacchio, A., Noble, M., Pauptit, R., Wierenga, R. & Saraste, M. Crystal structure of a Src-homology 3 (SH3) domain. *Nature* **359**, 851-5 (1992).
77. Rodaway, A.R., Sternberg, M.J. & Bentley, D.L. Similarity in membrane proteins. *Nature* **342**, 624 (1989).
78. Ren, R., Mayer, B.J., Cicchetti, P. & Baltimore, D. Identification of a ten-amino acid proline-rich SH3 binding site. *Science* **259**, 1157-61 (1993).
79. Yu, H., Rosen, M.K., Shin, T.B., Seidel-Dugan, C., Brugge, J.S. & Schreiber, S.L. Solution structure of the SH3 domain of Src and identification of its ligand-binding site. *Science* **258**, 1665-8 (1992).
80. Booker, G.W., Gout, I., Downing, A.K., Driscoll, P.C., Boyd,J., Waterfield, M.D. & Campbell, I.D. Solution structure and ligand-binding site of the SH3 domain of the p85 alpha subunit of phosphatidylinositol 3-kinase. *Cell* **73**, 813-22 (1993).
81. Koyama, S., Yu, H., Dalgarno, D.C., Shin, T.B., Zydowsky, L.D. & Schreiber, S.L. Structure of the PI3K SH3 domain and analysis of the SH3 family. *Cell* **72**, 945-52 (1993).
82. Yu, H., Chen, J.K., Feng, S., Dalgarno, D.C., Brauer, A.W. & Schreiber, S.L. Structural basis for the binding of proline-rich peptides to SH3 domains. *Cell* **76**, 933-45 (1994).
83. Kishan, K.V., Scita, G., Wong, W.T., Di Fiore, P.P. & Newcomer, M.E. The SH3 domain of Eps8 exists as a novel intertwined dimer. *Nat Struct Biol* **4**, 739-43 (1997).
84. Groemping, Y., Lapouge, K., Smerdon, S.J. & Rittinger, K. Molecular basis of phosphorylation-induced activation of the NADPH oxidase. *Cell* **113**, 343-55 (2003).
85. Harkiolaki, M., Gilbert, R.J., Jones, E.Y. & Feller, S.M. The C-terminal SH3 domain of CRKL as a dynamic dimerization module transiently exposing a nuclear export signal. *Structure* **14**, 1741-53 (2006).
86. Reid, H.H., Wilks, A.F. & Bernard, O. Two forms of the basic fibroblast growth factor receptor-like mRNA are expressed in the developing mouse brain. *Proc Natl Acad Sci U S A* **87**, 1596-600 (1990).

87. Safran, A., Avivi, A., Orr-Urtereger, A., Neufeld, G., Lonai, P., Givol, D. & Yarden, Y. The murine flg gene encodes a receptor for fibroblast growth factor. *Oncogene* **5**, 635-43 (1990).
88. Dionne, C.A., Crumley, G., Bellot, F., Kaplow, J.M., Searfoss, G., Ruta, M., Burgess, W.H., Jaye, M. & Schlessinger, J. Cloning and expression of two distinct high-affinity receptors cross-reacting with acidic and basic fibroblast growth factors. *EMBO J* **9**, 2685-92 (1990).
89. Keegan, K., Meyer, S. & Hayman, M.J. Structural and biosynthetic characterization of the fibroblast growth factor receptor 3 (FGFR-3) protein. *Oncogene* **6**, 2229-36 (1991).
90. Stark, K.L., McMahon, J.A. & McMahon, A.P. FGFR-4, a new member of the fibroblast growth factor receptor family, expressed in the definitive endoderm and skeletal muscle lineages of the mouse. *Development* **113**, 641-51 (1991).
91. Partanen, J., Makela, T.P., Eerola, E., Korhonen, J., Hirvonen, H., Claesson-Welsh, L. & Alitalo, K. FGFR-4, a novel acidic fibroblast growth factor receptor with a distinct expression pattern. *EMBO J* **10**, 1347-54 (1991).
92. Werner, M., Hermann-Le Denmat, S., Treich, I., Sentenac, A. & Thuriaux, P. Effect of mutations in a zinc-binding domain of yeast RNA polymerase C (III) on enzyme function and subunit association. *Mol Cell Biol* **12**, 1087-95 (1992).
93. Johnson, D.E., Lu, J., Chen, H., Werner, S. & Williams, L.T. The human fibroblast growth factor receptor genes: a common structural arrangement underlies the mechanisms for generating receptor forms that differ in their third immunoglobulin domain. *Mol Cell Biol* **11**, 4627-34 (1991).
94. Chellaiah, A.T., McEwen, D.G., Werner, S., Xu, J. & Ornitz, D.M. Fibroblast growth factor receptor (FGFR) 3. Alternative splicing in immunoglobulin-like domain III creates a receptor highly specific for acidic FGF/FGF-1. *J Biol Chem* **269**, 11620-7 (1994).
95. Miki, T., Bottaro, D.P., Fleming, T.P., Smith, C.L., Burgess, W.H., Chan, A.M. & Aaronson, S.A. Determination of ligand-binding specificity by alternative splicing: two distinct growth factor receptors encoded by a single gene. *Proc Natl Acad Sci U S A* **89**, 246-50 (1992).
96. Gilbert, E., Del Gatto, F., Champion-Arnaud, P., Gesnel, M.C. & Breathnach, R. Control of BEK and K-SAM splice sites in alternative splicing of the fibroblast growth factor receptor 2 pre-mRNA. *Mol Cell Biol* **13**, 5461-8 (1993).
97. Orr-Urtreger, A., Bedford, M.T., Burakova, T., Arman, E., Zimmer, Y., Yayon, A., Givol, D. & Lonai, P. Developmental localization of the splicing

alternatives of fibroblast growth factor receptor-2 (FGFR2). *Dev Biol* **158**, 475-86 (1993).

98. Alarid, E.T., Rubin, J.S., Young, P., Chedid, M., Ron, D., Aaronson, S.A. & Cunha, G.R. Keratinocyte growth factor functions in epithelial induction during seminal vesicle development. *Proc Natl Acad Sci U S A* **91**, 1074-8 (1994).
99. Yan, G., Fukabori, Y., McBride, G., Nikolaropolous, S. & McKeehan, W.L. Exon switching and activation of stromal and embryonic fibroblast growth factor (FGF)-FGF receptor genes in prostate epithelial cells accompany stromal independence and malignancy. *Mol Cell Biol* **13**, 4513-22 (1993).
100. Johnson, D.E. & Williams, L.T. Structural and functional diversity in the FGF receptor multigene family. *Adv Cancer Res* **60**, 1-41 (1993).
101. Ornitz, D.M. & Itoh, N. Fibroblast growth factors. *Genome Biol* **2**, REVIEWS3005 (2001).
102. McKeehan, W.L., Wang, F. & Kan, M. The heparan sulfate-fibroblast growth factor family: diversity of structure and function. *Prog Nucleic Acid Res Mol Biol* **59**, 135-76 (1998).
103. Schuller, A.C., Ahmed, Z. & Ladbury, J.E. Extracellular point mutations in FGFR2 result in elevated ERK1/2 activation and perturbation of neuronal differentiation. *Biochem J* **410**, 205-11 (2008).
104. Schuller, A.C., Ahmed, Z., Levitt, J.A. Suen, K.M., Suhling, K. & Ladbury, J.E. Indirect recruitment of the signalling adaptor Shc to the fibroblast growth factor receptor 2 (FGFR2). *Biochem J* **416**, 189-99 (2008).
105. Ahmed, Z., Schuller, A.C., Suhling, K., Tregidgo, C. & Ladbury, J.E. Extracellular point mutations in FGFR2 elicit unexpected changes in intracellular signalling. *Biochem J* **413**, 37-49 (2008).
106. Jackson, R.L., Busch, S.J. & Cardin, A.D. Glycosaminoglycans: molecular properties, protein interactions, and role in physiological processes. *Physiol Rev* **71**, 481-539 (1991).
107. Yayon, A., Klagsbrun, M., Esko, J.D., Leder, P. & Ornitz, D.M. Cell surface, heparin-like molecules are required for binding of basic fibroblast growth factor to its high affinity receptor. *Cell* **64**, 841-8 (1991).
108. Kan, M., Wang, F., Xu, J., Crabb, J.W., Hou, J. & McKeehan, W.L. An essential heparin-binding domain in the fibroblast growth factor receptor kinase. *Science* **259**, 1918-21 (1993).
109. Lin, X., Buff, E.M., Perrimon, N. & Michelson, A.M. Heparan sulfate proteoglycans are essential for FGF receptor signaling during Drosophila embryonic development. *Development* **126**, 3715-23 (1999).

110. Knox, S., Merry, C., Stringer, S., Melrose, J. & Whitelock, J. Not all perlecans are created equal: interactions with fibroblast growth factor (FGF) 2 and FGF receptors. *J Biol Chem* **277**, 14657-65 (2002).
111. Burgess, W.H. & Maciag, T. The heparin-binding (fibroblast) growth factor family of proteins. *Annu Rev Biochem* **58**, 575-606 (1989).
112. Gitay-Goren, H., Soker, S., Vlodavsky, I. & Neufeld, G. The binding of vascular endothelial growth factor to its receptors is dependent on cell surface-associated heparin-like molecules. *J Biol Chem* **267**, 6093-8 (1992).
113. Higashiyama, S., Abraham, J.A., Miller, J., Fiddes, J.C. & Klagsbrun, M. A heparin-binding growth factor secreted by macrophage-like cells that is related to EGF. *Science* **251**, 936-9 (1991).
114. Mansukhani, A., Dell'Era, P., Moscatelli, D., Kornbluth, S., Hanafusa, H. & Basilico, C. Characterization of the murine BEK fibroblast growth factor (FGF) receptor: activation by three members of the FGF family and requirement for heparin. *Proc Natl Acad Sci U S A* **89**, 3305-9 (1992).
115. Saksela, O., Moscatelli, D., Sommer, A. & Rifkin, D.B. Endothelial cell-derived heparan sulfate binds basic fibroblast growth factor and protects it from proteolytic degradation. *J Cell Biol* **107**, 743-51 (1988).
116. Saksela, O. & Rifkin, D.B. Release of basic fibroblast growth factor-heparan sulfate complexes from endothelial cells by plasminogen activator-mediated proteolytic activity. *J Cell Biol* **110**, 767-75 (1990).
117. Vlodavsky, I., Miao, H.Q., Medalion, B., Danagher, P. & Ron, D. Involvement of heparan sulfate and related molecules in sequestration and growth promoting activity of fibroblast growth factor. *Cancer Metastasis Rev* **15**, 177-86 (1996).
118. Turnbull, J.E. & Gallagher, J.T. Heparan sulphate: functional role as a modulator of fibroblast growth factor activity. *Biochem Soc Trans* **21**, 477-82 (1993).
119. David, G. Integral membrane heparan sulfate proteoglycans. *FASEB J* **7**, 1023-30 (1993).
120. Aviezer, D., Levy, E., Safran, M., Svahn, C., Buddecke, E., Schmidt, A., David, G., Vlodavsky, I. & Yayon, A. Differential structural requirements of heparin and heparan sulfate proteoglycans that promote binding of basic fibroblast growth factor to its receptor. *J Biol Chem* **269**, 114-21 (1994).
121. Feldman, B., Poueymirou, W., Papaioannou, V.E., DeChiara, T.M. & Goldfarb, M. Requirement of FGF-4 for postimplantation mouse development. *Science* **267**, 246-9 (1995).

122. Niswander, L., Tickle, C., Vogel, A., Booth, I. & Martin, G.R. FGF-4 replaces the apical ectodermal ridge and directs outgrowth and patterning of the limb. *Cell* **75**, 579-87 (1993).
123. Aviezer, D., Safran, M. & Yayon, A. Heparin differentially regulates the interaction of fibroblast growth factor-4 with FGF receptors 1 and 2. *Biochem Biophys Res Commun* **263**, 621-6 (1999).
124. Brickman, Y.G., Ford, M.D., Small, D.H., Bartlett, P.F. & Nurcombe, V. Heparan sulfates mediate the binding of basic fibroblast growth factor to a specific receptor on neural precursor cells. *J Biol Chem* **270**, 24941-8 (1995).
125. Powers, C.J., McLeskey, S.W. & Wellstein, A. Fibroblast growth factors, their receptors and signaling. *Endocr Relat Cancer* **7**, 165-97 (2000).
126. Wang, J.K., Gao, G. & Goldfarb, M. Fibroblast growth factor receptors have different signaling and mitogenic potentials. *Mol Cell Biol* **14**, 181-8 (1994).
127. Raffioni, S., Thomas, D., Foehr, E.D., Thompson, L.M. & Bradshaw, R.A. Comparison of the intracellular signaling responses by three chimeric fibroblast growth factor receptors in PC12 cells. *Proc Natl Acad Sci U S A* **96**, 7178-83 (1999).
128. Haugsten, E.M., Sorensen, V., Brech, A., Olsnes, S. & Wesche, J. Different intracellular trafficking of FGF1 endocytosed by the four homologous FGF receptors. *J Cell Sci* **118**, 3869-81 (2005).
129. Johnson, D.E., Lee, P.L., Lu, J. & Williams, L.T. Diverse forms of a receptor for acidic and basic fibroblast growth factors. *Mol Cell Biol* **10**, 4728-36 (1990).
130. Wang, F., Kan, M., Yan, G., Xu, J. & McKeehan, W.L. Alternately spliced NH2-terminal immunoglobulin-like Loop I in the ectodomain of the fibroblast growth factor (FGF) receptor 1 lowers affinity for both heparin and FGF-1. *J Biol Chem* **270**, 10231-5 (1995).
131. Olsen, S.K., Ibrahimi, O.A., Raucci, A., Zhang, F., Eliseenkova, A.V., Yayon, A., Basilico, C., Linhardt, R. J. & Schlessinger, J., Mohammadi, M. Insights into the molecular basis for fibroblast growth factor receptor autoinhibition and ligand-binding promiscuity. *Proc Natl Acad Sci U S A* **101**, 935-40 (2004).
132. Plotnikov, A.N., Schlessinger, J., Hubbard, S.R. & Mohammadi, M. Structural basis for FGF receptor dimerization and activation. *Cell* **98**, 641-50 (1999).
133. Plotnikov, A.N., Hubbard, S.R., Schlessinger, J. & Mohammadi, M. Crystal structures of two FGF-FGFR complexes reveal the determinants of ligand-receptor specificity. *Cell* **101**, 413-24 (2000).

134. Stauber, D.J., DiGabriele, A.D. & Hendrickson, W.A. Structural interactions of fibroblast growth factor receptor with its ligands. *Proc Natl Acad Sci U S A* **97**, 49-54 (2000).
135. Venkataraman, G., Raman, R., Sasisekharan, V. & Sasisekharan, R. Molecular characteristics of fibroblast growth factor-fibroblast growth factor receptor-heparin-like glycosaminoglycan complex. *Proc Natl Acad Sci U S A* **96**, 3658-63 (1999).
136. Pellegrini, L., Burke, D.F., von Delft, F., Mulloy, B. & Blundell, T.L. Crystal structure of fibroblast growth factor receptor ectodomain bound to ligand and heparin. *Nature* **407**, 1029-34 (2000).
137. Schlessinger, J., Plotnikov, A.N., Ibrahimi, O.A., Eliseenkova, A.V., Yeh, B.K., Yayon, A., Linhardt, R.J. & Mohammadi, M. Crystal structure of a ternary FGF-FGFR-heparin complex reveals a dual role for heparin in FGFR binding and dimerization. *Mol Cell* **6**, 743-50 (2000).
138. Ellis, L., Clauser, E., Morgan, D.O., Edery, M., Roth, R.A. & Rutter, W. J. Replacement of insulin receptor tyrosine residues 1162 and 1163 compromises insulin-stimulated kinase activity and uptake of 2-deoxyglucose. *Cell* **45**, 721-32 (1986).
139. Mohammadi, M., Schlessinger, J. & Hubbard, S.R. Structure of the FGF receptor tyrosine kinase domain reveals a novel autoinhibitory mechanism. *Cell* **86**, 577-87 (1996).
140. Hubbard, S.R., Wei, L., Ellis, L. & Hendrickson, W.A. Crystal structure of the tyrosine kinase domain of the human insulin receptor. *Nature* **372**, 746-54 (1994).
141. Piwnica-Worms, H., Saunders, K.B., Roberts, T.M., Smith, A.E. & Cheng, S.H. Tyrosine phosphorylation regulates the biochemical and biological properties of pp60c-src. *Cell* **49**, 75-82 (1987).
142. Feng, J., Witthuhn, B.A., Matsuda, T., Kohlhuber, F., Kerr, I.M. & Ihle, J.N. Activation of Jak2 catalytic activity requires phosphorylation of Y1007 in the kinase activation loop. *Mol Cell Biol* **17**, 2497-501 (1997).
143. Hubbard, S.R. Crystal structure of the activated insulin receptor tyrosine kinase in complex with peptide substrate and ATP analog. *EMBO J* **16**, 5572-81 (1997).
144. Johnson, L.N., Noble, M.E. & Owen, D.J. Active and inactive protein kinases: structural basis for regulation. *Cell* **85**, 149-58 (1996).
145. Hubbard, S.R. & Till, J.H. Protein tyrosine kinase structure and function. *Annu Rev Biochem* **69**, 373-98 (2000).

146. Reddy, M.M. & Rajasekharan, R. Serine/threonine/tyrosine protein kinase from Arabidopsis thaliana is dependent on serine residues for its activity. *Arch Biochem Biophys* **460**, 122-8 (2007).
147. Chen, H., Ma, J., Li, W., Eliseenkova, A.V., Xu, C., Neubert, T.A., Miller, W.T. & Mohammadi, M. A molecular brake in the kinase hinge region regulates the activity of receptor tyrosine kinases. *Mol Cell* **27**, 717-30 (2007).
148. Ornitz, D.M., Xu, J., Colvin, J.S., McEwen, D.G., MacArthur, C.A., Coulier, F., Gao, G. & Goldfarb, M. Receptor specificity of the fibroblast growth factor family. *J Biol Chem* **271**, 15292-7 (1996).
149. Xu, J., Liu, Z. & Ornitz, D.M. Temporal and spatial gradients of Fgf8 and Fgf17 regulate proliferation and differentiation of midline cerebellar structures. *Development* **127**, 1833-43 (2000).
150. Zhang, X., Ibrahimi, O.A., Olsen, S.K., Umemori, H., Mohammadi, M. & Ornitz, D.M. Receptor specificity of the fibroblast growth factor family. The complete mammalian FGF family. *J Biol Chem* **281**, 15694-700 (2006).
151. Ruoslahti, E. & Yamaguchi, Y. Proteoglycans as modulators of growth factor activities. *Cell* **64**, 867-9 (1991).
152. Spivak-Kroizman, T., Lemmon, M.A., Dikic, I., Ladbury, J.E., Pinchasi, D., Huang, J., Jaye, M., Crumley, G., Schlessinger, J. & Lax, I. Heparin-induced oligomerization of FGF molecules is responsible for FGF receptor dimerization, activation, and cell proliferation. *Cell* **79**, 1015-24 (1994).
153. Heldin, C.H. & Ostman, A. Ligand-induced dimerization of growth factor receptors: variations on the theme. *Cytokine Growth Factor Rev* **7**, 3-10 (1996).
154. Ornitz, D.M., Yayon, A., Flanagan, J.G., Svahn, C.M., Levi, E. & Leder, P. Heparin is required for cell-free binding of basic fibroblast growth factor to a soluble receptor and for mitogenesis in whole cells. *Mol Cell Biol* **12**, 240-7 (1992).
155. Roghani, M., Mansukhani, A., Dell'Era, P., Bellosta, P., Basilico, C., Rifkin, D. B. & Moscatelli, D. Heparin increases the affinity of basic fibroblast growth factor for its receptor but is not required for binding. *J Biol Chem* **269**, 3976-84 (1994).
156. Yarden, Y. & Schlessinger, J. Self-phosphorylation of epidermal growth factor receptor: evidence for a model of intermolecular allosteric activation. *Biochemistry* **26**, 1434-42 (1987).
157. Bellot, F., Crumley, G. ,Kaplow, J.M., Schlessinger, J., Jaye, M. & Dionne, C.A. Ligand-induced transphosphorylation between different FGF receptors. *EMBO J* **10**, 2849-54 (1991).

158. Pasquale, E.B. & Singer, S.J. Identification of a developmentally regulated protein-tyrosine kinase by using anti-phosphotyrosine antibodies to screen a cDNA expression library. *Proc Natl Acad Sci U S A* **86**, 5449-53 (1989).
159. Kumjian, D.A., Wahl, M.I., Rhee, S.G. & Daniel, T.O. Platelet-derived growth factor (PDGF) binding promotes physical association of PDGF receptor with phospholipase C. *Proc Natl Acad Sci U S A* **86**, 8232-6 (1989).
160. Margolis, B., Rhee, S.G.,Felder, S., Mervic, M., Lyall, R., Levitzki, A., Ullrich, A., Zilberstein, A. & Schlessinger, J. EGF induces tyrosine phosphorylation of phospholipase C-II: a potential mechanism for EGF receptor signaling. *Cell* **57**, 1101-7 (1989).
161. Mohammadi, M., Honegger, A.M., Rotin, D., Fischer, R., Bellot, F., Li, W., Dionne, C.A., Jaye, M., Rubinstein, M. & Schlessinger, J.A. Tyrosine-phosphorylated carboxy-terminal peptide of the fibroblast growth factor receptor (Flg) is a binding site for the SH2 domain of phospholipase C-gamma 1. *Mol Cell Biol* **11**, 5068-78 (1991).
162. Mohammadi, M., Dionne, C.A., Li, W., Li, N., Spivak, T., Honegger, A.M., Jaye, M. & Schlessinger, J. Point mutation in FGF receptor eliminates phosphatidylinositol hydrolysis without affecting mitogenesis. *Nature* **358**, 681-4 (1992).
163. Furdui, C.M., Lew, E.D., Schlessinger, J. & Anderson, K.S. Autophosphorylation of FGFR1 kinase is mediated by a sequential and precisely ordered reaction. *Mol Cell* **21**, 711-7 (2006).
164. Kouhara, H., Hadari, Y.R., Spivak-Kroizman, T., Schilling, J., Bar-Sagi, D., Lax, I. & Schlessinger, J. A lipid-anchored Grb2-binding protein that links FGF-receptor activation to the Ras/MAPK signaling pathway. *Cell* **89**, 693-702 (1997).
165. Hadari, Y.R., Gotoh, N., Kouhara, H., Lax, I. & Schlessinger, J. Critical role for the docking-protein FRS2 alpha in FGF receptor-mediated signal transduction pathways. *Proc Natl Acad Sci U S A* **98**, 8578-83 (2001).
166. Ong, S.H., Hadari, Y.R., Gotoh, N., Guy, G.R., Schlessinger, J. & Lax, I. Stimulation of phosphatidylinositol 3-kinase by fibroblast growth factor receptors is mediated by coordinated recruitment of multiple docking proteins. *Proc Natl Acad Sci U S A* **98**, 6074-9 (2001).
167. Lamothe, B., Yamada, M., Schaeper, U., Birchmeier, W., Lax, I. & Schlessinger, J. The docking protein Gab1 is an essential component of an indirect mechanism for fibroblast growth factor stimulation of the phosphatidylinositol 3-kinase/Akt antiapoptotic pathway. *Mol Cell Biol* **24**, 5657-66 (2004).

168. Kontaridis, M.I., Liu, X., Zhang, L. & Bennett, A.M. Role of SHP-2 in fibroblast growth factor receptor-mediated suppression of myogenesis in C2C12 myoblasts. *Mol Cell Biol* **22**, 3875-91 (2002).
169. Gotoh, N., Ito, M., Yamamoto, S., Yoshino, I., Song, N., Wang, Y., Lax, I., Schlessinger, J., Shibuya, M. & Lang, R.A. Tyrosine phosphorylation sites on FRS2alpha responsible for Shp2 recruitment are critical for induction of lens and retina. *Proc Natl Acad Sci U S A* **101**, 17144-9 (2004).
170. Hadari, Y.R., Kouhara, H., Lax, I. & Schlessinger, J. Binding of Shp2 tyrosine phosphatase to FRS2 is essential for fibroblast growth factor-induced PC12 cell differentiation. *Mol Cell Biol* **18**, 3966-73 (1998).
171. Ong, S.H., Lim, Y.P., Low, B.C. & Guy, G.R. SHP2 associates directly with tyrosine phosphorylated p90 (SNT) protein in FGF-stimulated cells. *Biochem Biophys Res Commun* **238**, 261-6 (1997).
172. Peters, K.G., Marie, J., Wilson, E., Ives, H.E., Escobedo, J., Del Rosario, M., Mirda, D. & Williams, L.T. Point mutation of an FGF receptor abolishes phosphatidylinositol turnover and Ca2+ flux but not mitogenesis. *Nature* **358**, 678-81 (1992).
173. Ahmed, Z., George, R., Lin, C.C., Suen, K.M., Levitt, J.A., Suhling, K. & Ladbury, J.E. Direct binding of Grb2 SH3 domain to FGFR2 regulates SHP2 function. *Cell Signal* **22**, 23-33 (2010).
174. Mason, I. Initiation to end point: the multiple roles of fibroblast growth factors in neural development. *Nat Rev Neurosci* **8**, 583-96 (2007).
175. Cantley, L.C., Auger, K.R., Carpenter, C., Duckworth, B., Graziani, A., Kapeller, R. & Soltoff, S. Oncogenes and signal transduction. *Cell* **64**, 281-302 (1991).
176. Clark, S.G., Stern, M.J. & Horvitz, H.R. C. elegans cell-signalling gene sem-5 encodes a protein with SH2 and SH3 domains. *Nature* **356**, 340-4 (1992).
177. Matuoka, K., Shibata, M., Yamakawa, A. & Takenawa, T. Cloning of ASH, a ubiquitous protein composed of one Src homology region (SH) 2 and two SH3 domains, from human and rat cDNA libraries. *Proc Natl Acad Sci U S A* **89**, 9015-9 (1992).
178. Fath, I., Schweighoffer, F., Rey, I., Multon, M.C., Boiziau, J., Duchesne, M. & Tocque, B. Cloning of a Grb2 isoform with apoptotic properties. *Science* **264**, 971-4 (1994).
179. Rey, I., Fath, I., Parker, F., Haun, F., Schweighoffer, F. & Tocque, B. A role for Grb2 in apoptosis? *Cell Death Differ* **2**, 105-11 (1995).

180. Matuoka, K., Shibasaki, F., Shibata, M. & Takenawa, T. Ash/Grb-2, a SH2/SH3-containing protein, couples to signaling for mitogenesis and cytoskeletal reorganization by EGF and PDGF. *EMBO J* **12**, 3467-73 (1993).
181. Skolnik, E.Y., Lee, C.H., Batzer, A., Vicentini, L.M., Zhou, M., Daly, R., Myers, M.J., Jr., Backer, J.M., Ullrich, A. & White, M.F. The SH2/SH3 domain-containing protein GRB2 interacts with tyrosine-phosphorylated IRS1 and Shc: implications for insulin control of ras signalling. *EMBO J* **12**, 1929-36 (1993).
182. Downward, J. Signal transduction. Rac and Rho in tune. *Nature* **359**, 273-4 (1992).
183. Ridley, A.J. & Hall, A. The small GTP-binding protein rho regulates the assembly of focal adhesions and actin stress fibers in response to growth factors. *Cell* **70**, 389-99 (1992).
184. Smith, M.R., DeGudicibus, S.J. & Stacey, D.W. Requirement for c-ras proteins during viral oncogene transformation. *Nature* **320**, 540-3 (1986).
185. Chardin, P., Camonis, J.H., Gale, N.W., van Aelst, L., Schlessinger, J., Wigler, M.H. & Bar-Sagi, D. Human Sos1: a guanine nucleotide exchange factor for Ras that binds to GRB2. *Science* **260**, 1338-43 (1993).
186. Egan, S.E., Giddings, B.W., Brooks, M.W., Buday, L., Sizeland, A.M. & Weinberg, R.A. Association of Sos Ras exchange protein with Grb2 is implicated in tyrosine kinase signal transduction and transformation. *Nature* **363**, 45-51 (1993).
187. Li, N., Batzer, A., Daly, R., Yajnik, V., Skolnik, E., Chardin, P., Bar-Sagi, D., Margolis, B. & Schlessinger, J. Guanine-nucleotide-releasing factor hSos1 binds to Grb2 and links receptor tyrosine kinases to Ras signalling. *Nature* **363**, 85-8 (1993).
188. Bowtell, D., Fu, P., Simon, M. & Senior, P. Identification of murine homologues of the Drosophila son of sevenless gene: potential activators of ras. *Proc Natl Acad Sci U S A* **89**, 6511-5 (1992).
189. Yang, S.S., Van Aelst, L. & Bar-Sagi, D. Differential interactions of human Sos1 and Sos2 with Grb2. *J Biol Chem* **270**, 18212-5 (1995).
190. Noble, M.E., Musacchio, A., Saraste, M., Courtneidge, S.A. & Wierenga, R.K. Crystal structure of the SH3 domain in human Fyn; comparison of the three-dimensional structures of SH3 domains in tyrosine kinases and spectrin. *EMBO J* **12**, 2617-24 (1993).
191. Goudreau, N., Cornille, F., Duchesne, M., Parker, F., Tocque, B., Garbay, C. & Roques, B.P. NMR structure of the N-terminal SH3 domain of GRB2 and

its complex with a proline-rich peptide from Sos. *Nat Struct Biol* **1**, 898-907 (1994).

192. Lim, W.A., Richards, F.M. & Fox, R.O. Structural determinants of peptide-binding orientation and of sequence specificity in SH3 domains. *Nature* **372**, 375-9 (1994).
193. Kohda, D., Terasawa, H., Ichikawa, S., Ogura, K., Hatanaka, H., Mandiyan, V., Ullrich, A., Schlessinger, J. & Inagaki, F. Solution structure and ligand-binding site of the carboxy-terminal SH3 domain of GRB2. *Structure* **2**, 1029-40 (1994).
194. Terasawa, H., Kohda, D., Hatanaka, H., Tsuchiya, S., Ogura, K., Nagata, K., Ishii, S., Mandiyan, V., Ullrich, A. & Schlessinger, J. Structure of the N-terminal SH3 domain of GRB2 complexed with a peptide from the guanine nucleotide releasing factor Sos. *Nat Struct Biol* **1**, 891-7 (1994).
195. Pelicci, G., Lanfrancone, L., Grignani, F., McGlade, J., Cavallo, F., Forni, G., Nicoletti, I., Pawson, T. & Pelicci, P.G. A novel transforming protein (SHC) with an SH2 domain is implicated in mitogenic signal transduction. *Cell* **70**, 93-104 (1992).
196. Camici, G.G., Schiavoni, M., Francia, P., Bachschmid, M., Martin-Padura, I., Hersberger, M., Tanner, F.C., Pelicci, P., Volpe, M., Anversa, P., Luscher, T.F. & Cosentino, F. Genetic deletion of p66(Shc) adaptor protein prevents hyperglycemia-induced endothelial dysfunction and oxidative stress. *Proc Natl Acad Sci U S A* **104**, 5217-22 (2007).
197. Ruff-Jamison, S., McGlade, J., Pawson, T., Chen, K. & Cohen, S. Epidermal growth factor stimulates the tyrosine phosphorylation of SHC in the mouse. *J Biol Chem* **268**, 7610-2 (1993).
198. Rozakis-Adcock, M., McGlade, J., Mbamalu, G., Pelicci, G., Daly, R., Li, W., Batzer, A., Thomas, S., Brugge, J. & Pelicci, P.G. Association of the Shc and Grb2/Sem5 SH2-containing proteins is implicated in activation of the Ras pathway by tyrosine kinases. *Nature* **360**, 689-92 (1992).
199. McGlade, J., Cheng, A., Pelicci, G., Pelicci, P.G. & Pawson, T. Shc proteins are phosphorylated and regulated by the v-Src and v-Fps protein-tyrosine kinases. *Proc Natl Acad Sci U S A* **89**, 8869-73 (1992).
200. Pronk, G.J., McGlade, J., Pelicci, G., Pawson, T. & Bos, J.L. Insulin-induced phosphorylation of the 46- and 52-kDa Shc proteins. *J Biol Chem* **268**, 5748-53 (1993).
201. Li, W., Nishimura, R., Kashishian, A., Batzer, A.G., Kim, W. J., Cooper, J. A. & Schlessinger, J. A new function for a phosphotyrosine phosphatase: linking GRB2-Sos to a receptor tyrosine kinase. *Mol Cell Biol* **14**, 509-17 (1994).

202. Buday, L. & Downward, J. Epidermal growth factor regulates p21ras through the formation of a complex of receptor, Grb2 adapter protein, and Sos nucleotide exchange factor. *Cell* **73**, 611-20 (1993).
203. Gale, N.W., Kaplan, S., Lowenstein, E.J., Schlessinger, J. & Bar-Sagi, D. Grb2 mediates the EGF-dependent activation of guanine nucleotide exchange on Ras. *Nature* **363**, 88-92 (1993).
204. Skolnik, E.Y., Batzer, A., Li, N., Lee, C.H., Lowenstein, E., Mohammadi, M., Margolis, B. & Schlessinger, J. The function of GRB2 in linking the insulin receptor to Ras signaling pathways. *Science* **260**, 1953-5 (1993).
205. Pronk, G.J., de Vries-Smits, A.M., Buday, L., Downward, J., Maassen, J.A., Medema, R.H. & Bos, J.L. Involvement of Shc in insulin- and epidermal growth factor-induced activation of p21ras. *Mol Cell Biol* **14**, 1575-81 (1994).
206. Benjamin, C.W. & Jones, D.A. Platelet-derived growth factor stimulates growth factor receptor binding protein-2 association with Shc in vascular smooth muscle cells. *J Biol Chem* **269**, 30911-6 (1994).
207. Maignan, S., Guilloteau, J.P., Fromage, N., Arnoux, B., Becquart, J. & Ducruix, A. Crystal structure of the mammalian Grb2 adaptor. *Science* **268**, 291-3 (1995).
208. Yuzawa, S., Yokochi, M., Hatanaka, H., Ogura, K., Kataoka, M., Miura, K., Mandiyan, V., Schlessinger, J. & Inagaki, F. Solution structure of Grb2 reveals extensive flexibility necessary for target recognition. *J Mol Biol* **306**, 527-37 (2001).
209. Hunter, T. Protein kinases and phosphatases: the yin and yang of protein phosphorylation and signaling. *Cell* **80**, 225-36 (1995).
210. Moorhead, G.B., De Wever, V., Templeton, G. & Kerk, D. Evolution of protein phosphatases in plants and animals. *Biochem J* **417**, 401-9 (2009).
211. Alonso, A., Sasin, J., Bottini, N., Friedberg, I., Osterman, A., Godzik, A., Hunter, T., Dixon, J. & Mustelin, T. Protein tyrosine phosphatases in the human genome. *Cell* **117**, 699-711 (2004).
212. Andersen, J.N., Jansen, P.G., Echwald, S.M., Mortensen, O., Fukada, T., Vecchio, R.D., Tonks, N.K. & Moller, N.P.H. A genomic perspective on protein tyrosine phosphatases: gene structure, pseudogenes, and genetic disease linkage. *FASEB J* **18**, 8-30 (2004).
213. Paul, S. & Lombroso, P.J. Receptor and nonreceptor protein tyrosine phosphatases in the nervous system. *Cell Mol Life Sci* **60**, 2465-82 (2003).
214. Kuhne, M.R., Pawson, T., Lienhard, G.E. & Feng, G.S. The insulin receptor substrate 1 associates with the SH2-containing phosphotyrosine phosphatase Syp. *J Biol Chem* **268**, 11479-81 (1993).

215. Lechleider, R.J., Freeman, R.M., Jr. & Neel, B.G. Tyrosyl phosphorylation and growth factor receptor association of the human corkscrew homologue, SH-PTP2. *J Biol Chem* **268**, 13434-8 (1993).
216. Cunnick, J.M., Dorsey, J.F., Munoz-Antonia, T., Mei, L. & Wu, J. Requirement of SHP2 binding to Grb2-associated binder-1 for mitogen-activated protein kinase activation in response to lysophosphatidic acid and epidermal growth factor. *J Biol Chem* **275**, 13842-8 (2000).
217. Kazlauskas, A., Feng, G.S., Pawson, T. & Valius, M. The 64-kDa protein that associates with the platelet-derived growth factor receptor beta subunit via Tyr-1009 is the SH2-containing phosphotyrosine phosphatase Syp. *Proc Natl Acad Sci U S A* **90**, 6939-43 (1993).
218. Bennett, A.M., Tang, T.L., Sugimoto, S., Walsh, C.T. & Neel, B.G. Protein-tyrosine-phosphatase SHPTP2 couples platelet-derived growth factor receptor beta to Ras. *Proc Natl Acad Sci U S A* **91**, 7335-9 (1994).
219. Vogel, W. & Ullrich, A. Multiple in vivo phosphorylated tyrosine phosphatase SHP-2 engages binding to Grb2 via tyrosine 584. *Cell Growth Differ* **7**, 1589-97 (1996).
220. Bennett, A.M., Hausdorff, S.F., O'Reilly, A.M., Freeman, R.M. & Neel, B.G. Multiple requirements for SHPTP2 in epidermal growth factor-mediated cell cycle progression. *Mol Cell Biol* **16**, 1189-202 (1996).
221. O'Reilly, A.M. & Neel, B.G. Structural determinants of SHP-2 function and specificity in Xenopus mesoderm induction. *Mol Cell Biol* **18**, 161-77 (1998).
222. Araki, T., Nawa, H. & Neel, B.G. Tyrosyl phosphorylation of Shp2 is required for normal ERK activation in response to some, but not all, growth factors. *J Biol Chem* **278**, 41677-84 (2003).
223. Sun, X.J., Crimmins, D.L., Myers, M.G., Jr., Miralpeix, M. & White, M.F. Pleiotropic insulin signals are engaged by multisite phosphorylation of IRS-1. *Mol Cell Biol* **13**, 7418-28 (1993).
224. Sugimoto, S., Wandless, T.J., Shoelson, S.E., Neel, B.G. & Walsh, C.T. Activation of the SH2-containing protein tyrosine phosphatase, SH-PTP2, by phosphotyrosine-containing peptides derived from insulin receptor substrate-1. *J Biol Chem* **269**, 13614-22 (1994).
225. Perrimon, N. The torso receptor protein-tyrosine kinase signaling pathway: an endless story. *Cell* **74**, 219-22 (1993).
226. Noguchi, T., Matozaki, T., Horita, K., Fujioka, Y. & Kasuga, M. Role of SH-PTP2, a protein-tyrosine phosphatase with Src homology 2 domains, in insulin-stimulated Ras activation. *Mol Cell Biol* **14**, 6674-82 (1994).

227. Milarski, K.L. & Saltiel, A.R. Expression of catalytically inactive Syp phosphatase in 3T3 cells blocks stimulation of mitogen-activated protein kinase by insulin. *J Biol Chem* **269**, 21239-43 (1994).
228. Deb, T.B., Wong, L., Salomon, D.S., Zhou, G., Dixon, J.E., Gutkind, J.S., Thompson, S.A. & Johnson, G.R. A common requirement for the catalytic activity and both SH2 domains of SHP-2 in mitogen-activated protein (MAP) kinase activation by the ErbB family of receptors. A specific role for SHP-2 in map, but not c-Jun amino-terminal kinase activation. *J Biol Chem* **273**, 16643-6 (1998).
229. Guy, G.R., Yusoff, P., Bangarusamy, D., Fong, C.W. & Wong, E.S. Dockers at the crossroads. *Cell Signal* **14**, 11-20 (2002).
230. Itoh, M., Yoshida, Y., Nishida, K., Narimatsu, M., Hibi, M. & Hirano, T. Role of Gab1 in heart, placenta, and skin development and growth factor- and cytokine-induced extracellular signal-regulated kinase mitogen-activated protein kinase activation. *Mol Cell Biol* **20**, 3695-704 (2000).
231. Liu, Y. & Rohrschneider, L.R. The gift of Gab. *FEBS Lett* **515**, 1-7 (2002).
232. Lock, L.S., Royal, I., Naujokas, M.A. & Park, M. Identification of an atypical Grb2 carboxyl-terminal SH3 domain binding site in Gab docking proteins reveals Grb2-dependent and -independent recruitment of Gab1 to receptor tyrosine kinases. *J Biol Chem* **275**, 31536-45 (2000).
233. Sachs, M., Brohmann, H., Zechner, D., Muller, T., Hulsken, J., Walther, I., Schaeper, U., Birchmeier, C. & Birchmeier, W. Essential role of Gab1 for signaling by the c-Met receptor in vivo. *J Cell Biol* **150**, 1375-84 (2000).
234. Weidner, K.M., Di Cesare, S., Sachs, M., Brinkmann, V., Behrens, J. & Birchmeier, W. Interaction between Gab1 and the c-Met receptor tyrosine kinase is responsible for epithelial morphogenesis. *Nature* **384**, 173-6 (1996).
235. Holgado-Madruga, M., Emlet, D.R., Moscatello, D.K., Godwin, A.K. & Wong, A.J. A Grb2-associated docking protein in EGF- and insulin-receptor signalling. *Nature* **379**, 560-4 (1996).
236. Yart, A., Laffargue, M., Mayeux, P., Chretien, S., Peres, C., Tonks, N., Roche, S., Payrastre, B., Chap, H. & Raynal, P. A critical role for phosphoinositide 3-kinase upstream of Gab1 and SHP2 in the activation of ras and mitogen-activated protein kinases by epidermal growth factor. *J Biol Chem* **276**, 8856-64 (2001).
237. Cunnick, J.M., Mei, L., Doupnik, C.A. & Wu, J. Phosphotyrosines 627 and 659 of Gab1 constitute a bisphosphoryl tyrosine-based activation motif (BTAM) conferring binding and activation of SHP2. *J Biol Chem* **276**, 24380-7 (2001).

238. Cunnick, J.M., Meng, S., Ren, Y., Desponts, C., Wang, H. G., Djeu, J. Y. & Wu, J. Regulation of the mitogen-activated protein kinase signaling pathway by SHP2. *J Biol Chem* **277**, 9498-504 (2002).
239. Agazie, Y.M. & Hayman, M.J. Molecular mechanism for a role of SHP2 in epidermal growth factor receptor signaling. *Mol Cell Biol* **23**, 7875-86 (2003).
240. Hof, P., Pluskey, S., Dhe-Paganon, S., Eck, M.J. & Shoelson, S.E. Crystal structure of the tyrosine phosphatase SHP-2. *Cell* **92**, 441-50 (1998).
241. Ravetch, J.V. & Lanier, L.L. Immune inhibitory receptors. *Science* **290**, 84-9 (2000).
242. Beebe, K.D., Wang, P., Arabaci, G. & Pei, D. Determination of the binding specificity of the SH2 domains of protein tyrosine phosphatase SHP-1 through the screening of a combinatorial phosphotyrosyl peptide library. *Biochemistry* **39**, 13251-60 (2000).
243. Neel, B.G., Gu, H. & Pao, L. The 'Shp'ing news: SH2 domain-containing tyrosine phosphatases in cell signaling. *Trends Biochem Sci* **28**, 284-93 (2003).
244. Pei, D., Lorenz, U., Klingmuller, U., Neel, B.G. & Walsh, C.T. Intramolecular regulation of protein tyrosine phosphatase SH-PTP1: a new function for Src homology 2 domains. *Biochemistry* **33**, 15483-93 (1994).
245. Lu, W., Gong, D., Bar-Sagi, D. & Cole, P.A. Site-specific incorporation of a phosphotyrosine mimetic reveals a role for tyrosine phosphorylation of SHP-2 in cell signaling. *Mol Cell* **8**, 759-69 (2001).
246. Zhao, Z., Larocque, R., Ho, W.T., Fischer, E.H. & Shen, S.H. Purification and characterization of PTP2C, a widely distributed protein tyrosine phosphatase containing two SH2 domains. *J Biol Chem* **269**, 8780-5 (1994).
247. Peraldi, P., Zhao, Z., Filloux, C., Fischer, E.H. & Van Obberghen, E. Protein-tyrosine-phosphatase 2C is phosphorylated and inhibited by 44-kDa mitogen-activated protein kinase. *Proc Natl Acad Sci U S A* **91**, 5002-6 (1994).
248. Poole, A.W. & Jones, M.L. A SHPing tale: perspectives on the regulation of SHP-1 and SHP-2 tyrosine phosphatases by the C-terminal tail. *Cell Signal* **17**, 1323-32 (2005).
249. Schuller, A. Protein Recruitment to receptor tyrosine kinase-mediated early signalling complexes. (PhD Thesis, *University College London*, 2007).
250. Yuzawa, S. Yokochi, M., Hatanaka, H., Ogura, K., Kataoka, M., Miura, K., Mandiyan, V., Schlessinger, J. & Inagaki, F. Solution structure of Grb2 reveals extensive flexibility necessary for target recognition. *J Mol Biol* **306**, 527-37 (2001).

251. Bae, J.H., Boggon, T.J., Tome, F., Mandiyan, V., Lax, I. & Schlessinger, J. Asymmetric receptor contact is required for tyrosine autophosphorylation of fibroblast growth factor receptor in living cells. *Proc Natl Acad Sci U S A* **107**, 2866-71.
252. McDonald, C.B., Seldeen, K.L., Deegan, B.J., Lewis, M.S. & Farooq, A. Grb2 adaptor undergoes conformational change upon dimerization. *Arch Biochem Biophys* **475**, 25-35 (2008).
253. van der Geer, P. & Pawson, T. The PTB domain: a new protein module implicated in signal transduction. *Trends Biochem Sci* **20**, 277-80 (1995).
254. Pawson, T. & Scott, J.D. Signaling through scaffold, anchoring, and adaptor proteins. *Science* **278**, 2075-80 (1997).
255. Jones, D.A. & Benjamin, C.W. Phosphorylation of growth factor receptor binding protein-2 by pp60c-src tyrosine kinase. *Arch Biochem Biophys* **337**, 143-8 (1997).
256. Li, S., Ilaria, R.L., Jr., Million, R.P., Daley, G.Q. & Van Etten, R.A. The P190, P210, and P230 forms of the BCR/ABL oncogene induce a similar chronic myeloid leukemia-like syndrome in mice but have different lymphoid leukemogenic activity. *J Exp Med* **189**, 1399-412 (1999).
257. Li, S., Couvillon, A.D., Brasher, B.B. & Van Etten, R.A. Tyrosine phosphorylation of Grb2 by Bcr/Abl and epidermal growth factor receptor: a novel regulatory mechanism for tyrosine kinase signaling. *EMBO J* **20**, 6793-804 (2001).
258. Minoo, P., Chughtai, N., Campiglio, M., Stein-Gerlach, M., Lebrun, J.J., Ullrich, A. & Ali, S. The adaptor function of SHP-2 downstream of the prolactin receptor is required for the recruitment of p29, a substrate of SHP-2. *Cell Signal* **15**, 319-26 (2003).
259. Haines, E., Minoo, P., Feng, Z., Resalatpanah, N., Nie, X.M., Campiglio, M., Alvarez, L., Cocolakis, E., Ridha, M., Di Fulvio, M., Gomez-Cambronero, J., Lebrun, J.J. & Ali, S. Tyrosine phosphorylation of Grb2: role in prolactin/epidermal growth factor cross talk in mammary epithelial cell growth and differentiation. *Mol Cell Biol* **29**, 2505-20 (2009).
260. Lew, E.D., Furdui, C.M., Anderson, K.S. & Schlessinger, J. The precise sequence of FGF receptor autophosphorylation is kinetically driven and is disrupted by oncogenic mutations. *Sci Signal* **2**, ra6 (2009).
261. Ahmed, Z., George, R., Lin, C.C., Suen, K.M., Levitt, J.A., Suhling, K. & Ladbury, J.E. Direct binding of Grb2 SH3 domain to FGFR2 regulates SHP2 function. *Cell Signal* **22**, 23-33 (2010).

262. Cherniack, A.D., Klarlund, J.K. & Czech, M.P. Phosphorylation of the Ras nucleotide exchange factor son of sevenless by mitogen-activated protein kinase. *J Biol Chem* **269**, 4717-20 (1994).
263. Corbalan-Garcia, S., Yang, S.S., Degenhardt, K.R. & Bar-Sagi, D. Identification of the mitogen-activated protein kinase phosphorylation sites on human Sos1 that regulate interaction with Grb2. *Mol Cell Biol* **16**, 5674-82 (1996).
264. Dong, C., Waters, S.B., Holt, K.H. & Pessin, J.E. SOS phosphorylation and disassociation of the Grb2-SOS complex by the ERK and JNK signaling pathways. *J Biol Chem* **271**, 6328-32 (1996).
265. Cherniack, A.D., Klarlund, J.K., Conway, B.R. & Czech, M.P. Disassembly of Son-of-sevenless proteins from Grb2 during p21ras desensitization by insulin. *J Biol Chem* **270**, 1485-8 (1995).
266. Waters, S.B., Yamauchi, K. & Pessin, J.E. Insulin-stimulated disassociation of the SOS-Grb2 complex. *Mol Cell Biol* **15**, 2791-9 (1995).
267. Waters, S.B., Holt, K.H., Ross, S.E., Syu, L.J., Guan, K.L., Saltiel, A.R., Koretzky, G.A. & Pessin, J.E. Desensitization of Ras activation by a feedback disassociation of the SOS-Grb2 complex. *J Biol Chem* **270**, 20883-6 (1995).
268. Selvin, P.R. The renaissance of fluorescence resonance energy transfer. *Nat Struct Biol* **7**, 730-4 (2000).
269. Weiss, S. Fluorescence spectroscopy of single biomolecules. *Science* **283**, 1676-83 (1999).
270. Nagai, T., Yamada, S., Tominaga, T., Ichikawa, M. & Miyawaki, A. Expanded dynamic range of fluorescent indicators for Ca(2+) by circularly permuted yellow fluorescent proteins. *Proc Natl Acad Sci U S A* **101**, 10554-9 (2004).
271. Kajihara, D., Abe, R., Iijima, I., Komiyama, C., Sisido, M. & Hohsaka, T. FRET analysis of protein conformational change through position-specific incorporation of fluorescent amino acids. *Nat Methods* **3**, 923-9 (2006).
272. Santoso, Y., Joyce, C.M., Potapova, O., Le Reste, L., Hohlbein, J., Torella, J. P., Grindley, N.D. & Kapanidis, A.N. Conformational transitions in DNA polymerase I revealed by single-molecule FRET. *Proc Natl Acad Sci U S A* **107**, 715-20.